

DEVELOPEMENT OF A FRAMEWORK FOR ASPHALT PERFORMANCE-RELATED SPECIFICATION AND PERFORMANCE PREDICTION

A Dissertation

presented to the Faculty of the Graduate School
at the University of Missouri, Columbia

In partial fulfillment
of the requirements for the degree of
Doctor of Philosophy in
Civil & Environmental Engineering

By

Behnam Jahangiri Koohbanani

Dr. William G. Buttlar, Dissertation Supervisor

December, 2020

The undersigned, appointed by the Dean of the Graduate School, have examined the dissertation entitled

**DEVELOPEMENT OF A FRAMEWORK FOR ASPHALT
PERFORMANCE-RELATED SPECIFICATION AND
PERFORMANCE PREDICTION**

presented by Behnam Jahangiri Koohbanani, a candidate for the degree of Doctor of Philosophy, and hereby certify that, in their opinion, it is worthy of acceptance.

William G. Buttlar, Ph.D., P.E

Amir H. Alavi, Ph.D.

Yaw Adu-Gyamfi, Ph.D.

Matthew R. Maschmann, Ph.D.

DEDICATION

To my Mother, Sister, and Grandparents – the most important people in my life.

To my friends and colleagues, my extended family.

ACKNOWLEDGEMENTS

First and foremost, I would like to thank my supervisor and committee chair, Professor William Buttlar, who has the attitude and the substance of a role model. He has been a great source of encouragement and tremendous support throughout my PhD program. Dr. Buttlar continually and convincingly conveyed a spirit of adventure in regard to research and an excitement in regard to teaching. Without his supervision and guidance, this dissertation would not have been possible

I am very thankful to my Ph.D. committee members, Dr. Amir Alavi, Dr. Yaw Adu-Gyamfi, and Dr. Matthew Maschmann for their inputs on my research. I would also like to thank Dr. Mohammad M. Karimi and Dr. Oliver Giraldo for helping with the modeling part of the study. Further, I would like to thank all the current/recent members of the research group including Mr. Hamed Majidifard, Dr. Puynaslok Rath, Dr. Bo Li, Mr. Kaveh Barri, Ms. Loreto Urra, Ms. Shishi Chen, Mr. Helmut Leodarta, and Ms. Nandita Gettu. All provided great support as a cohesive unit. I am blessed to have known them professionally and personally.

A special gratitude is reserved for my family and friends for their company during this stage of my life. I am extremely grateful to my mother, Fariba Motlagh, for her love, prayers, caring, and sacrifices for educating and preparing for my future. I am very thankful to Kaveh Barri, Farzaneh Azadi, Saria Goudarzvand, Nasser Yazdani, Liz Wilcox, and Amir Khederzadeh for their support. They all kept me going and the completion of this program was not possible without them.

TABLE OF CONTENTS

ACKNOWLEDGEMENTS	II
LIST OF FIGURES	VIII
LIST OF TABLES	XIV
ABSTRACT	XVI
1. INTRODUCTION	1
1.1. Overview	2
1.2. Research Approach/Detailed Work Plan	4
1.3. Organization of the Remainder of the Report.....	4
2. FIELD INVESTIGATION AND TESTING RESULTS ON FIELD CORES.....	11
2.1. Overview	12
2.2. Site Visit and Field Investigations	12
2.2.1. Ground-Tire Rubber Test Sections (Report Published in 2017) 13	
2.2.2. SMA Study (Published in 2016)	15
2.2.3. RAS Test Section on I90-Shoulder (Published in 2012).....	17
2.2.4. Other Sections	20
2.3. Cored Sections and Mixture Properties	20
2.4. Field Core Testing Results.....	26
2.4.1. DC(T) Testing Results	26
2.4.2. Repeatability of the Cracking Tests	29
2.4.3. Hamburg Testing Results	30

2.5.	Summary of Field Observations	32
3.	SAMPLING AND TESTING THE PLANT-PRODUCED MIXTURES	34
3.1.	Overview.....	35
3.2.	Sample and Fabrication.....	42
3.3.	Testing Results for Plant-Produced Mixtures	45
3.3.1.	DC(T) Testing Results	45
3.3.2.	HWTT Testing Results.....	51
3.3.3.	TSR Testing Results.....	61
3.3.4.	Boiling Water Test Results	65
3.3.5.	Performance Test Repeatability	68
3.3.6.	Performance-space Diagram	71
3.3.7.	Long-term Aging.....	76
4.	DEVELOPMENT OF THE SPECIFICATION BASED ON FIELD PERFORMANCE DATA AND ANALYSIS	83
4.1.	Overview.....	84
4.2.	Condition Rating Survey (CRS)	85
4.2.1.	CRS Trends in Service Life	86
4.2.2.	Distress Type and Severity.....	87
4.2.3.	Analysis of the Distress Data	89
4.3.	International Roughness Index (IRI)	94
4.4.	Rut Depth.....	95
4.5.	Specification Development.....	96
4.5.1.	Overview	96

4.5.2.	Performance Test Use in Asphalt Mix Design Specifications	97
4.5.3.	DC(T) Spec Calibration Process	106
4.5.4.	Hamburg Test in Mix Design Specification.....	108
4.5.5.	Effect of Depth on Pavement Response.....	109
4.5.6.	DC(T) Spec Development.....	117
4.5.7.	Performance-Based Specification Levels for DC(T) Fracture Energy	127
4.5.8.	Performance-Based Specification Thresholds for Hamburg Rut Depth	129
4.5.9.	Performance-Based Specification Thresholds for SIP and Use of TSR Test	131
5.	VISCOELASTIC CHARACTERIZATION OF ASPHALT MIXTURE USING DC(T) CREEP TEST	134
5.1.	Introduction.....	135
5.1.1.	Overview: Available Creep Test Set-ups	135
5.2.	Scope and Objectives	140
5.3.	Materials, Sample Fabrication, and Test Setup	141
5.3.1.	Sample Fabrication.....	144
5.3.2.	DC(T) Creep Test Set-up	144
5.4.	Analysis of Experimental Results.....	146
5.4.1.	Determining the Creep Compliance Factor.....	146
5.4.2.	Identification of Viscoelastic Properties	148
5.5.	Numerical Simulation	150

5.6.	Numerical Validation.....	152
5.6.1.	Comparing DC(T) Response Predictions with Experimental Measurements	152
5.6.2.	Comparing IDT Response Predictions with Experimental Measurements	156
5.7.	Illi-TC Modeling Results	168
5.8.	Summary and Conclusions	172
6.	ASPHALT MIXTURE PERFORMANCE GRADING	174
6.1.	Introduction.....	175
6.1.1.	Binder Specification.....	175
6.1.2.	Modern Mixture Characterization	177
6.1.3.	Illinois Tollway Mixture Sustainability and Performance Design 179	
6.1.4.	Challenges Associated with Binder Extraction and Recovery....	181
6.1.5.	Motivation for the Current Study	183
6.2.	Methodology	183
6.3.	Mixture Properties	186
6.4.	Results and Discussions	191
6.4.1.	Experimental Testing Results at Low Temperature.....	191
6.4.2.	Comparing the cracking performance of asphalt mixture with extracted and recovered binder	194
6.4.3.	Experimental Testing Results at High Temperature	200
6.4.4.	Comparing the rutting performance of asphalt mixture with	

recovered binder.....	202
6.4.5. Usable Temperature Interval of Mixtures and Binders	206
6.5. Summary and Conclusions	211
7. SUMMARY, CONCLUSIONS, AND FUTURE WORKS	213
REFERENCES	219
APPENDIX A: REVIEW ON THE PERFORMANCE TESTS	238
A.1. Mixture Tests to Mitigate Thermal Cracking	239
A.1.1. Overview of the IDT	240
A.1.2. Overview of TSRST Test.....	240
A.1.3. Overview of DC(T) Test	240
A.1.4. Overview of SCB Test	241
A.1.5. Overview of IDEAL-CT Test	242
A.2. Mixture Tests to Mitigate Rutting.....	242
A.2.1. Overview of WLA tests	243
A.2.2. Overview of APA test	244
APPENDIX B: OTHER PERFORMANCE TESTING RESULTS	245
B.1. I-FIT Testing Results	245
B.2. IDEAL-CT Testing Results.....	251
B.3. IDT Creep and Strength Testing Results.....	258
VITA.....	263

LIST OF FIGURES

Figure 1-1. Flowchart of performance-based specification	9
Figure 2-1. Pictures from I-88 at mile post 61 (EB shoulder and mainline)	14
Figure 2-2. Picture from I-88 at mile post 65.9-High ABR rubber modified asphalt (RMA) mix (EB shoulder and mainline)	15
Figure 2-3. Picture from I-294, mix G, mile post range: 25-27	16
Figure 2-4. Heavy Truck Traffic on I-294, near accident site	16
Figure 2-5. Pictures from I-90 route: a) Mix A (Gravel), WB, MP:3 ¾, b) Mix B (Diabase), EB, MP: 7 ¼	17
Figure 2-6. Pictures from I-90, WB shoulder, a) MP:4 ¼, b) MP: 5 1/2.....	18
Figure 2-7. Plan view and notes on the 2011 study section.....	19
Figure 2-8. Pictures of a) I-90 west to I-39 ramp and b) I-90 MP 17.0.....	20
Figure 2-9. Example of the field core pictures and details from Wang’s Report	21
Figure 2-10. Field cores located in Wang Engineering storage facility	23
Figure 2-11. Transferring the field cores from Wang Engineering storage facility to MAPIL	23
Figure 2-12. DC(T) testing results at -12 °C for the top lift of the field cores.....	28
Figure 2-13. Comparing fracture energies for top and bottom lifts of the field cores	29
Figure 2-13. Hamburg samples with 12mm PCC shims placed below asphalt specimens	31
Figure 2-14. Hamburg testing results for the top lift of the field cores	31
Figure 2-16. Comparing the rut depths for top and bottom lifts of the field cores.....	32
Figure 3-1. Sampling plant produced mixtures from different asphalt plants. a) Mix 1836,	

Wm Ch; b) Mix 1845, Curran, and; c) Mix 1807, Geneva	35
Figure 3-2. Temporarily storage of samples at Tollway maintenance yard	35
Figure 3-3. Aggregate gradations for the investigated plant-produced mixtures	40
Figure 3-4. Location of paved roads using the sampled mixtures on Google Earth.....	42
Figure 3-5. Splitting the bucket of mixture as per AASHTO R47	43
Figure 3-6. Preparing samples for theoretical maximum specific gravity (G_{mm}) testing ..	43
Figure 3-7. Comparing different G_{mm} values for the studied mixtures (Measured = Test performed in MAPIL; QC = Measured by quality control crew; JMF = job mix formula).....	44
Figure 3-8. Transferring the heated mix to the mold	44
Figure 3-9. DC(T) fracture energy at -12 °C using MAPIL samples	46
Figure 3-10. Comparing DC(T) fracture energy at -12 °C: current study vs. JMF	49
Figure 3-11. Pavement temperature at the surface in the northern part of the US (reliability=98%).....	50
Figure 3-12. Comparing DC(T) fracture energy at -12 and -18 °C.....	51
Figure 3-13. Hamburg testing results at required number of passes at 50 °C	54
Figure 3-14. Tested samples after 20K pass at 50 °C. a) 1828 mix, b) 1834 mix.....	56
Figure 3-15. Examples of determination of SIP: a) 1835, b) 1845, c) 1828, d) 1834 mixtures.....	58
Figure 3-16. Parallel creep and stripping lines for 1836 mix.	61
Figure 3-17. TSR sample conditioning. a) Dry set at 25 °C, b) Wet set at 60 °C.....	63
Figure 3-18. Wet and dry strengths and TSR values	64
Figure 3-19. Boiling water test samples and container residue for different mixtures.....	68

Figure 3-20. Average COV (%) of the tests	71
Figure 3-21. Hamburg-DC(T) performance-space diagram for 2018 mixtures	73
Figure 3-22. Required oven aging durations at 95°C to match level of field aging 6 mm below pavement surface for 8 years of field aging (Kim et al., 2018)	78
Figure 3-23. Aging the Tollway 2018 plant produced mixtures in oven at 95 °C for 6 days	79
Figure 3-24. Comparing the DC(T) fracture energies of short-term aged (STA) with long- term aged (LTA) samples	80
Figure 3-25. Comparing the FI of short-term aged (STA) with long-term aged (LTA) samples.....	81
Figure 3-26. Load-displacement response for aged mixtures under I-FIT testing: a)1835 b)1818	82
Figure 4-1. Comparing the CRS values as a function of year	87
Figure 4-2. Example of analyzed field performance data for I88-60.5	91
Figure 4-3. Average severity of centerline deterioration distress (S) as a function of service life.....	91
Figure 4-4. Average severity of longitudinal/center lane cracking distress (Q) as a function of service life	92
Figure 4-5. Average severity of transverse/reflective cracking distress (O) vs. service life	93
Figure 4-6. Comparison of IRI values vs. year in service	94
Figure 4-7. Comparison of rut depth values vs. year in service	96
Figure 4-8. Transverse cracking vs. DC(T) fracture energy (Buttlar et al., 2018)	98

Figure 4-9. Superimposed sections investigated in this study on the bubble plot	100
Figure 4-10. CRS loss for the investigated sections in Illinois and Missouri vs. DC(T) fracture energy	101
Figure 4-11. Correlation between CRS loss per year and DC(T) fracture energy ($R^2=66.54\%$)	102
Figure 4-12. CRS loss for the investigated sections in Illinois and Missouri vs. FI.....	103
Figure 4-13. Correlation between CRS loss per year and FI ($R^2=48.38\%$).....	103
Figure 4-14. Steps in DC(T) spec development.....	108
Figure 4-15. Effect of depth on the layer temperature as a function of depth (SHRP A357 Report, 1993- Location: Frazier, Minnesota)	110
Figure 4-16. Stress relaxation due to depth (SHRP A357 Report, 1993- Location: Frazier, MN).....	111
Figure 4-17. LTPP bind software outputs for pavement temperature in winter as a function of depth and reliability in Northern Illinois.....	112
Figure 4-18. LTPP bind software outputs for pavement temperature in summer as a function of depth and reliability in Northern Illinois.....	113
Figure 4-19. Comparing Hamburg testing results at two different temperatures, a) 1829, b) 1818, c) 1803, d) 1807.....	116
Figure 4-20. Computing a shift in number of passes for 1828 mix	117
Figure 4-21. Flowchart to Calibrate DC(T) spec for SMA friction surface mixtures	120
Figure 4-22. Flowchart to Calibrate DC(T) spec for SMA surface mixtures	121
Figure 4-23. Flowchart to Calibrate DC(T) spec for SMA binder mixtures	123
Figure 4-24. Flowchart to Calibrate DC(T) spec for shoulder surface mixtures including	

“Unmodified SMA”, and “Dense” shoulder surface mixtures	124
Figure 4-25. Comparing shoulders with different ages and fracture energies	125
Figure 4-26. Flowchart to calibrate DC(T) thresholds for shoulder binder mixtures	127
Figure 5-1. Study Framework	141
Figure 5-2. Aggregate gradations for the investigated plant-produced mixtures	143
Figure 5-3. A sample of the test output from DC(T) machine: three replicates (R1, R2, and R3) were tested for each temperature	145
Figure 5-4. The schematic of the generalized Kelvin-Voigt model	149
Figure 5-5. An example of DC(T) creep responses as simulated with viscoelastic FEM in Abaqus	153
Figure 5-6. CMOD response versus time at three temperature levels for mixture of: (a) 1844; (b) 1835; (c) 1824; (d) 1845; (e) 1836; (f) 1840	155
Figure 5-7. An example of DC(T) creep responses through FEM	158
Figure 5-8. Horizontal and vertical deflections from IDT testing for the 1844 mix: (a) at 0°C; (b) at -12°C; (c) at -24°C	160
Figure 5-9. Horizontal and vertical deflections from IDT testing for the 1835 mix: (a) at 0°C; (b) at -12°C (c) at -24°C	161
Figure 5-10. Horizontal and vertical deflections from IDT testing for the 1824 mix: (a) at 0°C; (b) at -12°C; (c) at -24°C	162
Figure 5-11. Horizontal and vertical deflections from IDT testing for the 1845 mix: (a) at 0°C; (b) at -12°C; (c) at -24°C	163
Figure 5-12. Horizontal and vertical deflections from IDT testing for the 1836 mix: (a) at 0°C; (b) at -12°C; (c) at -24°C	164

Figure 5-13. Horizontal and vertical deflections from IDT testing for the 1840 mix: (a) at 0°C; (b) at -12°C; (c) at -24°C.....	165
Figure 5-14. Screenshot of the Illi-TC window to plug in the material properties (Example: Mix 1844).....	169
Figure 5-15. Screenshot of the Illi-TC output for number of critical events (Example: Mix 1844).....	172
Figure 6-1. Proposed approach to determine the mixture PG.....	185
Figure 6-2. Aggregate gradation chart for the mixtures.	190
Figure 6-3. DC(T) fracture energy at -12°C.....	193
Figure 6-4. Comparing DC(T) fracture energy at -12°C and -18°C.	194
Figure 6-5. Comparing the mixture and extracted PGLT.	195
Figure 6-6. Determination of 1835 mix PGLT.	196
Figure 6-7. Hamburg testing results at 50°C.	201
Figure 6-8. Comparing Hamburg testing results at multiple temperatures.....	202
Figure 6-9. Comparing mix and binder performance grades.....	205
Figure 6-10. Mix vs. Binder UTI.....	209

LIST OF TABLES

Table 2-1. List of the selected sections for coring and their distress description	22
Table 2-2. Mixture properties for the cored sections (Top Lift).....	25
Table 2-3. Mixture properties for the cored sections (Bottom lift).....	26
Table 2-3. Variability of the cracking performance test results for field cores	30
Table 3-1. Mixture sampling details	36
Table 3-2.Details of mixture ingredients	39
Table 3-3. Location of the paved section using the studied mixtures.....	41
Table 3-4. Identifying the stripping mixtures based on SIP requirements	60
Table 3-5. Test COV averages for different mix categories	70
Table 3-6. Standard Deviation (STD) averages for different mix categories	70
Table 3-7. Illinois oven aging duration based per NCHRP-781 “(6 mm below the surface) (Elwardanya et al., 2018):.....	78
Table 4-1. Examples of CRS distress characterization and coding	89
Table 4-2. ANOVA results and Tukey ranking	106
Table 4-3. Number of passes to reach 2.5 mm rut depth	116
Table 4-4. DC(T) thresholds at -12 °C for different mix categories.....	129
Table 4-5. Hamburg rut depth thresholds at 50 °C for different mix categories	130
Table 4-6. SIP thresholds at 50 °C for different mix categories (applied when the slope ratio is ≥ 2.0).....	133
Table 5-1. Details of mixture ingredients	143
Table 5-2. Loading properties in DC(T) creep test.....	145
Table 5-3. Identified viscoelastic constant coefficient	150

Table 5-4. Repeatability of CMOD at 1000 s	156
Table 5-5. Loading properties in IDT creep test.....	157
Table 5-6. Repeatability of IDT creep horizontal displacement at 1000 s	166
Table 5-7. Repeatability of IDT creep vertical displacement at 1000 s.....	167
Table 5-8. Comparing IDT with DC(T) creep tests	168
Table 5-9: Input parameters in Illi-TC and resultant critical events and amount of cracking.....	171
Table 6-1. Illinois Tollway performance criteria for different mixture types.....	186
Table 6-2. Details of the mixture ingredients.	189

ABSTRACT

Traditional asphalt mixtures have generally involved relatively simple combinations of virgin asphalt binder and aggregates to meet load-bearing needs of the roads and surfaces. Accordingly, simple tests such as Marshall Stability and Flow were used in an effective manner for asphalt mixture screening and quality control purposes. In recent years, there has been a proliferation of asphalt ingredients available to designers, especially in the case of recycled materials, compaction aides, and mixture performance and/or sustainability promoting products. These include reclaimed asphalt pavement (RAP), recycled asphalt shingles (RAS), warm mix agents, antistripping agents, rejuvenators, ground tire rubber, and even waste plastic. These modern, heterogeneous asphalt mixtures exhibit more complex behavior as compared to earlier mixes containing fewer ingredients and predominantly virgin materials. As a result, recent asphalt mixes require advanced performance tests to account for these complexities, while factoring in traffic and environmental loads for the given mixture type being designed.

In this study, various existing roads including good and bad performing sections were selected in Illinois and Missouri and after conducting site visits. In field investigations, the main distresses on the Tollway in northern Illinois and across the state of Missouri were identified. Also, several field cores were obtained from mainline and shoulder sections to evaluate the laboratory performance of existing asphalt mixtures across a range in-situ aging levels. Analyzing the available field performance data such as international roughness index (IRI), condition rating system (CRS), and rut depths and comparing them with laboratory testing results provided a robust data set to establish updated performance test thresholds for the Tollway mixture design specification.

According to recent literature, mixture performance can be evaluated using various tests to mitigate different distress types such as cracking, rutting, and moisture damage. In this study, fourteen different mixtures produced in 2018 on mainline and shoulders sections across the Tollway system, and four mixtures in Missouri were selected to characterize performance testing trends and to study the ability of the different performance tests to predict pavement performance. To this end, performance tests such as the DC(T), I-FIT, IDEAL-CT, IDT, Hamburg, and TSR were conducted on the collected plant produced mixtures. The process of sample fabrication, ease of conditioning and testing, repeatability and ability to correctly rank various Tollway mix types was taken into consideration in selecting the appropriate performance tests to be used in the Tollway's mix design asphalt specification. The DC(T) test was found to possess the best correlation to field performance, and significantly outperformed the I-FIT test in terms of test repeatability. Both the I-FIT and IDEAL tests returned failing results for a number of SMA mixes, and dense-graded mixes with high recycling content, which have traditionally performed well on the Tollway. This provided additional motivation to retain the DC(T) test as the cracking test to be used in the Tollway's asphalt mixture design specification.

The analysis presented in this study, in conjunction with field observations, led to the identification of various cracking types as the primary distresses observed on Tollway mainline and shoulder sections surfaced with asphalt. Rutting and stripping were not found on Tollway asphalt surfaces, nor in Missouri at the present time. The Disk-shaped Compact Tension (DC(T)) test was chosen to be retained in the performance related specification (PRS) for the design of crack-resistant mixtures due to its high degree of correlation with

field results and best repeatability. A systematic approach was developed, which allowed different reliability levels to be addressed in the specification, along with a consensus step to take advantage of local practitioner experience. Similarly, for high-temperature performance, Hamburg thresholds for binder course mixtures were tailored for different mixture types and use cases. In some cases, by relaxing Hamburg requirements, designers have more leeway in building crack resistance into the mixture and/or to utilize higher amounts of recycled materials. For SMA mixtures, it was observed that low rut depth mixes were sometimes identified as having stripping potential in the Iowa method. However, similar mixtures have not exhibited stripping in the field. As a result, it is recommended that SMA mixtures with rut depths less than or equal to 4.0 mm after 20,000 passes should be characterized as non-stripping and do not need to be checked for stripping potential through the Iowa method. Based on experimental results, it is also recommended to use the Hamburg test in lieu of the TSR stripping test for moisture sensitivity evaluation. In the event of failing results, the TSR test can be used as a secondary method to assess adequate moisture resistance. Using the specification for both cracking and rutting, a novel grading system that takes into account the performance of the asphalt mixture was developed and the Tollway mixtures were graded based on this system. Also, the characterization of the viscoelastic behavior at low temperature through the DC(T) creep test led to validating the performance of the mixtures that could pass the cracking requirements.

Chapter 1

INTRODUCTION

1.1. Overview

Some eighty years ago, the Marshall stability and flow test and Hveem stabilometer and cohesiometer devices were developed to supplement asphalt binder purchase specifications and volumetrics-based mix design methods by providing ‘tests on the mix.’ In both cases, tests were developed to provide bookends on high and low temperature asphalt pavement performance, i.e., rutting and durability/cracking. These were necessarily very simple, empirical tests run at room temperature or higher, as it was difficult to test in the low in-service temperature range in that era, or to reliably measure fundamental material properties. In the late 80’s and early 90’s, the Strategic Highway Research Program (SHRP) undertook an ambitious program to radically improve asphalt binder purchase specifications, aggregate requirements, mixture compaction, and performance-based mixture tests with associated models. The SHRP program created ‘Superpave’ products such as the PG Binder specification, new collections of aggregate consensus and source property tests, a new standardized asphalt gyratory compactor, and provided minor changes and national standardization of mixture volumetric design principles and use of the AASHTO T-283 tensile strength ratio test to evaluate moisture damage.

In 2015, the Federal Highway Administration (FHWA) defined Balanced Mix Design (BMD) as “asphalt mix design using performance tests on appropriately conditioned specimens that address multiple modes of distress taking into consideration mix aging, traffic, climate and location within the pavement structure” [1]. The BMD involves two or more performance tests addressing pavement cracking and rutting to be added to the Superpave asphalt mixture design system in order to more reliably attain desired

pavement performance targets [2,3]. Currently, three approaches to BMD, each progressively more reliant on mixture performance tests, were identified by the group, including: volumetric design with performance verification, performance-modified volumetric design, and performance design [4]. In these approaches, cracking tests such as Texas overlay tester (OT) [5], Illinois Flexibility Index Test (I-FIT) [6], IDEAL-CT [7], and Disk-Shaped Compact Tension (DC(T)) have been evaluated (Mogawer et al., 2005). Also, flow number [8] and wheel tracking (e.g. Asphalt Pavement Analyzer (APA) and Hamburg Wheel tracking [9]) tests have been used to address rutting [10,11]. In addition to volumetric mix design requirements, a BMD should ideally involve systematically-developed and validated performance-related specification (PRS), outlining requirements (or minimum thresholds) to be attained by the mixture after subjecting it to the specified suite of performance tests. Normally, a PRS will contain requirements to limit rutting, moisture damage, and one or more forms of pavement cracking.

With the DOTs and agencies' emphasis on constructing and maintaining high volume expressways, high performing asphalt mixtures are needed to ensure durable, long-lasting pavements. The use of validated and improved performance-related specifications (PRS) could also lead to lower maintenance needs, saving cost, and reducing user delays.

Asphalt mixture test methods in a practitioner-friendly PRS should be repeatable, straightforward, commercially available and sufficiently standardized. They should also reliably control the most critical distresses identified by the owner. The types of critical distresses to be controlled may differ when developing PRS limits for surface mixes, binder course mixes, and shoulder mixes. In theory, a benefit arising from adoption of

performance-related mixture specifications is the ability to provide additional flexibility to the mix designer by relaxing or removing any over-constrained method-based requirements (gradation bands, dust-to-asphalt ratio range). This should be simultaneously investigated to shorten the PRS development and implementation cycle, saving time and money.

1.2. Research Approach/Detailed Work Plan

This study describes the findings of a comprehensive research conducted at Illinois Tollway, leading to a PRS for the design of mainline and shoulder asphalt mixtures. A novel approach was developed, involving the systematic establishment of specification requirements based on: (1) selection of baseline values based on minimally acceptable field performance thresholds; (2) elevation of thresholds to account for differences between short-term lab aging and expected long-term field aging; (3) further elevation of thresholds to account for variability in lab testing, plus variability in the testing of field cores, and; (4) final adjustment and rounding of thresholds based on a consensus process.

1.3. Organization of the Remainder of the Report

A comprehensive literature review was conducted and provided in Appendix A. The obtained insight from literature review along with consultation with the Technical Review Panel (TRP) assisted in the selection of projects to be shadowed in 2018, and in the selection of older projects for coring and collection of performance data. The overall dissertation organization is summarized as a flowchart in Figure 1-1. A description of the chapters covered in this dissertation is provided below.

Chapter two: Field Investigation and Testing Results on Field Cores

This chapter elaborates on site visits and field observations conducted to examine the performance of selected mainline pavements and shoulders, including the sampled 2018 sections. In addition, the site visits provided the opportunity to visit older, existing sections with the goal of identifying good and poor performing sections with varying service lives. These sections were later cored to obtain additional performance testing samples, and the corresponding field performance data versus time was obtained via collaboration with Applied Research Associates (ARA), LLC and MoDOT's ARAN portal. It presents the results of the laboratory testing, involving field core samples obtained in 2019. Results from field-aged cores were studied alongside test results on short-term aged samples such that the mixture PRS could be calibrated. This calibration enables the PRS to specify the use of short-term aged, laboratory-prepared specimens, along with suitably conservative property thresholds that take into account the expected property (and performance) effects of subsequent long-term aging in the field.

Chapter three: Sampling and Testing the Plant-Produced Mixtures

This part of the study provides details regarding the collected plant produced asphalt mixtures selected for sampling in this study. Fourteen mixtures, produced at six asphalt plants were selected in consultation with the TRP. These were sampled during production in the summer of 2018, with details on the sampling and storage techniques used, mix designs, etc., provided in this chapter. provides the laboratory testing results from the selected 2018 Tollway plant-produced mixtures. After transferring the collected samples from the asphalt plants to the Missouri Asphalt Pavement and Innovation Lab (MAPIL),

testing samples were fabricated and a suite of performance tests were conducted. The testing results were used to evaluate the pros and cons of the investigated performance tests, including their repeatability, practicality and their expected relationship to field performance. Furthermore, a long-term aging protocol was followed to age the loose mixtures in the oven for six days at 95 °C. Long-term aging of the selected loose mixtures provided the opportunity to verify the aging effect on performance tests that has been reported in the relevant literature. Preliminary recommendations for performance tests to be used in the revised asphalt mixture PRS for the Tollway were generated from the results obtained in this data set.

Chapter four: Development of the Specification based on Field Performance Data and Analysis

This chapter presents the field performance data provided by ARA and analyzed by the research team. The distress and overall performance data were used to set final thresholds in the revised asphalt mixture PRS developed herein. It also establishes the framework for the development of the recommended PRS threshold adjustments. Considering the selected performance tests and their thresholds from the previous chapters, this chapter describes the systematic process used for finalization of the performance specification. The framework utilizes a combination of laboratory and field investigation results, a straightforward statistical approach to conservatively account for test and sampling variability, and documents the consensus process used to incorporate practical

considerations and experience from selected experts on the project TRP, which led to verification and/or final rounding of PRS thresholds.

Chapter five: Viscoelastic Characterization of Asphalt Mixture Using DC(T) Creep Test

This section presents a framework to identify the low-temperature viscoelastic properties of asphalt concrete using the disk-shaped compacted tension (DC(T)) creep test. The DC(T) creep test was conducted on different asphalt mixtures comprised of various components and modifiers at three temperature levels of 0, -12, and -24 °C. The creep compliance function for each of these mixtures was modeled using a generalized Kelvin-Voigt spring-dashpot phenomenological representation. Numerical simulations of DC(T) creep tests using the identified viscoelastic properties are presented, which indicate the capability of the proposed approach to characterize the low-temperature linear viscoelastic behavior of the investigated asphalt mixtures. To further validate the viscoelastic properties obtained from DC(T) test through different stress-strain states, numerical simulation results from an Indirect Tensile Creep Test were compared to experimental results. The calibrated viscoelastic models were then used in a finite element based tool called Illi-TC to predict the amount of low temperature cracking on the surface of the pavements.

Chapter six: Asphalt Mixture Performance Grading

Advanced binder and mixture tests have steadily evolved towards the improvement of asphalt pavement serviceability and durability. More than ever before, asphalt mixture

performance tests are critical in the design and evaluation of modern, heterogeneous asphalt mixtures. The Illinois Tollway's current performance-engineered mix design specification requires compliance to both high and low temperature mixture test criteria. As part of a rigorous research investigation, results from disk-shaped compact tension (DC(T)) fracture and Hamburg wheel tracking tests conducted at multiple temperatures were used to develop a continuous performance grade (PG) system. The developed mixture PG testing and analysis system represents a new method to broadly fingerprint the performance range of Tollway mixtures, and asphalt mixtures in general. The calculated mix PG was then compared to the recovered binder continuous PG grade. The mixture PG appears to more realistically assess the mixture performance range since it takes into account the role of aggregates and additives such as crumb rubber and their interaction with the binder system. In addition, the uncertainties and difficulties associated with the binder extraction and recovery, especially for rubber-modified mixtures, is avoided in the mixture continuous grading approach.

Chapter seven: Summary, Conclusions, and Future Work

This chapter summarizes the conclusions and findings of this research investigation, and provides recommendations for future research.

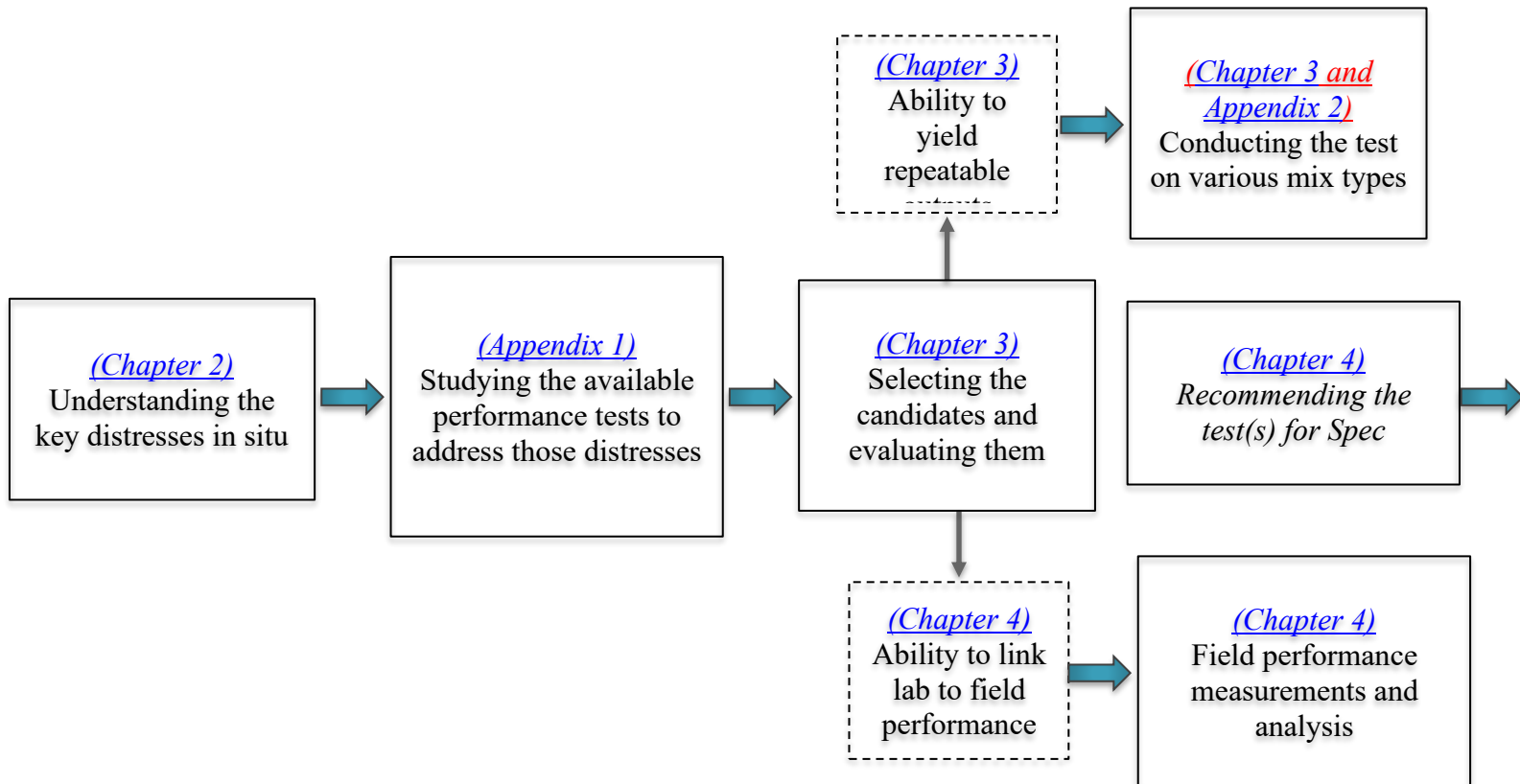


Figure 1-1. Flowchart of performance-based specification

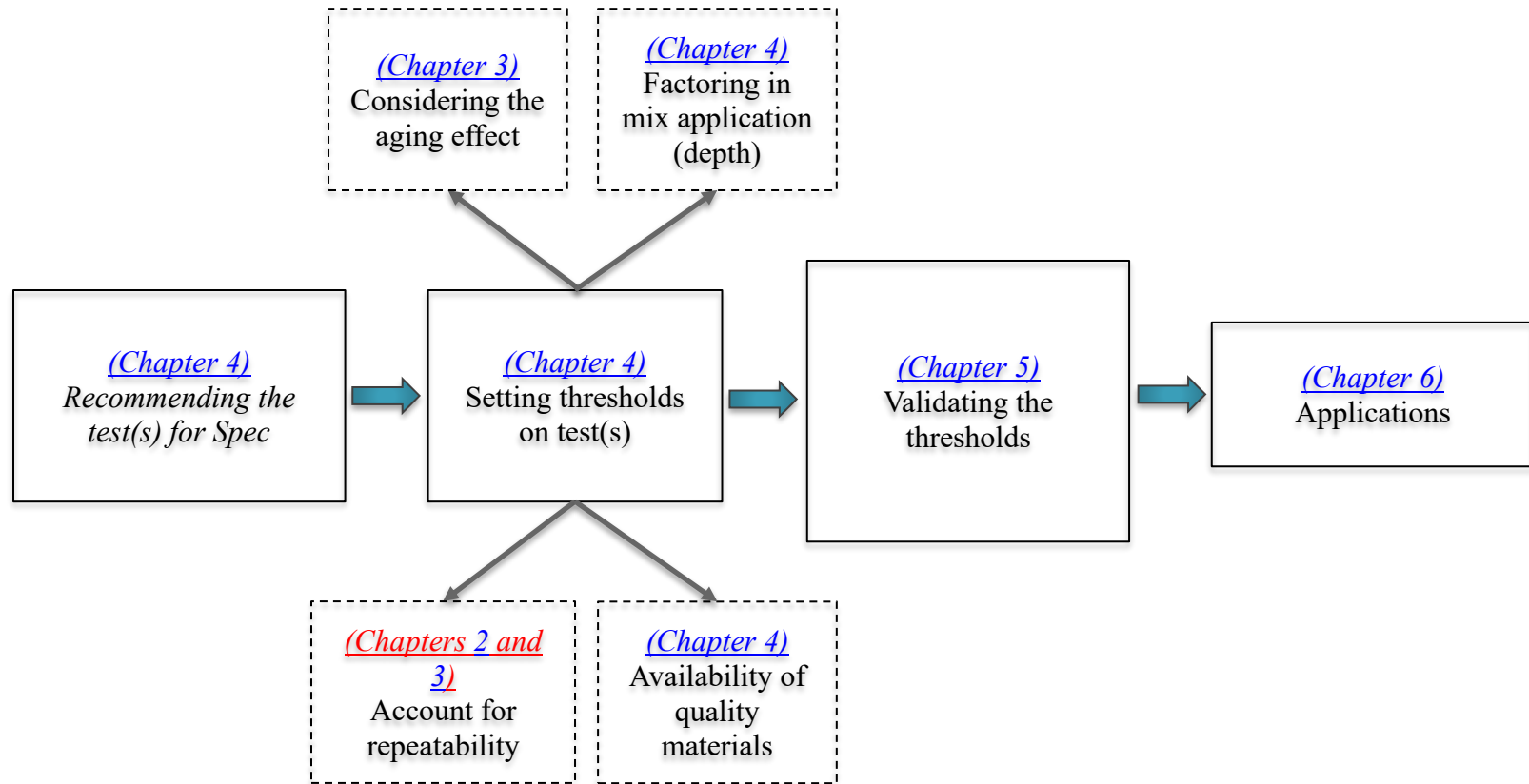


Figure 1.1 (cont.). Flowchart of performance-based specification

Chapter 2

FIELD INVESTIGATION AND TESTING RESULTS ON FIELD CORES

2.1. Overview

Development of a truly performance-based specification requires comprehensive laboratory testing combined with extensive field performance data. Besides overall condition, details regarding the type, extent and severity of individual distresses should be considered when trying to control rutting, cracking and moisture damage. This can be achieved through site visits (visual inspection), automated data collection vehicles or preferably both. Both types of data were used herein to assist in updating the Tollway's asphalt mix design performance test thresholds.

The plant-produced asphalt mixtures studied in this study were used to pave different sections in the Tollway road system during the summer of 2018. The sampled mixtures were used to fabricate testing samples and evaluate the efficiency of the performance tests and to assess the expected performance in these mixtures. Various performance tests were carried out, and the results were presented in the previous chapter. In order to observe the service quality of the mixtures in-situ, the MU team had a two-day site visit from May 30th to May 31st, 2019. After finalizing a location of the targeted sections and the milepost ranges in a meeting with the TRP subcommittee, and the condition of the sections was visually observed. Although the visited sections did not age considerably, they experienced a record-breaking winter and severe cooling events at the beginning of 2019 that provided an opportunity to reveal any poor performing mixtures in terms of low temperature cracking.

2.2. Site Visit and Field Investigations

In addition to the 2018 overlaid sections, other good and bad performing sections were located and observed as follows. Most of these selected sections were already studied in

previous projects, and their laboratory performance data either on field cores or plant produced mixtures were available. The list of the projects from which the sections were selected as follows.

- Illinois Tollway I-88 Ground Tire Rubber Test Sections: Laboratory Mix Designs and Performance Testing- Report Published in 2017
- Laboratory Investigation of Illinois Tollway Stone Matrix Asphalt Mixtures with Varied Levels of Asphalt Binder Replacement- Report Published in 2016
- Characterization of Hot Mix Asphalt Containing Post-Consumer Recycled Asphalt Shingles and Fractionated Reclaimed Asphalt Pavement- Report Published in 2010

2.2.1. Ground-Tire Rubber Test Sections (Report Published in 2017)

The Illinois Tollway constructed test sections for three Ground Tire Rubber (GTR) asphalt modifier technologies on the Reagan Memorial Tollway (I-88) in April 2016. Apart from estimating the performance characteristics of the new GTR technologies, the study also examined the effect of softer virgin binder and an increased amount of reclaimed asphalt on mix performance properties. Accordingly, the GTR technologies were incorporated into SMA mixes with 33% asphalt binder replacement (ABR) using a ‘standard’ base or virgin binder (PG 58-28) and a softer base binder (PG 46-34). A third design was also used, where the softer base binder was combined with an increased asphalt binder replacement (ABR) percentage (PG 46-34 with 47% ABR), obtained by increasing the content of recycled asphalt shingles (RAS).

- Route I-88: The 1636 mix (Elastiko PG 46-34 High ABR) on passing lane (EB)

- Mile post: 61.0
- Observations: Some thermal cracks were observed- Cores were taken from the mainline. Some cracks stopped once they reached the rubber modified mix on the inside lane (see Figure 2-1)



Figure 2-1. Pictures from I-88 at mile post 61 (EB shoulder and mainline)

- Route I-88: The 1631 mix (Evoflex PG 46-34 High ABR) on outside shoulder (EB)
 - Mile post 65.9
 - Observations: SMA shoulder- Many cracks in asphalt (Figure 2-2).



Figure 2-2. Picture from I-88 at mile post 65.9-High ABR rubber modified asphalt (RMA) mix (EB shoulder and mainline)

2.2.2. SMA Study (Published in 2016)

In order to maximize the environmental and economic benefits of RAP, RAS, and GTR, innovative pavement agencies and mix designers tend to utilize these recycled products in various combinations to reduce virgin asphalt and aggregate content to the maximum extent possible, leading to significant cost savings and enhanced sustainability. In general, SMA surface mixtures containing high percentages of asphalt binder replacement (ABR) from RAP/RAS would be more susceptible to thermal and block cracking as compared to virgin asphalt mixtures, unless specific measures are taken to counterbalance the recycled materials with a softer virgin binder base grade and/or through the use of a rejuvenating-type modifier. Such countermeasures have been taken in the design of Tollway high-traffic, stone matrix asphalt mixtures; however, the design of these mixtures pre-dated the existence of modern low temperature mixture cracking

tests. In addition, the Illinois Tollway made an early move to a lower design voids target in an effort to enhance mixture durability when recycled materials are used. The primary objectives of this study were to evaluate the low temperature characteristics and expected performance of cores obtained from seven Tollway projects constructed between 2008 to 2012 using stone-mastic asphalt (SMA) mixtures with varying ABR levels and virgin materials.

- Route I-294: Mix G (PG 70-28 SBS), overlaid in 2012
 - Mile post range: 25-27
 - Observations: Some potholes- Reflective cracking (some were skewed)- Fat spots- Rough ride (see Figure 2-3)
 - Heavy traffic load (see Figure 2-4)

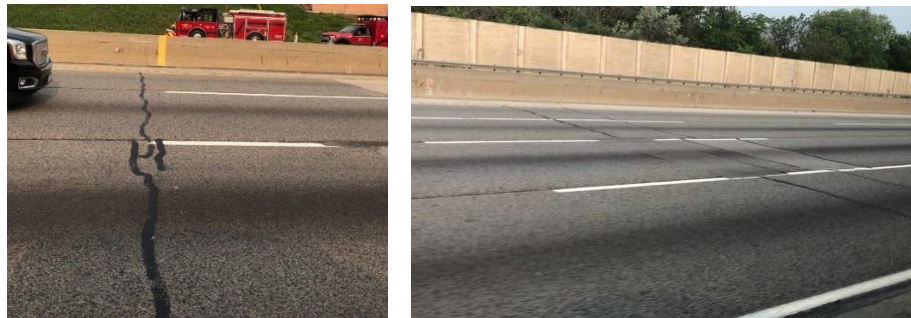


Figure 2-3. Picture from I-294, mix G, mile post range: 25-27



Figure 2-4. Heavy Truck Traffic on I-294, near accident site

- Route I-90: Mix A (on WB) and mix B (on EB)
 - Mile post range: 2-15
 - Observations: Mostly longitudinal and joint cracks (Figure 2-5)



(a)

(b)

Figure 2-5. Pictures from I-90 route: a) Mix A (Gravel), WB, MP:3 $\frac{3}{4}$, b) Mix B (Diabase), EB, MP: 7 $\frac{1}{4}$

2.2.3. RAS Test Section on I90-Shoulder (Published in 2012)

In summer of 2009, a field demonstration project was conducted by the Illinois Tollway on the Jane Addams Memorial Tollway (I-90). Eight mix designs containing zero or five percent RAS and varying percentages of FRAP were developed and placed in the pavement shoulder. With more transportation agencies studying the options of adding RAS or using higher amounts of RAP through fractionation, the Tollway became interested in adopting these techniques in their construction specifications. The objective of this new research was to determine how replacing five percent of the FRAP in these new mixes with five percent post-consumer RAS would affect the performance of asphalt pavements. Figure 2-6 provides sample images from the shoulder and Figure 2-7 presents the properties of the mixtures used

on the shoulder with the mile markers and description for each section superimposed on the plan view.



(a)



(b)

Figure 2-6. Pictures from I-90, WB shoulder, a) MP:4 1/4, b) MP: 5 1/2

2.2.4. Other Sections

- Route I-90: SMA mix, overlaid in 2018, GTR modified
 - Mile post range: 16.5-17.9 EB, and I-90 west to I-39 ramp
 - Observations: High density block cracking on the SMA mix (observable when walking, less noticeable when driving), ride is still reasonably good)
(Figure 2-8)



Figure 2-8. Pictures of a) I-90 west to I-39 ramp and b) I-90 MP 17.0

Based on these observations, a list of good and poor performing sections was prepared (see Table 2-1). In this list, sections from mainlines (SMAs) and shoulders (dense graded) with different levels of age ranging from three to eleven years of service life were selected. Obtaining field cores and testing the laboratory performance of these sections were the next phase carried out in this study. This table also shows the location and number of cores obtained from each section along with a short description of the distresses observed on each section.

2.3. Cored Sections and Mixture Properties

Previously, the selected sections for the field cores were introduced. These sections were selected to cover the wide range of the mixture types that Tollway used on both mainline

and shoulders. Also, considering the good- and poor performing sections could help with the specification calibration. It is also worth mentioning that these sections cover a wide range of service life and most of the sections have experienced at least eight years and many cold events. Wang Engineering collected 51 full-depth cores and 81 partial-depth cores at various locations along I-88, I-90 and I-294 shown in Table 2-1 in July and August 2019 (see Figure 2-9). The cores were obtained using a coring machine equipped with a 6.0-inch diameter core barrel. Figure 2-10 and Figure 2-11 show the field cores in the storage Wang’s facility and the transferring of these cores to MAPIL using a truck, respectively.

**Pavement Cores
WB I-90 at MP 6.6**



**Surface Cores
WB I-90 at MP 6.6**



PAVEMENT CORES: I-88/I-90/I-294 PAVEMENT CORES, ISTHA GJR CONTRACT RR-18-4410, TASK 0202G, LEE AND WINNEBAGO COUNTIES, ILLINOIS		
SCALE: GRAPHICAL	EXHIBIT 2-7	DRAWN BY: E. Yim CHECKED BY: A. Hamad
		1145 N. Main Street Lombard, IL 60148 www.wangeng.com
		FOR ILLINOIS TOLLWAY 166-01-08

Figure 2-9. Example of the field core pictures and details from Wang’s Report

Table 2-1. List of the selected sections for coring and their distress description

<i>Route</i>	<i>Lane</i>	<i>Mile Post Range</i>	<i>Total No. of Cores</i>	<i>No. of Mid-Depth*</i>	<i>No. of Surface layer**</i>	<i>Description</i>
I-88	Inside lane-Tangents	45.00-55.10	12	3	9	On rubblized JCP
I-88	Inside lane-Tangents	61.30-60.10	12	3	9	Control-SBS- located between the rubber sections
I-90	Mainline-Tangents	15.00-2.00	12	3	9	Gravel- Aged SMA-construction joints- crack sealants
I-90	Mainline	15.00-2.00	12	3	9	Diabase- Aged SMA
I-90	I-90 Ramps	17.80-16.50	12	3	9	High density block cracking
I-294	Mainline	30.50-36.50	12	3	9	Quartzite mix- Reflective cracking- Rough ride- Placed on jointed
I-88	Shoulder	45.00-55.10	12	3	9	<u>Visually good performing</u>
I-88	Shoulder	55.10-60.00	12	3	9	Poor performing- transverse cracks, low severe block cracks.
I-90	Shoulder	7.50-7.00	6	3	3	Poor performing- transverse and block cracks
I-90	Shoulder	6.60-6.25	6	3	3	Poor Performing- severe transverse and block cracks
I-90	Shoulder	6.25-5.25	6	3	3	Poor performing-3 ft. interval transverse cracks and block cracking
I-90	Shoulder	5.25-4.50	6	3	3	Poor performing- more transverse cracks than block
I-90	Shoulder	9.50-10.50	6	3	3	Good performing
I-90	Shoulder	9.50-10.50	6	3	3	Poor performing- transverse cracks

*Mid-depth core: 6” deep- **Surface layer core: 3-4” deep



Figure 2-10. Field cores located in Wang Engineering storage facility



Figure 2-11. Transferring the field cores from Wang Engineering storage facility to MAPIL

The details about those cored sections including the location of the core samples, mixture properties on first two lifts of the cores, and also the overlaying year will be discussed in this section.

Table 2-2 shows the properties of the cores' top lift. These cores were obtained from I-88, I-90, and I-294. The first six mixtures are SMAs including both SMA friction surface and SMA surface. The next six mixtures are shoulder sections located on I-88 and I-90. The description of each column is provided below.

- “Location” column, which will be used as the label of the sections later, includes the route and also a number that represents the mile post range and is unique for each section.
- “MP Range” represents the mile post range on the corresponding section.
- “Year” shows the overly time (year) of the section.
- “Base Binder” is the binder system including the PG grade and the modification.
- “Mix Type” can be SMA surface, SMA friction surface, or N70 dense graded mix.
- “NMAAS” and “ABR”s are the nominal maximum aggregate size and asphalt binder replacement by RAP or RAS, respectively.

As mentioned in the previous chapter, the performance-based specification covers various types of mixtures located within different levels of the pavement structure.

Therefore, in addition to the top lifts, it was attempted to study the bottom lifts of the field cores and evaluate their performance. The test results for the bottom lifts will be used to calibrate the spec for the corresponding mixture types. The details of bottom lifts

of the field cores were collected from JMF and presented in Table 2-3. The bottom lifts studied in this study are from seven sections. The first three mixtures are the SMAs used on the bottom lift, and the next four sections are N50 dense graded shoulder binders. The headings used in this table are similar to the ones used in

Table 2-2.

Table 2-2. Mixture properties for the cored sections (Top Lift)

Location	MP Range	Year	Base Binder	Mix. Type	NMAS	ABR by RAP	ABR by RAS
I88-47	45-55.1	2016	SBS 70-28	SMA Surface	12.5	11.6	19.8
I88-60.5	60.1-61.3	2015	SBS 70-28	SMA Friction S.	12.5	14.8	20.7
I90-6.6	2.0-15.0	2009	76-22+ GTR	SMA Surface	12.5	13.9	0
I90-6.0	2.0-15.0	2008	70-28+ GTR	SMA Friction S.	12.5	16.3	0
I90-17.8	16.5-17.9	2008	76-28+ GTR	SMA Friction S.	19.0	16.0	0
I294-34	30.5-36.5	2012	SBS 70-28	SMA Friction S.	19.0	15.5	16.2
I88-52	45.0-55.1	2015	58-28	N70D Surface	9.5	19.1	19.6
I88-57	55.1-60.0	2014	58-28	N70D Surface	9.5	22.8	17.8
I90-7.25	7.0-7.5	2009	58-22	N70D Surface	9.5	16.7	20.1
I90-5.12	4.0-5.25	2009	58-22	N70D Surface	9.5	24.4	0.0
I90-10E	9.9-10.1	2008	58-22	N70D Surface	9.5	24.0	0
I90-10W	9.9-10.1	2008	58-22	N70D Surface	9.5	16.2	0

Table 2-3. Mixture properties for the cored sections (Bottom lift)

Location	MP Range	Year	Mix. Type	Base Binder	NMAS	ABR by RAP	ABR by RAS
I90-6.6	2.0-15.0	2009	SMA Surface/Binder	76-22+ GTR	12.5	13.9	0
I90-6.0	2.0-15.0	2008	SMA Binder	76-22+ GTR	12.5	15.3	0
I294-34	30.5-36.5	2012	SMA Binder	SBS 70-28	12.5	17.1	19.2
I90-7.25	7.0-7.5	2009	N50 Binder	58-22	19.0	21.7	22.4
I90-6.06	6.0-6.12	2009	N50 Binder	58-22	19.0	32.9	24.2
I90-5.12	5.0-5.25	2009	N50 Binder	58-22	19.0	42.1	23.7
I90-4.75	4.5-5.0	2009	N50 Binder	58-22	19.0	31.2	23.7

2.4. Field Core Testing Results

2.4.1. DC(T) Testing Results

DC(T) samples were fabricated using the top lift of the collected field cores. The thickness of the top lift was at least 50 mm (2 inches) for all the sections, which made it possible to cut the DC(T) samples into 50 mm slices. Three replicates were tested for each section and the average of DC(T) fracture energies was calculated. Figure 2-12 shows the fracture energies tested at -12 °C. The error bars shown for each section covers the range of the obtained from testing the replicates. Also, mixture type and year of overlay are indicated for each section. The table attached to the figure provides the amount of recycled materials used in each mixture, including the ABR by RAP and RAS

and total ABR. The details of the mixture ingredients such as the NMAS, binder system, and modification are provided in

Table 2-2. The tested mixtures are divided into two categories, namely, SMAs and dense graded mixtures, using a gray dashed line. As expected, the DC(T) fracture energies of the SMAs are higher than the dense graded mixtures. Also noted were:

- I88-47 and I88-60.5 both used SBS 70-28 binder systems. However, benefiting from higher quality aggregates, I88-60.5 yielded a significantly higher fracture energy (436 v. 830 J/m²) although this section has aged one year longer than I88-47.
- The combination of higher aggregate quality and also a softer binder system (PG 70-28 GTR) used in the I90-6 mix (SMA friction surface) resulted in higher DC(T) fracture energy as compared to I90-6.6.
- Referring to the distress summary for I90-6.0 and I90-6.6 listed in Table 2-1, the section with lower fracture energy (I90-6.6) started to show transverse cracking while I90-6 with higher fracture energy did not.
- Although the I90-17.8 section experienced block cracking on its surface, the mixture performed well in the DC(T) test with a fracture energy value of 800 J/m². We believe this is due to the nature of aggregate in this mix, perhaps combined with mix volumetrics.
- The I294-34 mix was placed on jointed concrete pavement and has experienced significant reflective cracking. The fracture energy of this mix was low (451 J/m²).

- The fracture energy of all the shoulder mixtures including poor and good performing sections was around 400 J/m². This indicates that a long-term aged fracture energy level of 400 J/m² may be borderline with respect to ensuring adequate resistance to environmentally-based cracking in the Chicagoland area.

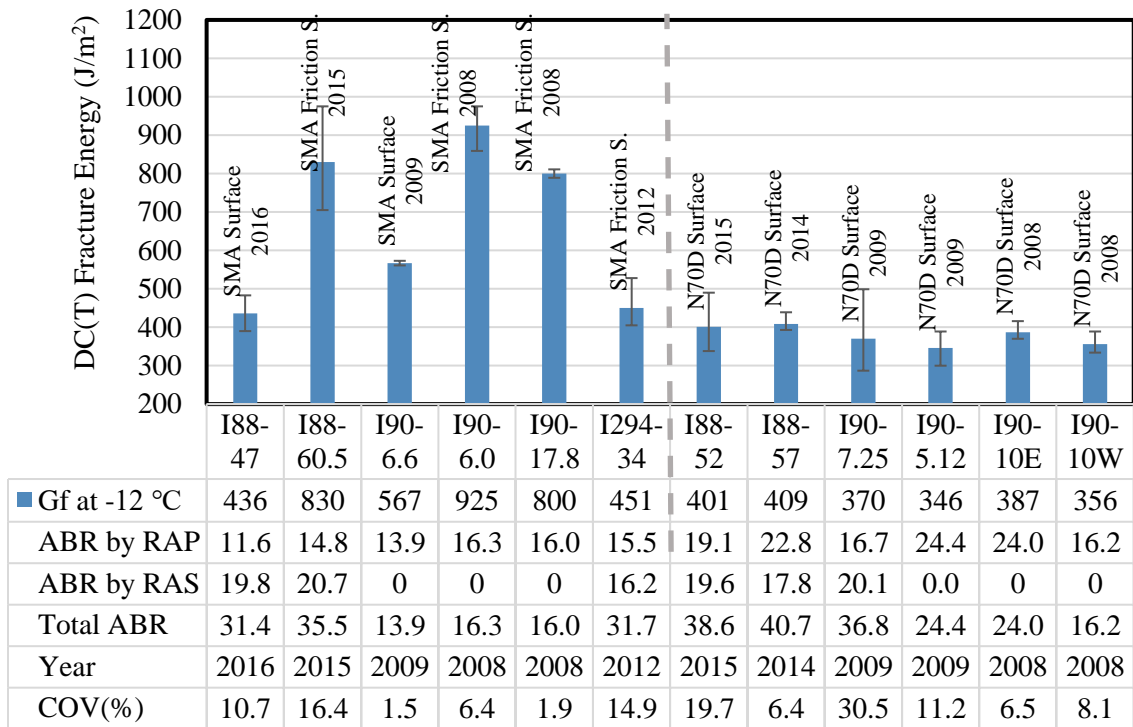


Figure 2-12. DC(T) testing results at -12 °C for the top lift of the field cores

Figure 2-13 shows the DC(T) fracture energies for two lifts of the studied sections.

Generally, no significant difference was observed in fracture energy for two different lifts of the same section. Although the mix used in the bottom lift may not be as crack resistant as the first lift, the environmental and traffic loading conditions that the first lift experiences are more severe than the bottom lift. Given the fact that the studied mixtures have aged for many years in-situ, the higher crack resistance could be balanced with harsher environmental conditions (i.e. cooling cycles their severity) such that the difference between fracture energies is not considerable.

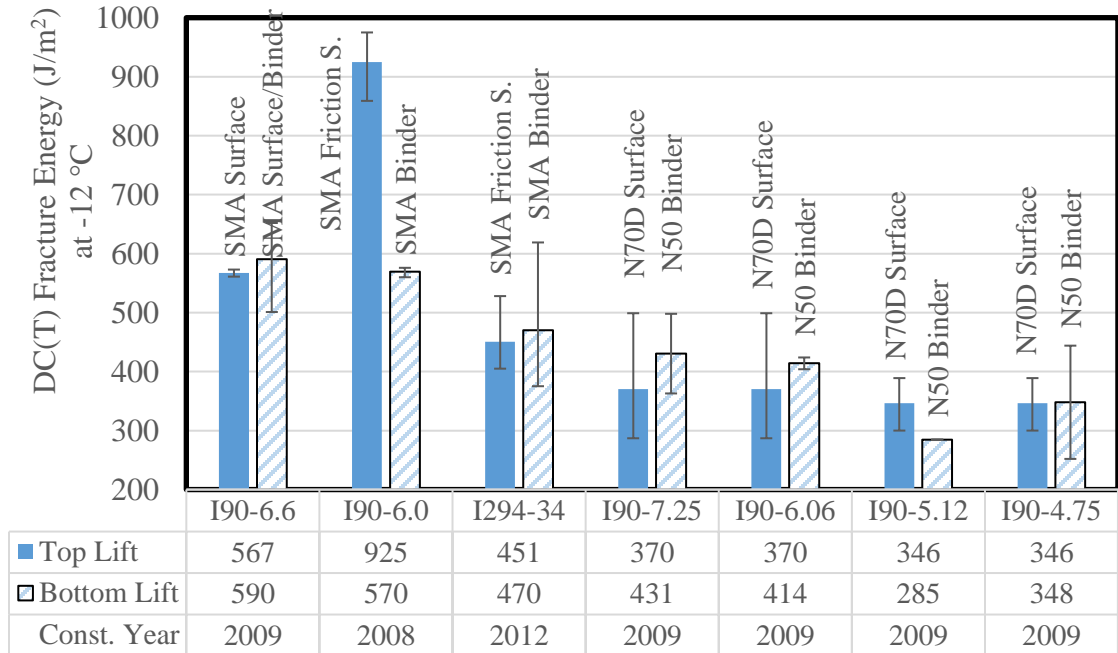


Figure 2-13. Comparing fracture energies for top and bottom lifts of the field cores

2.4.2. Repeatability of the Cracking Tests

Table 2-4 presents the COV and standard deviation (STD) of different cracking tests for different mixture types tested in this study. As mentioned before, the repeatability of a performance test should be a key consideration in selecting an appropriate test for specification development. As shown in the table, the DC(T) test has the lowest COV for all tests across each mix category. Note that the I-FIT and IDEAL-CT tests were not performed on the shoulder binder lift mixes so that enough materials could be retained to enable Hamburg testing.

Table 2-4. Variability of the cracking performance test results for field cores

Cracking Test:	DC(T) at -12 °C		FI (4 Reps)		CT	
Mix. Type	COV	STD	COV	STD	COV	STD
SMA F. S.	9.9	70	48.7	2.9	7.9	17
SMA S.	6.1	27	17.8	1.0	10.9	18
SMA B.	14.2	73	25.3	2.6	27.8	57
Shoulder S.	13.7	52	38.5	1.4	20	11
Shoulder B.	16.2	62	NA	NA	NA	NA

2.4.3. Hamburg Testing Results

Based on the Hamburg test specification and testing fixtures, 62 mm thickness samples are needed. In order to fit the samples into the Hamburg fixtures, concrete slices were fabricated at a thickness of about 12 mm and placed in the fixtures as vertical shims (see Figure 2-14). Figure 2-15 presents the rut depths measured in the Hamburg test on asphalt cores. The rut depth of the first six mixtures (SMAs) were recorded at 20,000 passes while for shoulder mixtures, 15,000 wheel passes were used. As already seen in the plant-produced mixtures in Chapter 3, rutting is not a concern for SMAs. The only SMA mix with a rut depth higher than 6 mm was I90-6.6 which had the lowest amount of recycled materials (ABR=13.9%). Similarly, the I90-5.12 section, which had the lowest ABR among the three tested shoulder mixtures with an ABR of 24.4%, recorded the highest rut depth (8.0 mm). It is also worth mentioning that the testing samples obtained from the field cores for the rest of the shoulder mixtures, including I90-7.25, I90-10E, and I90-10W, were used for the cracking tests, as cracking was the main distress on the shoulders. The relatively low rut levels on field cores are probably due to the age-

hardening of the mixes, but also indicate the proper performance characteristics in Tollway mixtures, such as resistance to stripping or aggregate degradation.



Figure 2-14. Hamburg samples with 12mm PCC shims placed below asphalt specimens

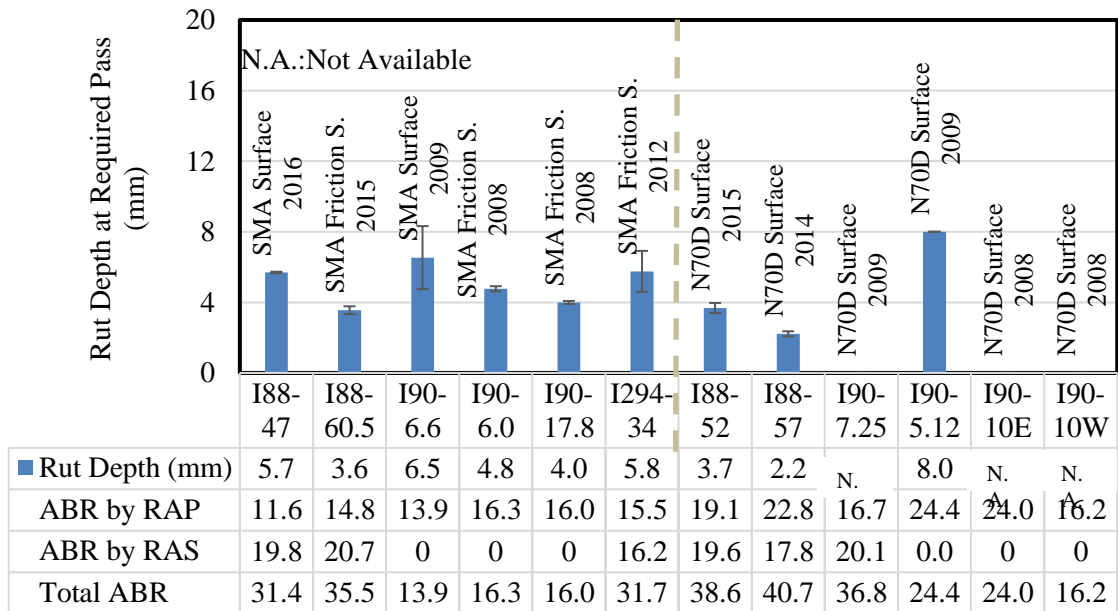


Figure 2-15. Hamburg testing results for the top lift of the field cores

Figure 2-16 compares the rut depths from testing of surface vs. top binder course lifts in the Hamburg on cores. For the SMA binders and shoulder binders the required number of Hamburg passes is 20,000 and 10,000, respectively. The bottom lift of the I90-6.6 section, which used the same mix as the top lift, did not perform well in the Hamburg test at 50 °C. It is not clear why this mix experienced poor scoring in the Hamburg.

However, due to its position in the pavement (shoulder, binder), rutting is not expected to be a concern.

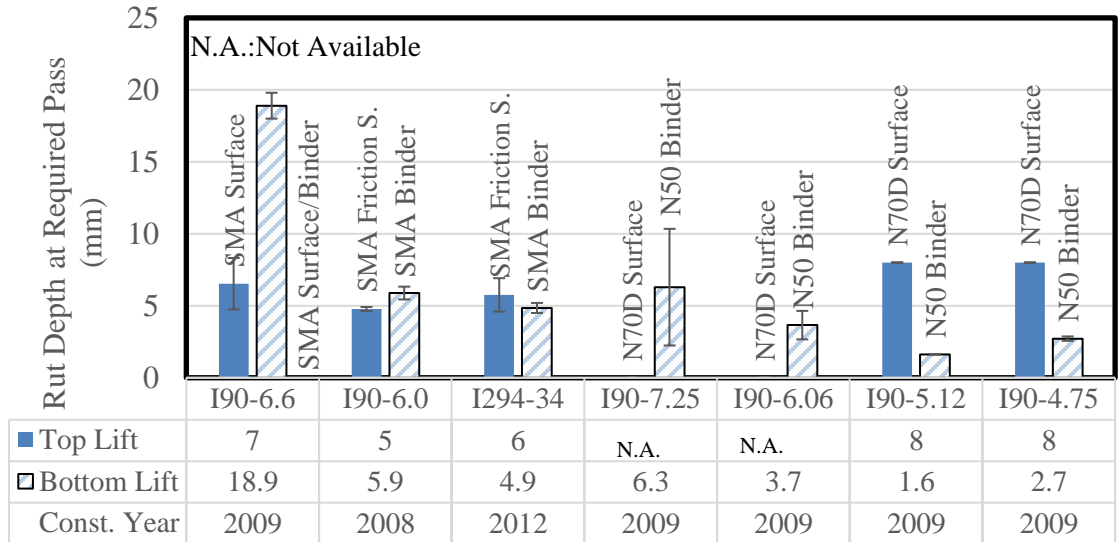


Figure 2-16. Comparing the rut depths for top and bottom lifts of the field cores

The results obtained from field cores were instrumental in validating and calibrating DC(T) and Hamburg thresholds in the Tollway asphalt performance specification, as described in Chapter 4.

2.5. Summary of Field Observations

In this two-day site visit, the MU team observed numerous sections both on mainline segments and shoulders. These sections were mainly paved using the asphalt mixtures that were previously tested through different projects. The most common distress observed on the surface of the roads was transverse cracking which calls for extra attention to selecting the appropriate cracking test and then setting the thresholds for the test output. A summary of the field observations is categorized based on the projects as follows.

Sections in Performance-Based Specification Project (2018 mixtures)

- Mixtures used in the 2018 study on the mainline did not have considerable transverse cracking. That being said, some reflective cracks were observed after the record-cold winter of 2018-2019.
- Mix 1845 which was used on the shoulder (Lehigh rubber mix) has begun to show thermal cracking after the 2018-2019 harsh winter.

Sections in Rubber Study

- All the mainline sections constructed in 2016 were performing very well (only a few, isolated thermal cracks were observed).
- The control sections (SBS) in-between the rubber sections (and west of them) exhibited more thermal cracks as compared to the GTR mainline sections.
- The dense-graded mix shoulders had frequent cracking.
- The SMA mix used on the shoulder (Evoflex RMA) showed extensive transverse cracking.

Sections in SMA Study

- The 2012 I-294 section now has many visible distresses, and is starting to ride rough. It should be mentioned that this mix has been placed on jointed concrete pavement.
- Heavy % trucks were observed.

Sections in RAS Study (Shoulders)

- The shoulders with RAP and RAS had many cracks, thermal and block.

Chapter 3

SAMPLING AND TESTING THE PLANT-PRODUCED MIXTURES

3.1. Overview

The selected plant-produced asphalt mixtures in this research were sampled per AASHTO T-168-03 across six asphalt plants in the Chicago Area, as shown in Figure 3-1. Mixtures were sampled into uncoated, 5-gallon steel pails with tight-fitting lids. A representative from the Missouri Asphalt Pavement and Innovation Lab (MAPIL) of the University of Missouri-Columbia conducted all sampling with the assistance of local quality control (QC) lab staff. At the time of sampling, daily G_{mm} , and asphalt plant 6-min reports and cumulative mix tons were recorded in most cases. Selected materials were temporarily stored at the Tollway maintenance yard in Naperville, IL (Figure 3-2) for approximately one month before collection by MAPIL researchers.



Figure 3-1. Sampling plant produced mixtures from different asphalt plants. a) Mix 1836, Wm Ch; b) Mix 1845, Curran, and; c) Mix 1807, Geneva

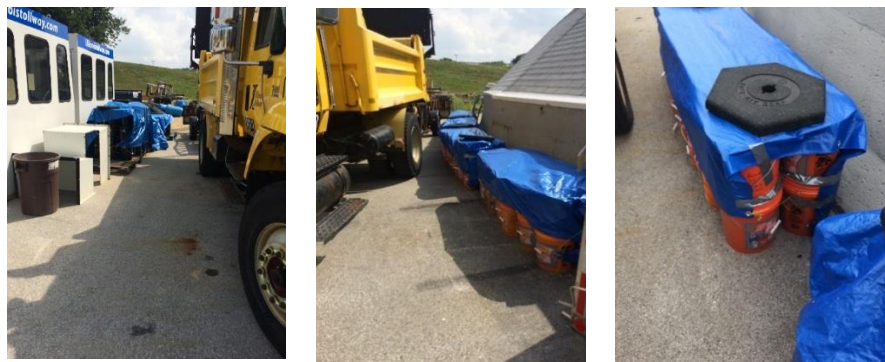


Figure 3-2. Temporarily storage of samples at Tollway maintenance yard

Table 3-1 provides details regarding the asphalt mixtures sampled from Chicago area plants producing Tollway asphalt mixtures in the summer of 2018. In total, six Illinois Tollway SMAs and eight dense graded mixtures were sampled from different asphalt plants in northern Illinois. Table 3-2 summarizes key asphalt mixture properties for each sampled section.

Table 3-1. Mixture sampling details

Date Sampled	No. of	Mix Type/Usage
9-Jul	10	N70 9.5mm Surface
9-Jul	10	N50 19.0mm Binder - 3.0 voids
9-Jul	10	N80 12.5 mm SMA Surface
9-Jul	10	N80 12.5 mm SMA Friction Surface
13-Jul	10	N80 12.5 mm SMA Surface
13-Jul	10	N80 12.5 mm SMA Friction Surface
16-Jul	10	N50 19.0mm Binder - 3.0 voids
16-Jul	10	N50 4.75mm IL-4.75
18-Jul	10	N70D 9.5mm Surface
18-Jul	10	N50 4.75mm IL-4.75
18-Jul	10	N50 4.75mm IL-4.75
18-Jul	10	N80 12.5 mm SMA Friction Surface
2-Aug	10	N80 12.5 mm SMA Friction Surface
12-Sep	10	N70E 9.5mm Surface

For the sake of simplicity, the common “90WMA” prefix in the Tollway Mix ID was omitted, and a shorter, four-digit sample ID was used throughout the report. The first four

mixtures (1844, 1835, 1824, and 1845) are friction-surface-type SMAs, denoted as ‘Friction S.’ (used on highway curves and ramps), and the last two SMA mixtures (1836 and 1840) are regular SMA surfaces (used in lower trafficked, non-curved or tangent road alignments). The next three mixtures (1829, 1828, and 1823) are finer HMA mixtures (IL-4.75), which are used on the mainline below SMAs to promote pavement smoothness. Some engineers also believe that the IL-4.75 helps to reduce the rate of reflective cracking emanating upward from underlying Portland cement concrete joints and cracks. The three mixtures labeled as 1818, 1834, and 1826 represent surface shoulder materials (Shoulder S.). Finally, the last two sample IDs (1803 and 1807) represent shoulder binders, which appear below shoulder surface mixtures on the Tollway. As shown in the table, the design number of gyrations (N_{Design}) of all SMAs is 80, while the N_{Design} for shoulder surface mixtures is 70. IL-4.75 and shoulder binder mixtures used an N_{Design} level of 50 gyrations.

Table 3-2 also shows the binder system and reported modifiers used in each mix. Among the mixtures investigated, four of them, including 1844, 1824, 1836, and 1823 involved SBS-polymer-modified binder systems. Five mixtures (1835, 1845, 1840, 1829, and 1828) involved ground tire rubber (GTR), either by a terminal-blend wet process or by dry process. The 1835 mix utilized a relatively soft, neat binder (Superpave PG 46-34) combined with 10% engineered crumb rubber (ECR) by weight of binder (a dry-process GTR system). This mix also had the highest amount of recycled materials in any of the SMAs investigated (41.2% ABR), including 25.1% ABR by RAP and 16.1% ABR by RAS. Similar to 1835, the 1845 mix also used PG 46-34 neat binder, which was later modified by 10.5% rubber by weight of the binder. The neat binder used in the 1840 mix

was PG 58-28. This binder in this mix possessed 12.0% GTR, added to the binder via a terminal-blend, wet process. The binder used in dense graded shoulder mixtures involved neat (unmodified) Superpave binders.

The plan grade of binder used in Tollway SMAs and IL-4.75s is PG 76-22. This implies that any extracted binder samples, which may include both a modifier (polymer or rubber), recycled binder components (usually RAP and RAS), and possibly rejuvenators and/or warm-mix and/or liquid antistripping additives, are expected to pass the performance grading criteria at 76°C for the PG high temperature (PGHT) and -22°C for the PG low temperature (PGLT). As for the shoulder mixtures, the plan grade is PG 64-22. The less stringent requirement on the PGHT of the shoulder plan grade is due to the lower traffic load that the shoulders experience throughout their service life. However, the plan PGLT requirement is the same for shoulder and mainline mixtures, as they experience the same low-temperature environmental conditions. Note also that the binder course mixtures on both shoulder and mainline sections undergo less critical low temperature and high temperature events, as they are thermally insulated and protected by the overlying surface mix. This should be considered when establishing PRS thresholds.

Aggregate gradations for the mixtures investigated are shown in Figure 3-3. It can be seen that the gradation of all SMAs investigated are quite similar, possessing a nominal maximum aggregate size (NMAS) of 12.5 mm. Likewise, the gradation of dense-graded mixtures within the groups, including IL-4.75, shoulder surface, and shoulder binder, are quite similar, within 4.5, 9.5, and 19 mm nominal maximum aggregate size (NMAS) groups, respectively. Despite the similarities in the aggregate gradations, it should be noted that the aggregate type used by each asphalt contractor can and does vary in the

Chicagoland area. Therefore, the overall characteristics of the aggregate skeleton in each mix investigated herein should be viewed as unique.

Table 3-2. Details of mixture ingredients

Mix. ID	Mix Type	Base Binder	Plan Grade	ABR by RAP	ABR by RAS	NMAS
1844	N80 SMA Friction S.	SBS 70-28	76-22	10.8	16.0	12.5
1835	N80 SMA Friction S.	46-34 +10%ECR	76-22	25.1	16.1	12.5
1824	N80 SMA Friction S.	SBS 64-34	76-22	20.4	16.7	12.5
1845	N80 SMA Friction S.	46-34 +10.5%Lehigh	76-22	23.9	15.4	12.5
1836	N80 SMA Surface	SBS 64-34	76-22	16.2	16.3	12.5
1840	N80 SMA Surface	58-28 +12%GTR	76-22	15.9	9.8	12.5
1829	N50 Dense IL-4.75	58-28 +12%GTR	76-22	17.8	9.3	4.75
1828	N50 Dense IL-4.75	46-34 +10%ECR	76-22	35.3	9.2	4.75
1823	N50 Dense IL-4.75	SBS 64-34	76-22	24.1	14.2	4.75
1818	N70 Dense Shoulder S.	64-22	64-22	20.4	0.0	9.5
1834	N70 Dense Shoulder S.	58-28	64-22	20.0	0.0	9.5
1826	N70 Dense Shoulder S.	46-34	64-22	27.6	18.1	9.5
1807	N50 Dense Shoulder Binder	46-34	64-22	34.4	14.0	19.0
1803	N50 Dense Shoulder Binder	58-28	64-22	26.5	16.6	19.0

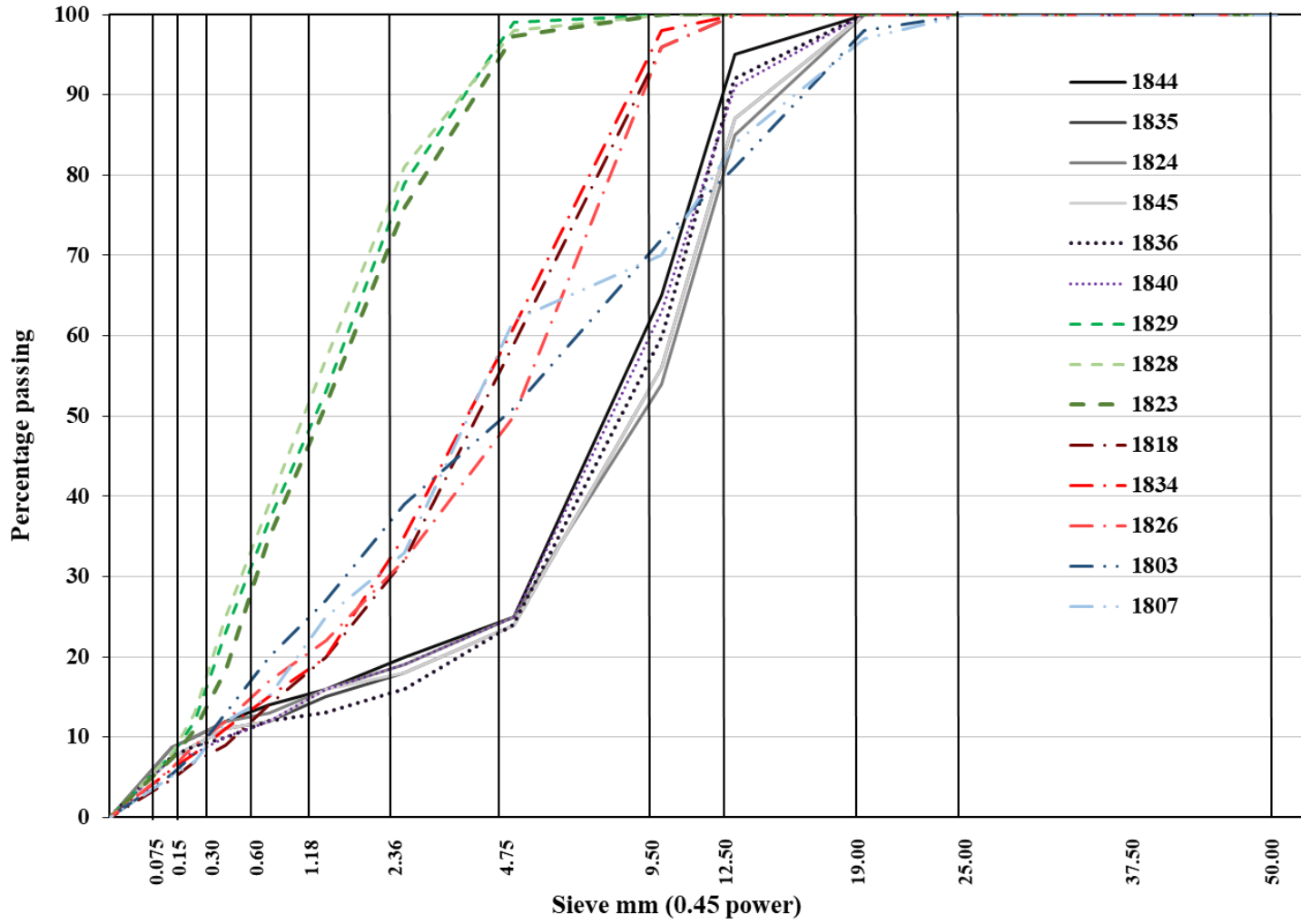


Figure 3-3. Aggregate gradations for the investigated plant-produced mixtures

Table 3-3 presents details regarding the sections that were paved in 2018. As indicated in Table 2-3 and shown on Figure 3-4, mixtures 1844 and 1834 were used to pave the mainline and shoulder, respectively, on route I-355 in starting from mile post (MP) 12 to 22. Mix1826 was used to pave the I-355 shoulder from MP 22 to 30. All other mixtures were used on I-88 between the indicated mile posts. The direction of the route is indicated in the ‘Mile Post’ column whenever the mixture appeared only in one direction.

Table 3-3. Location of the paved section using the studied mixtures

Mix. ID	Mix Type	Route	Mile Post	Location	Traffic (ADT, and % Commercial Vehicles-
1844	SMA Friction	I-355	12-22	Mainline	65,000 – 10% CV
1835	SMA Friction	I-88	93-103	Mainline	16,900 – 25% CV
1824	SMA Friction	I-88	EB 76-91	Mainline	10,600 – 25% CV
1845	SMA Friction	I-88	WB-105	Shoulder	16,900 – 25% CV
1836	SMA Surface	I-88	WB 76-91	Mainline	10,600 – 25% CV
1840	SMA Surface	I-88	103-113	Mainline	16,900 – 25% CV
1829	IL-4.75	I-88	103-113	Mainline	16,900 – 25% CV
1828	IL-4.75	I-88	92-103	Mainline	16,900 – 25% CV
1823	IL-4.75	I-88	WB 79-91	Mainline	10,600 – 25% CV
1818	Shoulder S.	I-88	EB 76-91	Shoulder	N.A.
1834	Shoulder S.	I-355	12-22	Shoulder	N.A.
1826	Shoulder S.	I-355	22-30	Shoulder	N.A.
1807	Shoulder	I-88	103-113	Shoulder	N.A.
1803	Shoulder	I-88	92-103	Shoulder	N.A.

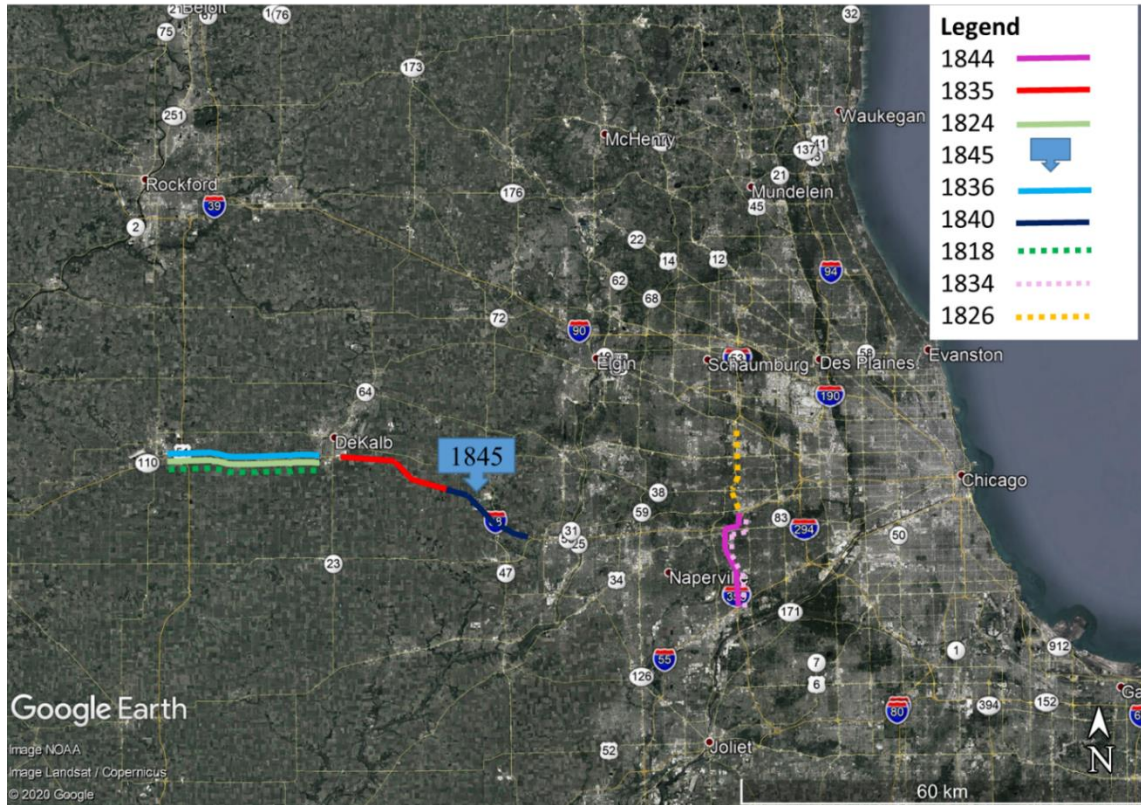


Figure 3-4. Location of paved roads using the sampled mixtures on Google Earth

3.2. Sample and Fabrication

The sampled plant-produced mixtures were brought back to MAPIL in 5-gallon steel pails. The plastic handles were removed and then pails were placed in a forced draft oven to heat the asphalt mixture to a workable consistency (~100 °C). The heated mixture was then reduced to the gyratory sample mass following the quartering method in AASHTO R47 (see Figure 3-5). After reduction, two 1500 gr sets were collected in order to measure the maximum specific gravity (G_{mm}) of the mixtures as per AASHTO T 209 (see Figure 3-6). Although the G_{mm} was mentioned on the job mix formula (JMF) of each mix, it was attempted to verify it as the G_{mm} at the time of production might vary from the one on JMF. Figure 3-7 shows three different G_{mm} values obtained for each mixture. The blue bars are the G_{mm} values measured at MAPIL after reheating the buckets and

collecting the G_{mm} samples. The orange bars are the G_{mm} measured at the night of mix production in the asphalt plant for quality control purposes, and the gray bars are the G_{mm} mentioned on the JMF sheets. It is also worth mentioning that the MAPIL measured values were used to measure the air void content of the gyratory compacted specimens. In order to avoid segregation during the sample production process, the heated asphalt mixture in the pans was transferred to a chute, as shown in Figure 3-8, and then was poured into the mold. A Pine GB2 Superpave gyratory compactor was used to compact the reheated samples and make cylindrical specimens.



Figure 3-5. Splitting the bucket of mixture as per AASHTO R47



Figure 3-6. Preparing samples for theoretical maximum specific gravity (G_{mm}) testing

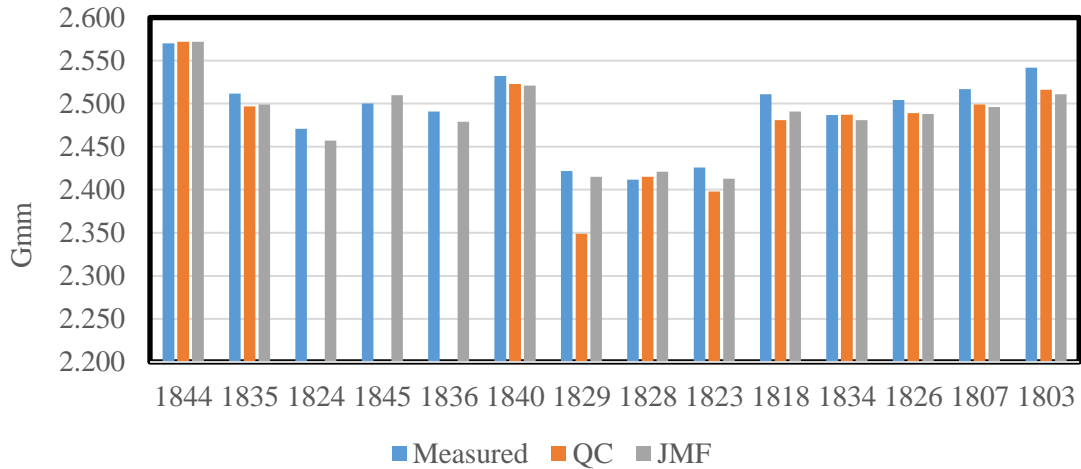


Figure 3-7. Comparing different G_{mm} values for the studied mixtures (Measured = Test performed in MAPIL; QC = Measured by quality control crew; JMF = job mix formula)



Figure 3-8. Transferring the heated mix to the mold

After splitting to desired mass, the asphalt mixture was heated to compaction temperature (155 and 143 °C for modified and unmodified mixes, respectively). All SMA testing samples were compacted to 6.0 % air voids while the target air void for dense graded mixtures was 7.0 %. For DC(T) and I-FIT samples, air voids were measured on the 50

mm slices before notching and coring for the DCT specimens, and before cutting the slice in half and notching in the case of I-FIT specimens. For Hamburg specimens, the original gyratory specimen (62 mm in height) was used for Gmb testing prior to cutting the flat face on one side. The TSR and IDEAL-CT tests were performed on 95 mm gyratory compacted samples.

3.3. Testing Results for Plant-Produced Mixtures

3.3.1. DC(T) Testing Results

The DC(T) test was developed to characterize the fracture behavior of asphalt concrete mixtures at low temperatures. The testing temperature is 10°C warmer than the PG low temperature grade of the mixture, per (ASTM D7313-13). Figure 3-9 shows the DC(T) fracture (G_f) testing results at -12 °C, using samples fabricated at MAPIL. The error bars provide the range of the values obtained for the three replicates tested in DC(T) fracture. In addition to the bars shown in the figure, the table attached to the figure provides the mix ID, the average fracture energy and also the ABR of each mix. Also, the type of the mix and the binder system are shown above each bar. The cracking resistance of the SMA friction surface (F. S.) mixes was expected to be the highest, followed by SMA surface mixes. Additionally, as the shoulder surface mixtures experience the same environmental conditions, they should ideally be designed with relatively high cracking resistance. The IL-4.75 and shoulder binder mixtures were expected to have lower cracking resistance as they are used in sublayers of the pavement. As shown in Figure 3-9, the expectations for relative crack resistance were found to be in close agreement with the measured DC(T) fracture energy results. This finding was among the early

indications that the DC(T) test is a viable candidate for the control of cracking in Tollway asphalt mixtures, at least from the standpoint of mixture performance.

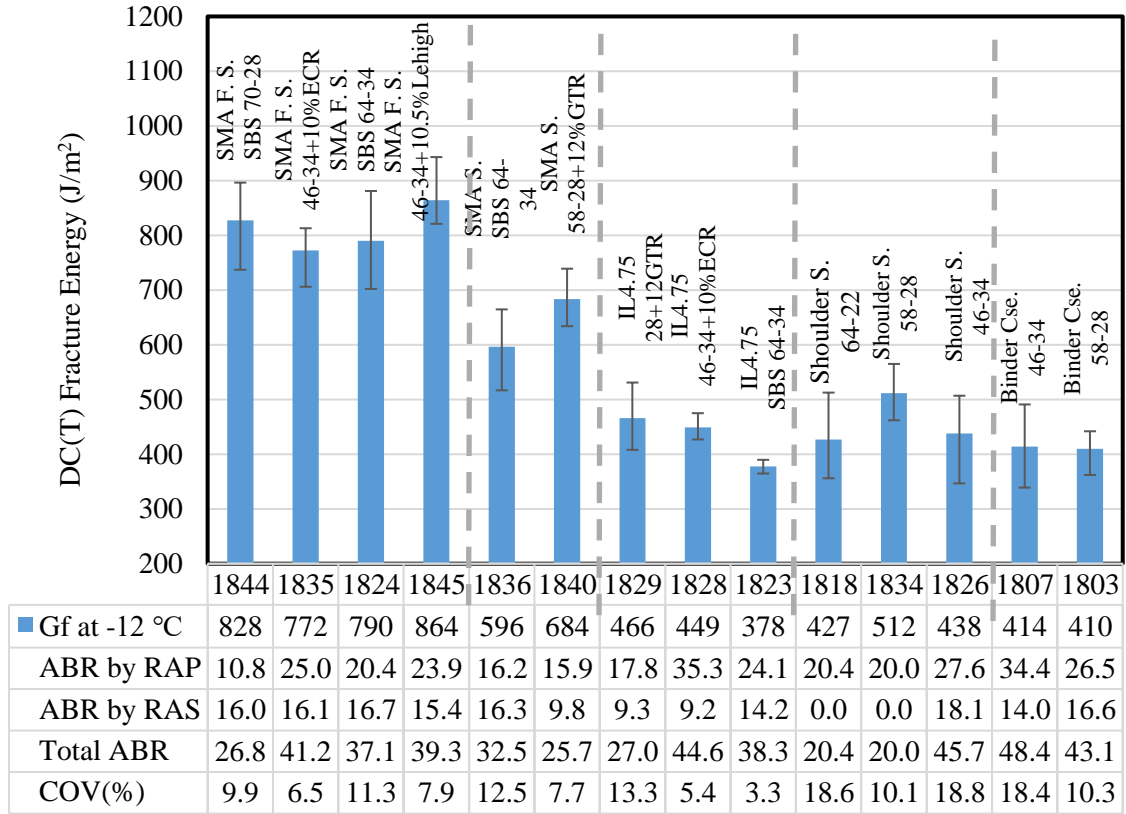


Figure 3-9. DC(T) fracture energy at -12 °C using MAPIL samples

As shown in the figure, all the SMA friction surface type mixtures were found to pass the 750 J/m² fracture energy threshold, which was specified by the Tollway in prior completion of this study (for instance, in the 2019 specification). The difference between the highest and lowest recorded fracture energy is less than 100 J/m² which implies that the resistance of the SMA Friction surface with respect to low temperature cracking is expected to be similar between sections. On the other hand, the SMA surface mixtures had significantly lower fracture energy than the SMA friction surface mixtures. The 1836 mix recorded the lowest fracture energy (596.5 J/m²) and similar to 1840 which had 684

J/m², the sampled production mix did not pass the formerly practiced 700 J/m² limit for SMA surface mixtures in design. This may be possibly attributed to the effects of aging during sample storage (3 months on average) followed by reheating of the mix. More observations from the results are summarized as follows:

- The base binder system used in the 1824 and 1836 mixtures is the same (SBS 64-34). Although the 1824 mixture had higher amount of ABR, it has an additional 270 J/m² of fracture energy. This comparison reveals the importance of aggregate quality and its significant role in low temperature cracking resistance of the mix.
- Although the 1840 mix had the lowest amount of recycling, it was not found to pass the existing Tollway fracture energy criteria. Using a softer base binder on the low temperature side, adding a rejuvenator (recycling agent), and/or utilizing higher quality aggregate are strategies that could be used in the future to boost the fracture energy in this mixture.
- Despite the high ABR (44.6%) incorporated in 1828 mix, using a softer binder system along with engineered crumb rubber (ECR) resulted in a relatively high fracture energy. In IL-4.75 mixtures, the 1823 mix with an SBS 64-34 binder system exhibited the lowest fracture energy.
- In the shoulder surface mix group, the 1826 mix benefited from the soft binder system and possessed a DC(T) fracture energy of 438 J/m² despite the high recycle content (ABR=45.7 %). Compared to 1818, the 1834 mix with a softer binder and similar recycle content performed notably better in terms of low temperature cracking. The softer binder system used in 1834 mix likely

contributed to the additional 75 J/m² of fracture energy as compared to mix 1818. Differences in aggregate quality might also contribute to the difference in DC(T) fracture energy of these two mixtures.

- The shoulder binder mixtures including mix 1807 and 1803 yielded similar DC(T) fracture energy values, close to the 400 J/m² level specified by the Tollway at the time of their design. In the future, incorporating GTR could assist in raising the fracture energy of these mixtures, as was the case for IL-4.75s.

Figure 3-10 compares the DC(T) fracture energy measured at MAPIL using plant-produced lab compacted mixtures with the ones reported on the JMF. As shown, in most of the cases (all except 1844) the measured DC(T) energy at MAPIL is lower than the reported fracture energy. Storage and reheating of the plant-produced samples might have resulted in additional aging of the mixtures, which often leads to lower DC(T) fracture energy values (Buttlar et al., 2019).

Figure 3-11 presents a contour map that provides the pavement temperature at the surface produced by MAPIL researchers using LTPP bind software at a level of 98 % reliability. This temperature is used in order to determine the required PGLT for the binder. As shown in the figure, the required PGLT of the binder in the state of Illinois is in the range of -22 to -27 °C. The PGLT of -22 °C is mainly required in the southern part of Illinois while the -27 °C limit is suitable for the very northern part of the state. Therefore, the PGLT of plan grade of the binder in the upper parts of Illinois should be lower than -22 °C to reach 98 % reliability. As per ASTM D-7313, the DC(T) test is performed at 10 °C warmer than the binder grade. The Illinois Tollway currently uses a -22 °C plan low

temperature grade, and thus testing at -12 °C used in the DC(T). Thus, the relatively high DC(T) thresholds specified by the Illinois Tollway reflect both the high project criticality of Tollway road surfaces, and also the fact that a slight adjustment has been factored in the specification based on the fact that Northern Illinois is somewhat colder than the assumed -22 °C PGLT used in the asphalt binder plan grades.

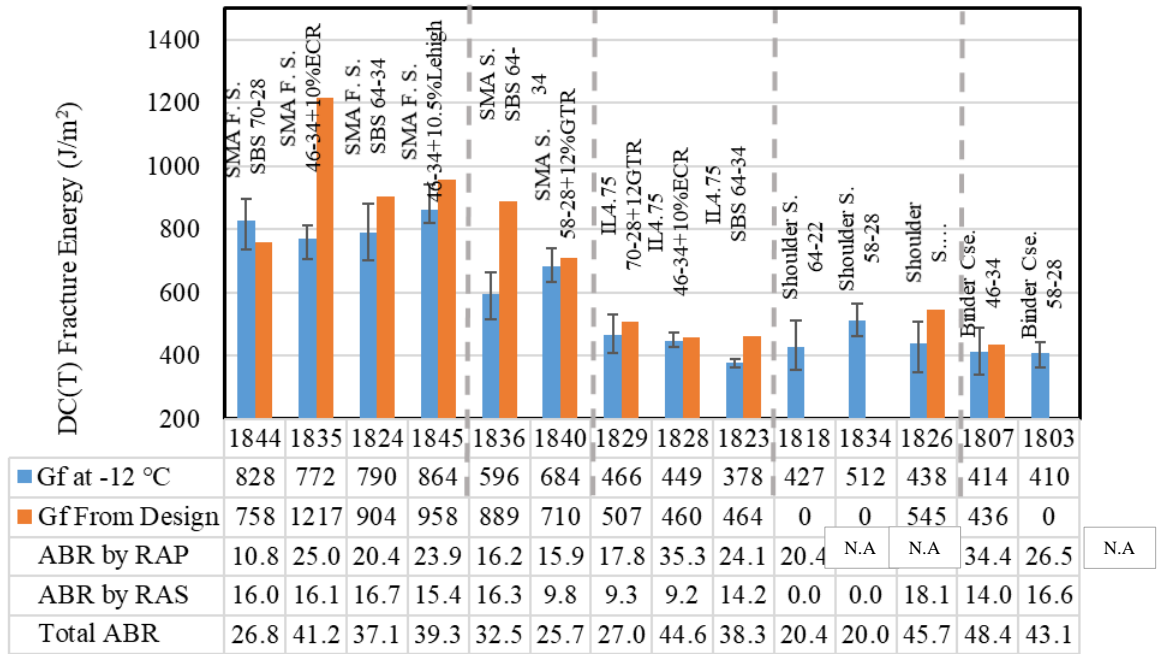


Figure 3-10. Comparing DC(T) fracture energy at -12 °C: current study vs. JMF

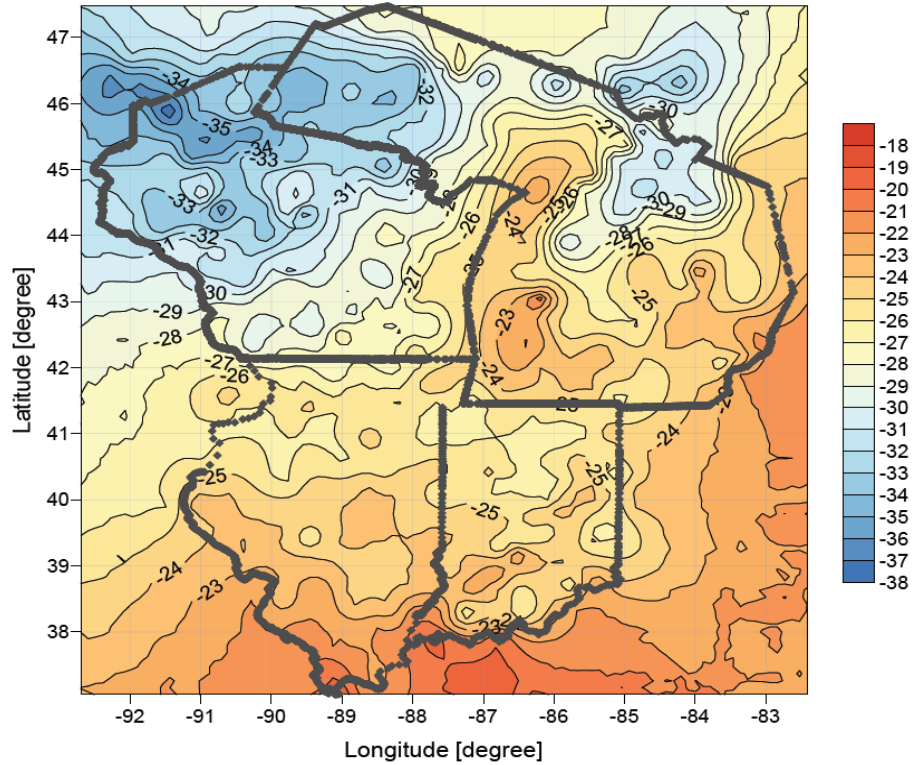


Figure 3-11. Pavement temperature at the surface in the northern part of the US (reliability=98%)

As testing temperature drops, asphalt binder becomes stiffer and as a result, the asphalt sample exhibits more brittle behavior and reduced fracture energy. Therefore, lower fracture energies are expected at $-18\text{ }^{\circ}\text{C}$ compared to $-12\text{ }^{\circ}\text{C}$. As shown in Figure 3-12, the DC(T) fracture energy of all the mixtures at $-18\text{ }^{\circ}\text{C}$ are indeed lower than those obtained at $-12\text{ }^{\circ}\text{C}$. Experiencing a drop of about 260 J/m^2 , the 1824, which is an SBS modified mix, showed the highest temperature sensitivity in the SMA friction surface category. On the other hand, the 1835 mix, which is modified with a dry process Engineered Crumb Rubber (ECR-type GTR) showed almost the same fracture energy at $-18\text{ }^{\circ}\text{C}$ as compared to $-12\text{ }^{\circ}\text{C}$. If the same DC(T) criteria were applied by Tollway at $-18\text{ }^{\circ}\text{C}$, only the 1835 would pass. The 1840 mix in the SMA surface group experienced a significant drop in

fracture energy after testing at -18 °C, which indicates that this mix may be highly temperature sensitive at low temperatures. Although the IL-4.75 and shoulder binder mixtures will not experience extreme low temperature events such as surface mixtures do, the DC(T) test at -18 °C was conducted nevertheless to evaluate their temperature sensitivity. Only the 1803 mix, which used a PG 58-28 base binder showed high sensitivity, where the DC(T) fracture dropped from 410 to 290 J/m² (a 28 % reduction in fracture energy).

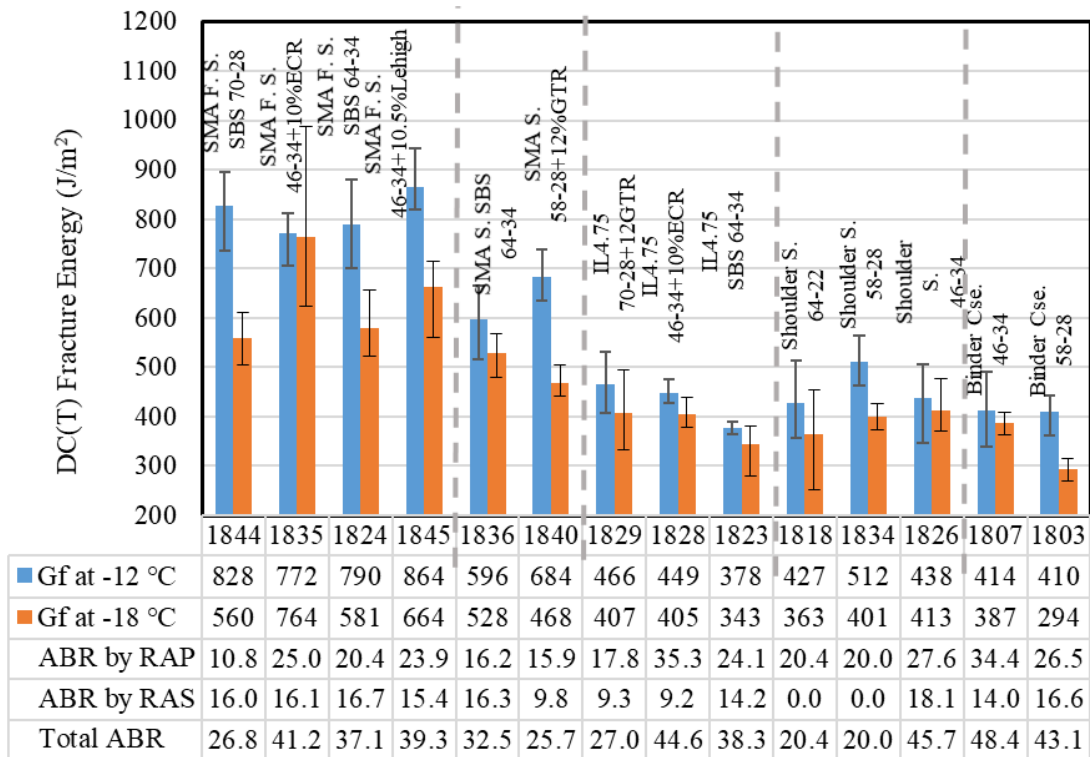


Figure 3-12. Comparing DC(T) fracture energy at -12 and -18 °C

3.3.2. HWTT Testing Results

The two most common WLT test devices are the Hamburg Wheel Tracking Test (HWTT) and the Asphalt Pavement Analyzer (APA) (formerly known as Georgia-loaded wheel tester). The HWTT is performed in accordance to the AASHTO T324 standard.

The vertical deformation of the specimen is recorded along with the number of wheel passes. In addition, conducting the test under water provides the opportunity to measure stripping potential. To this end, the concept of a stripping inflection point (SIP) has been defined and is currently used by state agencies in California, Wisconsin, Iowa, and Missouri. SIP is reported as the number of passes needed to reach the point at which the rutting vs. wheel pass curve displays a sudden increase in rut depth (inflection point in the curve). In this study, the Iowa method has been implemented to calculate the SIP as follows:

- Fit a 6th degree polynomial curve to the rut depth vs. wheel pass curve
- Take the first derivative of the fitted curve
- Determine the stripping line using the tangent at the point nearest to the end of the test where the minimum of the first derivative of the fitted curve occurs
- Determine the creep line using the tangent at the point where the second derivative of the fitted curve equals zero
- Intersect the creep and stripping lines - the wheel pass at which these two lines intersect is taken as the SIP

The Hamburg wheel tracking test was carried out in order to evaluate the rutting susceptibility of the mixtures. As mentioned before, the required number of wheel passes for Tollway SMAs is 20,000 and for shoulder surface mixtures is 15,000. Also, based on the current version of the Tollway asphalt mixture specification, the allowable rut depth at the required number of passes for SMA mixtures is 6 mm and 12.5 mm for shoulder

mixtures. The measured rut depth under the Hamburg test along with the requirements for each mixture type is shown in Figure 3-13. From the figure, clearly Tollway SMAs have low rutting levels, as the maximum rut depth recorded was 3.3 mm in mix 1835. This means that the studied SMAs benefit from a robust aggregate structure and binder system, which is consistent with the observed resistance to permanent deformation of similar mixtures placed in the field over the past decade (see section 6).

As for the IL-4.75 mixtures, the 1828 mix recorded the highest rut depth (12.2 mm) under 15,000 wheel passes required for this category (see Figure 3-14). This mix was the only mix that could not meet the rutting requirements among all the Tollway mixtures.

However, it is worth mentioning that the IL-4.75 mixtures are not placed on the surface of the pavement, and thus, they do not experience the same environmental and traffic conditions as the SMA mixtures. The lower number of wheel passes required for this category may reflect the fact that these mixtures do not undergo heavy traffic stresses.

However, choosing a more appropriate testing temperature and/or adjusting the number of wheel passes to more directly account for the temperature difference between the surface and the binder course depth was addressed in this study, as documented later in this report. In addition, setting less stringent (more appropriate) Hamburg requirements for this category would result in more economic and/or allow more crack resistant mixtures to be designed in a simpler fashion.

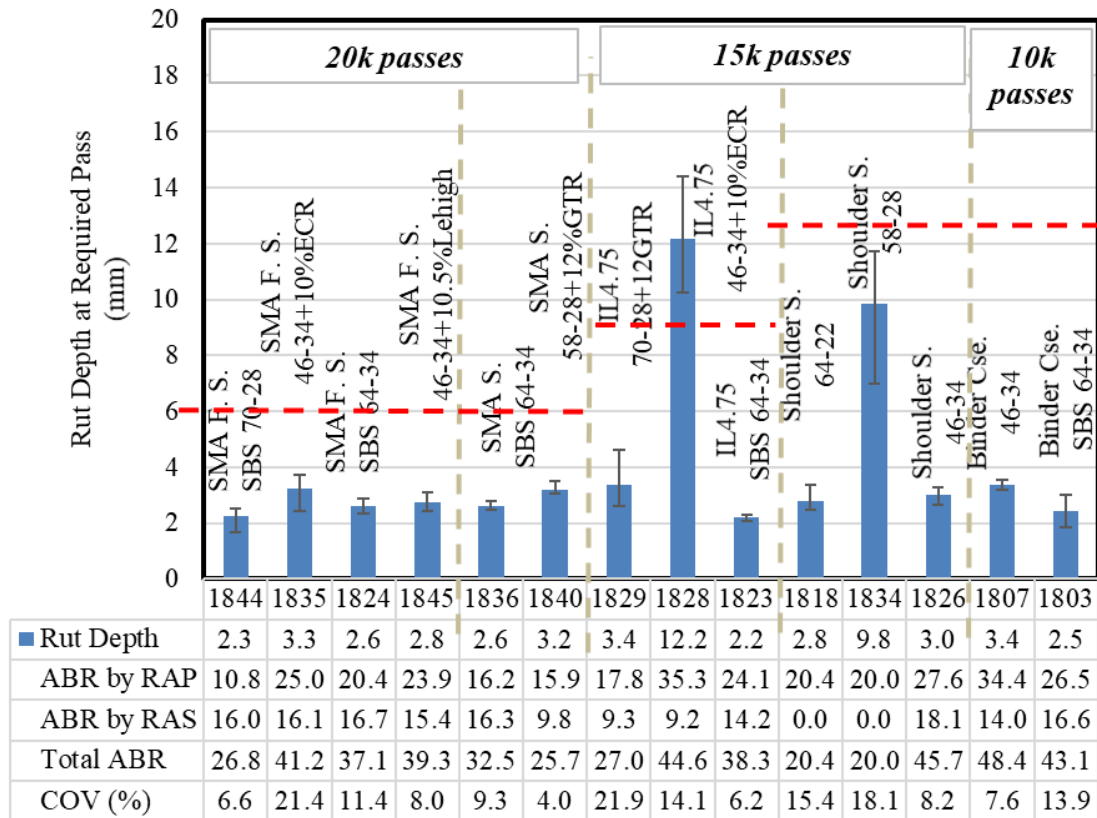


Figure 3-13. Hamburg testing results at required number of passes at 50 °C

In the shoulder surface mix category, the 1818 and 1826 shoulder mixtures possessed low Hamburg rut depths as compared to the allowable. However, the 1834 mix (see Figure 3-14), which used a softer binder system as compared to 1818, had the highest rut depth (9.8 mm) among the tested mixtures. This shoulder mix is not designed for heavy traffic loads, and the higher Hamburg rut depth opens the door to obtain higher fracture energy due to the softer binder grade while employing a relatively economical mix design.

Similar to the IL-4.75s, the number of required load pass is lower for shoulder binders due to the lower stress which is induced in the sublayers of the pavement. The 1807 mix had a slightly higher rut depth which is attributed to the softer binder as compared to the 1803 mix. As the maximum rut depth allowed for this category is the conventional 12.5

mm, in the future, these mixtures could benefit from a softer binder system – especially if new or more stringent fracture requirements are introduced for shoulder mixes as discussed later in this report.

As discussed earlier, the moisture damage potential of the mix can be evaluated through SIP determination. Higher SIP values indicate that the mix can tolerate more wheel passes prior to stripping. A minimum SIP threshold is thus specified for different mix types. Based on the Iowa method, a mix is first identified as potentially stripping when the ratio of the stripping line slope to the creep line slope exceeds 2.0. To illustrate the calculation of SIP, examples for four mixtures are provided in Figure 3-15.

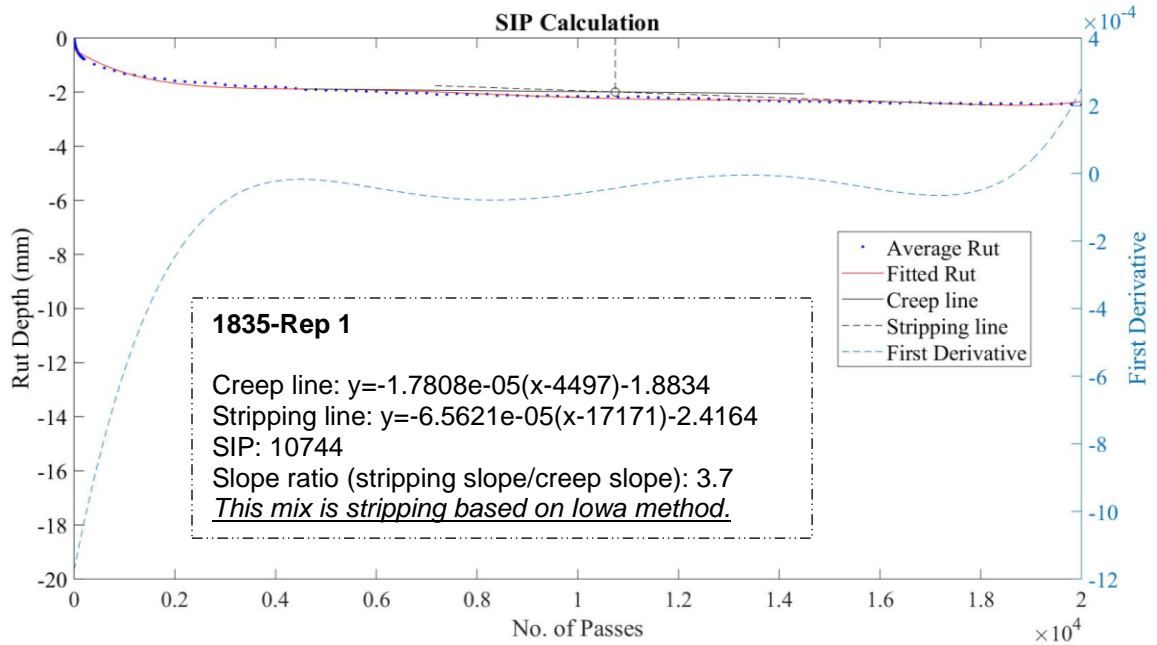
The first example is shown in Figure 3-15-a, which represents the first replicate of the 1835 mix. Recall that in Figure 3-13, the maximum rut depth recorded for this mix was relatively low, at 3.3 mm. However, as Figure 3-15-a shows, the slope of the creep line is very low, such that the slope ratio did in fact exceed 2.0. Thus, the Iowa method determines this mix to have stripping potential, and the SIP was subsequently recorded to occur at 10,744 passes. However, the visual inspection did not show any de-bonding between aggregate and binder, which is generally expected in the case of actual stripping. This example implies that the mathematical process used in the SIP calculation might lead to misleading results, especially in cases where the deformation rate at the end of the densification phase of plastic deformation (i.e., the creep slope) is very low. This makes the denominator of the slope ratio very small and results in relatively higher slope ratios even if the stripping phase followed by densification phase is not problematic (i.e. stripping slope is relatively low). Figure 3-15-b (1845-Rep 1) presents another example of what appears to be an incorrect indication of a stripping-prone mix. However, the 1845

mix did not show visible stripping, where the rut depth recorded at the end of 20,000 passes was also very small (just over 2 mm). In addition to the visual inspection, performing other moisture damage tests such as AASHTO T-283 and the Texas boiling water test were used to further evaluate the Iowa method based SIP parameter. Figure 3-15-c and d present the rut depths and slopes for the 1828 and 1834 Tollway mixtures, which incurred the highest rut depths among the studied mixtures.

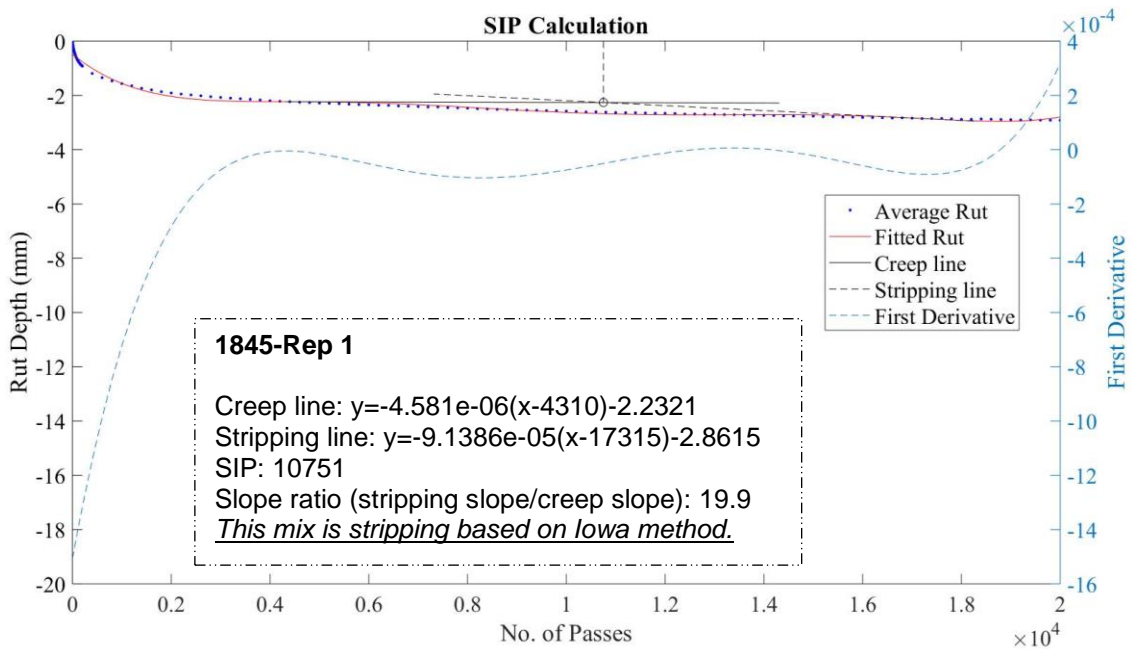


Figure 3-14. Tested samples after 20K pass at 50 °C. a) 1828 mix, b) 1834 mix

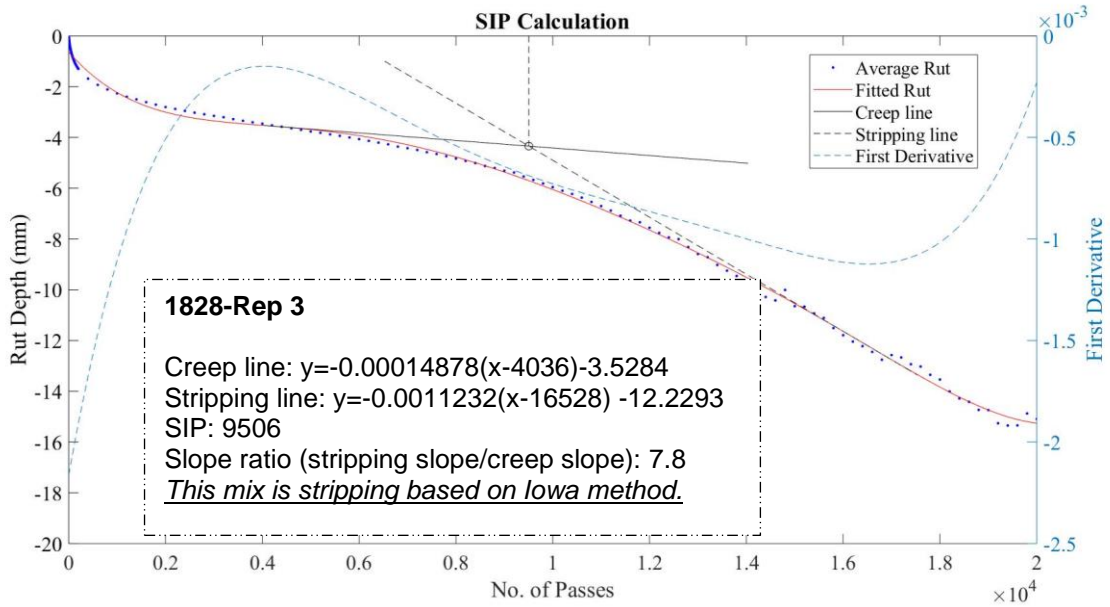
Table 3-4 shows the average of creep and stripping slopes, and the SIP of the plant produced 2018 Tollway mixtures investigated. Of these, five mixtures including 1835, 1845, 1829, 1828, and 1834 had slope ratios over 2.0, indicating stripping potential according to the Iowa method. It is also worth mentioning that although SIP could be calculated for all the mixtures, as long as the slope ratio is lower than 2.0, the mix is not considered as stripping based on the Iowa method. Mixture 1828 was found to be a stripping prone mix, although borderline ($9,861 < 10,000$).



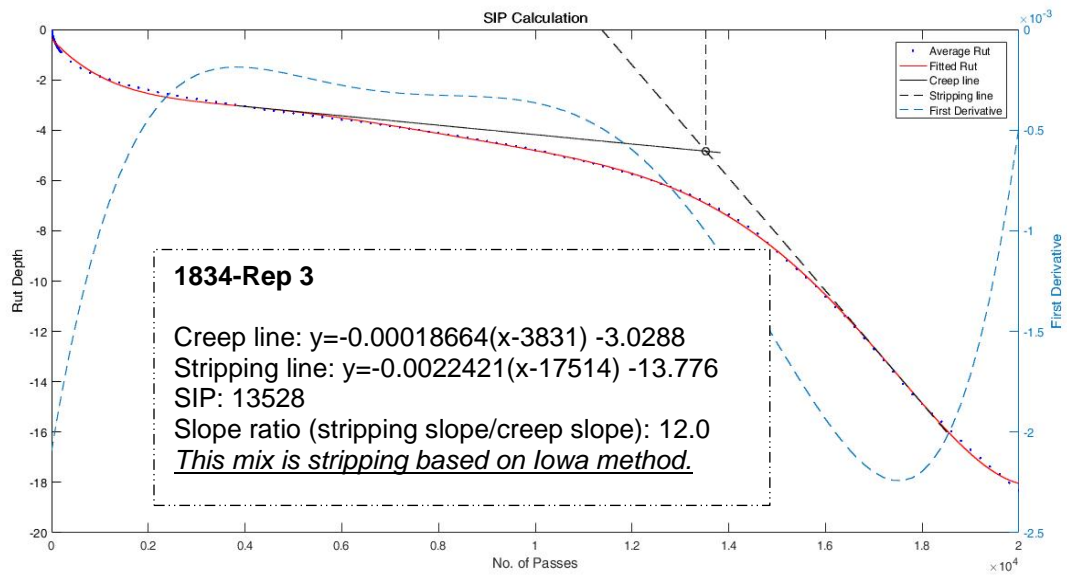
(a)



(b)



(c)



(d)

Figure 3-15. Examples of determination of SIP: a) 1835, b) 1845, c) 1828, d) 1834 mixtures

Table 3-4 also provides the minimum SIP required by the Tollway in their 2019 asphalt mixture specification for different mix categories. For all SMA categories, a minimum SIP of 15,000 passes is used. As highlighted, the average SIP measured on the plant-

produced, reheated, lab-compacted specimens for mixes 1835 and 1845 are lower than the required minimum values and were identified as stripping mixtures. On the other hand, since the average SIP of the other three mixtures with slope ratios greater than 2.0 is higher than the required SIP, they are not tagged as stripping mixtures.

Having very low creep and stripping slopes can result in extremely low or even negative SIPs. This phenomenon especially occurs when most of the deformation occurs during the densification phase and both the creep and stripping lines bear similar slopes. Given the average slopes and SIP values obtained for mix 1836 in Table 3-4, it can be seen that the Iowa method resulted in an average SIP of 1711 passes; however, the slope ratio was lower than 2.0 and did not trigger the stripping detection. As shown in Figure 3-16, in one of the replicates of the 1836 mix, the almost parallel creep and stripping lines has shifted the intersection back to negative computed wheel passes at the SIP (obviously not possible). Clearly, the model fitting and numerical steps used in Iowa method for the SIP calculation often fails to work well for mixtures such as SMAs, which experience a negligible rut depth during the densification stage. In addition to negative SIPs, positive creep slope (upward deflection) can also be observed due to curve fitting issues and numerical calculation in the SIP determination. For this reason, it is recommended that for SMA mixtures with very low rut depths, for instance, for those with no greater than 4.0 mm of rutting at 20,000 passes, that the mixture be considered as ‘non-stripping’ without the need to compute the slope ratio and SIP value.

Table 3-4. Identifying the stripping mixtures based on SIP requirements

Mix. ID	Creep Slope	Stripping Slope	Slope Ratio	SIP	Min. SIP	Status
1844	3.99E-05	6.47E-05	1.6	13430	15000	OK
1835	4.29E-05	9.85E-05	2.8	13562	15000	Stripping
1824	5.62E-05	6.20E-05	1.1	14375	15000	OK
1845	1.98E-05	8.18E-05	10.5	10633	15000	Stripping
1836	6.37E-05	7.32E-05	1.5	1711	15000	OK
1840	5.39E-05	9.45E-05	1.8	12382	15000	OK
1829	6.95E-05	1.60E-04	2.3	12450	10000	OK
1828	2.19E-04	1.56E-03	7.1	9861	10000	Stripping
1823	4.48E-05	7.49E-05	1.7	12565	10000	OK
1818	6.51E-05	1.07E-04	1.6	13107	10000	OK
1834	2.43E-04	1.83E-03	7.5	13149	10000	OK
1826	6.16E-05	1.01E-04	1.7	13608	10000	OK
1807	6.62E-05	1.26E-04	1.9	12084	10000	OK
1803	7.68E-05	9.65E-05	1.3	12222	10000	OK

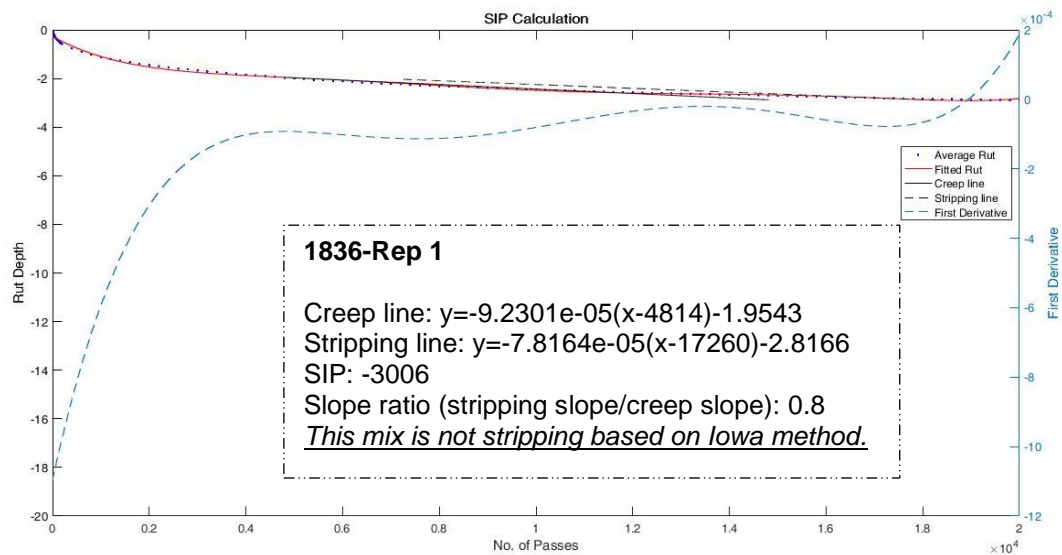


Figure 3-16. Parallel creep and stripping lines for 1836 mix

3.3.3. TSR Testing Results

Prior to the introduction of the Hamburg test, the tensile strength ratio (TSR) test was the preferred method to evaluate moisture damage resistance of Tollway asphalt mixtures. The TSR test was conducted using the Illinois modified version (accelerated moisture conditioning) of the AASHTO T283 specification. In this method, the indirect tensile strength ratio of two subsets of samples is measured and compared to the required TSR threshold. The first subset of samples included at least three replicates of gyratory compacted samples with 95 mm thickness. The air void content of the samples was kept within 6 ± 0.5 % for SMAs and 7 ± 0.5 % for dense-graded mixtures. After being compacted and cooled down at room temperature, the dry samples were conditioned in water bath at 25 °C (see Figure 3-17-a) for two hours. After conditioning, the samples were tested to measure the indirect tensile strength. Although the conditioning process is completed in water, this subset of samples is termed the dry subset.

The next subset of samples is called wet subset and includes at least three replicates with the same geometry and air void content as the dry subset. This subset is subjected to a vacuum saturation process, followed by soaking in warm water. To this end, specimens were placed in a vacuum container, supported a minimum of 25 mm (1 in.) above the container bottom by a perforated spacer. The container was then filled with potable water at room temperature so that the specimens had at least 25 mm (1 in.) of water above their surface. A vacuum of 13 to 67 kPa absolute pressure (10 to 26 in. Hg partial pressure) was applied for approximately 5 to 10 minutes. The vacuum pressure was then removed, and the specimen left submerged in water for a short time (approximately 5 to 10 min). The time required for some specimens to achieve the correct degree of saturation (between 70 and 80 percent) may in fact be less than 5 min. In addition, some specimens may require the use of an absolute pressure of greater than 67 kPa. After performing a first run of vacuum saturation trials, the saturation level is measured. If the degree of saturation is between 70 and 80 %, the sample will be ready for warm water conditioning. If the degree of saturation is less than 70 %, another period of saturation is needed. In case the saturation degree is over 80 %, the sample would not be representative and was discarded. After vacuum-saturating the samples, they were placed in warm water at 60 °C (see Figure 3-17-b) for 24 hours. After this warm conditioning prior to testing, the samples were placed in water at 25 °C for two hours. Finally, the IDT strength of the samples was measured. The minimum acceptable tensile strength is set at 60 psi for mixtures containing unmodified asphalt binders and 80 psi for mixtures containing modified asphalt binders.

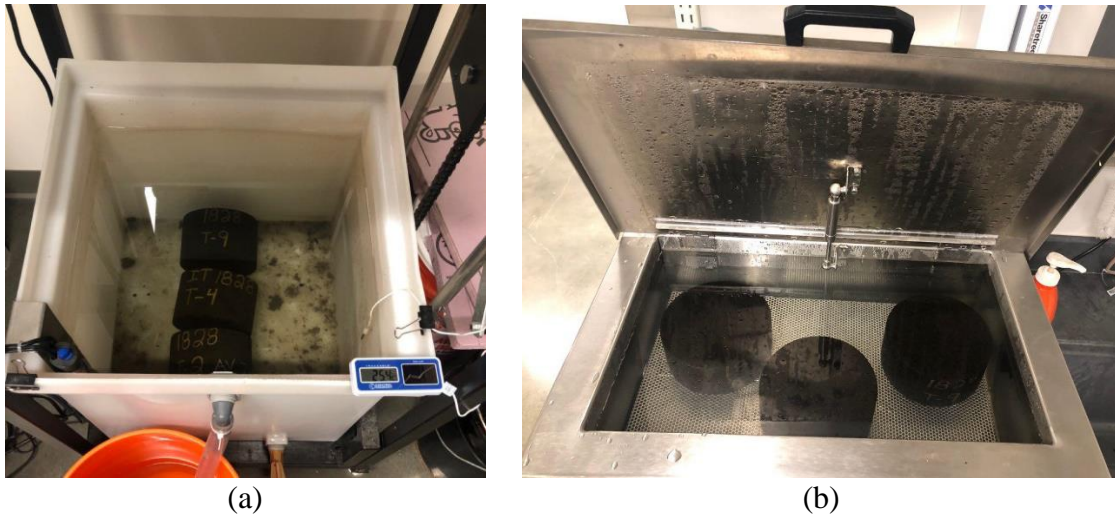


Figure 3-17. TSR sample conditioning. a) Dry set at 25 °C, b) Wet set at 60 °C

Figure 3-18 presents the tensile strength of the sample subsets on the left axis in form of the bars (dry in orange and wet in dark blue colors). Also, the tensile strength ratio (TSR) is shown on the right axis as indicated by the green data points. Clearly, most of the mixtures possessed strength values in both dry and wet conditions in excess of 80 psi, indicating that the IDT strength minimums were easily met. The only mix which could not meet the minimum strength of 80 psi (set for modified mixtures) was 1828. Referring to the Hamburg testing results, the rut depth of this mix was also high, although its SIP was found to meet the requirement. The TSR calculated for this mix is 77.3 which is below the minimum TSR of 85% required in the Tollway specification. Therefore, the 1828 mix showed moisture damage potential in both the Hamburg and TSR tests. Fortunately, the IL-4.75 mixes, which yielded TSR values less than 85%, are used in the sublayers of the pavement structure and will not experience the intensity of freeze-thaw cycles and traffic loads as a surface mixture endures.

The TSR values for the 1835 and 1845 mixtures, which were marked as stripping mixtures by the Iowa method, were more than 96 % with their strength values greater

than 90 psi in both wet and dry conditions. The rut depth of these mixtures in the Hamburg test was very low, but the slope ratios were high, and the mixes were detected as stripping by Iowa method. Therefore, these two performance tests do not completely match in terms of detecting the stripping. This finding supports the recommendation of waiving the Iowa SIP calculation and requirement for SMA mixtures with low total rut depths at 20,000 wheel passes. Based on these findings, it is also recommended that the Hamburg wheel track test be the primary test for moisture damage assessment. If the Hamburg test indicates stripping potential, the designer may opt to run the AASHTO T-283 procedure. If the TSR meets the required value, then the mixture can be passed and considered as non-stripping.

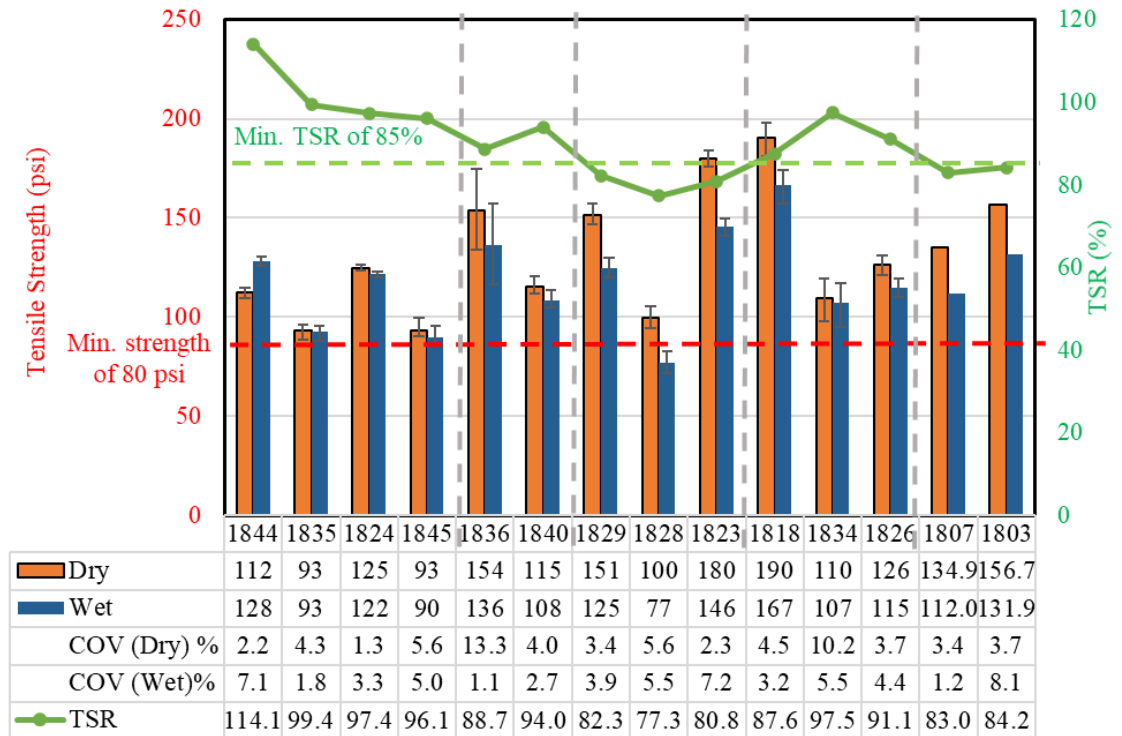


Figure 3-18. Wet and dry strengths and TSR values

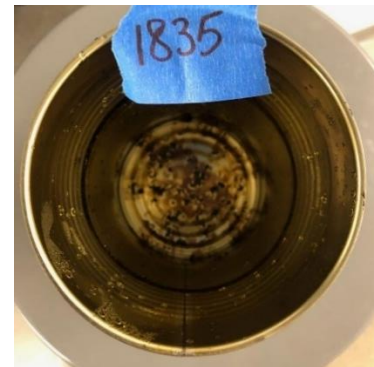
3.3.4. Boiling Water Test Results

In order to investigate the discrepancy between the Hamburg and TSR tests, a third test – the Texas boiling water test, was conducted per ASTM D3625-12. In this test, two, 250-gram samples of loose mixture were collected. After warming the samples to about 100 °C, one sample is placed in boiling water (100 °C) and the other sample is kept in water at room temperature for ten minutes. Then, the samples are carefully drained and visually compared with one other. If the bituminous coating of the aggregates conditioned in the boiling water was removed or observed to change in color, the mixture is identified as having stripping potential. In addition, residual material deposited on the wall and bottom of the water container can also help to indicate the separation of binder from aggregates and thus the potential for stripping in the evaluated mix. Figure 3-19 presents the pictures from nine conditioned loose mixtures in both boiling water and room temperature water and the binder residual on the wall and the bottom of the boiling water container. As Figure 3-19-b and Figure 3-19-d show, there is not a significant difference observed between the boiling water conditioned and room temperature water conditioned 1835 and 1845 samples. In addition, the residual remaining on the boiling water container is relatively negligible. As expected, the 1828 mix, which showed stripping potential though SIP and TSR parameter, had higher concentration of residual after being conditioned in boiling water for 10 minutes (Figure 3-19-g). However, due to the very fine particles present, it was difficult to detect any difference between the two differently conditioned samples from this mix with the naked eye. Based on these results and those of the previous sections, the boiling water test does not seem to be worth pursuing at the present time as a simple alternative to the Hamburg or TSR stripping tests. However,

from a research perspective, the test provided a useful outside perspective when comparing Hamburg and TSR results.



a)1844 mix



b)1835 mix



c)1824 mix



d)1845 mix



e)1836 mix



f)1840 mix



g)1828 mix



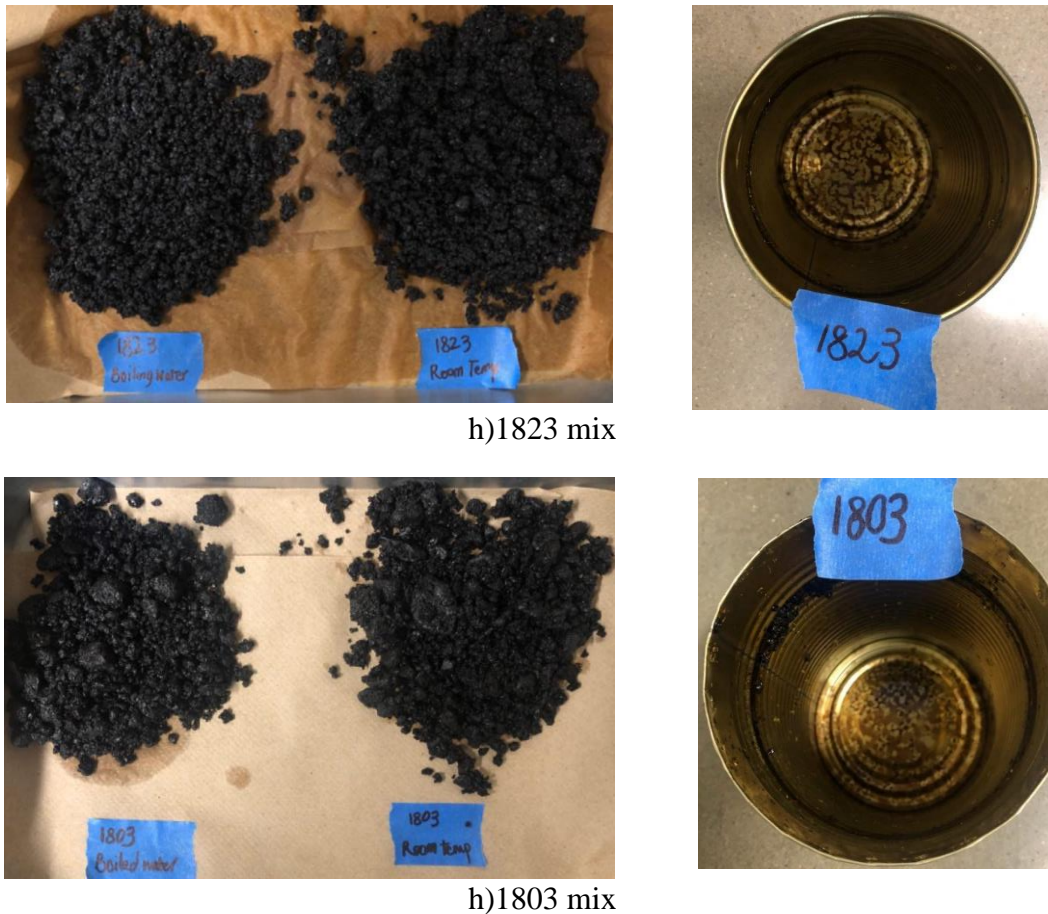


Figure 3-19. Boiling water test samples and container residue for different mixtures

3.3.5. Performance Test Repeatability

In the previous section, the capability of various performance tests and associated parameters to mitigate different distresses such as cracking, rutting, and moisture damage has been presented. Error bars were provided on figures to graphically illustrate the variability of the tests with respect to their mean values. In this section, the coefficient of variation (COV) values are summarized and compared to assess the relative repeatability of the tests. Except for I-FIT test, where four replicate specimens were tested for each mix, all other tests involved three test replicates. The COV parameter allows scaling of the standard deviation with respect to the mean value of the result obtained. The COV is

computed as the standard deviation of the replicate test results divided by the mean of the test results. Thus, the COV can be interpreted as the standard deviation of the test results expressed as a percentage of the mean. For instance, a 30% COV computation would estimate that 68% of test results would fall within +/- 30% of the true mean value. The dispersion can come from a number of sources, including variability in the material sampled, variability in procuring or producing the sample (gyratory compaction, coring and core procurement and handling/shipping/storage), variability in splitting samples, variability in fabricating the sample, human variability introduced during testing and possibly in data analysis, and finally, variability introduced by the testing device. By comparing similar materials evaluated with different testing approaches, one can obtain a general sense of the relative proportion of the COV that is attributable to the test device versus the inherent variability of the samples being tested. Lower COVs are generally associated with factors such as: fine-grained materials, homogeneous materials, samples and ligament areas larger than their representative volume element (RVE) dimensions, factory-produced materials, low-strain tests, modulus tests, and other highly controlled variables (temperature, loading rate, aging levels, specimen geometry). Higher COVs are generally associated with coarse-grade materials, heterogeneous materials, smaller samples tested below the RVE size, field produced materials, chaotic processes such as fracture or plastic shear flow in heterogeneous materials, and poorly or difficult to control variables. Clearly, our industry has its hands full when considering the realities of our material, our construction environment, and the desire to use simple test geometries and to test small samples with low number of replications when possible.

Table 3-5 and Table 3-6 show the averaged COVs and standard deviations (STDs) of the performance tests for different mix categories. It can be seen that the maximum COV of the DC(T) test for both -12 and -18 °C temperatures is less than 17 %. The COV of CT parameter is comparable to the FI (four replicate result). The IDT strengths in the TSR test (both wet and dry conditions) yielded the lowest COVs. The Hamburg rut depth COV never exceeded 15 % for the tested mix categories. By far, the SIP parameter had the highest variability when considering two mix categories - SMA surface (**131.7%**) and shoulder binder (**38.6%**). The average COVs for the performance tests are summarized in Figure 3-20.

Table 3-5. Test COV averages for different mix categories

Mix. Type	DC(T) at -12 °C	DC(T) at -18 °C	FI (4 Reps)	CT	Strength (Wet)	Strength (Dry)	Hamburg (Rutting)	SIP
SMA F. S.	8.9	15.1	23.8	26.9	4.3	3.3	11.9	14.1
SMA S.	10.1	7.8	20.3	11.5	1.9	8.6	6.6	131.7
IL-4.75	7.3	14.5	25.2	15.1	5.5	3.8	14.1	15.0
Shoulder S.	15.8	16.2	21.4	23.2	4.4	6.1	13.9	12.5
Binder Cse.	14.3	6.9	21.3	22.0	4.7	3.5	13.2	38.6

Table 3-6. Standard Deviation (STD) averages for different mix categories

Mix. Type	DC(T) at -12 °C	DC(T) at -18 °C	FI (4 Reps)	CT	Strength (Wet)	Strength (Dry)	Hamburg (Rutting)	SIP
SMA F. S.	71	102	2.2	39	4.9	3.3	0.3	3871
SMA S.	64	39	1.5	18	2.2	12.5	0.2	3132
IL-4.75	33	56	2.3	13	6.5	5.0	0.9	1770
Shoulder S.	71	62	2.0	20	5.4	8.1	0.8	1744
Binder Cse.	59	23	1.0	15	6.1	5.2	0.3	4711

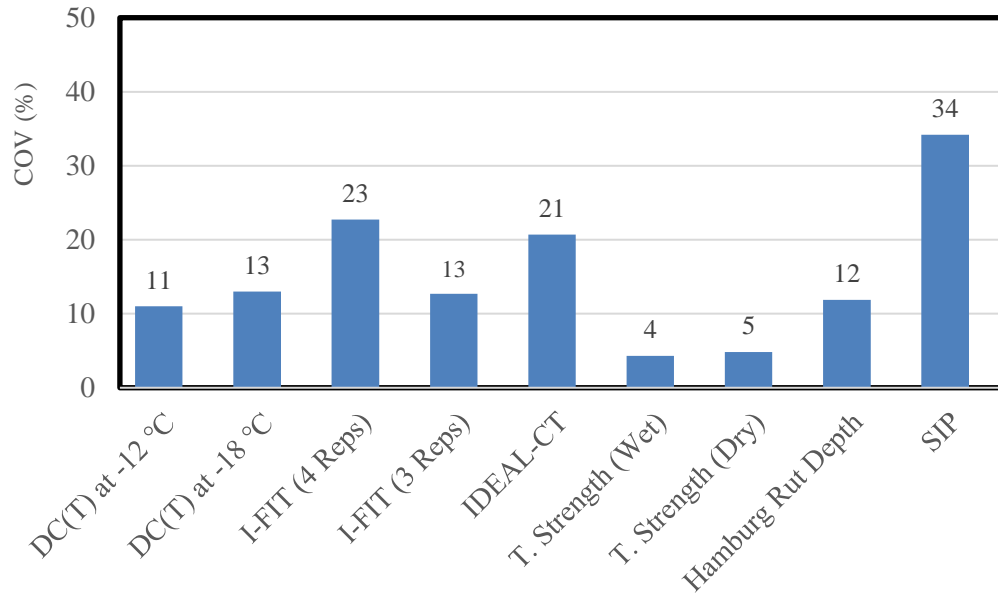


Figure 3-20. Average COV (%) of the tests

3.3.6. Performance-space Diagram

Figure 3-21 presents a useful x-y plotting form known as the ‘performance space diagram,’ or more specifically in this case, the Hamburg-DC(T) plot (Buttlar et al., 2016; Jahangiri et al., 2019). This plot allows the simultaneous evaluation of rutting and cracking behavior. Some useful trends that can often be observed when viewing data in this form are:

- The best overall performing mixtures will appear in the upper-right corner of the diagram (low rutting depth, high fracture energy). These can be considered as high ‘total energy’ mixtures; i.e., rut and crack (or damage) resistant. These are high toughness mixtures, and the best candidates for surfacing materials especially in demanding climates and for high traffic volumes.

- Mix variables that increase net total energy in the mix and thus ‘move’ mixtures in the direction of the upper-right corner of the plot include:
 - Higher quality binder (low temperature susceptibility, higher Useful Temperature Interval, or UTI), degree of polymer modification;
 - Higher quality aggregate (stronger, more angular, better bond with asphalt), and;
 - The presence of crack interceptors or rut mitigators, such as fibers, rubber particles, and even RAS (but only if properly used).

- Other salient features of the plot include:
 - Binders with different grades but similar UTI tend to move a mixture along a ‘binder tradeoff axis’, or roughly speaking, diagonal lines moving in the upwards-left or downwards-right directions, for stiffening and softening, respectively;
 - Pure stiffening elements, such as RAP, tend to move points upwards and to the left;
 - Pure softening elements, such as rejuvenators, tend to move points downwards and to the right;
 - Binders with higher UTI, where the grade bump is on the high temperature grade, tend to move points mainly upwards, but also slightly to the right due to the benefits of polymer in intercepting cracks, and;
 - Binders with higher UTI, where the grade bump is on the low temperature grade, tend to move points mainly to the right, but also slightly upwards, again, due to the benefits of polymer in intercepting cracks.

- Data points that appear in the undesirable middle-to-lower-left portion of the plot are sometimes those that contain RAP and insufficient binder bumping, and possibly poor bond, where the RAP tended to cause lower DC(T) values, and the nature of the RAP-virgin material combination led to a moisture-susceptible mix with high Hamburg rut depth value.

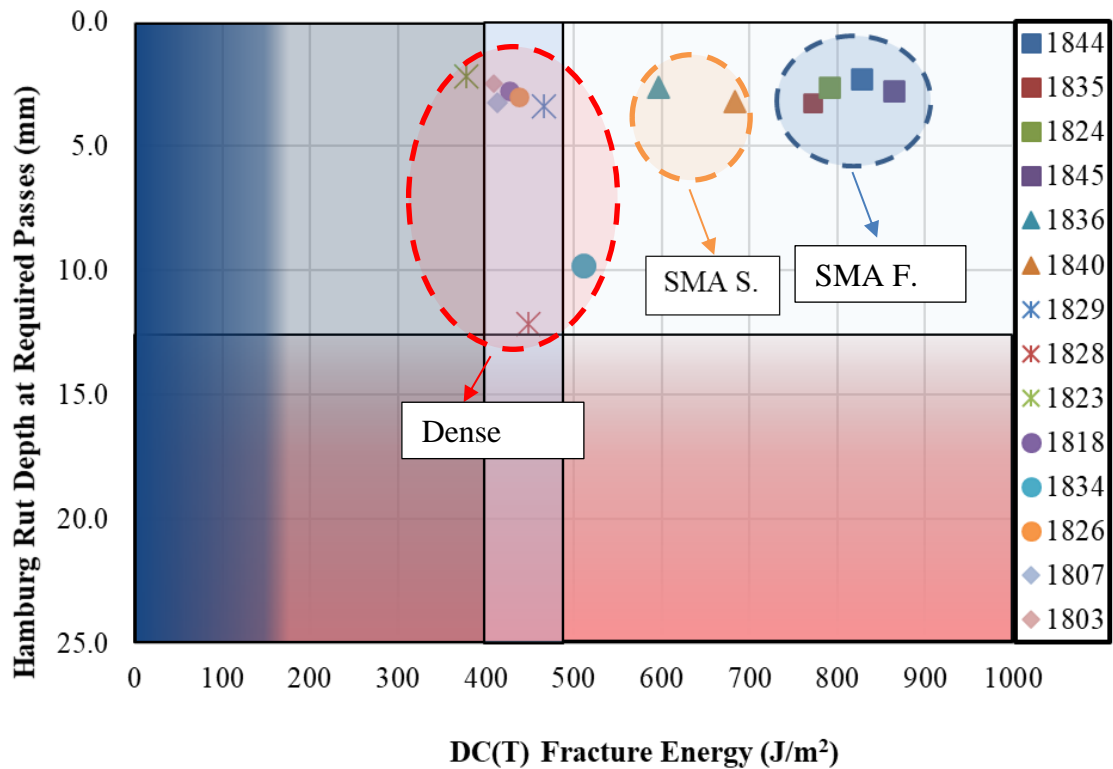


Figure 3-21. Hamburg-DC(T) performance-space diagram for 2018 mixtures

A number of interesting findings can be extracted from the results Tollway 2018 mixtures, including:

- The SMA friction surface mixtures (solid squares) are located on the upper right corner of the performance-space meaning that these mixtures have the highest fracture energy and very low rutting potential.

- Given the fact that there is still room between the recorded rut depth and the 6 mm threshold, these mixtures could benefit from a softer binder system and/or rejuvenator to further improve the DC(T) fracture energy.
- The two SMA surface mixtures (solid triangles), including 1836 and 1840, are placed on the left-hand side of the SMA friction surface mixtures.
 - The horizontal alignment observed for SMA surface and SMA friction surface mixtures underlines the importance of aggregate quality in DC(T) fracture energy.
 - The rutting and cracking performance of the 1836 mix could be more balanced by employing strategies to soften the mix.
- The IL-4.75 mixtures (asterisks) studied in this study exhibited greatly varying behavior based on Hamburg-DC(T) plot.
 - 1823 mix showed an excellent resistance to rutting, although its DC(T) fracture energy was the lowest among the studied mixtures.
 - The GTR used in 1829 mix along with the fine aggregate structure resulted in a rut-resistant mix that also possessed reasonable cracking resistance.
 - Unlike the 1829 mix, the 1828 mix (the other rubber modified mix in this category) did not perform very well in the Hamburg test. Similar cracking resistance was measured. Lack of room for the swelling of the dry-processed rubber modification in the fine aggregate structure could have possibly led to the poor performance of this mix in the Hamburg test.

- The three shoulder mixtures (solid circles) performed similar to the other dense graded categories. Since the shoulder surface mixtures experience the same environmental conditions as the SMAs do, their DC(T) fracture energy should also be expected to be relatively high. That being said:
 - The 1834 mix recorded a higher DC(T) fracture energy than the other two mixes in this category. However, its rut depth in Hamburg test was high. However, the poor Hamburg performance may not be problematic in practice due to the low load intensity typically experienced on the shoulder.
 - The 1818 mix had a similar amount of recycled materials (~20 %) as compared to mix 1834. However, the base binder used in mix is one PG grade stiffer. In the future, to improve the fracture energy of the 1834 mix, a softer binder system should be considered.
 - The 1826 mix has the highest amount of recycling (~46 %) and accordingly used the softest binder system (PG 46-34) in this category. This mix design strategy seemed to pay off, as the mix is characterized as one of the better overall performers based on the performance-space diagram.
 - None of the shoulder mixtures tested in this research were modified with rubber or SBS. Incorporation of GTR, as a recycled material, might improve the sustainability and also performance (especially cracking resistance) of these mixtures.

- The two shoulder binder mixtures including 1807 and 1803 (solid diamonds) performed very similarly in terms of their relatively low and high temperature test results.
 - As a result of high levels of recycled materials used (more than 43 % ABR), these mixtures are very stiff and showed negligible rutting in the Hamburg.
 - Similar to the shoulder surface mixtures, softer binders and GTR modification should be considered in future designs.

3.3.7. Long-term Aging

DC(T) testing has generally been performed on short-term aged laboratory mixes.

However, the rheological properties of the binder keep changing during the service life of the pavement resulting in higher cracking potential due to stiffening. The DC(T) was inherently calibrated to account for these differences during its development in the National Pooled Fund Study on Low Temperature Cracking (Pooled Fund Study #776). However, the calibration contained many sections from Minnesota, along with other participating states (mostly northern). This calibration had not been performed for the Illinois Tollway specification prior to this study. Thus, a targeted laboratory and field study was performed towards this end.

AASHTO R 30, which is the most commonly used method to simulate long term aging of the asphalt mixtures, suggests keeping the compacted samples at 85 °C for five days. However, given the highly variable climatic conditions across the US, this description likely does not closely simulate the environmental conditions in Chicago area. In addition, oven aging of the compacted samples could result in non-uniform aging,

distortion, and change in air voids of the testing samples. Recent studies have suggested that loose mix oven aging at 95 °C may be the most promising long-term aging method to simulate field aging for asphalt mixtures, at least for research purposes. For example, NCHRP Report 781 generated aging duration maps for mixtures aged in a forced-draft oven at 95 °C (see Figure 3-22) for the U.S. Three field age targets (4 years, 8 years, and 16 years) were selected for the purpose of matching field aging effects at three depths (6 mm, 20 mm, and 50 mm) with oven aged results at 95 °C. The recommended aging protocol was developed by means of a series of laboratory experiments on field cores and asphalt binders along with a system to select the aging index properties (AIPs) that were integrated with pavement aging models.

The limited literature available suggested using a 15% increase in DC(T) fracture energy thresholds on short-term aged specimens during mix design to account for the eventual fracture energy loss expected during long-term aging (Braham et al., 2009). However, this fracture energy reduction was recommended for one specific type of hot mix asphalt (HMA) and did not cover the various mix types used by the Tollway. To validate the recommended value and also to establish the aging characteristics for all of the Tollway mix types, University of Missouri (UM) researchers attempted to apply the NCHRP aging protocol on the loose mixtures to simulate eight years of aging on Tollway pavements placed in the Chicagoland area. In addition to DC(T) fracture energy, the sensitivity of FI parameter to aging was also studied. Table 3-7 shows the duration of oven aging needed to simulate different field aging times. For this study, the surface mixtures were aged for 6 days in a forced-draft oven at 95 °C (see Figure 3-23) to account for eight years of in-situ aging. It should be noted that the plant-produced

mixtures were sampled in mid-2018 and were kept in the storage facility until late 2019. However, any steric (thixotropic) hardening occurred would likely be reversed by sample heating and stirring.



Figure 3-22. Required oven aging durations at 95°C to match level of field aging 6 mm below pavement surface for 8 years of field aging (Kim et al., 2018)

Table 3-7. Illinois oven aging duration based per NCHRP-781 “(6 mm below the surface) (Elwardanya et al., 2018):

Field Aging Time	Oven Aging Time at 95 °C
4 years	3 days
8 years	6 days
16 years	12 days



Figure 3-23. Aging the Tollway 2018 plant produced mixtures in oven at 95 °C for 6 days

- Surprisingly, mix 1835 which is an SMA friction surface mix modified by dry-process GTR did not experience a drop in DC(T) fracture. This mix also had the smallest drop in FI score (63% drop) among the tested mixtures. Possibly the combination of GTR (containing carbon black, an antioxidant) along with a high amount of pre-aged recycled materials (ABR=41.2%) in this mix led to the relatively stable aging behavior.
- Mix 1836, which is an SBS-modified SMA surface mix, was measured to have a 19% decrease in fracture energy. However, the FI score underwent a decrease of 86% upon this aging. The DC(T) fracture energy ‘bump’ inherently considered in

the current Tollway specification is thought to be around 15%, which is very close to aging effect measured in this mix.

- Mix 1818, which is an unmodified shoulder surface mix, experienced 17% drop in DC(T) fracture energy after aging. This mix had the highest drop in FI score (96%). It is worth mentioning that the peak load in I-FIT exceeded 10 kN for this mix and a snap-back (very brittle) behavior was observed for this mix such that the slope of Load-Deflection curve could not be properly calculated.
- The average drop in DC(T) fracture energy for the investigated surface mixtures (including both SMA's and dense graded mixtures) was calculated as 16.5 %. Therefore, the recommended 15% in the literature is reasonably close to the obtained experimental results in the lab.

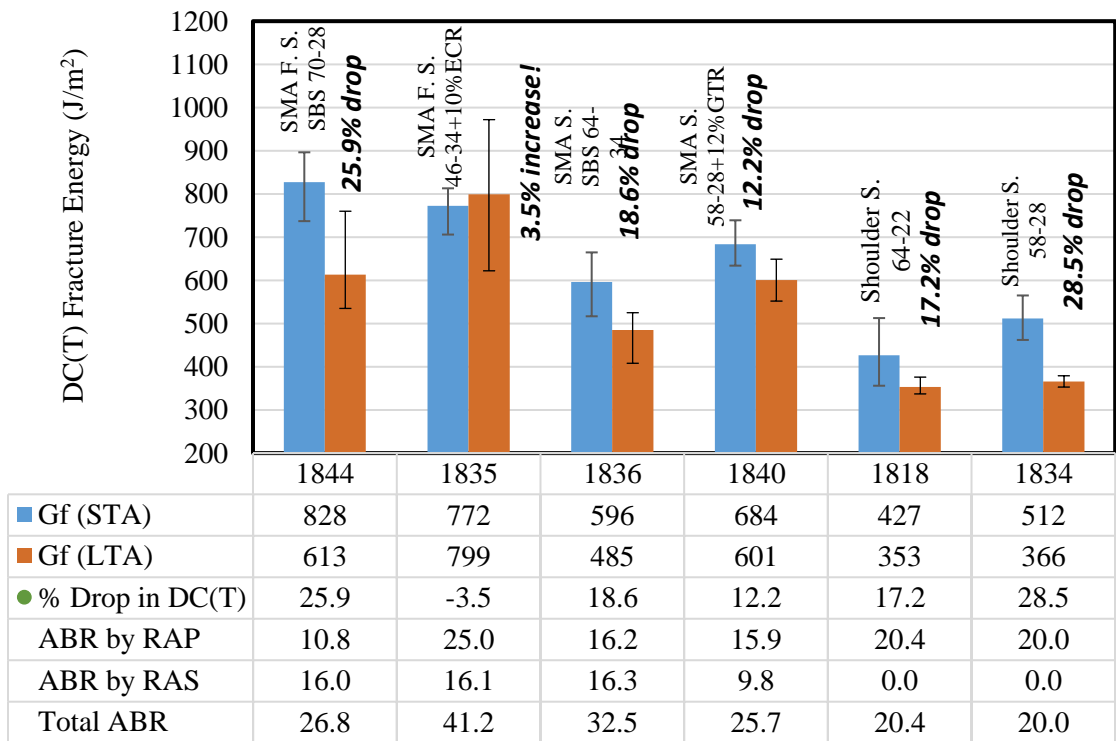


Figure 3-24. Comparing the DC(T) fracture energies of short-term aged (STA)

with long-term aged (LTA) samples

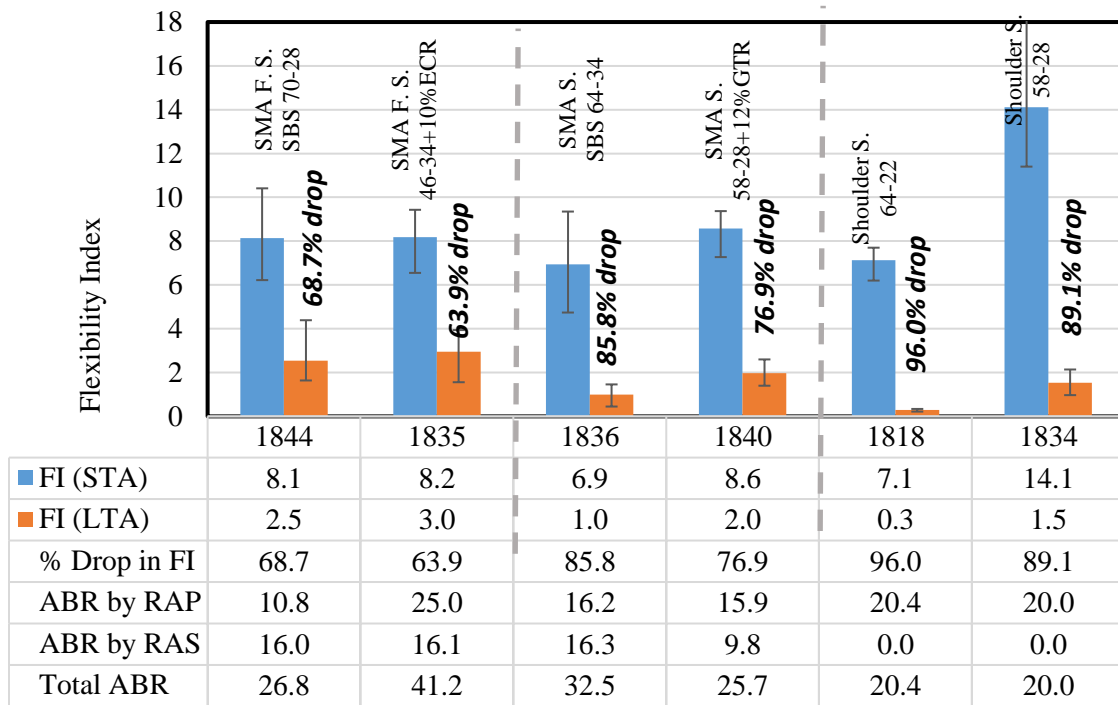


Figure 3-25. Comparing the FI of short-term aged (STA) with long-term aged (LTA) samples

Some of the tested aged samples (e.g. the 1835 mix) showed normal load-displacement curves (Figure 3-26a) while there were mixtures such as 1818 that had straight-line (due to a fast moving crack that outpaced the data acquisition rate used in the test) and snap-back shaped load-displacement plots (Figure 3-26b) with peak loads in excess of 10 kN. This behavior led to a very low FI value, less than 1.0, and in some cases, nearly zero. These specimens exhibited very brittle behavior in the I-FIT test, with snap-back type softening curves and very few data points following the peak load, indicating a very brittle failure. Analysis of data sets with very steep post-softening curves is not adequately described in the test specification, and requires analyst judgement. These mixes often possess the highest variability between test replicates. These observations

underscore the difficulty in using the I-FIT test with respect to mix specification calibration on long-term aged materials.

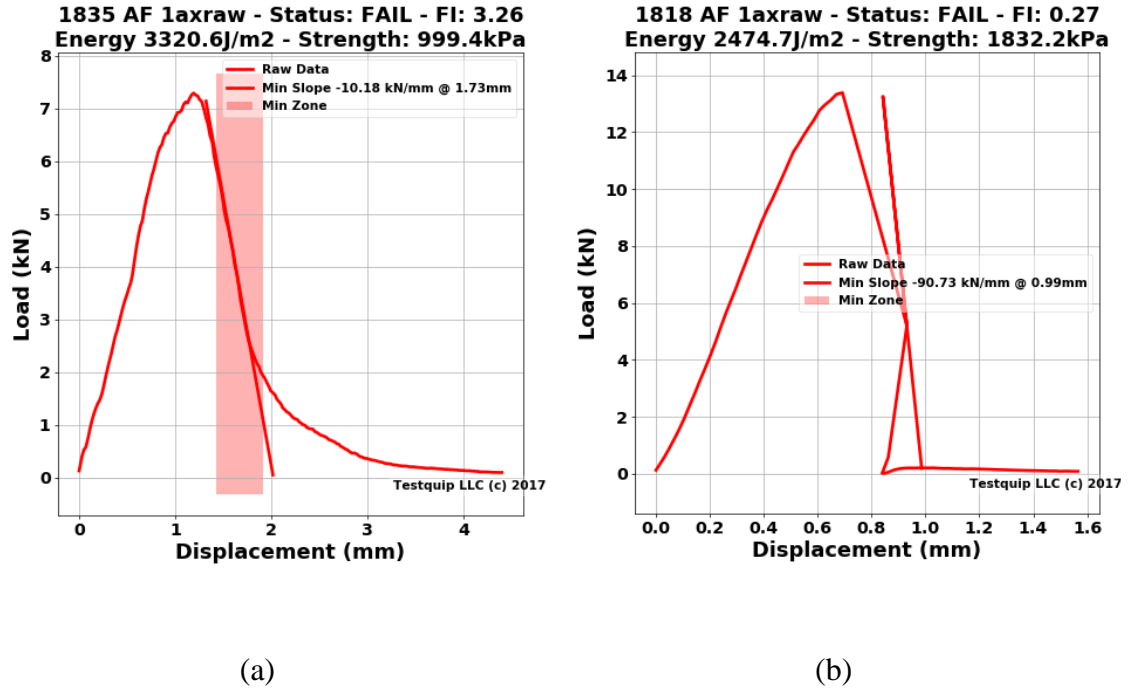


Figure 3-26. Load-displacement response for aged mixtures under I-FIT testing:
a)1835 b)1818

Chapter 4

DEVELOPMENT OF THE SPECIFICATION BASED ON FIELD PERFORMANCE DATA AND ANALYSIS

4.1. Overview

Pavements serve as an important and critical part of a nation's infrastructure, and it is essential to preserve its functioning to maintain national development and prosperity. Pavements, like all other infrastructure assets, deteriorate over time and thus require routine maintenance activities to be conducted by transportation agencies in order to avoid any loss of serviceability. The first step towards planning a pavement maintenance activity is to be aware of the pavement condition, and that is achieved through systematic Pavement Condition Surveys (PCSs).

PCSs refer to activities that quantify the pavement serviceability and its physical condition and are mainly comprised of three aspects: data collection, condition rating, and quality management. The data collection, which is mostly semi-automated or automated, provides a measure of the distresses prevalent in an existing pavement section. The data might also include other details about the pavement construction, such as length and width of the section, location of underlying structures, and details of last conducted preservation or maintenance activity. The condition rating is usually index- or scale-based to quantify the condition of a pavement section. Various systems for condition rating exist, and adoption of a particular system depends on available resources and familiarity with the said rating system. Finally, based on which pavement section falls below the set condition rating thresholds, adequate maintenance treatments are applied to retain a certain minimum serviceability. Condition rating data collected over time could provide an overall performance of any particular section and could provide an objective basis for selecting future maintenance techniques, affecting the short- and long-term budget planning of a transportation agency.

In this chapter, the field performance data collected by Applied Research Associates (ARA) are presented based on further processing and analysis by the research team. These data consist of condition rating survey (CRS) results including the severity of the observed asphalt pavement distresses, International Roughness Index (IRI), and rut depth collected from the mainline sections. Since all of the studied mainline sections are located in Northern Illinois, it is assumed that they experienced the same environmental conditions and their low-temperature cracking performance can be compared. The asphalt mixtures used on the studied mainlines have been tested in the lab, and the results were presented in Chapter 2. The objective of the field performance data analysis is to establish a link between the field performance and laboratory testing results. The link will ultimately be used to determine the thresholds and calibrate the performance specification.

4.2. Condition Rating Survey (CRS)

As mentioned before, a historical record of pavement condition rating allows for a) the proper planning of maintenance activities to be undertaken, b) the adequate allocation of funds to maintain a minimum amount of serviceability in the existing pavement network, and c) the ability to predict future requirements for maintenance leading to adoption of relevant preservation techniques. The Condition Rating System (CRS), used in this study, is an index between 1 and 9, representing a failed and a new pavement condition respectively.

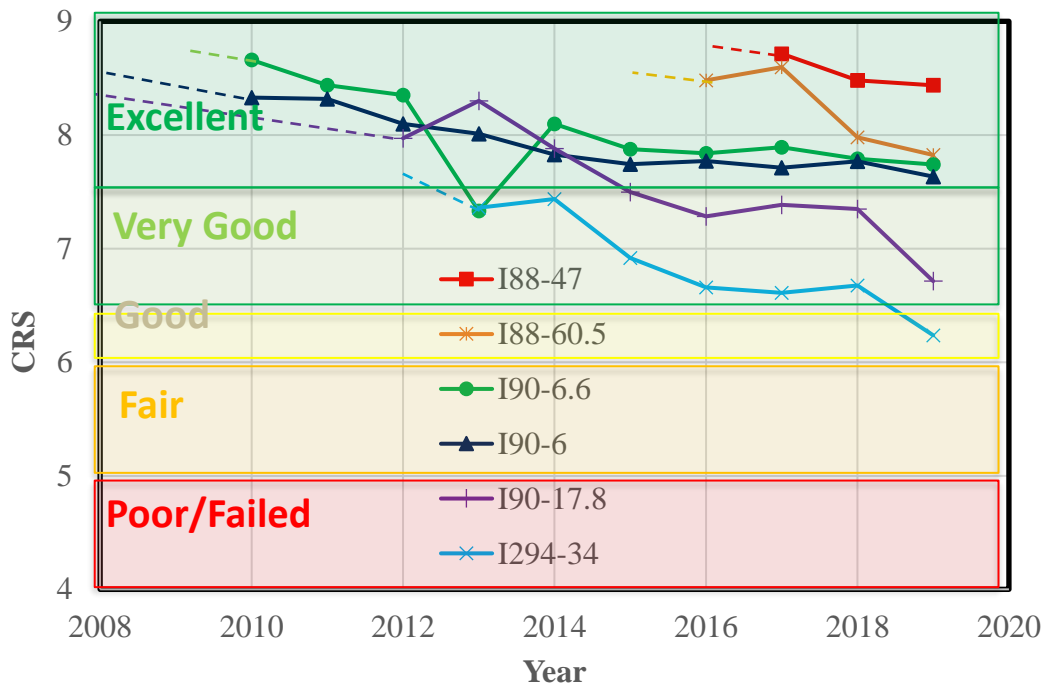
4.2.1. CRS Trends in Service Life

Figure 4-1 shows the CRS measurements for six different mainline sections that were already introduced in Chapter 2 and evaluated for performance. Different zones ranging from “Excellent” to “Poor/Failed” were superimposed on the figure to more clearly identify the condition of the sections based in CRS values. The CRS of each section is plotted in different years. Where the data was not available, a dashed line was used to extrapolate the CRS values, especially at the early years of the sections’ service life. As seen in

Table 2-2, the I88-47 section is the newest section (overlaid in 2016) and has the highest CRS score. Also, noted were:

- The lowest CRS is recorded for the I294-34 section which is placed on a jointed concrete pavement and undergoes heavy traffic loads as discussed in Chapter 2 (refer to Figure 2-4). In addition, I294-34 is the only section with an existing CRS value below 6.5, and the section entered the “good” condition based on CRS score.
- The I90-6.6 and I90-6.0 sections show similar trend and CRS values at different years and both hold CRS values in “Excellent” condition after more than 10 years of service life.
- Although the DC(T) fracture energy of I90-6.6 (567 J/m²) was much lower than that of I90-6.0 (925 J/m²), it was high enough to maintain the CRS values similar to I90-6.0.

- I90-17.8 showed block cracks on the surface as shown in Figure 2-8. Accordingly, the CRS decreased at a high rate especially in 2018 and 2019 such that the CRS went below the “Very Good” condition and into the “Good” zone.
- Despite the fact that I88-60.5 section is in its early stages of life, the CRS deterioration rate was high such that this section is approaching the “Very Good” CRS zone.



--- Dashed lines show extrapolated CRS to the year of last overlay

Figure 4-1. Comparing the CRS values as a function of year

4.2.2. Distress Type and Severity

The presented CRS values were determined based on the type, extent, and severity of different distresses. The CRS system has a pavement distress guide which can be used to characterize the distress identification and coding. This guide contains distresses for both concrete and asphalt pavements. Some of the important distresses which were frequently

observed on the studied sections are presented in Table 4-1. As noticed, these specific distresses are all cracking type distresses which highlight the importance of this mode of deterioration in the Tollway system. As shown, “centerline deterioration”, “longitudinal/center of lane cracking”, “transverse cracking/joint reflection cracking”, and “block cracking” are denoted as “S”, “Q”, “O”, and “M”, respectively. Each distress has different severity levels that can be identified using the digit after the distress code. For instance, S4 is used to characterize “centerline deterioration” that is “frequent”. It should be noted that the “S” distress is mainly due to the construction and is referred to as cold joint. Although this study does not attempt to mitigate this crack, improving the construction methods for paving patterns are expected to address it. Centerline cracks (Q) are developed mostly due to traffic load and could form block cracks after joining the transverse cracks. Finally, the transverse and reflective cracks (O) can be formed due to cooling cycles and propagation of the cracks from underneath layers, respectively.

Table 4-1. Examples of CRS distress characterization and coding

Distress Type	Severity Levels
Centerline Deterioration	S1 – Tight cracking with little or no spalling.
	S2 – Cracking with low to medium spalling.
	S3 – Infrequent: Cracks are open with medium to severe spalling.
	S4 – Frequent: Cracks are open with medium to severe spalling
Longitudinal/ Center of Lane Cracking	Q1 – Beginning Stage: Cracks are tight (width is less than or equal to ¼”) with little or no spalling.
	Q2 – Infrequent: Cracks are between ¼” and ½” and may have minor spalling.
	Q3 – Frequent: Cracks are between ¼” and ½” and may have minor spalling.
	Q4 – Infrequent: One or more of the following conditions exist: Cracks are greater than ½” in width Cracks have severe spalling Major maintenance activity has been performed on the crack
Transverse Cracking /Joint Reflection Cracks	O1 – Beginning Stage: Hairline cracks at any frequency.
	O2 – Infrequent: Cracks are open and less than or equal to ¼” in width and may have low to moderate levels of associated distress.
	O3 – Frequent: Cracks are open and less than or equal to ¼” in width and may have low to moderate levels of associated distress.
	O4 – Infrequent: Cracks are greater than ¼” in width and may have moderate to severe levels of associated distress.
Block Cracking	M1 – Low level: Hairline cracks with none or only a few interconnecting cracks. Cracks are not spalled.
	M2 – Medium level: Further development of interconnecting cracks into a pattern. Cracks may be lightly spalled.
	M3 – High level – Infrequent: Cracks have progressed so that the pieces are well defined and/or spalled at the edges.

4.2.3. Analysis of the Distress Data

The studied sections have different length and the CRS system provides the field performance data for subsections (typically) with a length of one mile. For each of these subsections, the field performance data such as CRS, IRI, and rut depth are provided. In addition to the aforementioned performance indices and parameters, each subsection determines the observed distresses and their severity. Figure 4-2 shows an example

(section I88-60.5) which is divided into two one-mile subsections (60.0 to 61.0 and 61.0 to 62.0). This figure also shows the number of lanes and the type of pavement. These data are organized and presented based on the year. As seen in this figure, the first subsection had three distresses including O2, Q1, and S2 in 2019. However, the severity of “O” distress was 1 (O1) on the second subsection in 2019, which indicates that the transverse/reflective cracks had relatively lower severity within the second subsection. A weighted average (based on the length of the subsection) is implemented to calculate the average severity of distresses. In this example, the average severity of O distress is calculated as 1.5 in 2019 as the two subsections of I88-60.5 had equal length (1 mile). This section was overlaid in 2015 and did not show any distresses from 2016 to 2017. There were some subsections (especially long ones such as I90-6.0 and I294-34) paved with concrete pavement as concrete subsections are commonly used next to bridges. Those subsections were excluded from the average severity calculation. The averaged severity of the important distresses was calculated for all of the studied sections in their service lives and will be discussed later. It should be mentioned that the only section which showed block cracking (“M” type distress) according to the ARA data is the I90-17.8 section. This section started to develop the “M1” crack in 2019. As no other sections developed block cracking, the average severity for “M” is not presented.

	Route	Station (mi)		No of Lanes	New Pvmnt Type	Distresses					Avg. Severity			
		From	To			1	2	3	4	5	S	Q	O	
2019	EWEB	60.00	61.00	2	HMAC	O2	Q1	S2				2	1	1.5
	EWEB	61.00	62.00	2	HMAC	O1	Q1	S2						
2018	EWEB	60.00	61.00	2	HMAC	Q1	S2					2	1	0.5
	EWEB	61.00	62.00	2	HMAC	S2	Q1	O1						
2017	EWEB	60.00	61.00	2	HMAC							0	0	0
	EWEB	61.00	62.00	2	HMAC									
2016	EWEB	60.000	61.000	2	HMAC							0	0	0
	EWEB	61.000	62.000	2	HMAC									

Figure 4-2. Example of analyzed field performance data for I88-60.5

The average severity of the centerline deterioration distress (S) is calculated for each section and presented in Figure 4-3. As shown in the figure, the severity of all the sections reached at least one after three years of service life. The I88-60.5 and I294-34 showed the highest rate of the distress development and reached the average of 2 at the fourth year of their service life. The calculated average severity of this distress for different sections suggests that the centerline deterioration stops growing after five years of service life. However, maintenance strategies should be applied in order to prevent the development of joint deterioration as surface water can penetrate through the cold joint and affect the structural capacity of the sublayers.

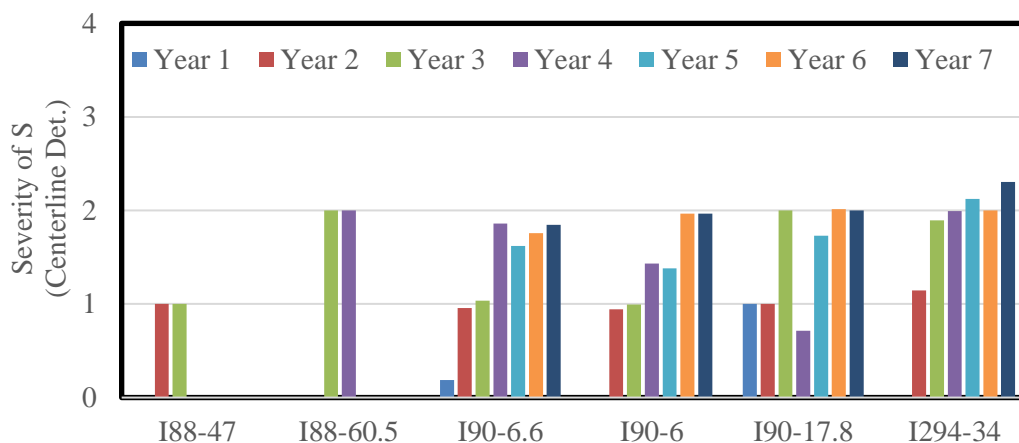


Figure 4-3. Average severity of centerline deterioration distress (S) as a function

of service life

As shown in Figure 4-4, Section I88-47 did not have longitudinal/center lane crack problem after three years of life. On the other hand, the severity of this distress reached one on section I88-60.5 after four years in service. Similar to the CRS and “S” distress, the I90-6.6 and I90-6.0 performed alike in terms of “Q” distress and did not grow considerable longitudinal/center lane cracks. I90-17.8 was the worst performing section in “Q” distress based on CRS data. This is aligned with the block cracks observed on this section. The I294-34 section developed some “Q” cracks after seven years of service life. Given the high traffic load that this section carries, it was expected to observe “Q” cracks on this section.

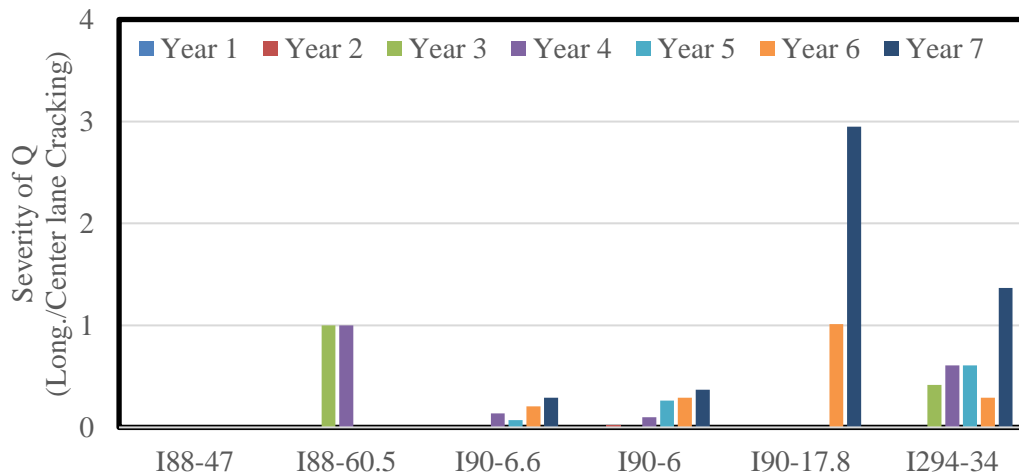


Figure 4-4. Average severity of longitudinal/center lane cracking distress (Q) as a function of service life

Figure 4-5 shows the average severity of “O” distress in the studied sections. As expected, the I294-34 section developed the highest severity of “O” distress. As mentioned before, the asphalt layer is placed on jointed concrete and the cracks observed on the surface (see Figure 2-3) are reflected from the concrete joints. Similar to the

previous performance indices and distresses, I90-6.6 and I90-6.0 are performing comparably. This similarity will be used later to set the criteria on the DC(T) fracture energy of the mainline mixtures. Section I90-17.8 was performing very well in terms of “Q” distress but suddenly started to grow the transverse cracks at year six. It appears that the I88-60.5 section has high potential for the transverse cracking and does not benefit from a crack resistant mix. That being said, this mix performed very well in all of the cracking tests and was one of the two best performers in the DC(T), I-FIT, and IDEAL-CT tests. It should be mentioned that this section was the shortest among the studied sections (less than two miles) and there might be difficulties associated with a comprehensive survey due to this short length. Another possible reason for this discrepancy between laboratory and field performances is the quality of construction. According to Table 2-1, this short section is paved using SBS modified asphalt mixture and is located between the rubber modified test sections and might have been placed on rubblized concrete pavement.

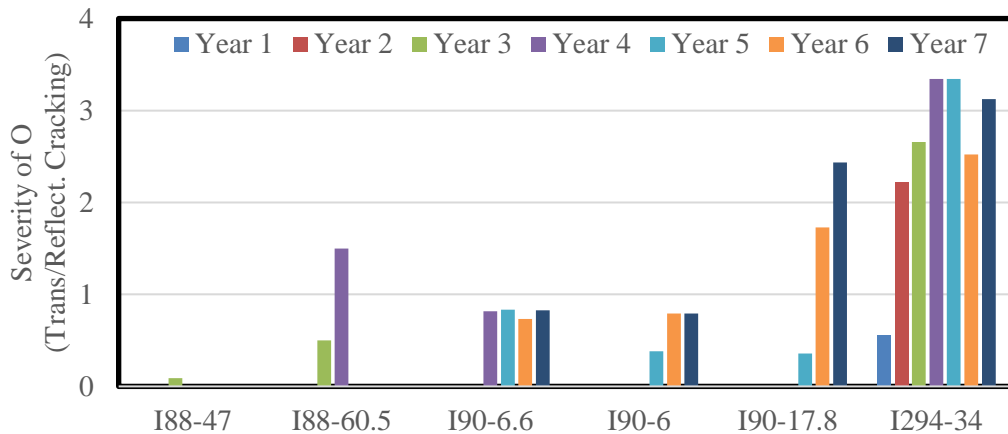


Figure 4-5. Average severity of transverse/reflective cracking distress (O) vs. service life

4.3. International Roughness Index (IRI)

Pavement roughness is generally defined as an expression of irregularities in the pavement surface that adversely affect the ride quality of a vehicle (and thus the user). Roughness is an important pavement characteristic because it affects not only ride quality but also vehicle delay costs, fuel consumption, and maintenance costs. Roughness is also referred to as “smoothness” although both terms refer to the same pavement qualities. IRI is a standardized measure of the reaction of a vehicle to roadway profile and roadway roughness as expressed in “inches per mile”. Generally, higher IRI values represent rougher roads and vice versa. IRI is used to define a characteristic of the longitudinal profile of a traveled wheel track and constitutes a standardized roughness measurement. The commonly recommended units are meters per kilometer (m/km) or millimeters per meter (mm/m). Figure 4-6 shows the IRI values for the six studied sections by year. As shown in the figure, the IRI trends are very similar to those of CRS presented in Figure 4-1.

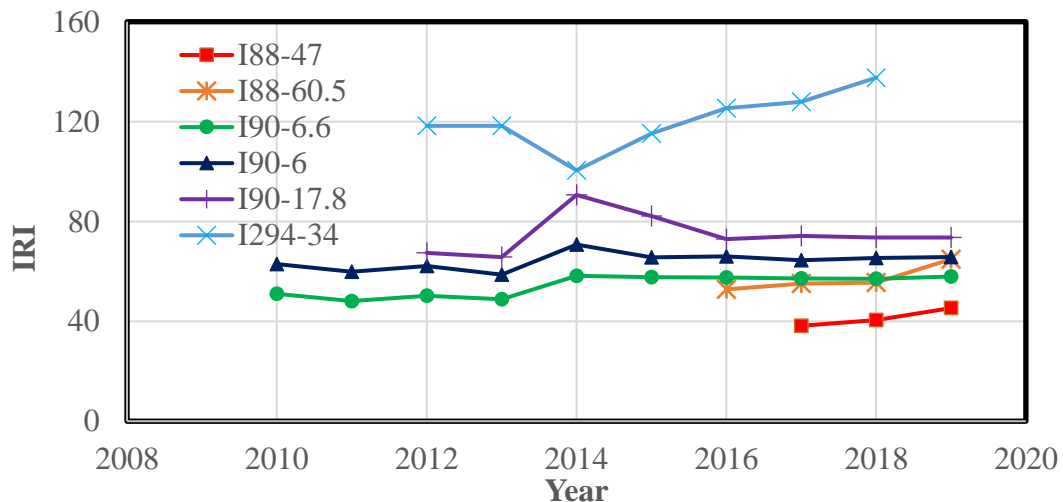


Figure 4-6. Comparison of IRI values vs. year in service

The I294-34 section recorded the highest roughness, which accumulated at a high rate. It is noted that the block cracks observed on I90-17.8 did not affect the ride quality and the IRI did not increase considerably even in recent years as compared to CRS values. The I90-6.0 and I90-6.6 sections performed well and had smooth ride quality. The other two sections, I88-47 and I88-60.5, did not have considerable aging and are at early stages of service life.

4.4. Rut Depth

The permanent deformation measured on the surface of the studied sections is presented in Figure 4-7. It is noted that the measured rut depths sometimes exhibit a decrease in rut depth in specific years. These unexpected rebounds are likely data anomalies, especially since they are such low values. That notwithstanding, and somewhat coincidentally, the final rut depths measured in 2019 are similar to the rut depths measured in the lab using the Hamburg test. Referring to Figure 2-15, the I90-6.6 mix had the highest rut depth (6.6 mm) at 20,000 passes under Hamburg wheels which is in accordance with the field performance. Also, I88-60.5 was the best field performer in terms of rutting and accordingly recorded the lowest rut depth (3.6 mm) in Hamburg test. These correlations and comparable field and laboratory rut depths show that the Hamburg test was able to mitigate the rutting distress, and the requirements already set for this test (20,000 at 50 °C) for mainline sections appear to be quite conservative.

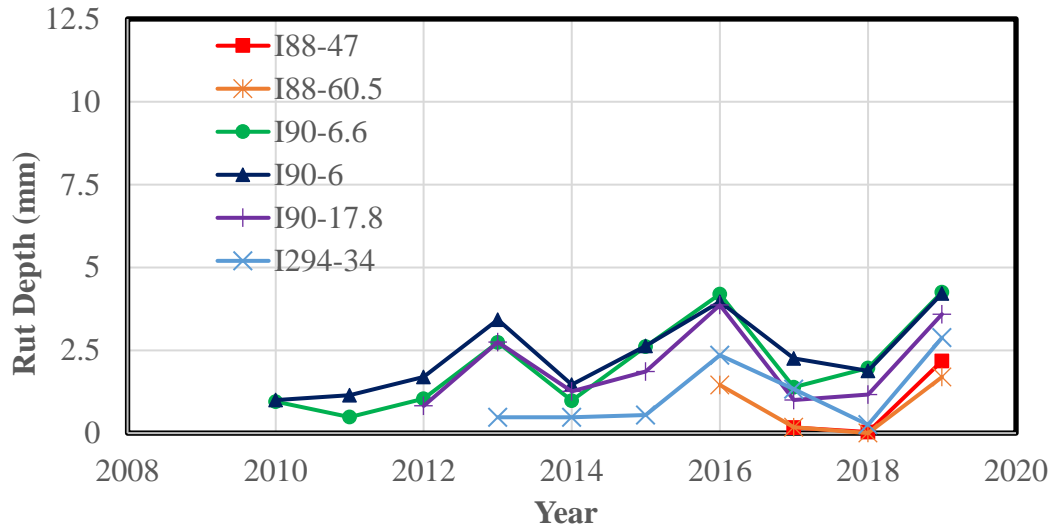


Figure 4-7. Comparison of rut depth values vs. year in service

4.5. Specification Development

4.5.1. Overview

This chapter presents the data and methods used to validate and calibrate the Illinois Tollway asphalt mixture design specification. Based on observations from the site visit (Chapter 2) along with the field performance data (Chapter 4), various forms of cracking occur more frequently on Tollway pavements as compared to rutting. That notwithstanding, a systematic process was developed and deployed to validate, and to calibrate the Tollway’s asphalt mix performance test thresholds as they relate to cracking, rutting and moisture damage. Adding and/or consolidating mix type categories was also addressed in an effort to match the recommended specification with current and future mix design practices. The concept of using the Hamburg as the primary screening method to evaluate moisture damage is also discussed.

4.5.2. Performance Test Use in Asphalt Mix Design Specifications

As presented earlier in this report, it is recommended that the Tollway retain its existing asphalt mix design performance tests in its asphalt mix design specification, namely the DC(T) fracture energy and Hamburg wheel tracking tests. Before reviewing/adjusting specification limits, a brief review of the testing parameters used in the existing specification and their link to performance is presented.

The Illinois Tollway has considerable experience in using the DC(T) test as part of mix design and material characterization. In this section, the data leading to the recommendation to retain the DC(T) test in the Tollway's mix design specification are reviewed. The ability to closely correlate a performance test criterion (or multiple criteria) to field performance should be a key consideration in selecting a performance test for a given distress category. Figure 4-8 shows an existing correlation between transverse cracking and fracture energy (colloquially referred to as "the bubble plot"), using data collected from field sections in various northern states in the US such as Minnesota, Missouri, and Illinois. As shown, there is a clear trend between DC(T) fracture energy and transverse cracking. The data in this plot has a rectangular hyperbola shape; mixtures with fracture energy above certain threshold have low-to-medium transverse cracking, while mixtures with low fracture energy values tend to have thermal cracking levels that 'bubble upwards' with age. As fracture energy of the asphalt mixture drops, the observed transverse cracking in the field increases (and the data dispersion, which is a factor in design reliability), with a sharp upward trend in the curve in the range of 400 J/m². The steep upward tick in the curve is likely related to the delineation between more brittle and more ductile binder systems. This is binder, aggregate, mix

design, recycling and age dependent. Mixtures that behave as brittle when tested in the DC(T) at 10 °C warmer than the PG low temperature plan grade (whether or not this happens may depend on the age of the mixture) are found to have low fracture energy values. Mixtures with fracture energies in excess of 600 J/m² are clearly found to have very low transverse cracking in this data set, and probably will not develop significant thermal cracking even in later stages of their service life (higher reliability design).

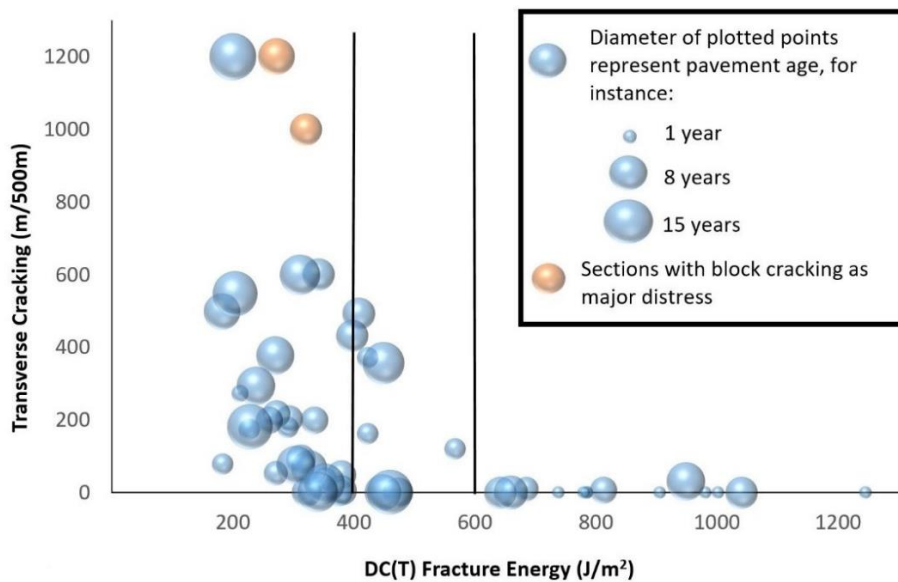


Figure 4-8. Transverse cracking vs. DC(T) fracture energy (Buttlar et al., 2018)

Figure 4-9 shows the amount of cracking for five SMA sections in Illinois and eleven dense graded sections in Missouri. These sections are added to the previous sections in Figure 4-9 to further investigate the correlation between the cracking potential and DC(T) fracture energy. To this end, the previous sections are shown as faded bubbles while the new sections have less transparency to be more distinguished. The relation between the cracking amount and the DC(T) fracture energy appears to be very similar to the one observed in the original bubble plot shown in Figure 4-8. This indicates that the

investigated sections in this study can be used to extract the correlation between the cracking in-situ and DC(T) fracture energy calculated in the lab.

As mentioned before, the CRS is the parameter used by Illinois Tollway to quantify the condition of the roads based on the type, extend, and severity of the distresses. As cracking, especially transverse cracking, is the main type of distress observed in Illinois and Missouri roads, it is attempted to use this parameter to establish a correlation between CRS loss per year and DC(T) fracture energy. To this end, the change (drop) in CRS during the life of each section is calculated and then is divided by the age of the section in years. The resultant parameter is called CRS loss per year and is shown in Figure 4-10 for sixteen sections in Illinois and Missouri. In this plot, the Mo151 section with a fracture energy of 180 J/m² recorded the highest CRS loss per year (≈ 0.9), whereas the I90-6.0 section in Illinois benefitted from a high quality SMA friction surface type mix and yielded the highest fracture energy and lowest CRS lost per year.

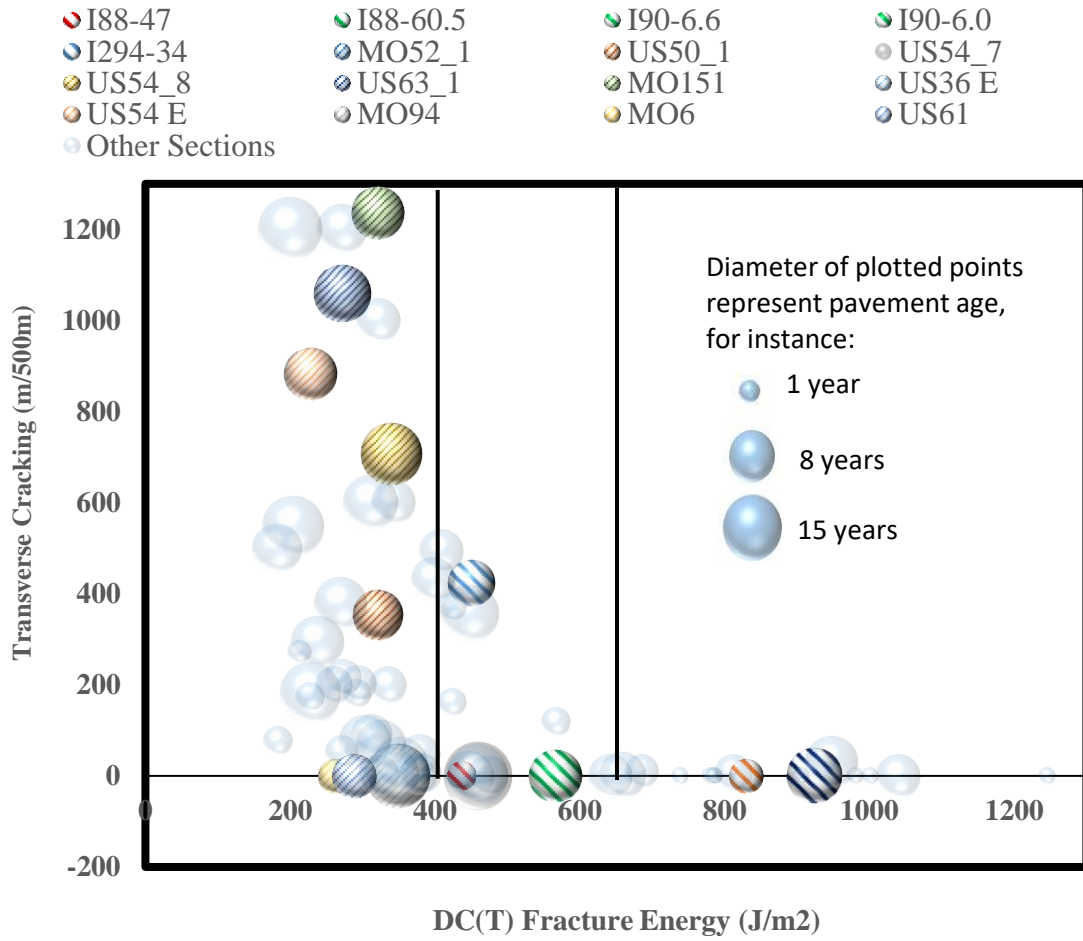


Figure 4-9. Superimposed sections investigated in this study on the bubble plot

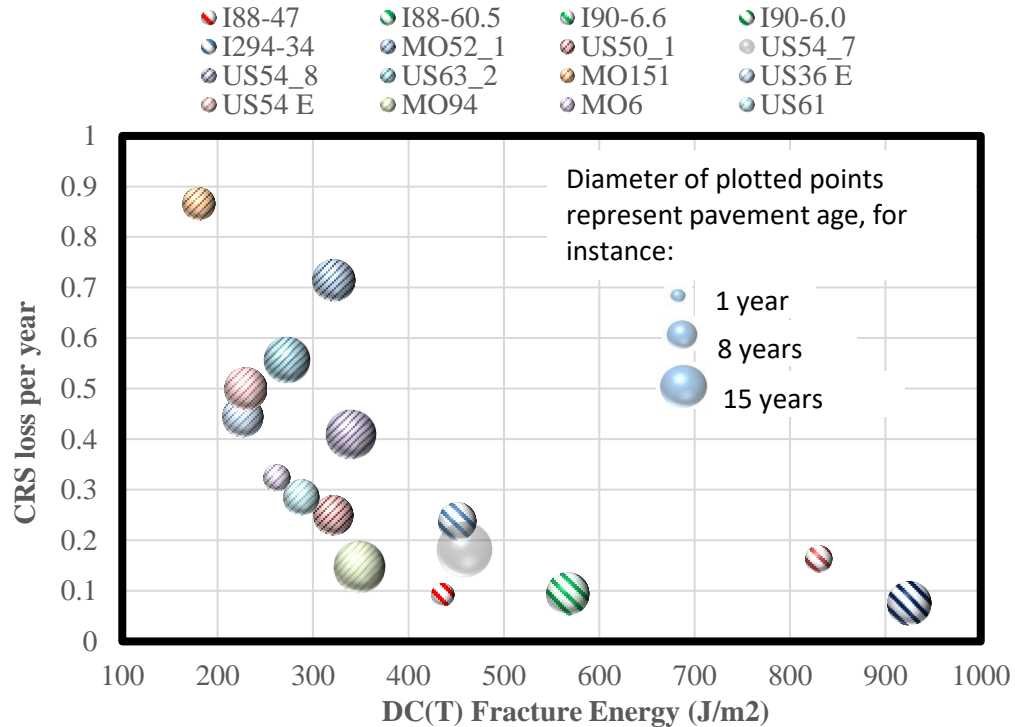


Figure 4-10. CRS loss for the investigated sections in Illinois and Missouri vs. DC(T) fracture energy

an inverse function $[y=a/(x+b)]$ is used to fit the data already presented in Figure 4-11. In this function, y is the IRI deterioration rate, x is the DC(T) fracture energy, and a and b are model coefficients. Yielding an R^2 of 66.5%, this function is believed to properly describe the correlation between the field performance and DC(T) fracture energy. It can be noted that the CRS loss starts to increase with a higher rate when the DC(T) fracture energy approaches 400 J/m^2 . Also, a section with fracture energy close to 600 J/m^2 appears to benefit from high reliability of withstanding the cold events and losing a low CRS value of 0.15 per year. These observations are aligned with the recommendations in Buttlar et al., 2018.

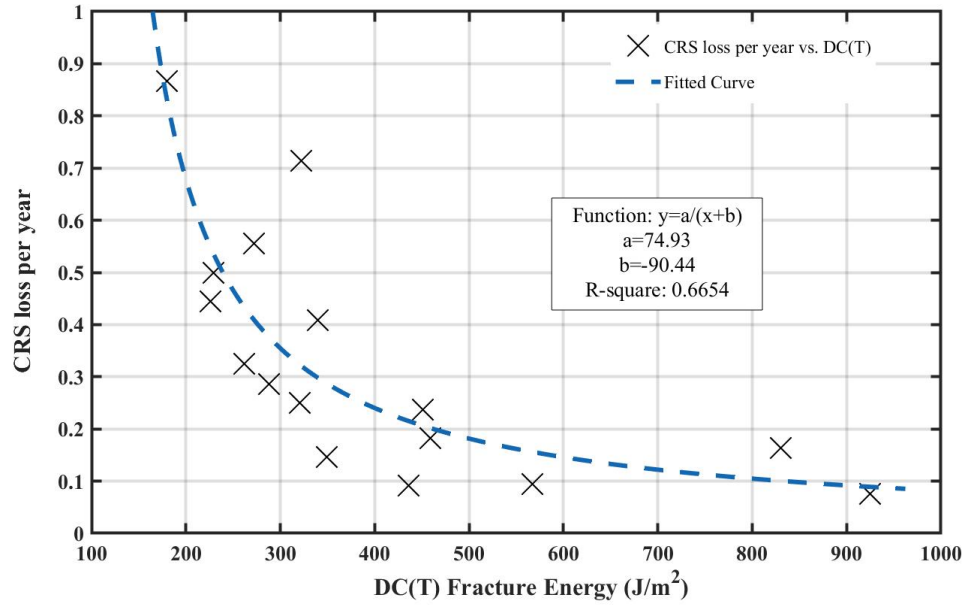


Figure 4-11. Correlation between CRS loss per year and DC(T) fracture energy ($R^2=66.54\%$)

Similar to the DC(T) test, the capability of the I-FIT to predict the field performance has been investigated through the correlation between the FI parameter and CRS loss per year. To this end, Figure 4-12 depicts the sections investigated in Illinois and Missouri. Overall, it is observed that as the FI increases, the CRS loss lowers as a result of a better cracking resistance. The FI of I88-60.5 section has the highest but does not have the lowest CRS loss per year. According to the results presented in Chapter 3, FI parameter is significantly dependent on the aging. Therefore, it is expected to see a drop in the FI parameter as this relatively young section ages. The same inverse function [$y=a/(x+b)$] was employed to study the quality of the fit and an R2 of 48.38% was obtained. Compared to the DC(T) correlation with the field performance, the FI parameter described lower variability in the field measurement, meaning that the DC(T) could be a better choice for the spec development.

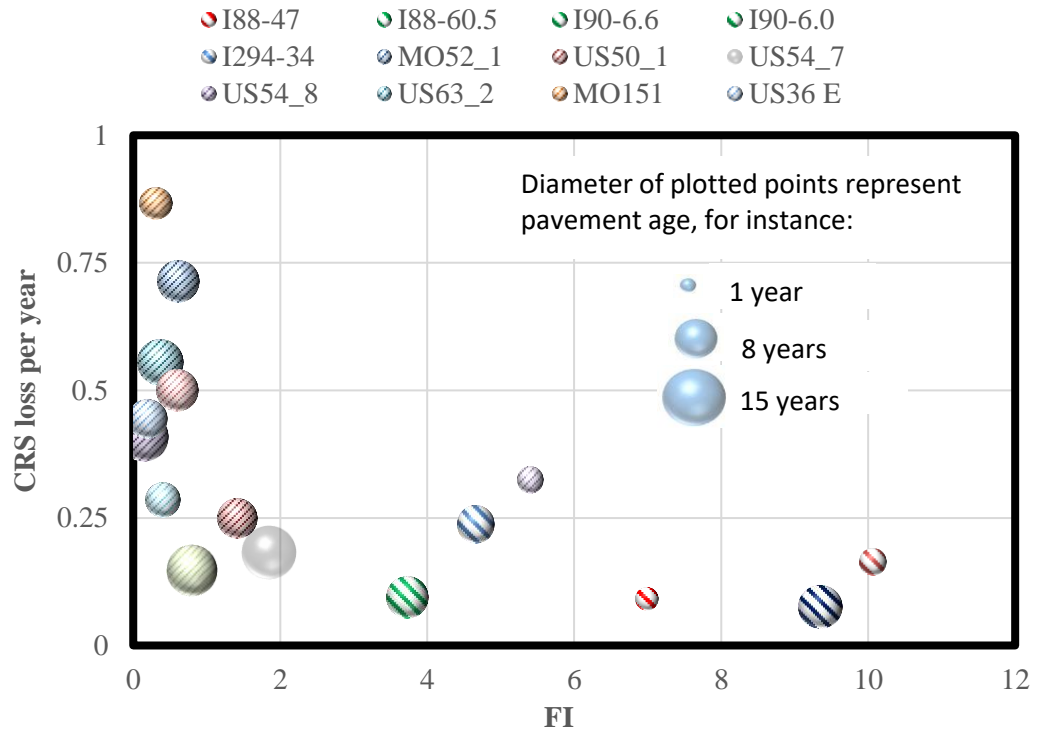


Figure 4-12. CRS loss for the investigated sections in Illinois and Missouri vs. FI

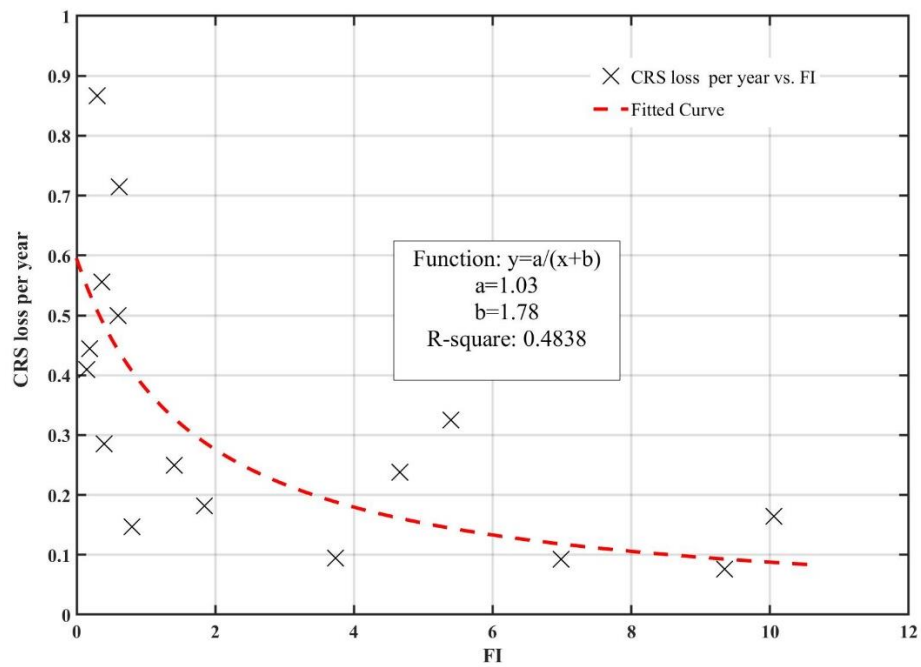


Figure 4-13. Correlation between CRS loss per year and FI ($R^2=48.38\%$)

As discussed in sections 2.5.2 and 3.3.5, the repeatability of the test is another key factor that should be considered when a performance test is being selected. As shown in Table 3-5 and Table 2-4, the DC(T) test produced low COV's for both plant-produced and field-cored samples, lower than either the IDEAL-CT or I-FIT tests. Lower COV values allow laboratories and transportation authorities to make more confident decisions, especially when borderline results are obtained.

Another key consideration in performance test selection is its ability to characterize and score (or to rank) asphalt mixes based on clear performance expectations. In other words, an expensive mix (such as SMAs) containing high quality aggregates and modified binder system along with premium volumetrics (e.g. high VMA) had led to nearly two decades of outstanding rut and cracking resistance in the field for the Illinois Tollway. Therefore, SMAs are expected to attain better cracking scores than dense-graded mixes, those containing unmodified binders, and mixes with lower aggregate quality or volumetric requirements (binder/shoulder mixes). In addition to meeting this expectation better than the I-FIT or IDEAL tests, the DC(T) was found to logically capture the effects of different mix ingredients. For example, although a similar binder system was used in both the 1824 and 1836 mixes, mix 1824 was categorized as an SMA friction surface mix due to its higher aggregate quality. This difference has been reflected in DC(T) fracture energy, where mix 1824 had almost 200 J/m² higher fracture energy than 1836 mix at -12 °C. On the other hand, the I-FIT and IDEAL tests sometimes scored dense-graded mixtures higher than SMA mixes. Finally, the DC(T) is more stable and predictable with respect to sample air void levels and mixture aging level, rendering it easier to calibrate based on testing on field cores.

In addition to the notes learned from the Illinois Tollway's mixtures, a statistical analysis of the four plant mixtures in Missouri was conducted in terms of each performance test conducted. As reported in Table 4-2 Total Degrees of Freedom (total DF=total number of replicates -1), F-value and P-value results obtained from the ANOVA test are included in the tabulated results. A significance level of 0.05 was used, as described earlier. As mentioned before, four replicates for each section were tested under the DC(T) and I-FIT cracking tests; while three replicates were used in IDEAL-CT, IDT, and HWTT based on material availability. As the p-value results suggest, only the IDT test failed to make some distinction between mixtures (P-value>0.05). The other performance tests yielded p-values greater than 0.05, indicating statistically significant differences between the measured performance indicators for at least two sections investigated. The DC(T) fracture and Hamburg tests ranked US54_1 as the best performer, while MO13_1 ranked the best in the I-FIT and IDEAL-CT tests. The DC(T) test exhibited three ranking groups (A, B, and C), while the other tests had a maximum of two ranked groups. This implies that DC(T) could more distinctly rank the performance of these four mixture types. In terms of test evaluation, the statistical method used herein has advantages over simply comparing test repeatability, such as COV, or the spread in test data across the sections investigated. Rather, the statistical method looks at these factors in a simultaneous fashion. Thus, the DC(T) exhibited the best combination of test repeatability and data spread, such that three distinct data groupings were observed. For the purposes of mix design, and QC/QA, the DC(T) would be a better delineator between mixes as compared to the other methods, at least for the four mixtures studied herein.

Table 4-2. ANOVA results and Tukey ranking

Statistical Parameter	DC(T) G_f	IDT	I-FIT	IDEAL-CT	HWTT
Total DF	15	11	15	11	11
F-value	16.64	2.27	12.43	12.45	15.58
P-value	0.000	0.157	0.001	0.002	0.001
Section (Plant Mix)	Ranking				
US54_1 (33-0-33)	A	A	B	B	A
MO13_1 (17-17-0)	A-B	A	A	A	B
US54_6 (31-31-0)	B	A	B	B	B
US63_1 (35-35-0)	C	A	B	B	B

4.5.3. *DC(T) Spec Calibration Process*

Following the recommendation to retain the DC(T) as the cracking test in the Tollway mix design specification, Figure 4-14 presents the approach developed by the research team to calibrate the specification for various mix types. In the first box, the threshold for DC(T) fracture energy must be chosen for different mix types based on field performance observations and testing results obtained on field cores. For example, by comparing poor performing and good performing sections and their corresponding DC(T) fracture energy results, baseline thresholds can be established. These can also be compared to the bubble plot which includes data from other studies (Figure 4-8) to ensure that recommendations are in range with broader national trends. However, it is acknowledged that the Tollway thresholds should be set towards the most stringent extreme of national thresholds because: (1) at DC(T) test temperature of -12 °C is desired by local practitioners, but this is more than 10 °C warmer than the PG low temperature for Chicagoland for a 98% reliability level and therefore somewhat unconservative (suggesting that fracture energy

thresholds should be adjusted upwards to account for the warmer test temperature used), and; (2) a very high reliability should be used in Tollway pavement material specifications, considering the very high traffic levels, high speeds, and in consideration of the high user delay costs associated with construction and maintenance activities on the Tollway.

The core samples tested and used to define the DC(T) threshold have been long-term aged in the field. However, in order to circumvent the impracticalities associated with long-term aging of mixtures in the lab prior during mix design, the effect of the aging must be calibrated into the specification limits for tests carried out on short-term aged specimens. In the next box shown in Figure 4-14, standard deviations associated with DC(T) testing will be used to account for test variability as a means to instill a high degree of reliability into the thresholds. SMA friction surfaces should have the highest reliability levels, as they are used on the surface of the mainline pavement in high traffic load sections and/or on the curves to provide skid resistance. Therefore, SMA friction surface type mixes have been assigned the highest level of reliability, as discussed later. The reliability approach developed is also intended to cover the uncertainties associated with field performance data collection and evaluation, and variabilities associated with test scores. Finally, comments and recommendations from experts serving on the study TRP were used, as shown in the last box (consensus step), to capture practical limitations which, for instance, can help avoid high bid prices for certain mix types based on limitations in locally available materials with respect to reaching certain DC(T) thresholds for certain mix types. Consensus adjustment can also create more uniform and logical spreads between thresholds assigned to various mix types in the specification.

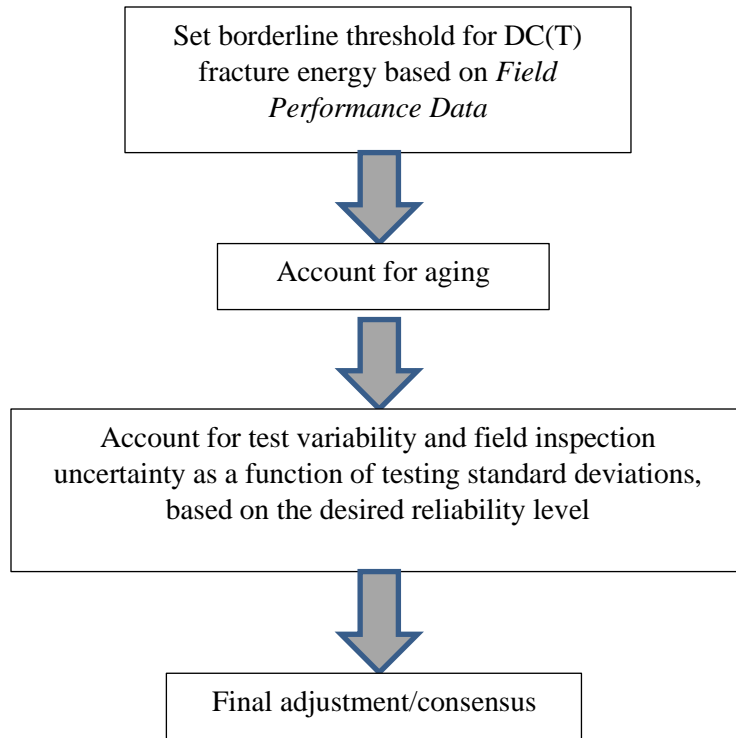


Figure 4-14. Steps in DC(T) spec development

4.5.4. Hamburg Test in Mix Design Specification

The Hamburg wheel tracking test has been used by many agencies across the U.S. to evaluate both rutting and stripping potential of the asphalt mixtures. The test has the capability to be performed at different temperatures as the water tank temperature is adjustable. Often, the test is performed at 50 °C and up to 20,000 wheel passes are used, based on traffic level. Limits such as 12.5 mm rut depth or lower are established, based on traffic level. Given the fact that the traffic load on the Tollway road facilities is relatively high (with AADT values up to 66,000 with 10% commercial vehicles), perhaps more than 20,000 wheel passes should be used. Instead, for practical reasons, the number of wheel passes is kept to 20,000 for SMAs and the maximum allowable rut depth is decreased to 6.0 mm to increase mix reliability (since this level is easily met with high quality aggregates, especially in higher ABR mixes). Following this approach, the

Tollway has not experienced rutting issues on mainline pavement in the era of Hamburg use. For the binder mixtures (both shoulders and mainlines) and shoulder surface mixtures, lower wheel pass levels and higher rut levels are allowed in the specification. As no evidence of stripping has been observed, it is suggested to maintain SIP requirements. However, it is recommended that the mix be declared as non-stripping for mixes with Hamburg rut depths lower than 4.0 mm, to avoid erroneous slope ratio and SIP values that sometimes occur in very stiff mixes.

4.5.5. Effect of Depth on Pavement Response

The Tollway performance specification covers not only surface mixtures, but also binder course mixtures that are used in both mainline and shoulder layers. Therefore, the loading and environmental conditions for binder course layers need to be considered and factored into the test criteria. In this section, the effect of depth for low temperature (cracking) and high temperature (rutting) performance and its implications on adjustment of PRS thresholds will be discussed.

Asphalt pavements experience the most extreme cold temperatures on the pavement surface during cold winter nights; temperatures in binder courses never reach these extreme levels. Figure 4-15 presents a pavement temperature analysis for very cold, 48-hour duration on a section located in Frazier, Minnesota which was investigated during the SHRP project in 1993. As shown, the difference in temperature at the top and a point 2 in. deep in the pavement is almost 4 °C at the lowest temperature peak. The difference in temperature extremes, and accordingly, the lower temperature gradients (cooling rates) in binder courses leads to lower tensile stress in these deeper layers of the pavement. Based on typical viscoelastic properties at low temperatures and using a convolution

integration, the tensile stress induced at different depths has been calculated as shown in Figure 4-16. This analysis reveals that there is approximately 40 % difference between the stress levels at the surface and 2 in. deep in the pavement (reduction from 500 to 300 psi) during critical conditions. This significant difference in material response provides motivation to develop less stringent performance test requirements for binder course mixes to allow economical designs. To the end, an analysis of Illinois temperature data, and simple methods to apply the results to the adjustment of specification values were developed

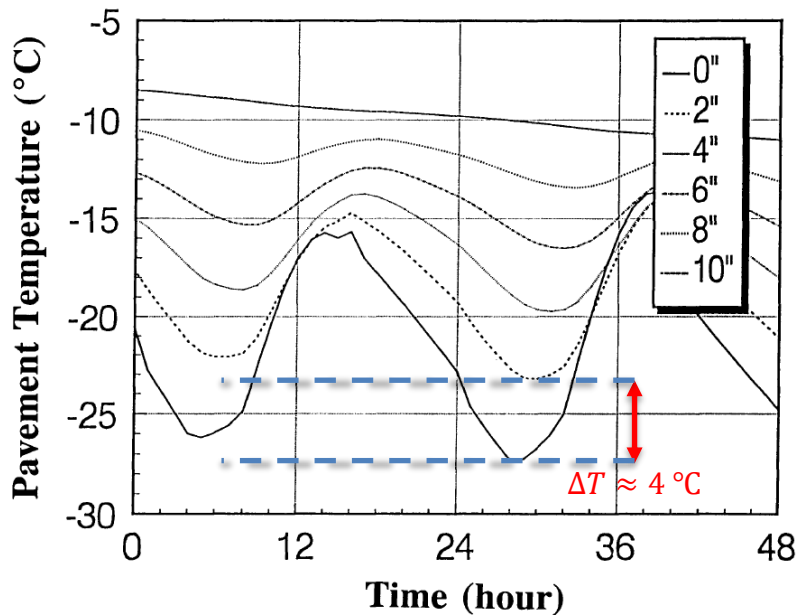


Figure 4-15. Effect of depth on the layer temperature as a function of depth (SHRP A357 Report, 1993- Location: Frazier, Minnesota)

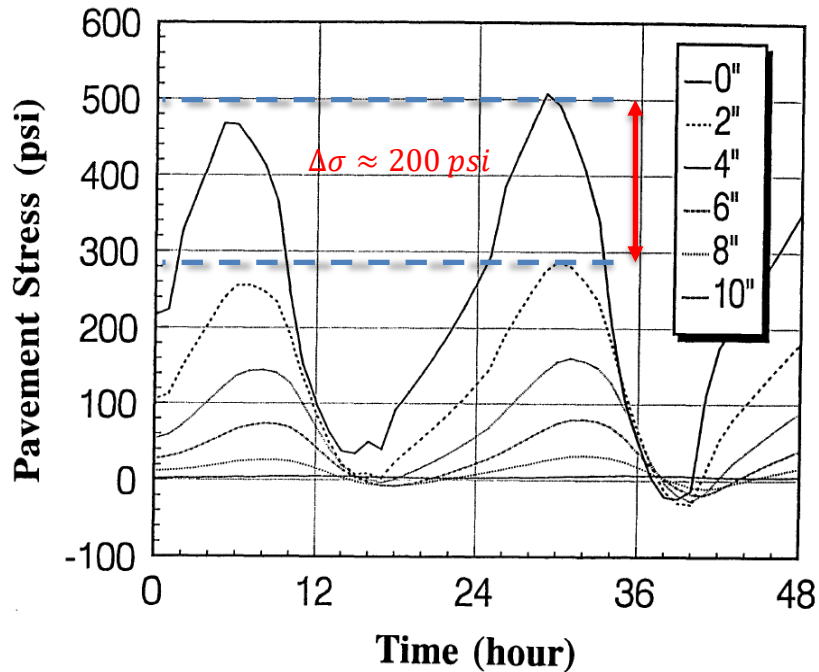


Figure 4-16. Stress relaxation due to depth (SHRP A357 Report, 1993- Location: Frazier, MN)

Using LTPP bind software, the pavement temperature data for the Chicago area at different pavement depths and reliability levels were extracted as presented in Figure 4-17. The station used for the pavement low temperature analysis is very close to the sections that were cored on I88 route (Station Name: Rochelle, ID: IL7354, MP=76 on I88). This provides the chance to investigate the temperature conditions of the sections whose field performance were studied. Considering 98 % reliability, the temperature of the pavement was determined as $-27.2 \text{ }^{\circ}\text{C}$ while it was calculated to be $-24.3 \text{ }^{\circ}\text{C}$ at a level of 50 mm of depth in the pavement. Following the temperature analysis shown in Figure 4-15, there was a $3 \text{ }^{\circ}\text{C}$ difference between the temperature determined at the surface and at depth of 50 mm ($\sim 2 \text{ in.}$). Scaling based the assumption of linear viscoelastic behavior, a 30% drop in thermal-induced stress is expected. Although a more rigorous viscoelastic analysis of specific creep data obtained on Tollway pavements would yield higher

accuracy, this estimate was instead used for brevity and considering the need to calibrate the model to account for other uncertainties that exist in practical mix design.

Clearly, data from the LTPPBind software suggest that a lower testing temperature should be used for DC(T) testing in the Chicagoland area. The DC(T) test temperature of -12 °C corresponds to a low pavement temperature of -22 °C, as normally the DC(T) test is performed at 10 °C warmer than the pavement temperature. Based on the determined pavement temperature at the 98 % reliability level (-27.2 °C), the DC(T) test should be performed at -17.2 °C. However, as the Tollway has been previously conducting the DC(T) test at -12 °C, this temperature has been retained, and the temperature difference will be accounted for as part of the calibration of the performance specification.

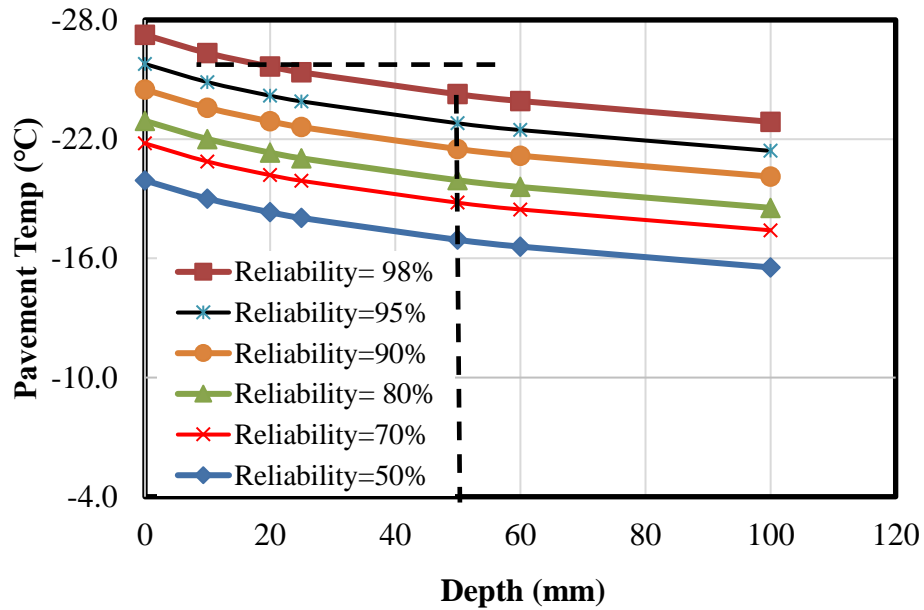


Figure 4-17. LTPP bind software outputs for pavement temperature in winter as a function of depth and reliability in Northern Illinois

The LTPPBind software was used to extract the pavement temperature data during summertime in the Chicago area. A weather station entitled Lake Villa (ID: IL4837),

which has a similar latitude as the I90-6.6 and I90-6.0 sections, was selected. As shown in Figure 4-18, the temperature difference between the surface and 50 mm depth in the pavement was determined to be 6.7°C (52.5-45.8=6.7 °C). This is clearly more significant compared to the low temperature differences computed. Although the Hamburg test is normally performed at 50 °C, the environmental conditions are less stringent for the sublayers in terms of pavement high temperature. Therefore, a less stringent criteria (or lower number of passes) should be considered for the binder course mixtures.

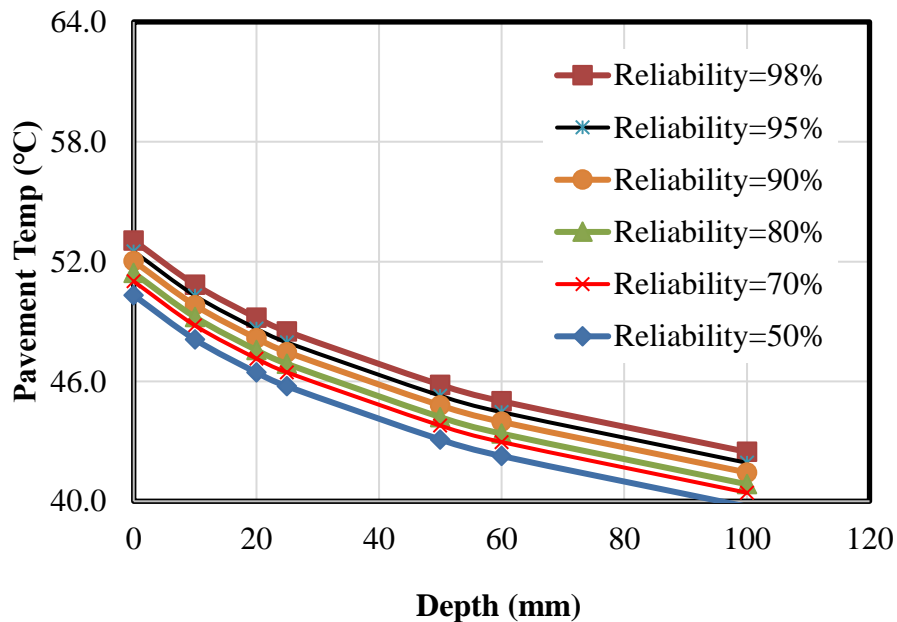
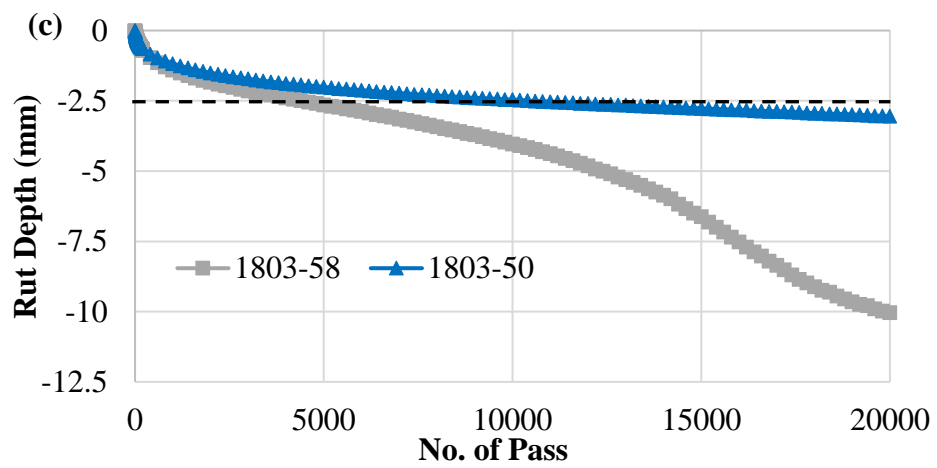
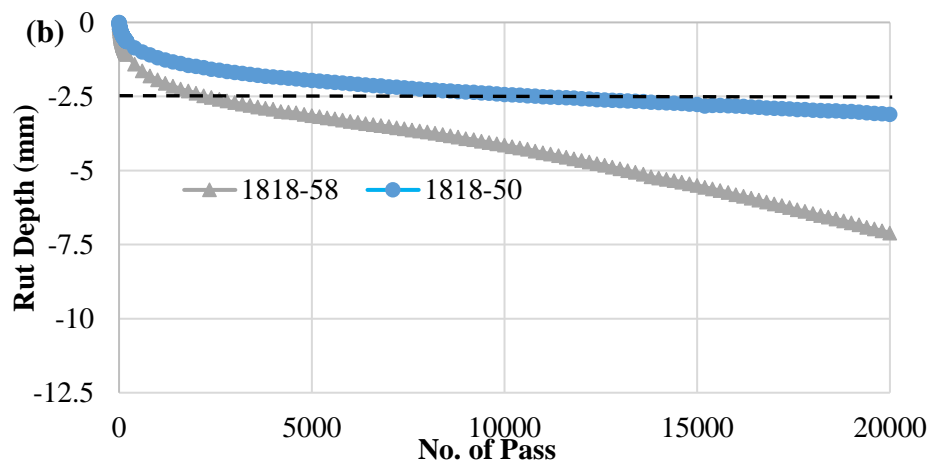
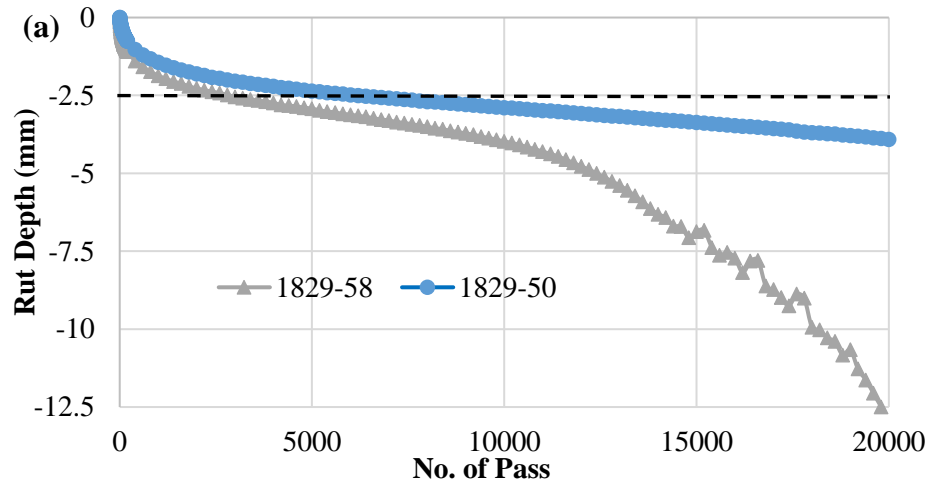


Figure 4-18. LTPP bind software outputs for pavement temperature in summer as a function of depth and reliability in Northern Illinois

To investigate the effect of temperature on the rutting performance of the asphalt mixtures, Hamburg tests at temperatures other than 50 °C were performed on the plant-produced mixtures. Figure 4-19 shows the rut depth as a function of wheel passes at 50

and 58 °C. Although the pavement temperature is not expected to reach 58 °C, as discussed above and shown in Figure 4-18, this testing temperature was selected such that a higher rut depth could be measured. Also, the 8 °C difference between these two testing temperatures is in the range of the 6.7 °C temperature difference determined using the LTPP bind temperature data. The difference between the observed rut depths at these two temperatures will be used to identify the number of passes that could be reduced from the requirements for the binder course mixtures. In essence, a wheel pass-to-temperature superposition principle has been established.

To this end, a rut depth of 2.5 mm was selected as the reference point. This rut depth was chosen because in most cases at 50 °C, the rut depth recorded by the test sample will attain this level just after the densification phase. The difference in the number of passes to reach this level of rut depth at 50 and 58 °C was then determined to account for the less severe environmental conditions in the subsequent layers. Table 4-3 summarizes the number of wheel passes to reach 2.5 mm for different mixtures at 50 and 58 °C. The average of this wheel pass difference was then calculated as 4,680 passes. After rounding, 5,000 is proposed to be used to reduce the number of required wheel passes for IL-4.75 mixtures to account for the lower temperature present at that depth in the pavement.



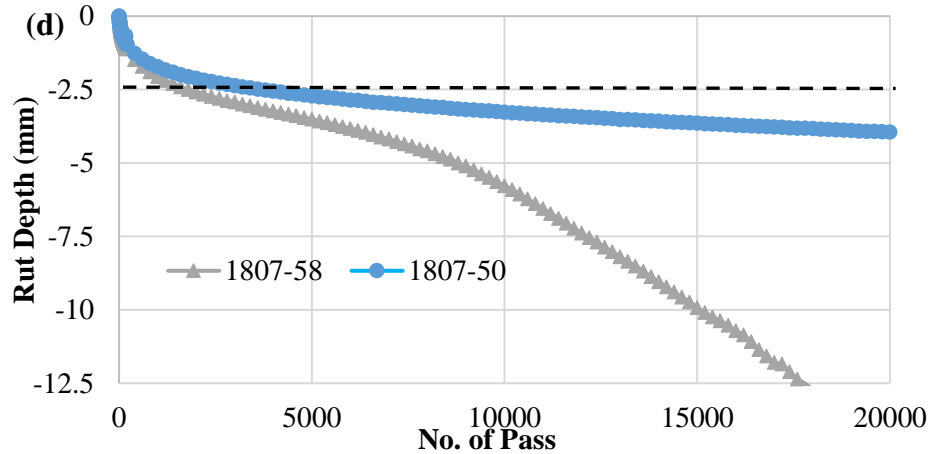


Figure 4-19. Comparing Hamburg testing results at two different temperatures, a) 1829, b) 1818, c) 1803, d) 1807

Table 4-3. Number of passes to reach 2.5 mm rut depth

Mix	58 °C	50 °C	Diff. in No. of Passes
1829	2900	6200	3300
1823	1100	4500	3400
1818	2400	11000	8600
1803	4500	10600	6100
1807	1800	3800	2000
	AVG		4680

As already shown in Chapter 3, Figure 3-13, the only mixture which could not meet the existing Hamburg requirements was the 1828 mix. This mix is an IL-4.75 type mixture, which is used below the road surface (at least 2 in. underneath the top of the pavement). Previously, the Tollway called for maximum rut depth of 9 mm under 15,000 passes. As the traffic load in the binder course is not as high as the surface due to the reduction in vertical stress with depth, the required number of wheel passes was reduced from 20,000 to 15,000. Further considering the effect of depth on pavement temperature, another

5,000 pass reduction in the number of required wheel passes is recommended. Figure 4-20 shows the recorded rut depth by this mix at two different temperatures including 50 and 40 °C. As shown in Chapter 3, this mix did not perform well at 50 °C and exceeded the existing rut threshold at 15,000 passes. However, now considering a lower recommended required number of wheel passes of 10,000, the rut depth would decrease to 7.5 mm, which is within the allowable rut depth. Assuming that this mix will be used 100 mm (4 in.) below the surface, the pavement temperature would be around 42.2 °C, using the LTPP bind data presented in Figure 4-18. In this case, the rut depth measured at 40 °C (shown in Figure 4-20) assures that the maximum rut depth even at 20,000 passes will be less than 4 mm, which is quite negligible.

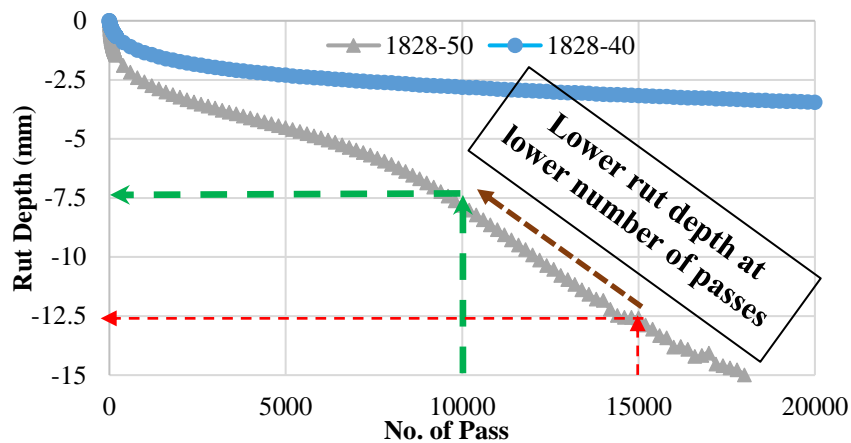


Figure 4-20. Computing a shift in number of passes for 1828 mix

4.5.6. DC(T) Spec Development

In this section, the flowchart introduced in Figure 4-14 is applied to develop the baseline DC(T) thresholds for different mixture types, which is used in the final consensus/adjustment step. Different borderlines were selected for DC(T) fracture energy based on field observations and stress analysis, such that designing below those limits

would very likely result in crack prone mixtures. Reliability was then built in by building on these thresholds. The first upwards adjustment was to take the borderline DC(T) fracture energy levels and raise them to account for the aging that the field samples have experienced. Two levels of aging adjustments (15 and 10%) have been considered for surface and binder mixtures, respectively. Afterwards, assuming that the DC(T) fracture energies obtained from testing the replicates follow a normal distribution, standard deviations according to different reliability levels for differing mixture types were developed. We now review these calculations for each mix type investigated.

Figure 4-21 presents the framework of DC(T) specification development for SMA friction surface mixtures. Considering the SMA mixtures used in sections such as I294, I90-6.6, and I90-6.0, the fracture energy recorded in I90-6.6 (560 J/m^2) was selected as the borderline for the SMA friction surface mixture category. The I90-6.0 section had an SMA fracture surface mix with fracture energy of 830 J/m^2 (see Figure 2-12) and performed very well in-situ. On the other hand, the I294-34 SMA friction surface mix possessed a fracture energy of 451 J/m^2 and experienced significant field cracking. Although the I90-6.6 section used an SMA surface mix, this section is near the I90-6.6 section and therefore had similar environmental and loading conditions. It is also worth mentioning that based on the field performance information, especially “O” cracking data, this section just reached the “O1” severity level meaning that the transverse cracking severity is changing from hairline cracking to infrequent open cracks (see Table 4-1). The 560 J/m^2 borderline set for this mixture type is obtained after testing the sections that are at least eight years old. Based on available literature (Braham et al., 2009) and also preliminary age testing results on laboratory aged samples in this study, a

15% increase was applied to account for aging on the tested field cores and switching the reference aging level for the DC(T) for the short-term aging level used in design.

Increasing by an additional 15 % resulted in DC(T) fracture energy of 644 J/m².

Like all performance tests, the DC(T) test has an inherent, non-zero COV. SMA friction surface type mixtures have been tested in both plant produced and field core sample types. The standard deviations for both sample types were reported in Chapter 2 and Chapter 3. As a highly simplified and conservative statistical approach, adding the two averaged standard deviations (plant and field core samples) to the previously calculated 644 J/m² results in DC(T) fracture energy threshold of 784 J/m². After rounding this value to the nearest 25 J/m², a DC(T) fracture energy threshold of 775 J/m² is completed and recommended for the DC(T) specification for this mix type. It should be mentioned that the two standard deviation level selected for this mix type corresponds to a minimum 95 % reliability (higher due to rounding), which is believed to be an appropriately high level for SMA friction surfaces. This mix is of high criticality, as SMA surface friction mixtures are used on sections with high traffic load (high criticality projects) and/or curves to provide skid resistance. Therefore, this high reliability level helps ensure a high degree of cracking resistance in the mixture, especially in terms of controlling low temperature cracking. This very high fracture energy level will also slow the rate of reflective cracking. Finally, after discussion, consensus was reached to use a threshold of 775 J/m² for this mix type, which was supported by the fact that almost all of the plant SMA friction surface mixtures produced in 2018 met this threshold.

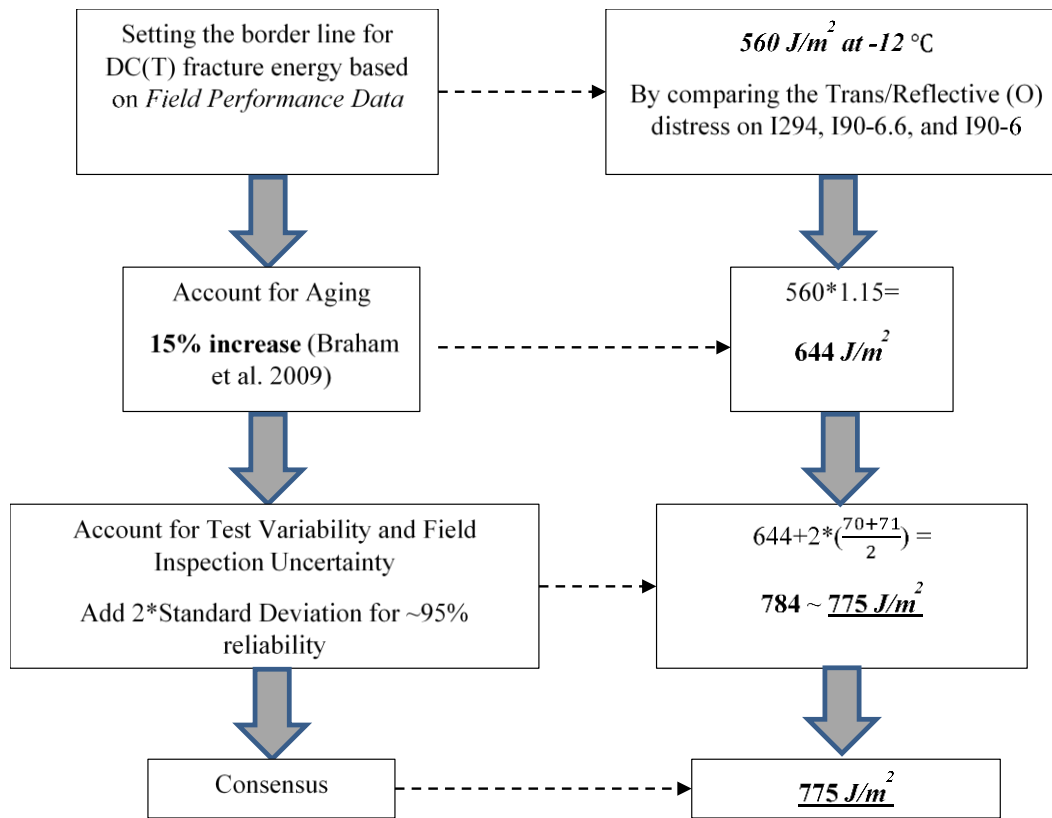


Figure 4-21. Flowchart to Calibrate DC(T) spec for SMA friction surface mixtures

The DC(T) specification for SMA surface mixtures is very similar to the one developed for SMA friction surfaces. The only difference in the DC(T) threshold setting is the reliability selected for this type of the mix. For the SMA surface mixtures, 1.5 times the averaged standard deviations was selected, which corresponds to a minimum 87 % reliability in DC(T) fracture energy results based on testing variability. After rounding the calculated threshold to the nearest 25 J/m², a fracture energy threshold of 725 J/m² was proposed to TRP. However, according to the TRP experience regarding the aggregate types normally used in this mixture type, a consensus to round down to 700 J/m² for mix economy was reached. This also provides more spread between the SMA

friction surface and SMA surface mixes, which will encourage tailored, unique mix design for the two different categories.

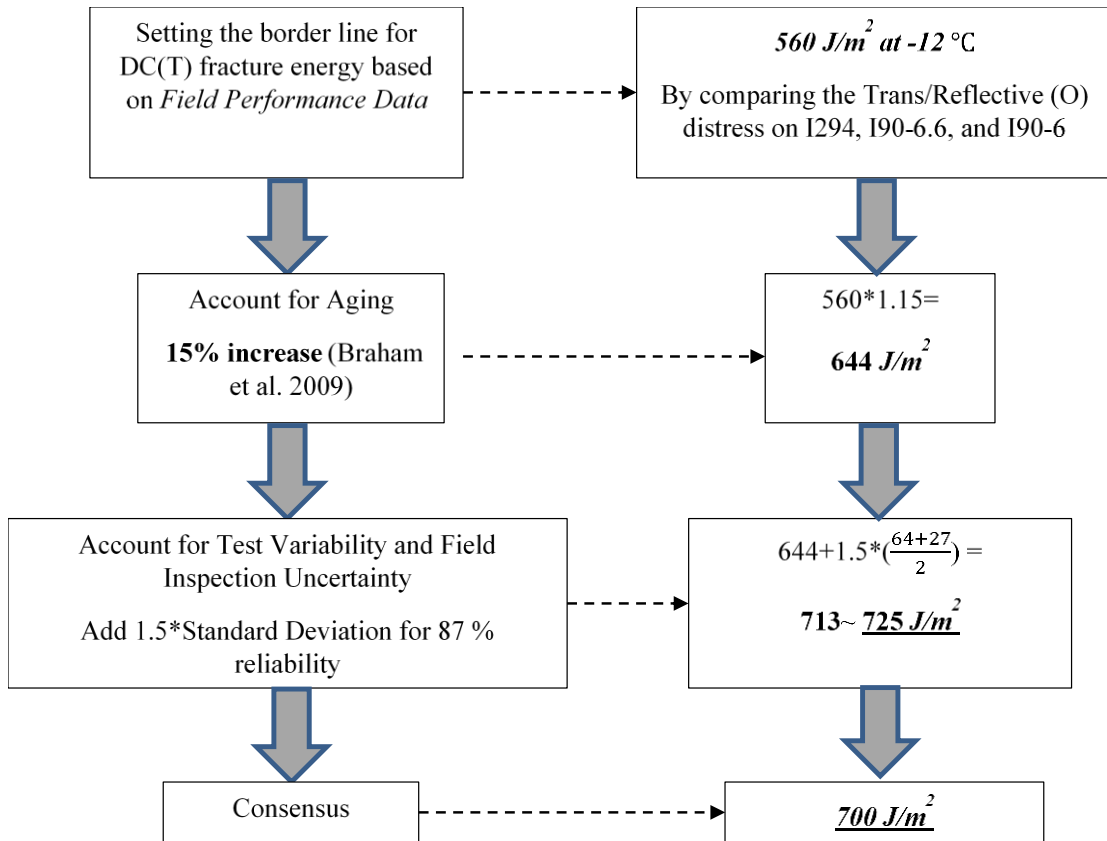


Figure 4-22. Flowchart to Calibrate DC(T) spec for SMA surface mixtures

According to the stress analysis discussed in earlier, linear scaling in fracture energy suggests that 70 % of the fracture energy required for the surface mixture should be used to establish a baseline for the SMA binders ($560 \times 70/100 = 392 \text{ J/m}^2$). In order to consider the effect of aging, a 10 % increase in DC(T) fracture energy was assumed. This acknowledges that the aging experienced in pavement sublayers will be lower than that of the surface layer. As the SMA binder mix was only tested in the form of field cores, a reliability of 95 % was achieved by taking two standard deviations based on the field core

test results for this high criticality mainline layer. This led to a DC(T) fracture energy threshold of 600 J/m^2 after rounding. During consensus discussions, it was acknowledged that Tollway has already been using a 650 J/m^2 limit for this layer, which encourages higher quality ingredients. Also, since this mix is normally used on jointed concrete pavement, additional fracture energy is thought to help slow down the rate of reflective cracking. Therefore, a consensus was reached that 650 J/m^2 should be retained for the SMA binder type mixture. In the future, this can be revisited, if full-depth asphalt sections gain popularity for major Tollway rehabilitation efforts such as rubblization projects. Less expensive mainline binder courses could be used in these instances where reflective cracking is not of concern. In this case, the 600 J/m^2 fracture energy threshold could be used.

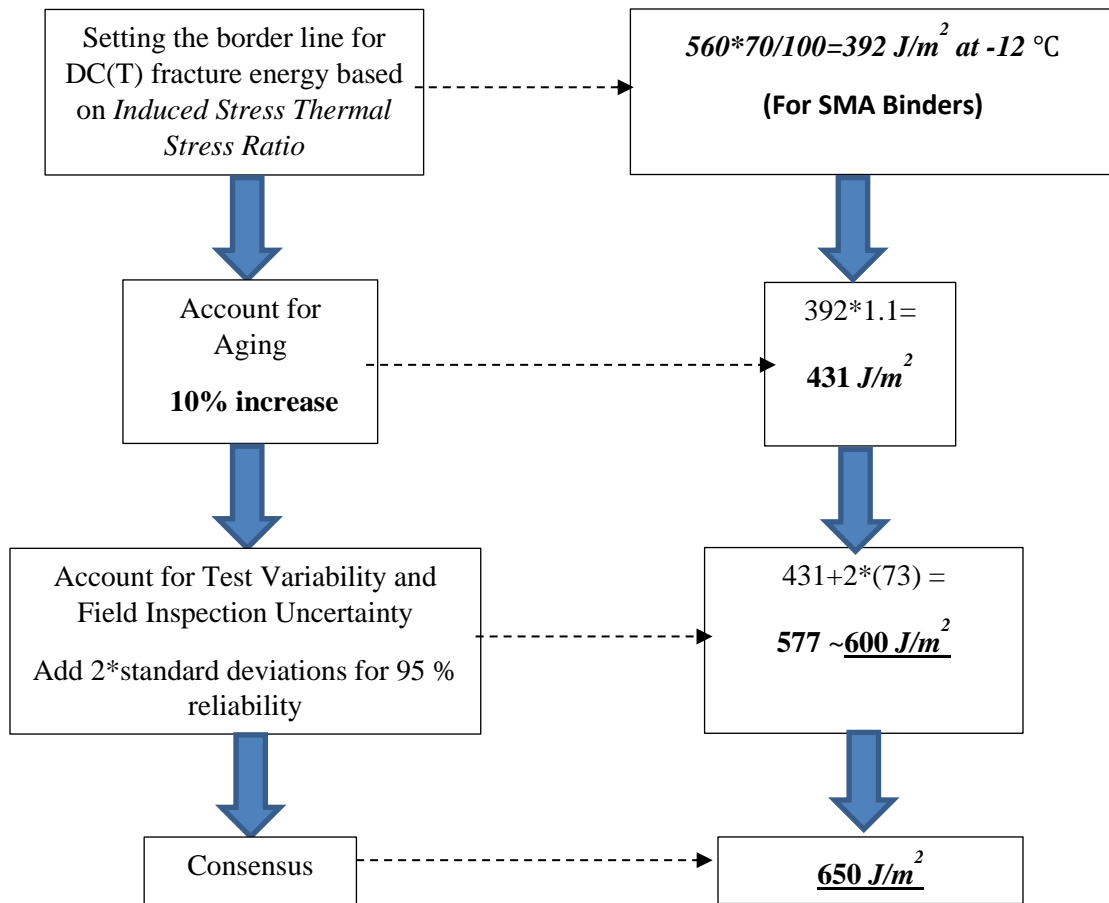


Figure 4-23. Flowchart to Calibrate DC(T) spec for SMA binder mixtures

The DC(T) specification for two types of shoulder mixtures, including unmodified SMA and dense graded is shown in Figure 4-24. As already shown in Figure 4-8 ("bubble plot"), a DC(T) border line of 400 J/m² was set as a limit between highly cracked and low cracked sections in previous studies. Looking at the DC(T) fracture test results shown in Chapter 2 (see Figure 2-12), it can be noted that both good and poor performing sections yielded fracture energy levels around 400 J/m². Also, Figure 4-25 indicates that there is a considerable difference between the performance of the shoulder mixtures when the DC(T) fracture energy is above 500 J/m². Given all these pieces of evidence, the DC(T) borderline for shoulder mixtures was set to 400 J/m² as a starting point in the flow chart.

Both mixture types (unmodified SMA and dense graded) are expected to experience the same aging level as SMA surface mixtures. The only difference between unmodified SMA and dense graded shoulders is the criticality of the project such that a higher reliability (87 % or 1.5*SD as opposed to 68 % for dense graded) is set for the unmodified SMA as this mixture type might be exposed to higher traffic during construction. After discussion with the TRP, thresholds of 500 J/m² and 450 J/m² were selected for unmodified SMA and dense graded shoulder surface mixtures, respectively.

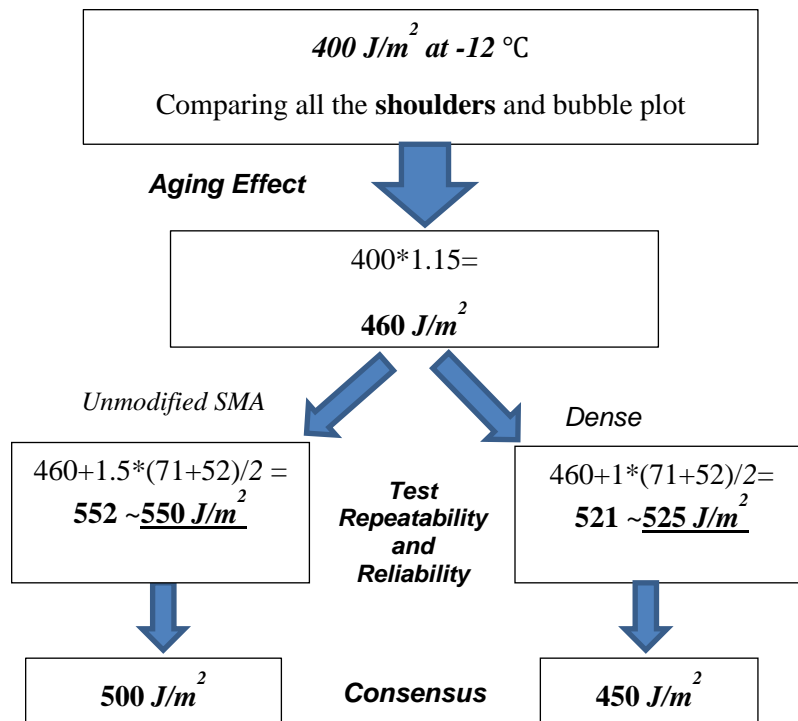


Figure 4-24. Flowchart to Calibrate DC(T) spec for shoulder surface mixtures including “Unmodified SMA”, and “Dense” shoulder surface mixtures





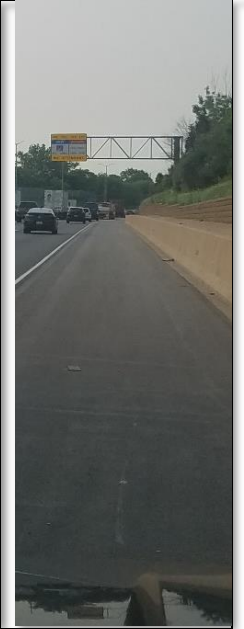
					
Section	I90-5.12	I90-7.25	I88-57	I-88 (MP:78- Mix:1818)	I355 (Mix1834)
Year	2009	2009	2014	2018	2018
DC(T)	345 J/m ²	370 J/m ²	409 J/m ²	426 J/m ²	512 J/m ²

Figure 4-25. Comparing shoulders with different ages and fracture energies

The final category for DC(T) specification development is the shoulder binder. This pavement layer can be constructed in different lifts (thicknesses). In this section, two different lifts are studied. The first shoulder binder lift is placed below the shoulder surface and will have a cover of about 2 inches (50 mm) on top; whereas the second binder lift is constructed prior to the top lift binder lift and benefits from a thicker cover (more than 4 inches or 100 mm). Therefore, the required DC(T) fracture energy can be relaxed for the bottom lift of shoulder binder. Considering two different categories (lifts) for the shoulder binder mixture type can result in more economical asphalt mixtures while the environmental and loading conditions have been considered.

Figure 4-26 shows the procedure to calibrate fracture energy for the two different lifts of the shoulder binder mixtures. As shown, a higher reliability is applied for the first lift as compared to the bottom lift. After this step, 450 and 400 J/m² were arrived at as thresholds for the top and lower shoulder binder course lifts, respectively. After consultation with the TRP, it was decided that these two thresholds should be consolidated into a single category, using the average value of the two categories, namely 425 J/m²).

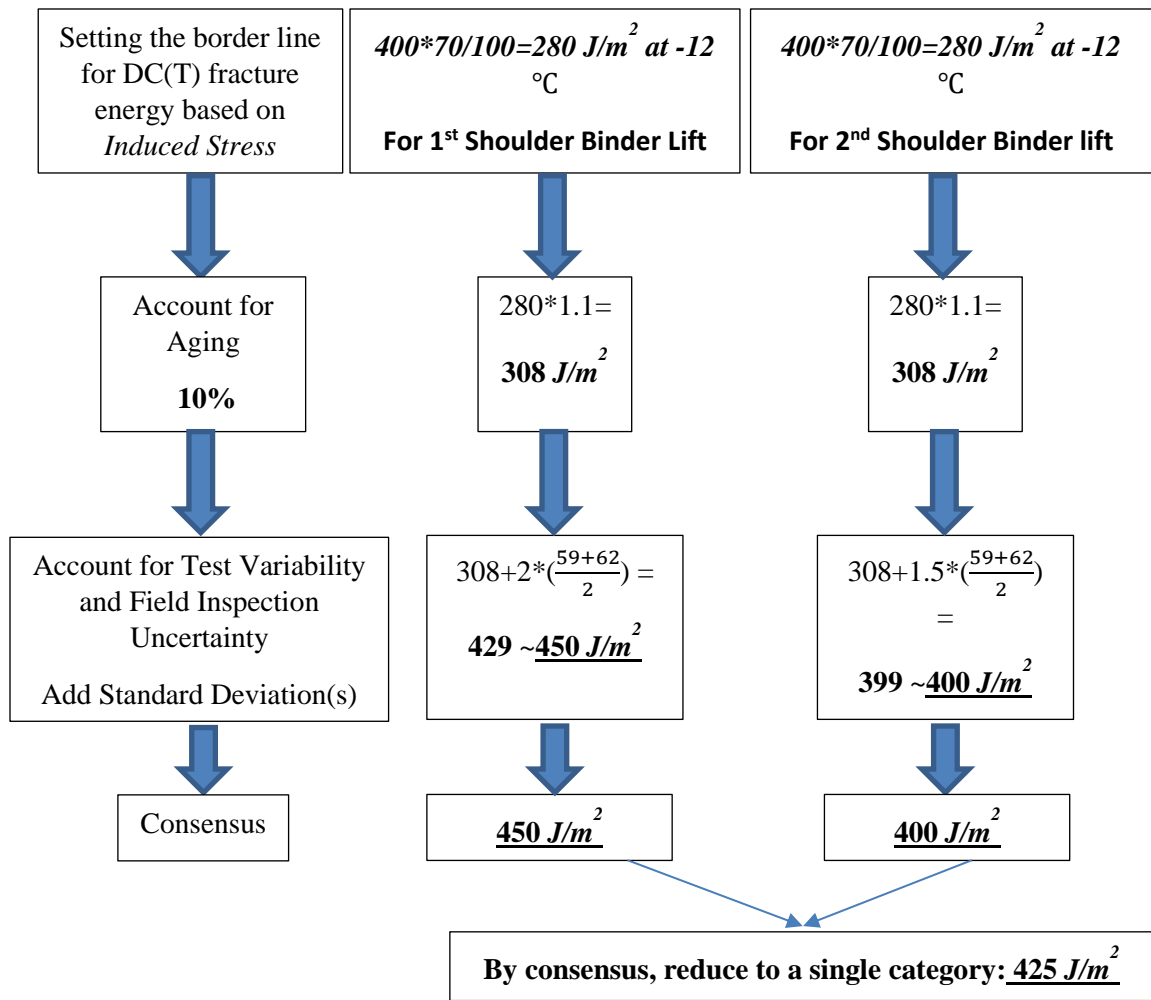


Figure 4-26. Flowchart to calibrate DC(T) thresholds for shoulder binder mixtures

4.5.7. Performance-Based Specification Levels for DC(T) Fracture Energy

Recommended DC(T) thresholds for different mixture categories are presented in Table 4-4. Experimental results, field performance data, statistical analysis and a final consensus step were used to validate or to adjust the thresholds. The SMA friction surface mixture threshold is recommended to be raised to 775 J/m^2 , as shown in Table 7-2. Given the higher aggregate quality used in this mixture and the results from testing of SMAs produced in 2018, it is expected that asphalt producers will be able to meet this threshold with well-designed mixes and high quality materials. In the case of shoulder

mixes, it is believed that the elevated DC(T) requirements will lead to lower thermal and block cracking occurrence. Comparing the dense graded shoulder surface mixtures produced in 2018 with the recommended threshold (450 J/m^2), the 1818 mixture would need to be redesigned to meet the new criterion in 2020. This mix used a PG 64-22 binder along with more than 20 % ABR. A softer binder system (e.g. PG 58-28) could help this mixture pass the newly recommended threshold without sacrificing recycled content.

In addition to the mixture types studied herein, the Tollway has two additional mainline binder course mixes in their latest specification: Mainline Binder ($N_{\text{design}} > 50$) and Mainline Binder ($N_{\text{design}} = 50$). Although not common on the Tollway, these mixes can be used as economical lower layers in full-depth asphalt pavement structures. In setting thresholds for these mixes, it was first acknowledged that shoulder binder course mixture requires a minimum of 425 J/m^2 for durability against environmental cracking. This value was applied to the Mainline Binder ($N_{\text{design}} > 50$) mixture, which is near the middle of the pavement structure and has the lowest requirements in terms of cracking resistance. This provides an opportunity to utilize mixtures with higher ABR. On the other hand, the $N_{\text{design}} = 50$ mixture will be at-or-near the bottom of the full-depth pavement structure and will therefore carry more bending-related tension. It was decided by consensus to require a slightly higher fracture energy value of 450 J/m^2 for this layer. Some agencies refer to lifts placed at the bottom of full-depth pavement structures as rich-bottom base mixtures, and likewise use specification criteria to promote extra cracking resistance.

Table 4-4. DC(T) thresholds at -12 °C for different mix categories

Mix. Type	Category	Existing	Recommended
SMA	Friction Surface	750 J/m ²	775 J/m ²
	Surface	700 J/m ²	700 J/m ²
	Binder	650 J/m ²	650 J/m ²
	Unmodified	500 J/m ²	500 J/m ²
Dense graded	IL 4.75	450 J/m ²	450 J/m ²
	Mainline Binder (N_{design}>50)	N/A	425 J/m ²
	Mainline Binder (N_{design}=50)	N/A	450 J/m ²
	Shoulder Surface (N_{design}≤70)	N/A	450 J/m ²
	Shoulder Binders	N/A	425 J/m ²

4.5.8. Performance-Based Specification Thresholds for Hamburg Rut Depth

The recommended thresholds for the Hamburg test to mitigate rutting are presented in Table 4-5. As mentioned before, there were no rutting prone section identified on the Tollway system. This indicates that Tollway has been screening the mixtures in an effective manner in terms of high temperature performance. Therefore, only minor changes have been proposed in the Hamburg requirements. In addition, a procedure was developed to use the Hamburg test as the primary screening tool for mixture stripping, with the classic TSR test used as a second screening step only when failing results are obtained (as explained in section 7.7). This procedure is recommended as a way to avoid the time and testing expense associated with the TSR test in cases where the Hamburg test returns a non-stripping determination.

An SMA binder category has been added to the previous thresholds, which uses the same number of passes (20,000) and similar maximum rut depth threshold compared with the

SMA friction surface and SMA surface mixtures. For unmodified SMAs, which are used on shoulders, the existing maximum rut depth of 9 mm is suggested to be relaxed to a threshold value of 12.5 mm. This recommendation was made in order to provide additional room for mixture designers to increase the cracking resistance as the shoulders were mainly exhibiting thermal and block cracking, rather than rutting. This threshold is also recommended for the IL4.75 mixtures (9.0 mm limit also recommended to be increased to 12.5 mm). In the Hamburg specification, the effect of pavement depth on reducing temperature has been considered and the required number of passes recommended for the binder course mixtures was decreased by 5,000 as compared to the existing limits (except for the IL-4.75 mixtures).

Table 4-5. Hamburg rut depth thresholds at 50 °C for different mix categories

Mix. Type	Category	Existing		Recommended	
		No. of Passes	Max. Rut Depth	No. of Passes	Max. Rut Depth
SMA	Friction Surface	20,000	6.0 mm	20,000	6.0 mm
	Surface	20,000	6.0 mm	20,000	6.0 mm
	Binder	20,000	6.0 mm	20,000	6.0 mm
	Unmodified	15,000	9.0 mm	15,000	12.5 mm ¹
Dense graded	IL 4.75	15,000	9.0 mm	15,000	12.5 mm
	Mainline Binder ($N_{design} > 50$)	15,000	12.5 mm	15,000	12.5 mm
	Mainline Binder ($N_{design} = 50$)	10,000	12.5 mm	10,000	12.5 mm
	Shoulder Surface ($N_{design} \leq 70$)	15,000	12.5 mm	10,000	12.5 mm
	Shoulder Binders	10,000	12.5 mm	7,500	12.5 mm

¹By consensus, the TRP decided to retain a maximum rut depth of 9.0 mm until more field data is available. This is a new mix category for the Tollway.

As mentioned in the previous section, in addition to the mixture types studied herein, the Tollway has two additional mainline binder course mixes in their latest specification: Mainline Binder ($N_{\text{design}} > 50$) and Mainline Binder ($N_{\text{design}} = 50$). Based on consultation with the TRP, it was agreed that an intermediate requirement of 12.5mm maximum rut depth at 15,000 wheel passes would be appropriate.

4.5.9. Performance-Based Specification Thresholds for SIP and Use of TSR Test

Table 4-6 presents the recommended SIP thresholds (minimum number of wheel passes at SIP) to control moisture damage. Similar to other Hamburg specifications, the SIP thresholds are either 5,000 or 2,500 cycles less than the required number of passes recommended for a given mix type. The field investigations did not indicate any stripping prone sections, implying that major changes to component material composition or to mix volumetrics is unnecessary for the Tollway. Therefore, the existing thresholds for SIP parameter are recommended to be only modestly changed.

First, recall that the Iowa method for SIP computation involves a pre-screening step. In other words, the first opportunity to specify a mix as non-stripping is in cases where the computed stripping slope-over-creep slope is below the 2.0 threshold. In this pre-screening step, if the criterion is met, there is no need to compute the SIP. There is also no need to check that value against the SIP threshold. In addition, multiple observations led to the recommendation of a second pre-screening step (to be applied only to SMA mixes), to specify a mix as non-stripping (and likewise, eliminating the need to compute SIP and check versus the SIP threshold). The data leading to this observation can be summarized as follows:

- Referring to the SIP results presented in Chapter 3, the slope ratio recorded by SMA mixtures, including sections 1835 and 1845, was above 2.0, while the rut depth accumulated at the end of 20,000 passes was remarkably low (less than 4.0 mm), showing no evidence of moisture susceptibility.
- In addition, the TSR and boiling water test results further evidenced adequate resistance to moisture damage in those SMA mixtures.
- Further investigation revealed that the very low creep slope (close to zero) were the cause of stripping-over-creep slope ratios greater than 2.0. The greater than 2.0 slope ratio triggered the SIP computation, and the flat curves appeared to produce arbitrary SIP numbers. This led to a false-positive stripping detections in the 1835 and 1845 mixes.
- In order to avoid false-positive determinations in highly rut-resistant SMA mixes, a second pre-screen step is recommended: when the rut depth at 20,000 passes is less than or equal to 4 mm, the mix is specified as non-stripping. A subsequent SIP calculation is not required.

While the use of the Hamburg test as the primary screening tool will certainly save time and testing expense in the mix design stage, it is acknowledged that over-screening of stripping resistant mixes may occur. Thus, until more field data is available, the classic TSR test may be utilized by mix designers as a secondary stripping determination. More specifically, if the asphalt mixture under evaluation does not pass via the Hamburg pre-screening steps or the SIP requirement, the TSR test can be subsequently performed. For

mixes meeting or surpassing the 85 % retained tensile strength and 80 psi tensile strength criteria in the TSR, the mix can be specified as non-stripping.

Table 4-6. SIP thresholds at 50 °C for different mix categories (applied when the slope ratio is ≥ 2.0)

Mix. Type	Category	Existing	Recommended
SMA*	Friction Surface	15,000	15,000
	Surface	15,000	15,000
	Binder	15,000	15,000
	Unmodified	15,000	10,000
Dense graded	IL 4.75	10,000	10,000
	Mainline Binder ($N_{\text{design}} > 50$)	10,000	10,000
	Mainline Binder ($N_{\text{design}} = 50$)	5,000	7,500
	Shoulder Surface ($N_{\text{design}} \leq 70$)	10,000	7,500
	Shoulder Binders	5,000	5,000

* If the measured rut depth for SMA mixes at the required number of passes (determined based on Table 7-3) is lower than 4.0 mm, the mix shall be specified as non-stripping without the need to compute the SIP.

Chapter 5

VISCOELASTIC CHARACTERIZATION OF ASPHALT MIXTURE USING DC(T) CREEP TEST

5.1. Introduction

Asphalt concrete suffers from low temperature cracking in cold regions. This type of pavement distress occurs due to the stress built-up in the pavement structure under temperature fluctuation. To calculate the thermally induced stress, viscoelastic characteristics of the asphalt mixture need to be characterized. Creep compliance provides a simple measure of the linear viscoelastic nature of asphalt concrete at low temperatures, and is often employed in thermal cracking models and can be used to evaluate the ability of the asphalt concrete to relax thermal stresses in response to rapid cooling events in the field. This material property can be characterized using experimental data from a creep test conducted by applying a rapidly applied, ‘step-stress’, which is then held constant as the time-dependent creep displacement is measured [1]. Various thermal cracking prediction models (e.g. TCMODEL [2,3] and ILLI-TC [4]) use viscoelastic creep compliance as a key input to the models, mainly for response calculation. In some cases, parameters derived from the creep compliance curve are also used in cracking models, such as measures of the slope of the creep compliance curve at long loading times [2, 3], which is often called the ‘m-value.’

5.1.1. Overview: Available Creep Test Set-ups

Researchers have proposed different test setups, such as uniaxial cylindrical [5,6] semi-circular bending (SCB) [7], indirect tension (IDT) [8,9], and bending beam geometries [10,11] to determine the creep compliance of asphalt mixtures. The uniaxial test can be performed in either pure tension or pure compression modes. Moreover, the stress level in uniaxial test is constant throughout the cylindrical sample, providing a straightforward creep compliance calculation method. However, the uniaxial test requires testing

specimens that cannot be fabricated from field cores due to the limited thickness of the asphalt lifts in a pavement structure. On the other hand, the SCB-type configuration benefits from a simple specimen fabrication process and can be performed on field cores as well. However, the bending moment (flexural stress) within the SCB sample is assumed to result in non-linear behavior and damaging of the sample. Besides, most of the available tests performed on the SCB configuration are performed at room temperature (25°C) and, therefore, do not need a temperature-control chamber. Due to the highly temperature dependent behavior of asphalt mixtures and the duration of the creep test (100 to 1000 s), the testing temperature needs to be controlled and maintained throughout the experiment. As a result, the uniaxial and SCB creep tests are not suitable for a considerable amount of applications in research and industry. In the following sections, the frequently applied creep tests including IDT and bending beam rheometer (BBR) tests are reviewed.

Following AASHTO T322-2007, the Superpave IDT test can be used to measure the creep compliance and strength of asphalt concrete. The field-cored or gyratory-compacted samples with heights ranging from 38 to 50 mm and diameters in the range of 150 ± 9 mm are generally used. Three testing temperatures with 10 °C intervals are recommended, which are often taken as 0, -10, and -20 °C. Alternatively, temperatures can be selected to encompass the low-performance grade (PG) of the asphalt binder and can use a different temperature spacing, such as 0, -12, and -24 °C. A creep test duration of 1000 seconds is generally required to ensure overlap between creep curves for master curve development. Since the creep compliance should normally be characterized in the linear viscoelastic range, loading levels should be kept sufficiently low to retain this

linearity. Therefore, a maximum deformation on the horizontal clip gage of 0.019 mm for 150 mm diameter samples is suggested to stay within the linear range. Besides, to circumvent the noise problems and drift inherent in sensors (displacement extensometers), a minimum deformation of 0.00125 mm at a 30-second loading time is recommended [8]. The IDT test setup and loading configurations pose both tensile and compressive stresses in both horizontal and vertical directions. Therefore, the stress and strain states in the IDT test are not as simple as those in uniaxial loading. Due to this complexity, a geometrical coefficient (or creep compliance correction factor) is calculated using the horizontal and vertical deflection and is applied in the creep compliance formula per AASTO T322.

The IDT test has been the most frequently applied test by researchers and agencies to calculate the creep compliance at low temperatures and evaluate the cracking potential of asphalt mixtures [12–15]. For example, Behnia et al. [16] fitted a power law function on IDT creep compliance master curves to characterize low temperature behavior of four mixtures with PG 64-22 and PG 58-28 binder types containing 20 and 40% reclaimed asphalt pavement (RAP). Dave et al. [4] introduced the IlliTC software, which simulates low temperature cracking in asphalt pavements using a 2D viscoelastic finite element (FE) analysis with cohesive zone fracture modeling. Hill et al. [17] used bio-based modifiers to improve thermal cracking resistance of recycled mixtures. To this end, DC(T) fracture and IDT bulk viscoelastic characterization tests were used. The m-value increases as the bio-based modifier is added to hot mix asphalt (HMA). Moreover, the addition of RAP resulted in a significant reduction in m-value. To numerically study the effect of material heterogeneity on the fracture of asphalt concrete, Wills et al. [18]

performed IDT creep tests on mixtures containing different air void contents and found that higher air voids lead to higher compliance in asphalt mixtures.

The creep compliance of the asphalt mixtures obtained from the BBR test involves three-point loading of the asphalt samples fabricated in the form of a beam with standard dimensions of 115×12.7×6.35 mm (length*width*thickness) per AASHTO TP 125.

Normally, three testing temperatures are chosen for this test. Test temperatures equal to 4, 10, and 16 °C above the low performance grade (PG) of the binder used in the mix have been successfully employed. The testing specimens could be obtained from both gyratory compacted and field core samples. Fifteen to twenty BBR specimens can be fabricated out of each gyratory sample and a minimum of five replicates is recommended by the standard for each temperature. A loading level of 4000 mN is applied on the beam specimen for 240 seconds. The viscoelastic properties of the asphalt mixture are calculated using the deflection measured in time.

Zokfa et al. [10] tested 20 different mixture types consisting of 10 binder types and 2 aggregate sources. The BBR apparatus was utilized to obtain creep compliance of thin asphalt mixture specimens. Due to the small cross sectional dimensions of BBR specimens (12.7 mm by 6.35 mm), the representative volume element (RVE), which accounts for reliability and repeatability to set the minimum dimensions of the testing sample, was not met [10]. The maximum aggregate size is often larger than the specimen width, and much larger than the specimen thickness. Nevertheless, due to the averaging effect along the relatively long beam, the BBR and the reference IDT creep compliance values were found to be in reasonable agreement [19]. Also, using measured IDT creep compliance and predicted IDT creep compliance from BBR creep data, it was shown that

similar crack depths and amount of cracking were predicted by TCMODEL [19]. The BBR mixture test is especially attractive for characterizing near-surface asphalt mixture creep properties, where high property gradients exist [20]. The AASHTO TP 125 procedure has been used by researchers to investigate the effect of aging on low temperature cracking potential and also to find the equivalent aging time between the loose mixture and gyratory compacted specimen aging protocols [21–24].

The DC(T) fracture test was introduced by Wagoner et al. in 2005 [25] to investigate the fracture resistance of the asphalt mixtures. One of the main advantages of the DC(T) geometry compared to the available SCB-type fracture tests is its larger ligament length such that the ratio between the average aggregate size and the fracture area is low. In other words, the number of aggregates acting as obstacles to crack propagation is high. This allows the complete release of fracture energy, and credits the role of aggregates [26]. The DC(T) test set-up benefits from a robust cooling chamber and uses a crack mouth opening displacement (CMOD) system to control the deflection at the top of a notched specimen [27]. The DC(T) fracture test has been used by various researchers and agencies during the last decade and is found to establish a good correlation with the pavement thermal cracking potential [28–30]. The DC(T) test has also been used for mixture characterization and to investigate the effect of the mix constituents on the low temperature cracking resistance [31–34].

The IDT test set-up requires an expensive loading frame and cooling chamber, which limits its practical use in routine mixture design and evaluation. In addition, the extensometers used to measure the vertical and horizontal deflections in the IDT test are costly and need continuous maintenance and calibration. The BBR test tries to avoid this

issue as the test is performed in a Superpave binder BBR test, which is relatively more available in asphalt labs. However, there is concern whether or not the thin beam specimens can properly represent the properties of asphalt mixture, due to size effect concerns, as the dimensions of the aggregates used in asphalt concrete are generally larger than the thickness of the BBR specimen. In this research, to address the difficulties and uncertainties associated with the IDT and BBR mixture creep tests, the DC(T) geometry is employed as a practical alternative. Although typically used to evaluate asphalt mixture fracture resistance, the DC(T) test is employed herein, where one of the industry standard test devices was upgraded to permit creep testing.

5.2. Scope and Objectives

- Calculating a geometrical coefficient for the DC(T) test which allows for a simple calculation of viscoelastic creep compliance from data streams collected from the industry standard DC(T) test device;
- Characterizing the viscoelastic behavior of asphalt mixtures at low temperatures using CMOD versus time results at low temperatures, along with creep load and the new geometrical coefficient and comparing results to the well established Superpave indirect tension test (IDT);
- Conducting test simulations using the finite element method (FEM) to predict the viscoelastic response and to validate the new geometrical coefficient.

To fulfill these objectives, a step-by-step approach was followed, as shown in Figure 5-1.

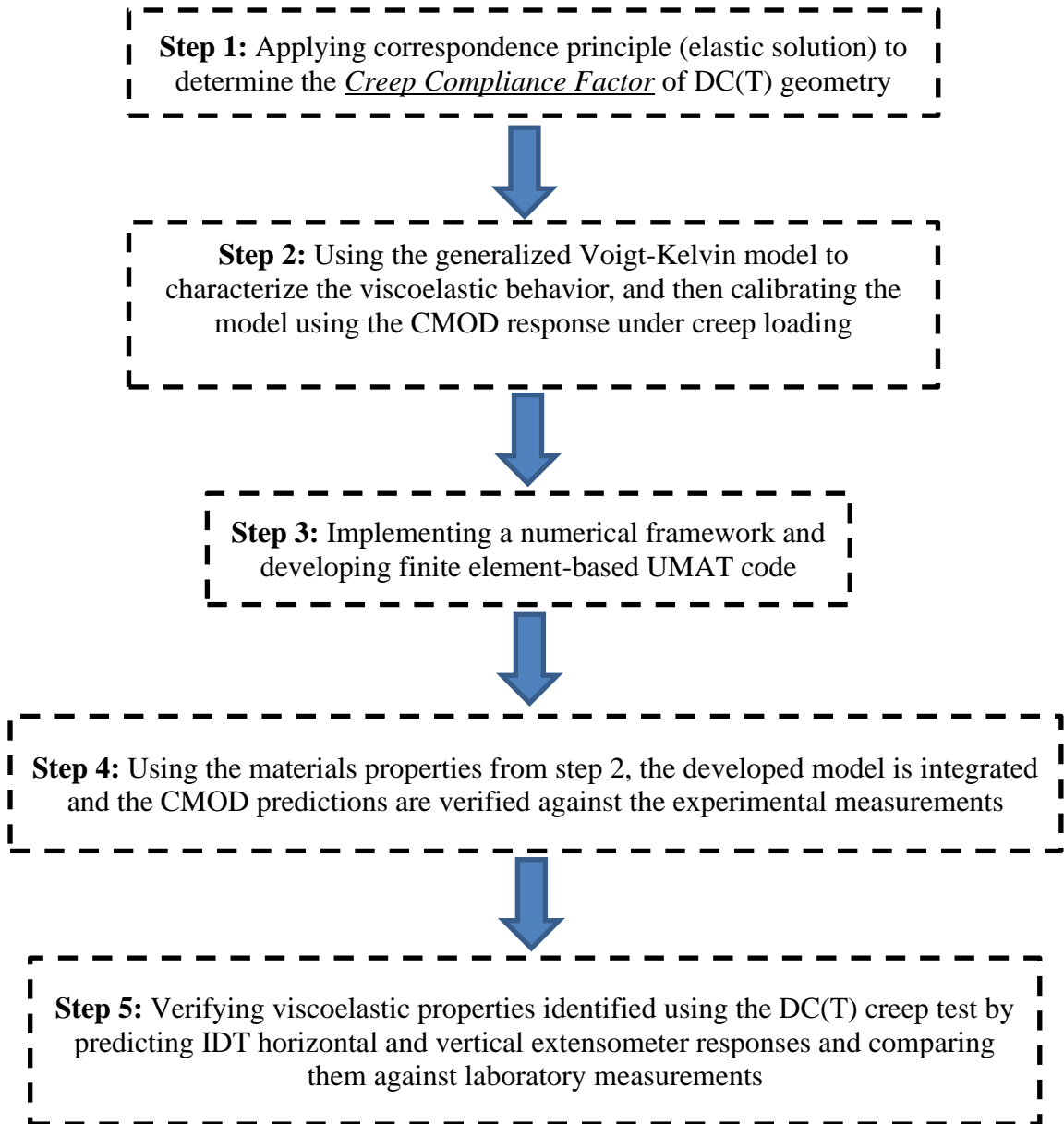


Figure 5-1. Study Framework

5.3. Materials, Sample Fabrication, and Test Setup

In the experimental portion of this study, six stone-matrix asphalt (SMA) type mixtures were produced and used to fabricate testing samples for the DC(T) and IDT creep tests.

The selected plant-produced asphalt mixtures were sampled per AASHTO T-168-03

across asphalt plants in the Chicago Area. Mixtures were sampled into uncoated, 5-gallon steel pails with tight-fitting lids. A representative from the Missouri Asphalt Pavement and Innovation Lab (MAPIL). After fabrication of the testing samples, the DC(T) and IDT test set-ups were used to conduct static creep tests (constant load) of 1000 second duration, where viscoelastic deflections were measured as a function of time. More details regarding data collection and analysis are provided later in this paper.

Table 2-1 presents compositional properties of the mixtures used in this study. The first four mixtures (labeled as 1844, 1835, 1824, and 1845) are friction-surface-type SMAs, used on highway curves and ramps, while the last two SMA mixtures (1836 and 1840) are regular SMA surface mixtures, used in lower trafficked, non-curved or tangent road alignments. Among these mixtures, three of them (1844, 1824, and 1836) involved SBS-polymer-modified binder systems and the other three (1835, 1845, and 1840) involved ground tire rubber (GTR), modified either by a terminal-blend, wet process or by the so-called dry process. The 1835 mix utilized a relatively soft, neat binder (Superpave PG 46-34) combined with 10% engineered crumb rubber (ECR) by weight of binder (a dry-process GTR system). This mix also had the highest amount of recycled materials among all of the SMAs investigated (41.2% ABR), including 25.1% ABR by RAP and 16.1% ABR by RAS. Similar to 1835, the 1845 mix was also made of PG 46-34 neat binder, which was later modified by 10.5% rubber by weight of the binder. The neat binder used in the 1840 mix was PG 58-28. The binder in this mix possessed 12.0% GTR, added to the binder via a terminal-blend, wet process. Aggregate gradations for all mixtures are shown in [Fig. 2](#). It can be seen that the gradation of all SMAs investigated are quite similar, all with a nominal maximum aggregate size (NMAS) of 12.5 mm.

Table 5-1. Details of mixture ingredients

Mix. ID	SMA Type	Base Binder	ABR by RAP	ABR by	NMAS
1844	Friction Surface	SBS 70-28	10.8	16.0	12.5
1835	Friction Surface	46-34 +10%ECR	25.1	16.1	12.5
1824	Friction Surface	SBS 64-34	20.4	16.7	12.5
1845	Friction Surface	46-34 10.5%GTR	23.9	15.4	12.5
1836	Surface	SBS 64-34	16.2	16.3	12.5
1840	Surface	58-28 +12%GTR	15.9	9.8	12.5

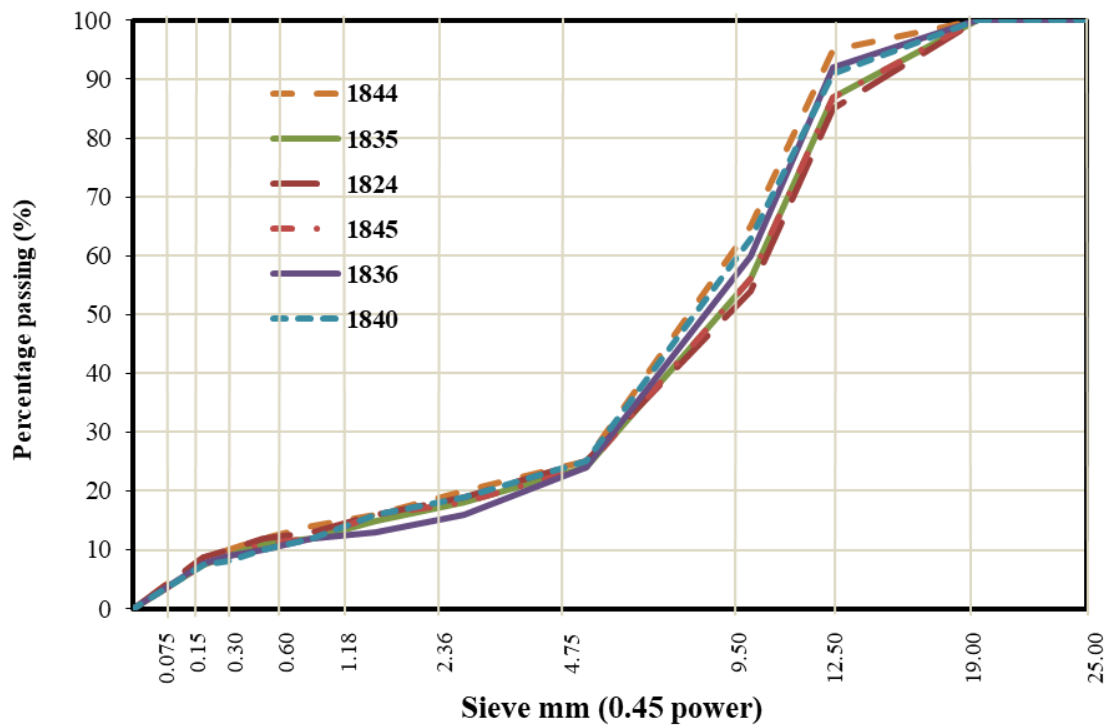


Figure 5-2. Aggregate gradations for the investigated plant-produced mixtures

5.3.1. *Sample Fabrication*

The sampled plant-produced mixtures were brought back to the MAPIL facility in 5-gallon steel pails. The plastic handles were removed and then pails were placed in a forced draft oven to heat the asphalt mixture to a workable consistency (~100 °C). The heated mixture was then reduced to mass of the gyratory sample following the quartering method in AASHTO R47. A Pine GB2 Superpave gyratory compactor was used to compact the reheated samples and make cylindrical specimens. After splitting to desired mass, the asphalt mixture was heated to compaction temperature (155 and 143 °C for modified and unmodified mixes, respectively). All SMA testing samples were compacted to 6.0 % air voids. For DC(T) samples, air voids were measured on the 50 mm slices before notching and coring for the DC(T) specimens.

5.3.2. *DC(T) Creep Test Set-up*

DC(T) specimens were fabricated as per ASTM D7313 with a diameter of 150 mm, thickness of 50 mm and ligament length of 84.5 mm, along with two loading holes, each 25 mm in diameter. The dimensions of each DC(T) sample, including thickness, diameter, and ligament length were measured, recorded, and then CMOD gage points were glued to the crack mouth of the specimen. The specimen was then placed into the DC(T) chamber for conditioning at the testing temperature for a minimum of 2 hours and maximum of 4 hours. Next, samples were suspended from the cylindrical loading fixtures. To avoid damaging the samples, creep loading levels as low as 0.3, 0.4, and 0.5 kN were chosen for the testing temperatures of 0, -12, and -24 °C, respectively. These levels were determined after a non-trivial, trial-and-error process. Choosing an overly low load level is undesirable, as it will lead to noises in deflection measurements; whereas selecting an overly high creep load leads to nonlinear behavior, either localized

damage or crack initiation and propagation at the crack tip. Prior to the application of the creep test load, a seating load of 0.1 kN was applied on the sample. The aim of the seating load is to ensure that the sample had been engaged by the loading platens, and to minimize movement of the sample when the main creep load is applied. As seen in Figure 5-3, three replicates were conducted on each mixture type. Table 5-2 presents the loading details of the DC(T) creep test at each temperature.

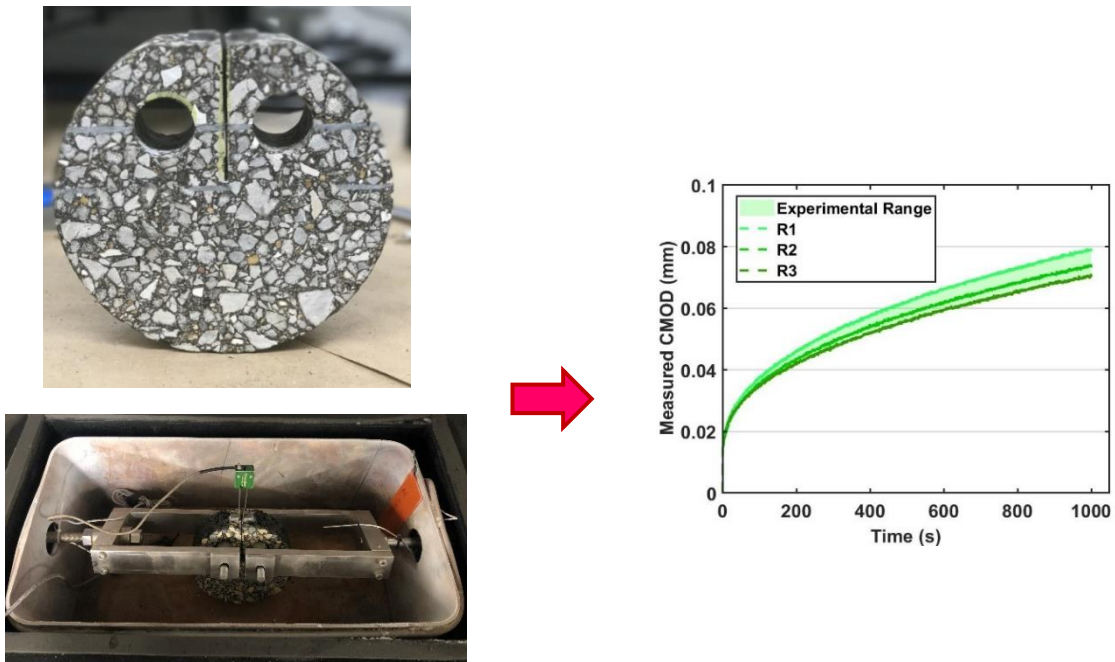


Figure 5-3. A sample of the test output from DC(T) machine: three replicates (R1, R2, and R3) were tested for each temperature

Table 5-2. Loading properties in DC(T) creep test

Test	Testing Temp. (°C)	Chamber Temp. (°C)	Seating Load (kN)	Ramp Time (s)	Creep Load (kN)	Creep Time (s)
DC(T) creep	0	0	0.1	0.1	0.3	1000
	-12	-12			0.4	
	-24	-24			0.5	

5.4. Analysis of Experimental Results

5.4.1. Determining the Creep Compliance Factor

The viscoelastic properties of asphalt concrete are often experimentally determined using a uniaxially-loaded, cylindrical specimen because of the simple and straightforward stress-strain relationship. The stress level under uniaxial loading σ is assumed constant at every point throughout the sample and is simply calculated as the load level divided by the cross-sectional area. The strain is simply calculated as the ratio of displacement measured by the loading machine divided by the original height of the specimen, or by using simple, surface-mounted displacement sensors (ASTM D-3497). However, a more complex, three-dimensional geometry exists in the DC(T) test, which leads to much more complex stress-strain states in the specimen, especially considering the added complexity associated the time-dependent (viscoelastic) behavior of bituminous materials. The correspondence principle provides a powerful tool for the analysis of viscoelastic boundary value problems (BVPs) for homogeneous and non-homogenous materials [35,36]. Using the correspondence principle, the 3-D viscoelastic solutions can be developed based on the elastic solution [37][38]. To this end, first, an elastic solution for a given specimen geometry is obtained as a function of applied load, geometry, and elasticity properties. Then, the viscoelastic solution of the investigated sample geometry is produced in accordance with the correspondence principle, where viscoelastic constitutive models are substituted in place of the elastic constants.

Considering the dimension compatibility in continuum mechanics, the relationship between the applied load, P , the specimen thickness, B , elasticity modulus, E , and crack mouth opening displacement ($CMOD$) is assumed as follows:

$$CMOD = \alpha \frac{P}{E \times B} \quad (1)$$

where α is the geometry coefficient, depending on the geometrical configuration of the ASTM D7313-17 DC(T) specimen. As shown in Eq. (1), the geometry coefficient completes the relationship between the mechanical and geometrical features of the DC(T) specimen. To calculate the geometry coefficient, the CMOD for various values of elasticity modulus, sample thickness, and load was calculated using the finite element method and applied to the elastic solution. Then, considering Eq. (1) and results obtained from the elastic solution, the geometry coefficient was back calculated from simulation results as $\alpha=25.0$. Therefore, Eq. (1) can be re-written as follows.

$$D = \frac{1}{E} = 0.04 \frac{B}{P} CMOD \quad (2)$$

where D is the inverse of the elastic modulus and is referred to as elastic compliance.

According to the definition of viscoelastic creep compliance (i.e., $\varepsilon(t) = \sigma_0 D(t)$; ε : strain; σ_0 : constant stress), for the case of constant applied load, the viscoelastic solution and then the viscoelastic creep compliance for the DC(T) geometry was determined as follows:

$$D(t) = 0.04 \frac{B}{P_0} CMOD(t) \quad (3)$$

where $D(t)$ is the viscoelastic creep compliance and P_0 is the constant applied load in the DC(T) test.

Moreover, for the case of time-dependent applied load, the viscoelastic solution can be defined in accordance with Boltzmann (hereditary) integral, such that:

$$CMOD(t) = \frac{1}{0.04B} \left[D(t)P(0) + \int_{0^+}^t D(t-\tau) \frac{\partial P(\tau)}{\partial \tau} d\tau \right] \quad (4)$$

where $P(t)$ is the time-dependent applied load in the DC(T) test.

5.4.2. Identification of Viscoelastic Properties

In this research, the DC(T) creep tests were conducted at three temperatures under a constant load applied for 1000 seconds, as shown in Table 5-2. The CMOD measurements collected at every 0.1 seconds are implemented to calculate the creep compliance according to Eq. (3). Three replicates were used for each mix type and the average creep compliance used in the subsequent analysis. The generalized Kelvin-Voigt model is then used to describe the elastic and viscoelastic behavior of asphalt concrete at low-temperature by fitting the model to the measured creep compliance. The model consists of multiple Voight-Kelvin elements accounting for the delayed elastic behavior assembled in series with one Maxwell element, resulting in a model that characterizes both elastic and creep responses (see Figure 5-4). The creep compliance function of the generalized Voight-Kelvin model is presented in Eq. (5),

$$D(t) = D_0 + \eta t + \sum_{i=1}^N D_i (1 - \exp[-\lambda_i t]) \quad (5)$$

where D_0 and η are the spring instantaneous creep compliance and the viscosity of the dashpot, respectively, in the Maxwell element. Also, D_i are creep compliance parameters and λ_i denotes the inverse of retardation time for each Voight-Kelvin element.

Considering four Kelvin elements, and minimizing the sum of squared error (SSE), the

model constant coefficients including D_0 , D_i , and η were calculated as shown in Table 5-3. It should be mentioned that the inverse of retardation time values (λ_i) are assumed (judiciously spread across the typical time spectrum of the creep compliance master curves) and were therefore not calibrated.

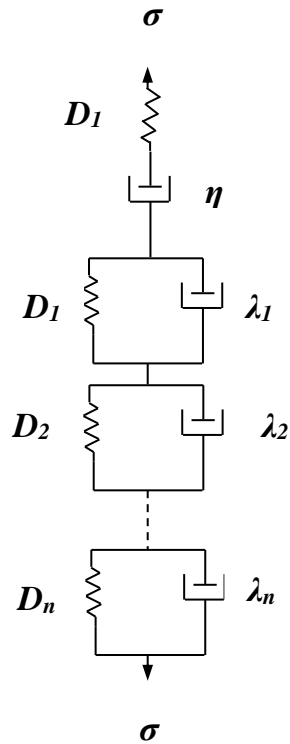


Figure 5-4. The schematic of the generalized Kelvin-Voigt model

Table 5-3. Identified viscoelastic constant coefficient

				λ_1 (1/s)	λ_2 (1/s)	λ_3 (1/s)	λ_4 (1/s)
				0.3162	0.1000	0.03162	0.0100
ID	Temp (°C)	D_0 (1/MPa)	η (1/s/MPa)	D_1 (1/MPa)	D_2 (1/MPa)	D_3 (1/MPa)	D_4 (1/MPa)
1824	0	6.23e-05	3.95e-07	4.14e-05	1.51e-05	2.49e-17	1.9e-04
	-12	4.52e-05	6.67e-08	1.32e-05	2.92e-06	1.04e-08	4.81e-05
	-24	3.12e-05	1.37e-08	4.53e-06	1.87e-06	5.6e-07	1.54e-05
1835	0	6.13e-05	1.76e-07	2.52e-05	1.08e-05	1.42e-08	1.07e-04
	-12	4.73e-05	4.4e-08	1.03e-05	1.4e-06	1.56e-07	3.53e-05
	-24	3.23e-05	1.71e-08	4.45e-06	2.11e-06	1.86e-06	1.49e-05
1836	0	6.53e-05	1.56e-07	2.08e-05	1.65e-05	2.2e-09	1.02e-04
	-12	4.39e-05	4.06e-08	9.22e-06	3.05e-06	4.47e-07	3.14e-05
	-24	3.02e-05	1.17e-08	2.5e-06	2.13e-06	1.3e-06	1.57e-05
1840	0	6.09e-05	2.42e-07	1.81e-05	2.19e-05	4.39e-15	1.3e-04
	-12	4.61e-05	4.61e-08	2.28e-06	1.08e-05	7.87e-06	2.12e-05
	-24	2.91e-05	1.51e-08	2.06e-06	1.74e-06	1.19e-06	1.19e-05
1844	0	5.89e-05	1.74e-07	2.86e-05	7.87e-06	5.89e-09	1.01e-04
	-12	4.13e-05	4.29e-08	1.08e-05	2.76e-06	1.29e-07	3.26e-05
	-24	2.99e-05	1.74e-08	2.9e-06	2.27e-06	1.08e-07	1.78e-05
1845	0	7.23e-05	2.72e-07	3.68e-05	1.45e-05	2.88e-11	1.46e-04
	-12	4.15e-05	5.28e-08	8.27e-06	7.27e-06	5.47e-08	3.99e-05
	-24	3.08e-05	1.27e-08	5.56e-06	1.1e-06	1.05e-08	1.8e-05

5.5. Numerical Simulation

This section presents the numerical framework for the generalized Voight-Kelvin model used to represent the viscoelastic behavior of asphalt concrete at low temperatures. It is worth mentioning that the generalized Voight-Kelvin model is not available in the Abaqus library and needs to be implemented as a user-defined subroutine [47].

According to the schematic of the generalized Voight-Kelvin model shown in Fig. 4, the one-dimensional hereditary (Boltzmann) integration of the viscoelastic constitutive relationship results in a viscoelastic strain at time of t , which is described by:

$$\varepsilon^t = D_0 \sigma^t + \int_0^t \Delta D^{(\psi^t - \psi^\tau)} \frac{d(\sigma^\tau)}{d\tau} d\tau + \int_0^t \eta (\psi^t - \psi^\tau) \frac{d(\sigma^\tau)}{d\tau} d\tau \quad (6)$$

where D_0 is the instantaneous compliance, ΔD is the transient creep compliance, η is the dashpot constant coefficient, τ denotes integration variable. The ε^t and σ^τ indicate strain and stress at time t , respectively. Similarly, ψ^t is the reduced time at time t , which is a function of time-temperature shift factor (a_T), as that $\psi^t = \int_0^t \frac{1}{a_T} d\xi$. The transient

compliance ΔD can be expressed using a Prony series:

$$\Delta D^{\psi^t} = \sum_{r=1}^N D_r \left(1 - \exp[-\lambda_r \psi^t] \right) \quad (7)$$

where N is the number of Prony series terms and D_r is the r th term of compliance associated with the r th retardation time, $1/\lambda_r$.

In order to solve Eq. (6) numerically, the stress, strain and internal state variables need to be determined at each time increment. Given the variables at last time increment ($t-\Delta t$), the stress, strain, and internal state variables are calculated at the current time increment (t) and are stored for the next time increment. As a displacement-strain-based numerical scheme, the strain tensor increment at time t (i.e., $\Delta \varepsilon_{ij}^t$) is given at the beginning of each increment. Then, given the relationship between the increment of viscoelastic strain and internal state variables stored at the last increment, the stress increment at the current time increment ($\Delta \sigma^t$) can be calculated. Finally, having the stress tensor at the last time increment ($\sigma^{t-\Delta t}$), the stress tensor at the current increment (σ^t) can be calculated as:

$$\begin{aligned}
\sigma_{kl}^t = & \left[D_{ijkl,0} + \sum_{r=1}^N D_{ijkl,r} - \sum_{r=1}^N D_{ijkl,r} \frac{1 - \exp[-\lambda_r \Delta\psi^t]}{\lambda_r \Delta\psi^t} + \frac{1}{2} \Delta\psi^t \eta_{ijkl} \right]^{-1} \times \\
& \left[\Delta\epsilon_{ij}^t + \left[D_{ijkl,0} + \sum_{r=1}^N D_{ijkl,r} - \sum_{r=1}^N D_{ijkl,r} \frac{1 - \exp[-\lambda_r \Delta\psi^{t-\Delta t}]}{\lambda_r \Delta\psi^{t-\Delta t}} + \frac{1}{2} \Delta\psi^{t-\Delta t} \eta_{ijkl} \right] \sigma_{kl}^{t-\Delta t} \right. \\
& - \left[\sum_{r=1}^N D_{ijkl,r} \frac{1 - \exp[-\lambda_r \Delta\psi^t]}{\lambda_r \Delta\psi^t} - \sum_{r=1}^N D_{ijkl,r} \frac{1 - \exp[-\lambda_r \Delta\psi^{t-\Delta t}]}{\lambda_r \Delta\psi^{t-\Delta t}} \right] \sigma_{kl}^{t-\Delta t} \\
& - \left[\frac{1}{2} \Delta\psi^{t-\Delta t} \eta_{ijkl} + \frac{1}{2} \Delta\psi^t \eta_{ijkl} \right] \sigma_{kl}^{t-\Delta t} - \left[\sum_{r=1}^N D_{ijkl,r} - \sum_{r=1}^N D_{ijkl,r} \exp[-\lambda_r \Delta\psi^t] \right] q_{kl,r}^{t-\Delta t} \\
& \left. + \Delta\psi^t \eta_{ijkl} \sigma_{kl}^0 \right]
\end{aligned} \tag{8}$$

The expression above is given in indicial notation, and thus, the summation convention applies. Once the variables are obtained for the current time increment, the stress and strain tensors, and the internal state variables (i.e., $q_{kl,r}^t$ and p_{kl}^t), are all updated and stored for the next time increment. The numerical implementation of the generalized Voight-Kelvin model was implemented in the finite element code Abaqus via a user material subroutine (UMAT), following an implicit scheme.

5.6. Numerical Validation

5.6.1. Comparing DC(T) Response Predictions with Experimental Measurements

In this section, the constitutive model and the introduced numerical framework are integrated to predict the time-dependent CMOD response obtained from the DC(T) test. To this end, the geometry of the DC(T) sample was modeled in Abaqus. The viscoelastic properties calculated in Section 5.3 were considered as constant coefficients of the model implemented in Section 5.4. The corresponding creep loads shown in Table 5-3 were applied in the model and the CMOD versus time is calculated. For instance, Figure 5-5

depicts the displacement, strain, and stress fields within a DC(T) specimen at the end of a creep test.

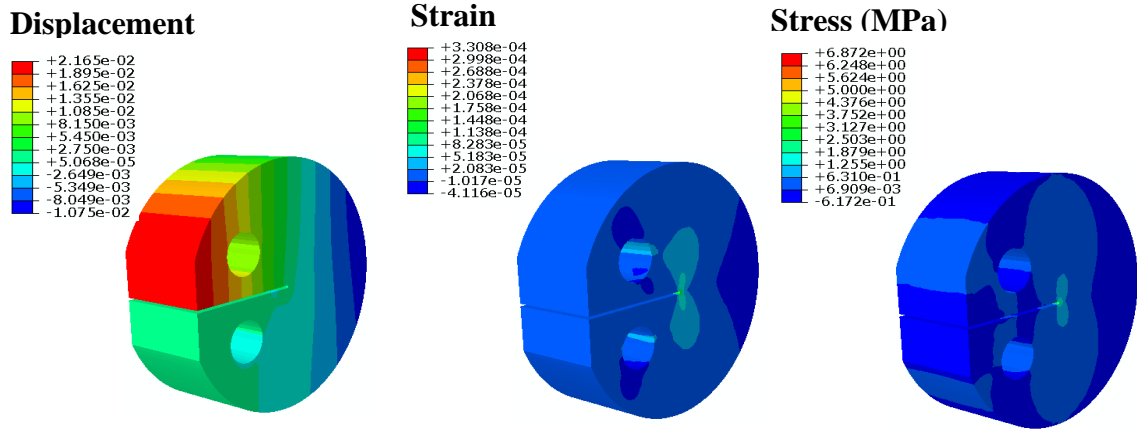


Figure 5-5. An example of DC(T) creep responses as simulated with viscoelastic FEM in Abaqus

Figure 5-6 shows the CMOD response of three replicates and the corresponding FEM result for each mix compared at three different temperatures. In this figure, the range of CMOD recorded by three replicates is highlighted for each temperature. As expected, despite being subjected to the highest level of creep load, the measured CMOD response at -24°C is always lower than the ones at -12 and 0°C. Also, the main proportion of accumulated CMOD at -24°C occurred at the early stages of the creep test (first ten seconds), indicating the predominant elastic behavior of the investigated asphalt mixtures at this temperature. On the other hand, the delayed elastic deformation increases as the temperature increases. As a result, the CMOD at 0°C accumulates much more gradually in time.

The CMOD responses presented in Figure 5-6 are used to validate the ability of the model to predict the DC(T) creep test results. To this end, the viscoelastic properties

shown in Table 5-3 are implemented in the numerical framework to calculate the CMOD responses at different temperatures. Comparing the obtained CMOD responses using FEM (dashed lines in the figures) with the range of laboratory-measured CMODs in time for three replicates shows the capability of the implemented numerical framework to successfully predict the DC(T) creep test responses. As indicated in Section 2, the studied mixtures use various combinations of binder systems and recycled materials. However, the 1824 mix is believed to benefit from the softest binder system (SBS 64-34 binder with total ABR of 37.1% by RAP and RAS) among the SMA friction surface type mixtures. This is reflected in the CMOD response as it recorded the highest CMOD among the mixtures especially at 0 and -12 °C.

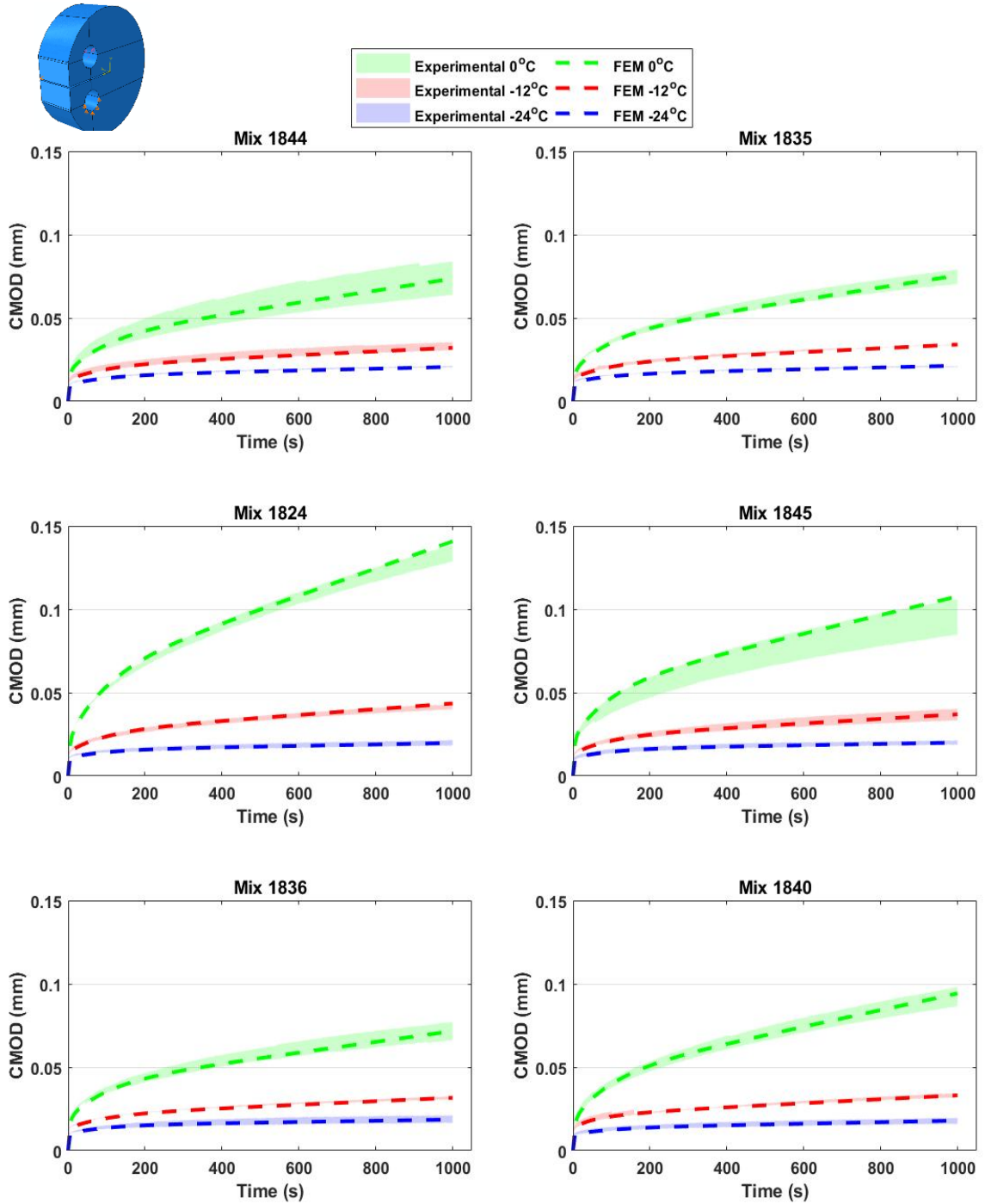


Figure 5-6. CMOD response versus time at three temperature levels for mixture of: (a) 1844; (b) 1835; (c) 1824; (d) 1845; (e) 1836; (f) 1840.

The repeatability of the DC(T) test is investigated based on the CMOD measurements at the 1000 s for three replicates of each mix. Table 5-4 shows the standard deviation along

with the measured coefficient of variance (COV) for replicate testing of the various mixture types at three temperatures. All averaged COVs are less than 10%, indicating the high level of repeatability of the DC(T) test. The highest average COV was recorded at 0 °C, which implies higher variability with higher test temperature. The higher variability of CMOD measurements at 0 °C can also be observed in Figure 5-6.

Table 5-4. Repeatability of CMOD at 1000 s

	-24°C		-12°C		0°C	
Mix. ID	STD (mm)	COV (%)	STD (mm)	COV (%)	STD (mm)	COV (%)
1844	0.0004	2.0	0.0029	8.8	0.0102	14.0
1835	0.0002	1.1	0.0005	1.5	0.0044	6.0
1824	0.0016	8.3	0.0028	6.7	0.0050	3.7
1845	0.0015	7.3	0.0035	9.5	0.0107	11.0
1836	0.0022	11.8	0.0013	4.2	0.0062	8.8
1840	0.0017	9.2	0.0012	3.7	0.0102	14.0
AVG	0.0013	6.6	0.0020	5.7	0.0078	9.6

5.6.2. Comparing IDT Response Predictions with Experimental Measurements

Viscoelastic properties of the mixtures along with the finite element method were implemented to show the capability of the numerical framework to predict the DC(T) creep responses. In this section, the viscoelastic properties obtained from DC(T) creep test are used to predict IDT creep responses. The differences in the stress state and strain distribution between the IDT and DC(T) geometries provide the opportunity to validate the DC(T) creep compliance properties and the numerical approach used in this study.

The IDT creep tests were carried out using a universal testing machine (UTM) with a capacity of 100 kN. The IDT creep test was performed on slices with 50 mm in thickness

and 150 mm in diameter, following AASHTO T-322. To carry out the IDT creep test, three replicates were conditioned at 0, -12, and -24 °C. For the sample to reach the desired testing temperature, the IDT cooling chamber needed to be set at a slightly lower temperature (see Table 5-5). Each sample was kept at the cooling chamber for 2 hours. The horizontal and vertical extensometers were then attached to the two faces of the IDT specimens, and the sample was placed into the IDT fixture. To compensate for the temperature loss due to opening the chamber door and installing the extensometers, the sample was kept for another half an hour to reach the testing temperature. Similarly to the DC(T) creep test, a seating load of 0.1 kN was applied to the sample. The seating load fixes the sample position in the IDT fixture, ensures rapid creep loading without impact, and eliminates some of the slight nonlinearity exhibited at low load levels. In the test, the load level is rapidly increased as a steep slope-load function until the target creep load is reached. The closed-loop controls are tuned such that the creep load is attained in less than one second. As Table 5-5 shows, the creep load was then maintained for 1000 seconds while horizontal and vertical displacements were recorded.

Table 5-5. Loading properties in IDT creep test

Test	Testing Temp. (°C)	Chamber Temp. (°C)	Seating Load (kN)	Ramp Time (s)	Creep Load (kN)	Creep Time (s)
IDT creep	0	-1.5	0.1	1	4	1000
	-12	-14		1	8	
	-24	-26		1	20	

Figure 5-7 shows the 3-D model of the IDT geometry along with the mechanical responses such as vertical stress and strain in Abaqus software. The viscoelastic properties identified from the DC(T) creep test, as in Section 3, were used in numerical

simulations. These mechanical responses are calculated using the viscoelastic parameters presented in Table 5-3 obtained from the DC(T) creep test. It is worth mentioning that the IDT test possesses a multiaxial stress state such that the vertical and horizontal stresses are imposed in vertical and horizontal directions, respectively. Given that the stress state in the DC(T) test is different than that in the IDT test (both in magnitude and distribution), a comparison between the results from both tests provides a meaningful way to verify and validate the ability of the proposed approach to identify the viscoelastic properties of asphalt mixtures at low temperatures.

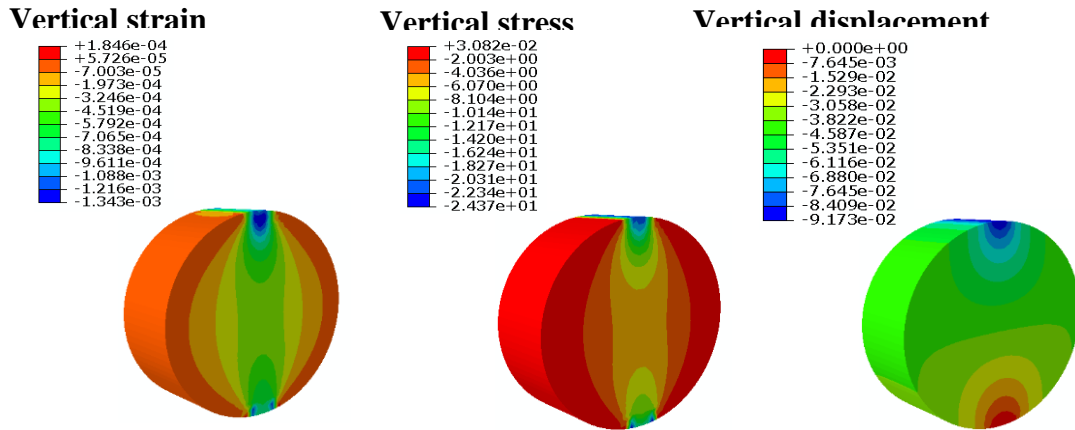


Figure 5-7. An example of DC(T) creep responses through FEM

To conduct the IDT test per AASHTO T-322, three replicates were tested for each mixture at three temperatures. As the extensometers are mounted on both sides of the IDT sample, six horizontal and six vertical sets of deflections were collected. Then, the maximum and minimum measure deflection were discarded (trimmed) per AASHTO T-322 and four extensometer results were used to analyze the results. Figure 5-8 to Figure 5-13 show the response range of the four extensometer measurements at each direction and the corresponding FEM result for mixtures at three different temperatures under the

IDT test. The horizontal and vertical displacements measured in each test were compared against the corresponding numerical results. The close agreement between the numerical simulations and experimental measurements validates the viscoelastic properties acquired through the proposed approach and the DC(T) creep test results.

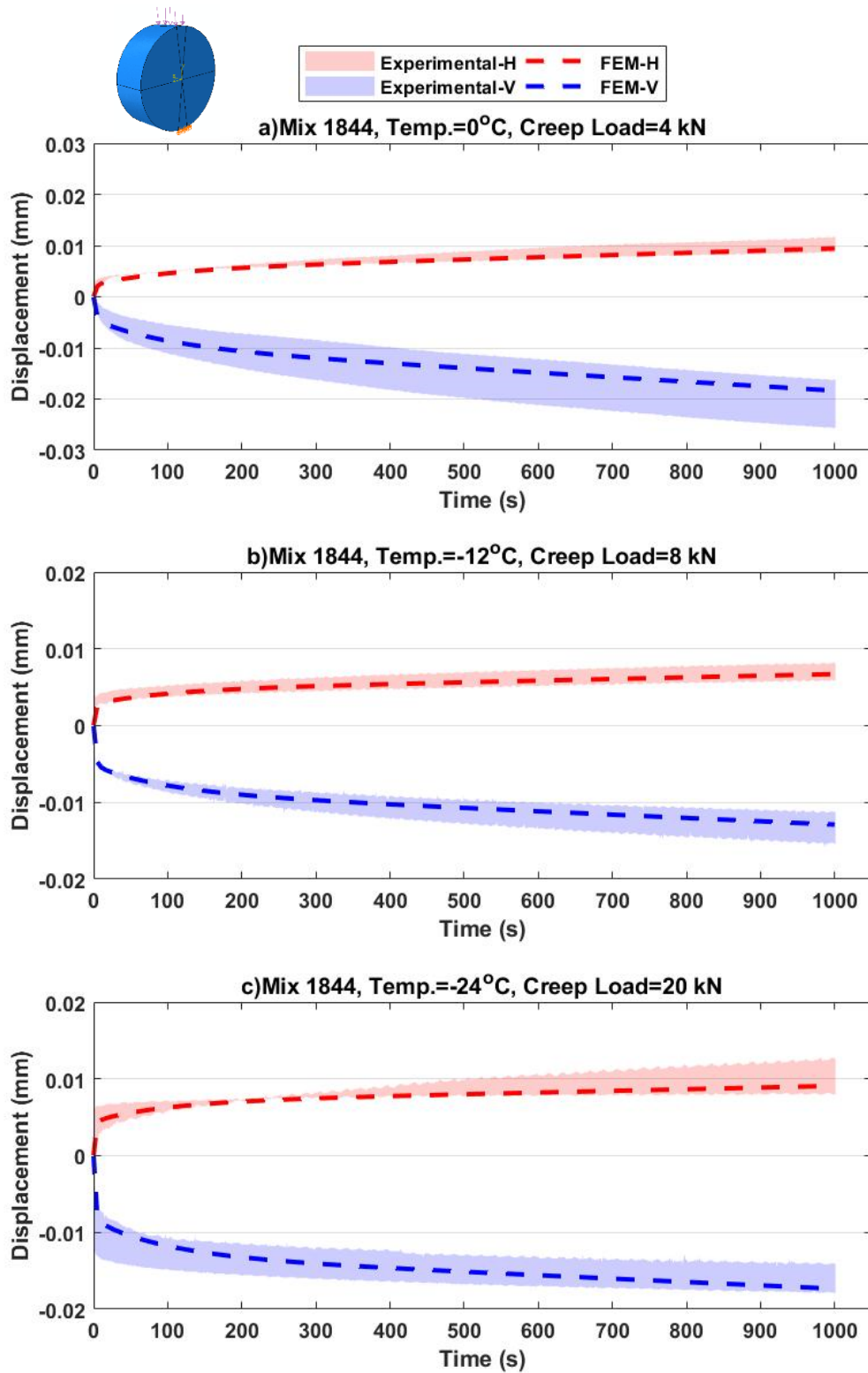


Figure 5-8. Horizontal and vertical deflections from IDT testing for the 1844 mix: (a) at 0°C; (b) at -12°C; (c) at -24°C

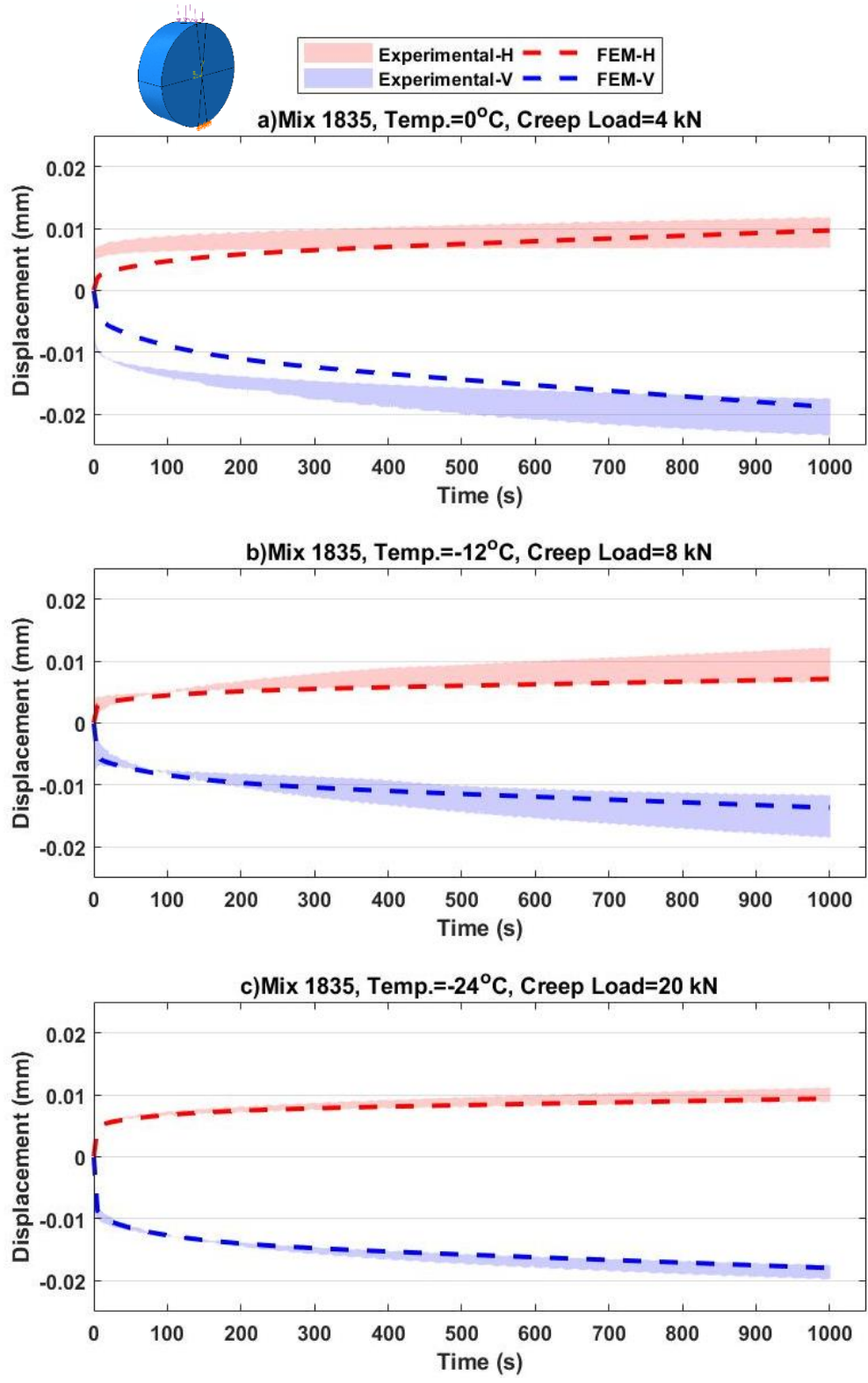


Figure 5-9. Horizontal and vertical deflections from IDT testing for the 1835 mix: (a) at 0°C; (b) at -12°C (c) at -24°C

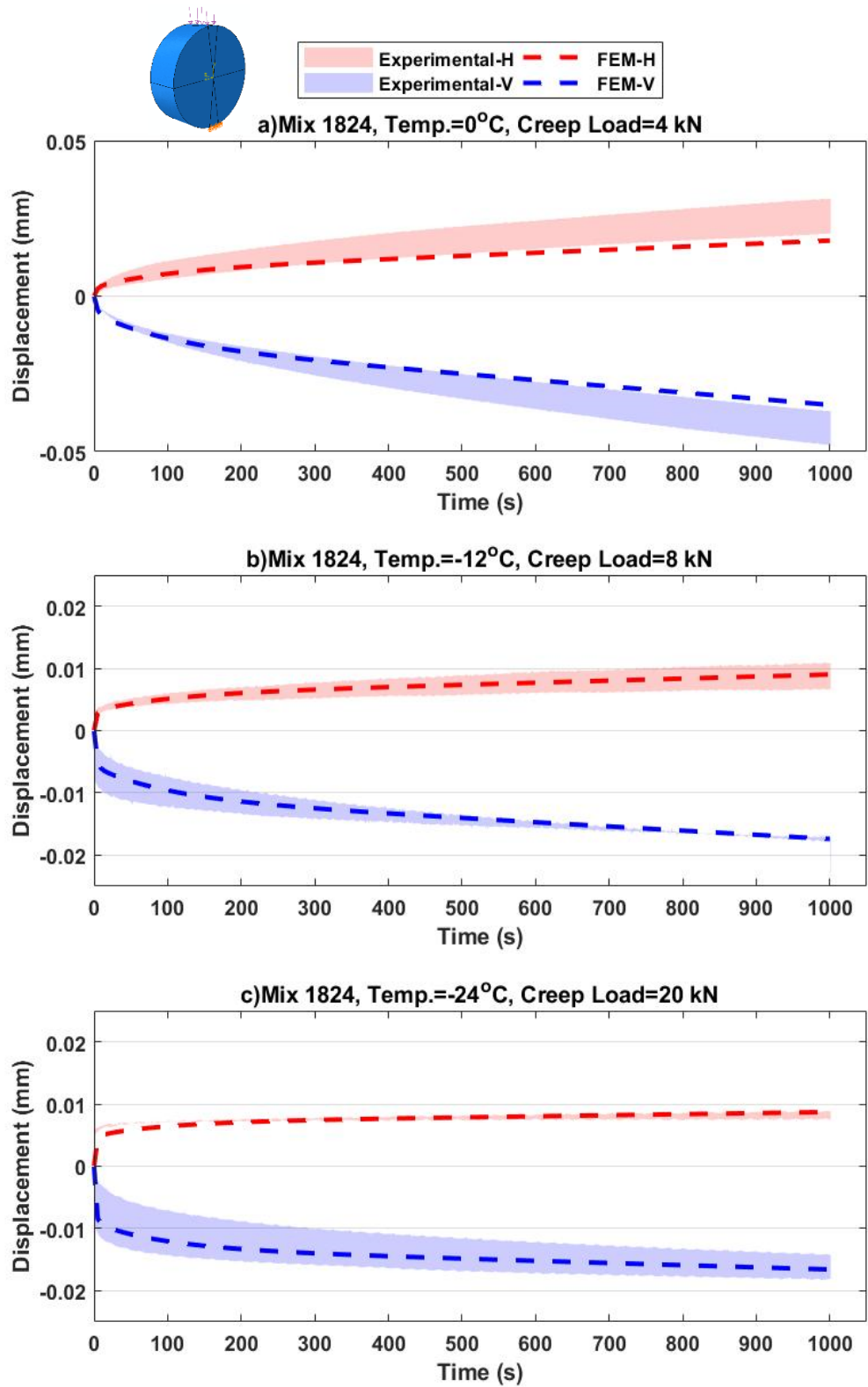


Figure 5-10. Horizontal and vertical deflections from IDT testing for the 1824 mix: (a) at 0°C; (b) at -12°C; (c) at -24°C

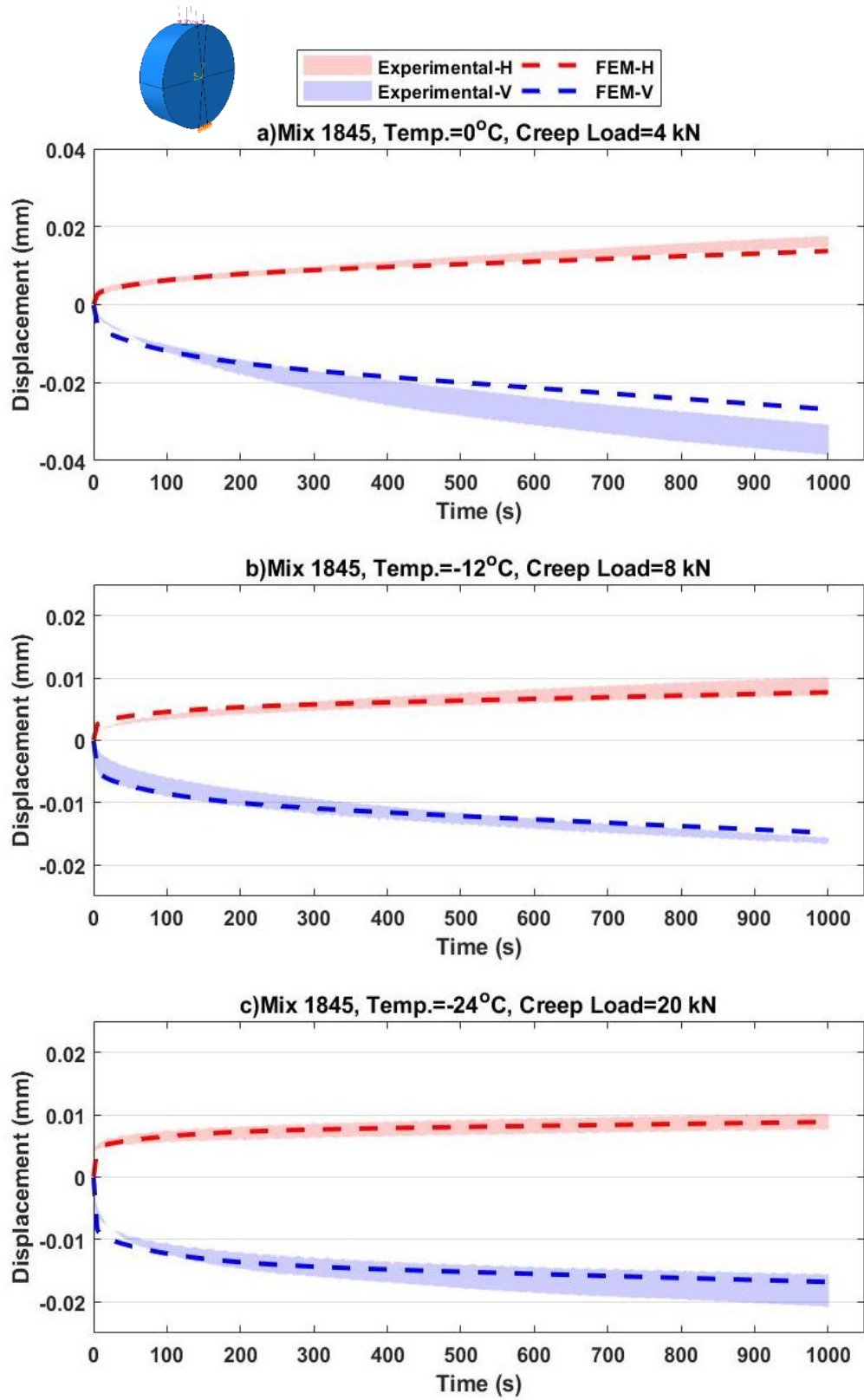


Figure 5-11. Horizontal and vertical deflections from IDT testing for the 1845 mix: (a) at 0°C; (b) at -12°C; (c) at -24°C

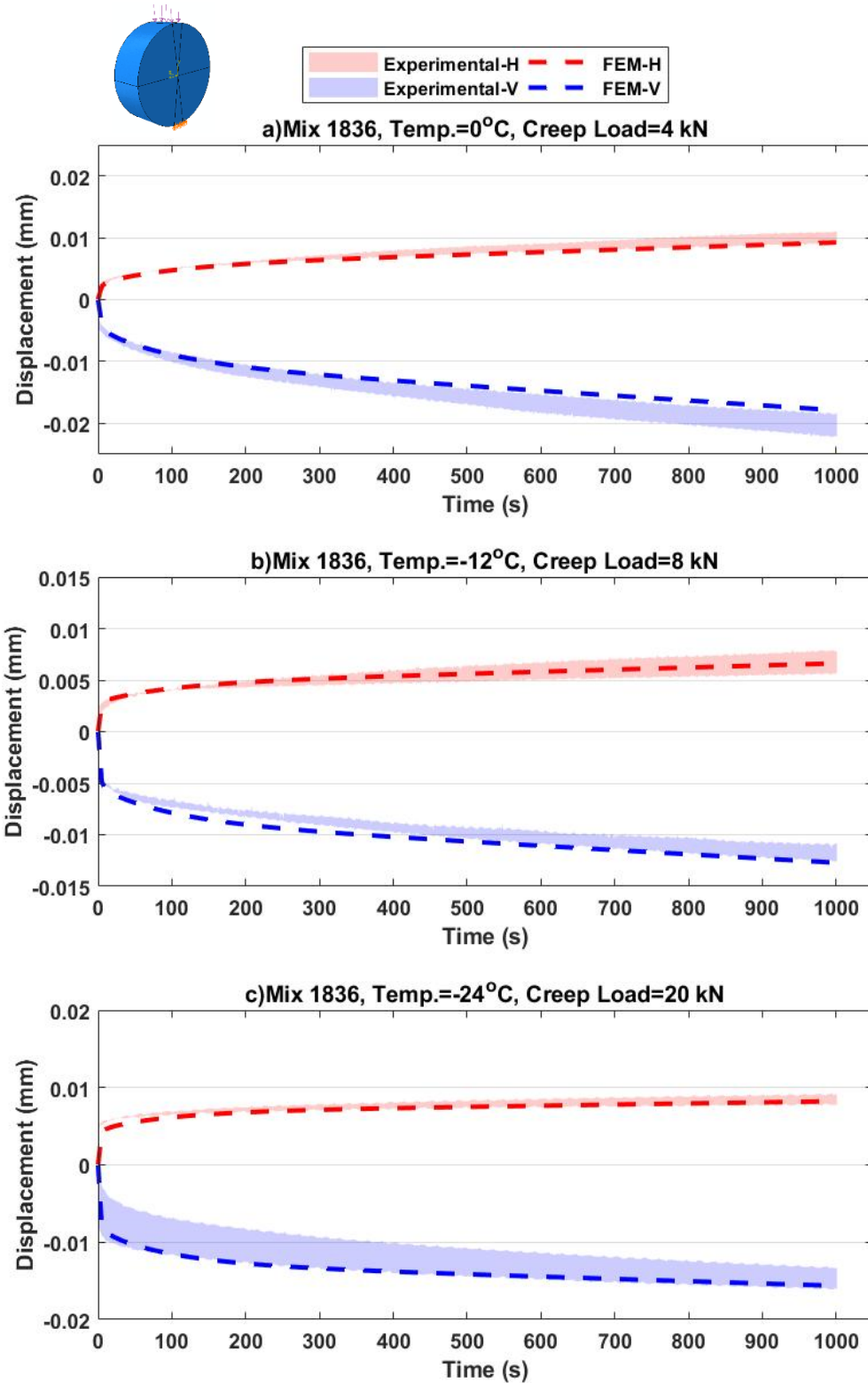


Figure 5-12. Horizontal and vertical deflections from IDT testing for the 1836 mix: (a) at 0°C; (b) at -12°C; (c) at -24°C

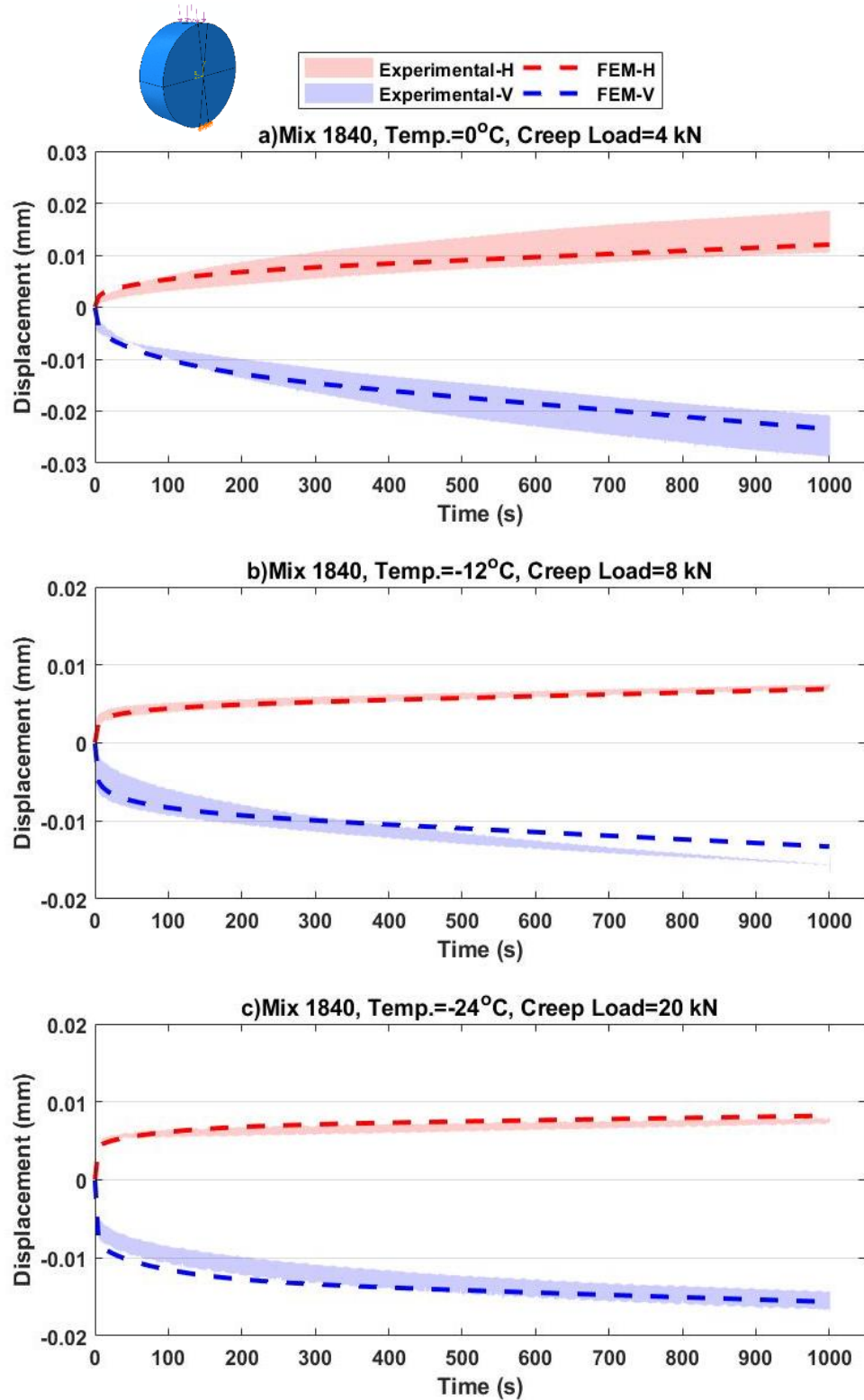


Figure 5-13. Horizontal and vertical deflections from IDT testing for the 1840 mix: (a) at 0°C; (b) at -12°C; (c) at -24°C

Table 5-6 and Table 5-7 provide the IDT test repeatability measures in the horizontal and vertical directions, respectively, using the extensometer measurements at 1000 seconds. The STD and COV parameters are calculated after discarding the lowest and highest measured deflections and considering the results from the remaining four extensometers in each direction, following AASHTO T-322. Using the trimmed data set from the three tested replicates leads to a lower coefficient of variation. According to Table 5-6 and Table 5-7, the averaged COV of the mixtures ranges from 9.0 to 16 % in horizontal and 9.8 to 12.7 % in vertical directions. Comparing to the DC(T) creep test repeatability, the COV of the IDT creep test is slightly higher. Also, it could be observed in both DC(T) and IDT tests that warmer test temperature leads to a higher standard deviation. As a result, a higher discrepancy is observed between the measured deflections and FEM predictions at 0 and -12 °C as compared to -24 °C (Figure 5-8 to Figure 5-13).

Table 5-6. Repeatability of IDT creep horizontal displacement at 1000 s

Mix. ID	-24°C		-12°C		0°C	
	STD	COV (%)	STD	COV (%)	STD	COV (%)
1844	0.0020	18.8	0.0009	13.2	0.0014	13.1
1835	0.0010	10.6	0.0027	31.8	0.0020	21.6
1824	0.0007	8.0	0.0017	19.8	0.0050	18.4
1845	0.0011	12.3	0.0013	15.4	0.0011	7.0
1836	0.0005	6.1	0.0012	17.5	0.0008	7.8
1840	0.0003	3.6	0.0005	7.5	0.0038	28.1
AVG	0.0009	9.9	0.0014	17.5	0.0023	16.0

Table 5-7. Repeatability of IDT creep vertical displacement at 1000 s

Mix. ID	-24°C		-12°C		0°C	
	STD	COV (%)	STD	COV (%)	STD	COV (%)
1844	0.0017	11.0	0.0017	12.5	0.0041	19.7
1835	0.0012	6.0	0.0033	24.5	0.0024	11.9
1824	0.0018	11.1	0.0035	18.4	0.0054	12.9
1845	0.0024	12.9	0.0006	3.7	0.0033	9.2
1836	0.0013	8.8	0.0008	7.0	0.0017	8.1
1840	0.0014	8.8	0.0012	8.2	0.0035	14.5
AVG	0.0016	9.8	0.0019	12.4	0.0034	12.7

Table 5-8 presents a variety of items that could be considered to further compare the IDT and DC(T) creep tests. The DC(T) sample fabrication involves additional steps such as making the notch and coring the holes. Therefore, the IDT sample fabrication is easier than that of the DC(T) sample. Although the vertical and horizontal extensometers on the sample surface make the instrumentation of the IDT test more difficult than that of the DC(T), it provides the chance to determine the Poisson's ratio of the mixture. Due to the measurement of the deflection in only one dimension in the DC(T) test, the calculation of Poisson's ratio is not possible through the presented DC(T) test setup. Monitoring the temperature of the asphalt sample in the cooling chamber indicated that the shorter duration of conditioning times is needed for temperature equilibrium in the DC(T) test. Also, opening the chamber door to load the testing into the test fixture has a small negative effect on the temperature of the conditioned sample. These resulted in selecting the DC(T) creep test as the more efficient test in terms of temperature controlling system. Given the lower COV calculated for these two tests, despite the trimmed data procedure applied for IDT displacing measurements, it was concluded that the DC(T) test is more

repeatable than the IDT creep test. The DC(T) creep test is also preferable in terms of the equipment cost and ease of data analysis.

Table 5-8. Comparing IDT with DC(T) creep tests

	DC(T) creep	IDT creep
Easier sample fabrication		✓
Also measures Poisson's ratio		✓
Easier instrumentation	✓	
Better temperature control	✓	
Higher test repeatability	✓	
Less expensive equipment	✓	
Simpler analysis	✓	

5.7. Illi-TC Modeling Results

Researchers at the University of Illinois at Urbana-Champaign developed a thermal cracking analysis software program called Illi-TC as a part of a national pooled funded study on low-temperature cracking [61]. Illi-TC tool simulates thermal cracking using three main types of data input, including climate, materials, and layering of the pavement to be evaluated. The default software includes a set of temperature profiles at various depths for specified geographical locations, calculated through Integrated Climatic Model (ICM) simulations. For material properties, the user inputs the tensile strength in MPa calculated from the IDT test or extracted from the DC(T) test, the DC(T) fracture energy in J/m^2 , raw creep data from the IDT (or DC(T)) test, and either the mixture coefficient of thermal expansion and contraction (CTEC) or the aggregate CTEC and mixture VMA (see Figure 5-14). In this study, results from DC(T) creep testing are used in Illi-TC software to account for the viscoelastic response and calculate the thermally induced

stress. Previously, the IDT creep compliance results were applied in the software. Introducing the DC(T) creep test and the creep compliance obtained from the test would result in a more convenient and less time consuming process to calculate the viscoelastic parameters.

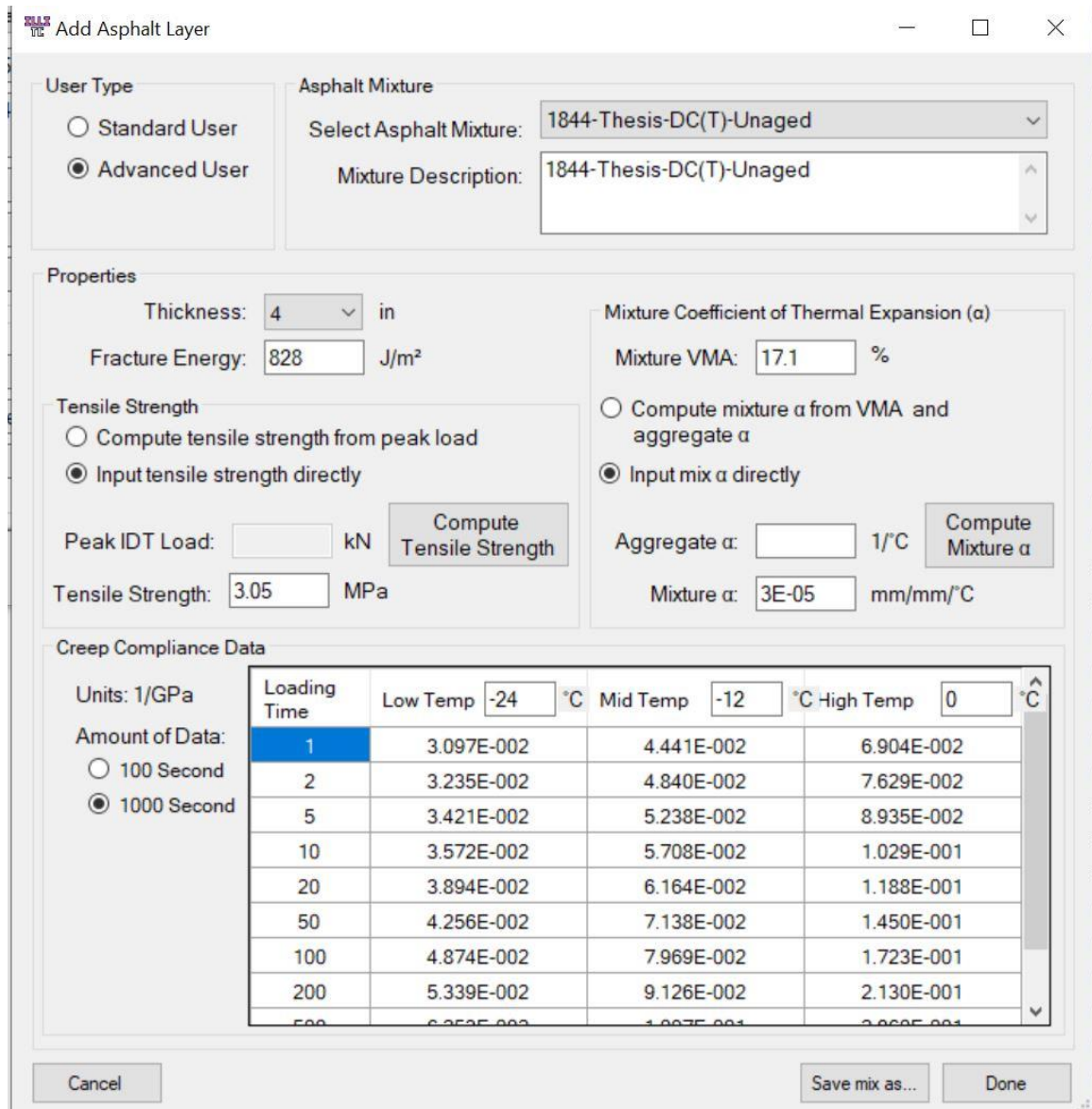


Figure 5-14. Screenshot of the ILLI-TC window to plug in the material properties (Example: Mix 1844)

The tool creates a finite element mesh depending on the specified geometry (pavement depth) and uses cohesive zone fracture elements in the finite element (FE) mesh to simulate thermal cracking. Field validation of this tool has been presented by Dave et al. (2013). More recently, Dave and Hoplin (2015) showed that Illi-TC is sensitive to the variation in fracture energy of asphalt mixtures and shows a difference in transverse cracking of asphalt pavements when the fracture energy is varied by values as low as 25 J/m². Following the usual practice, mixture CTEC values were estimated based on the primary geological composition of the aggregate stockpiles used in the study mixtures. In this study, a typical CTEC value of 3.00E-05 mm/mm/°C was assumed for all of the sections [63].

The inputs for the mixtures used for Illi-TC modeling and the modeling results are shown in Table 5-9. An example of temperature profile vs. time and resulting tensile stress at the surface of the pavement as computed by the Illi-TC software are provided in Figure 5-15. The number of critical events and also the amount of cracking are presented in the last two rows of the table. In addition to the six SMAs that were used on the surface of the Tollway facilities, another mix called US54_1 that has been used to pave sections across Missouri is investigated. This US54_1 mix is dense graded and generally possesses a lower cracking and rutting resistance as compared to the Tollway mixtures. Therefore, this mix was expected to develop higher amount of cracking and number of critical events. Although most of the Tollway SMA mixtures experienced critical one or two critical events (e.g. 1844, 1835, 1836, and 1840), the amount of cracking was not considerable due to the high DC(T) fracture energy. Therefore, based on the Illi-TC modeling results, these mixtures are not expected to develop transverse cracking in the

first five years of their service life. On the other hand, the US54_1 mix was found to experience nine critical events and more than 200 m per 500 m length of the road. This high level of cracking indicates that unlike the SMAs, this mix is not suitable to be used on the surface of the Tollway facilities. In addition, the modeling results show that all the friction surface type mixtures that could meet the proposed DC(T) criteria can properly withstand the cold environment in Chicagoland in terms of low temperature cracking. Although the 1836 and 1840 mixtures did not meet the proposed DC(T) fracture energy criteria for normal SMAs, the viscoelastic behavior and their stress relaxation capability helped with developing zero cracking amount. Further improvement of the binder system and aggregate system for these mixtures to meet the proposed DC(T) fracture energy requirements results in a higher reliability and can assure their cracking performance even after the first five years of their service life.

Table 5-9: Input parameters in Illi-TC and resultant critical events and amount of cracking

Section	1844	1835	1824	1845	1836	1840	US54_1
Fracture Energy (J/m²)	828	872	790	846	596	684	448
Mix CTEC (mm/mm/°C)	3.00E-05	3.00E-05	3.00E-05	3.00E-05	3.00E-05	3.00E-05	3.00E-05
IDT Strength (MPa)	3.05	3.1	3.4	3.2	3.5	3.5	3.9
VMA	17.1	16.2	16.2	16.1	16.1	16.0	14.4
Layer Thickness (cm)	10	10	10	10	10	10	7.5
Critical Events (output)	1	1	0	0	2	1	9
Cracking Amount per 500 m Length	0 m	0 m	0 m	0 m	0 m	0 m	>200 m

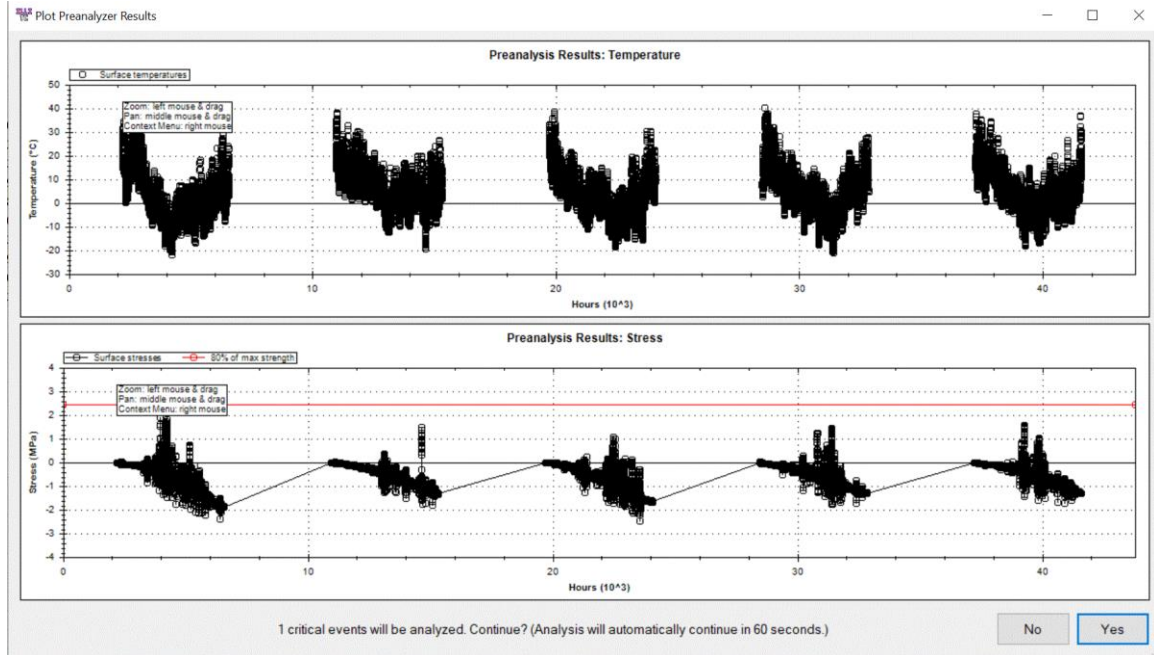


Figure 5-15. Screenshot of the Illi-TC output for number of critical events (Example: Mix 1844)

5.8. Summary and Conclusions

In this study, a new method called the DC(T) creep test was introduced to characterize the viscoelastic behavior of asphalt mixtures at low temperatures. To this end, the CMOD responses of six SMA type mixtures were measured under a constant load applied to the sample in 1000 seconds at three temperatures including -24, -12, and 0 °C. According to the well-known correspondence principle in viscoelasticity studies, the CMOD measurements under the DC(T) test along with a correction factor that accounts for the sample geometry were used to calculate the creep compliance as a function of time. A generalized Voight-Kelvin model including an isolated spring, a dashpot, and four Kelvin elements was employed and calibrated for each mix at each of the test temperatures. The viscoelastic constitutive relationship was implemented in the finite element code Abaqus via a user material subroutine. The proposed numerical framework was used to predict

the DC(T) response under creep loading. In addition, IDT creep tests were conducted at the same temperatures and the horizontal and vertical displacements were measured. The developed framework and determined viscoelastic parameters from the DC(T) creep tests were implemented to predict the IDT responses. The following conclusions could be drawn from the test results and analysis presented:

- The relationship between the CMOD response measured in aDC(T) creep test and the resulting viscoelastic creep compliance obtained by applying the simple geometrical constant developed herein can be used to simply and accurately characterize the viscoelastic creep behavior of asphalt concrete at low temperatures.
- The developed numerical framework and UMAT subroutine for the generalized Voight-Kelvin model can be used to simulate the viscoelastic response of asphalt mixtures in the commercial FEM code ABAQUS.
- The close agreement between the laboratory-measured displacements in IDT test and the FEM predicted displacements validated the viscoelastic properties obtained with the newly proposed DC(T) creep test and analysis method.
- The DC(T) creep test yields a lower COVs and is deemed to be more repeatable than the IDT creep test, even after applying the trimmed mean approach to the displacements measured in the IDT test.
- Except for the easier sample fabrication and the possibility to calculate Poisson's ratio, the DC(T) creep test may be viewed as preferable over the IDT creep test in terms of the added simplicity and reduced cost for instrumentation, temperature control, and data analysis.

Chapter 6

ASPHALT MIXTURE PERFORMANCE GRADING

6.1. Introduction

The performance of asphalt concrete depends heavily on both environmental and traffic loading conditions. In colder regions, low temperature and block cracking are common distresses observed in asphalt pavements, while rutting is the prevalent mode of deterioration at high temperatures and under heavy traffic. To ensure adequate asphalt pavement durability and serviceability, one must control not only asphalt binder properties, but also those of other components such as recycled materials, additives, aggregates, and mixture volumetrics. Ideally, the performance properties of a given asphalt mixture should also be evaluated based on its position in the pavement and should consider the entire layering system present in the pavement (i.e., the pavement structure). In summary, a comprehensive mix design system would set performance criteria in accordance with traffic, climate, and pavement structure.

6.1.1. Binder Specification

A key outcome of the Strategic Highway Research Program (SHRP) was the introduction of climate and traffic based performance grading of the asphalt binder. Unlike previous asphalt binder grading systems, the Superpave Performance-Graded (PG) binder system opened the door for the production and specification of a wide range of binders, including those with the ability to hold up in harsh, mid-continental climates such as the Midwest USA. In these regions, the binder must possess the ability to withstand rutting during hot summers, and low temperature cracking during very cold winters. These binders have a wide spread between the Superpave high and low temperature grades, which is sometimes called the Useful Temperature Interval (UTI). Following early asphalt technology terminology, these binders were said to possess low temperature

susceptibility. In the years following SHRP, the effect of traffic level was more comprehensively captured in a revised asphalt binder grading specification (AASHTO M332) using the multiple stress and creep recovery (MSCR) test [64]. Later, Anderson et al. (2011) investigated the environmentally-related binder cracking and introduced the ΔT_c parameter in order to characterize the relaxation loss due to aging.

As a step closer to fingerprinting the actual binder system in a modern, heterogeneous mixture, aged binder systems (e.g., field aged mixtures, mixtures containing recycled materials, etc.), the ASTM D2172 and ASTM D5404 procedures can be used to extract and recover binder from lab and field mixes [66–69] Binder extraction and recovery on polymer modified mixtures has also been reported. Mohammad et al. 2003 [70] performed chemical and mechanical tests on recovered polymer modified binder and showed the effect of extraction and recovery on the binder system to be minimal. Morea et al. (2012) [71] also reported on the ability to successfully perform extraction and recovery on polymer modified binder systems. Differences in binder viscosity and subsequent differences in rutting performance of SBS modified as compared to unmodified mixtures have also been reported [72]. On the other hand, difficulties associated with the extraction of crumb rubber modified binders have been reported in the literature [73,74]. Despite being a step closer to capturing actual mixture behavior, binder testing of extracted and recovered binder systems falls short of capturing effects caused by actual binder, mastic, and mixture morphology. The binder extraction gets even more complicated when the recycled materials such as RAP, RAS have been incorporated into the asphalt mixture. Due to the different blending levels of virgin and

recycled binders, the extracted and recovered binder may not represent the blended binder within the asphalt mixture [75].

6.1.2. Modern Mixture Characterization

Decades ago, traditional asphalt mixtures were mainly made of virgin asphalt binder, aggregates, and air voids, while modern, heterogeneous mixes contain various recycled components (RAP, RAS, GTR), recycling agents, fibers and more. Decades ago, simple mixture tests such as Marshall Stability and Flow proved to be adequate screening tools for the design and control of traditional asphalt mixtures. Recently, performance tests such as semi-circular bending [76], IDEAL-CT [77], and disk-shaped compact-tension (DC(T)) [78] tests have been widely used as relatively simple means for assessing the cracking potential of modern asphalt mixtures. For the high temperature response regime, the flow number [79] and Hamburg wheel tracking tests [80] are among several tests that have been carried out to characterize the rutting resistance of asphalt concrete.

Currently, the DC(T) test is one of the limited standardized methods to evaluate the fracture energy of asphalt mixtures at low [62,78] The DC(T) test has been widely used by researchers and agencies alike to determine the low temperature characteristics of asphalt mixtures [28]. Currently, several upper-Midwest US states and other agencies in cooler regions have adopted the DC(T) for the purposes of thermal and block cracking control in modern asphalt mixture design specifications, such as the Minnesota Department of Transportation, the Chicago Department of Transportation, and the Illinois Tollway. The DC(T) test offers various advantages that include straightforward sample configuration- both from plant/lab-compacted gyratories and from the field cores, and its standard fracture test configuration. In terms of mixture characterization, the DC(T)

fracture energy test has shown the capability to differentiate between varying mixture constituents such as RAP/RAS or WMA additives, and also between varying mixture properties, such as aging [28,81–83]. According to ASTM D7313, the DC(T) test is performed at 10 degrees warmer than the PGLT of the binder. Researchers in [78] performed the DC(T) fracture energy on four different asphalt mixtures at three different temperatures (-20, -10 and 0°C). They observed that as temperature decreases, the mixtures appear to yield lower fracture energy. This was attributed to the distinct transition from quasi-brittle fracture with softening response to brittle fracture with minimal softening after the peak. Zegeye et al. 2012 [84] reported similar findings. Li et al. 2008 [85] concurred with ASTM D7313 that DC(T) testing temperatures should be defined relative to the PG of the binder. Test temperatures such as PGLT-2 °C, PGLT+10 °C, and PGLT+22 °C temperatures were studied to evaluate the fracture resistance of 28 mixture types. Statistical analysis showed that testing temperature is a significant parameter in DC(T) fracture energy.

The most recent asphalt mixture specification used by the Illinois Tollway shows differing DC(T) fracture energy thresholds for different mixture types and positions in the pavement (surface vs. binder course asphalt; mainline vs. shoulder mixes). This was done to balance mixture performance vs. mixture economy, where higher reliability thresholds (higher fracture energy requirements) are used in more critical locations and vice-versa. More details regarding the Tollway DC(T) and Hamburg specification requirements are provided in the following section.

Rutting involves consolidation and shear flow resulting from the accumulation of shear strains caused by repeated traffic loading [86]. The rutting performance of asphalt

mixtures depends on mix design and environmental conditions including traffic and climate. The Hamburg Wheel Tracking Test (HWTT) is designed to investigate the rutting characterization by simulating traffic on the HMA mixtures through running standardized wheels on specimens at a given temperature. This test has been employed by many researchers to characterize the rutting potential of the asphalt mixtures [87–89]. Walubita et al. [90] argued that the average temperature and maximum temperature measured from the surface of some randomly selected in-service highways in Texas are 58.3 and 63.1, respectively. Therefore, specific rutting failures observed in Texas were attributed to the lower Hamburg testing temperature used as compared to actual pavement temperatures. To address this issue, Walubita et al. performed the Hamburg test at 50, 60 and 70°C. Swiertz et al. [91] also investigated the appropriate testing temperature for the Hamburg wheel tracking test. In this study, tests were carried out at 40, 45 and 50°C. Based on WisDOT specifications, in order for a mixture to pass the Hamburg test, unmodified and modified mixes should undergo at least 5000 and 15000 wheel passes, respectively, before accumulating 12.5 mm in rut depth. Regardless of the mixture combination, most mixes investigated in this relatively cold climate could not pass the criteria at the default Hamburg test temperature of 50°C, probably due to the presence of the relatively soft binders in Wisconsin. Both of the aforementioned studies suggest that a climate-dependent Hamburg test temperature may be needed in the United States.

6.1.3. Illinois Tollway Mixture Sustainability and Performance Design

The Illinois Tollway accomplishes the dual goals of achieving long term asphalt pavement durability with sustainability and economics by maximizing the amount of recycled materials in its asphalt mixtures and testing the mixtures to ensure the

pavements achieve long-term life. To increase asphalt pavement sustainability, the Tollway adopted the use of fractionated RAP in 2008; evaluated and implemented reclaimed asphalt shingles (RAS) in 2009 [92]; and began requiring warm mix asphalt (WMA) in all of its mixes in 2012 [93]. All of the Tollway mainline asphalt pavements are surfaced with stone-matrix asphalt (SMA) for long-term strength and durability.

The Tollway has used the shoulder pavement of its 286-mile system as the testbed for these asphalt mix innovations, to ensure the sustainable efforts do not sacrifice long-term durability. Full-scale pavement test sections have been used to evaluate the production and construction viability, and increasingly modern test procedures have been incorporated into these durability evaluations. Beam fatigue, dynamic modulus, flow number, indirect tensile strength, disk compact tension DC(T), and Hamburg wheel tracking have all been part of the evaluations to demonstrate that the Tollway's sustainability efforts have not affected long-term durability. The DC(T) and Hamburg test procedures have been incorporated into the Tollway's performance-based mix design and production specifications [94].

The results of these evaluations have confidently allowed the Tollway to permit up to 50 percent asphalt binder replacement (ABR) in all of its asphalt mixtures, with several mixes allowing even greater ABR [95]. The Tollway is continuing to conduct research, including field trials, towards extending their performance related specifications to include more asphalt material types, and to calibrate the system with additional lab and field data. The Tollway encourages industry and contractor innovation, and new materials are routinely considered in asphalt mixtures. The current mix design specifications allow both wet- and dry-process ground tire rubber, softer asphalt binders, and recycling agents.

These innovations have maximized the contractor's flexibility in designing their asphalt mixtures. The expectation is that the incorporation of performance-based specifications will result in even more advancements and innovation in the design and construction of the Tollway's asphalt pavements.

6.1.4. Challenges Associated with Binder Extraction and Recovery

As a step closer to fingerprinting the actual binder system in a modern, heterogeneous mixture, aged binder systems (e.g., field aged mixtures, mixtures containing recycled materials, etc.), the ASTM D2172 and ASTM D5404 procedures can be used to extract and recover binder from lab and field mixes [66–68,96]. Binder extraction and recovery on polymer modified mixtures has also been reported. Mohammad et al. [70] performed chemical and mechanical tests on recovered polymer modified binder and showed the effect of extraction and recovery on the binder system to be minimal. [71] also reported on the ability to successfully perform extraction and recovery on polymer modified binder systems. Differences in binder viscosity and subsequent differences in rutting performance of SBS modified as compared to unmodified mixtures has also been reported [72].

The main possible reasons of the high COV calculated for the tests on extracted and recovered binders, including the hardening effect of the solvent, existence of the solvent in the recovered binder, and partial extraction of the binder from aggregates, have been discussed in literature [97–102]. As an example, Burr et al. in [103] implemented the infrared (IR) spectroscopy to characterize the hardening effect of the solvent on the recovered binders. However, the extent of the aging was binder dependent and could be reduced through cold extraction and a rapid recovery. The binder extraction gets even

more complicated when the recycled materials such as RAP, RAS have been incorporated into the asphalt mixture. Due to the different blending levels of virgin and recycled binders, the extracted and recovered binder may not represent the blended binder within the asphalt [104,105] Researchers in [26] recommended mixture testing as more informative method for performance evaluation. The practicality of the extraction and recovery of the rubber modified binders has been discussed in research studies [73,106], Heitzman [106] mentioned the inaccurate binder and rubber content measurements through extraction because the complete solubility of rubber in the solvent is under question.

To eliminate the uncertainties about the extracted and recovered binders, researchers have tried to characterize the recycled binders without extracting them from the mixtures [107]. Ma et al. [99] conducted BBR tests on mortar and binder samples to estimate the RAP binder properties. The Hirsh model developed by Christensen et al. [108] was applied to back calculate the shear complex modulus in the mixtures containing different percentages of RAP [109]. It was observed that the back calculated binder G^* from complex modulus testing results of the mixture through the Hirsh model was lower than the one obtained from testing on the extracted binder. This observation was attributed to the higher level of blending of virgin binder with the RAP binder that the extracted binder would experience [109]. Hajj et al. in [110] tried blending chart, mortar method, Hirsch model, and Huet-Sayegh model to indirectly determine the PG in RAP mixtures and compared the results with the extracted binder PG. In addition, the fracture temperature obtained from TSRST test correlated very well with the PGLT from the mortar procedure.

6.1.5. Motivation for the Current Study

As the relevant literature suggests, asphalt materials need to be characterized and evaluated based on the environmental and loading conditions that they will experience during the service life. In order to assure the performance of asphalt mixture at different climatic conditions, the cracking and rutting potential of different mixtures were investigated in this study through testing of both recovered binder, and of as-produced Tollway mixtures. DC(T) and Hamburg tests benefit from a temperature control system that allows the user to conduct the test at multiple temperatures. This capability was used to determine the continuous performance grade of different types of mixture. This was then compared to the continuous binder grade of the recovered binders. A detailed summary of results, including a comparison of high- and low- temperature binder and mixture continuous grades, mixture useful temperature interval (UTI), and suggestions for future mixture improvement are provided. Suggestions for further development and local calibration of this method for use by other agencies is also provided.

6.2. Methodology

In this study, the performance of the SMAs and dense graded mixtures were evaluated at low and high temperatures. To investigate the cracking performance, DC(T) testing at -12°C was carried out and the fracture energy of the asphalt mixtures was measured. In addition to the crack resistance at -12°C, the temperature sensitivity of the studied mixtures was evaluated through performing DC(T) fracture test at -18°C. Then, a linear interpolation (or extrapolation) was applied to calculate the temperature at which the DC(T) fracture energy reaches the predefined fracture energy criteria as mentioned in Table 6-1. The determined threshold temperature was then used to arrive at the

performance grade (PG) of the mixture at low temperature, by subtracting 10°C. The same numerical approach was implemented on Hamburg testing results at two different temperatures to calculate the temperature at which the maximum rut depth allowed by Illinois Tollway (Table 6-1) is reached. For high temperature, a 'shift factor' of 14 degrees Celsius was added to the threshold test temperature to arrive at the high temperature performance grade. While Figure 6-1 shows the proposed approach to determine the mixture PG, more details regarding the new continuous mix PG system are provided in a later section. The performance tests carried out in this study are explained in the following section.

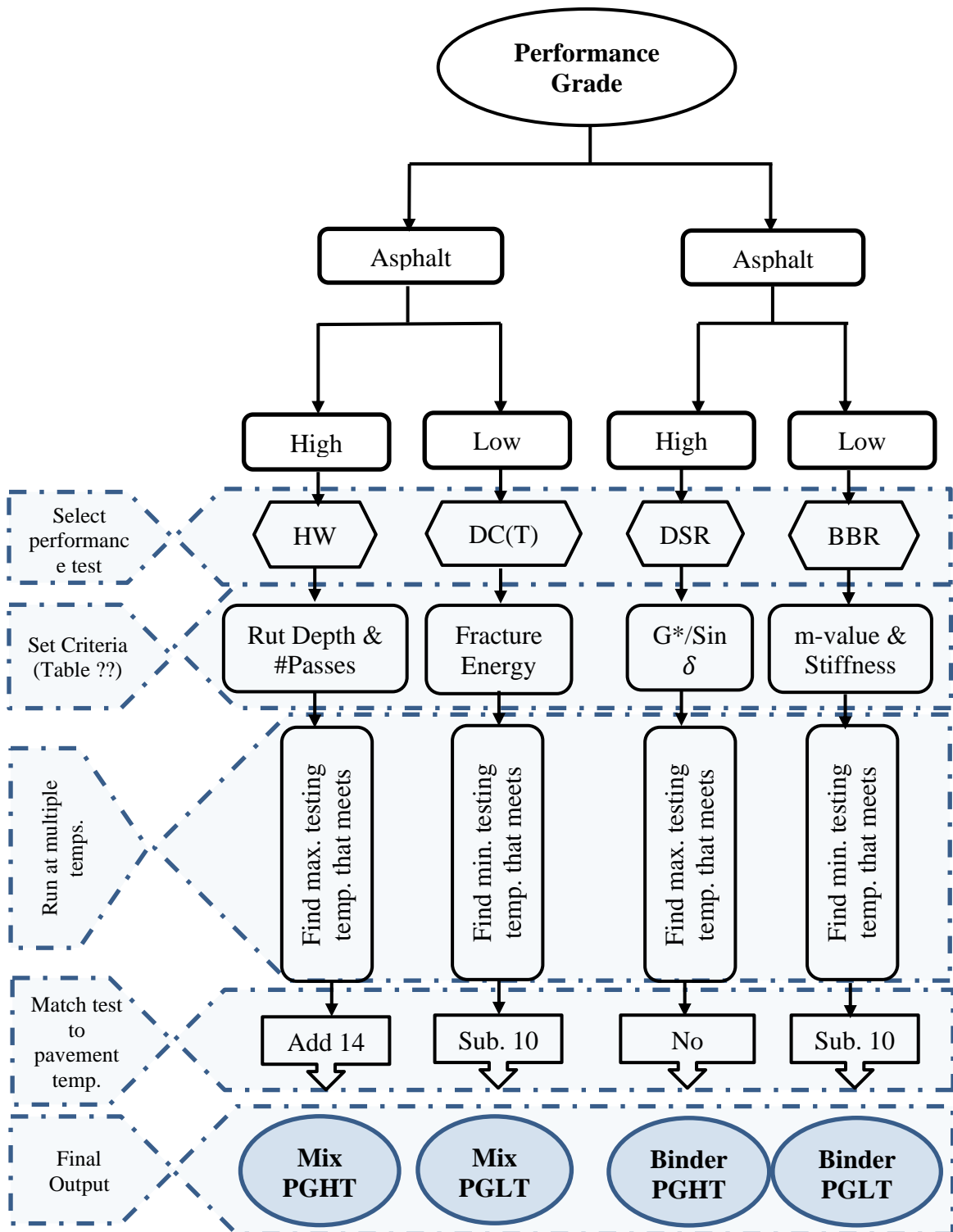


Figure 6-1. Proposed approach to determine the mixture PG

Table 6-1. Illinois Tollway performance criteria for different mixture types

Mixture Type	Minimum Fracture Energy	Maximum Rut Depth
SMA-Friction Surface	750 J/m ²	6 mm at 20000 passes
SMA- Surface	700 J/m ²	6 mm at 20000 passes
Shoulder Surface Course	425 J/m ²	12.5 mm at 15000 passes

6.3. Mixture Properties

In this study, six Illinois Tollway SMAs and two dense graded mixtures were sampled from different asphalt plants in Chicago. Mixtures were collected in steel buckets and then transferred to the lab for sample fabrication and testing. Table 6-2 shows the properties of each mixture type. As shown in the table, the design number of gyrations (NDesign) of all the SMAs is 80, while the NDesign for shoulder surface mixtures is 70. The first four mixtures (1844, 1835, 1824, and 1845) are friction-surface-type SMAs (used on curves and ramps) and the last two SMA mixtures are regular SMA surfaces (for use in full-speed, non-curved, or tangent, road alignments). The average daily traffic (ADT) on the routes paved with these mixtures ranges from 11000 to 17000 including 25% of commercial vehicles. Finally, the last two mixtures (1818 and 1834) were used to pave the surface of the shoulders.

Among the mixtures investigated, three of them, including 1844, 1824, and 1836 mixtures utilized SBS modified binder systems. Although the UTI of these binder systems was identical (70+28=98°C), the base binder used in 1844 was found to be stiffer, probably due to its use with a mix containing a relatively lower amount of recycled materials. The other three mixtures (1835, 1845, and 1840) involved rubber-

modified binder or mixture systems (contained GTR either by terminal blend or dry process). The 1835 mix utilized a soft neat binder of Superpave grade PG46-34 combined with 10% engineering crumb rubber (ECR) by weight of binder, added to the mixture through a dry process [111]. This mix also had the highest amount of recycling materials (41.2% ABR) including 25.1% ABR by RAP and 16.1% ABR by RAS. Similar to 1835, the 1845 mix also used PG46-34 neat binder which was later modified by 12.5% rubber by weight of the binder. The neat binder used in the 1840 mix is PG58-28. This binder was then modified by 12.0% of ground tire rubber (GTR), added to the binder through the wet process. Unlike the SMAs, the binder used in dense graded mixtures to pave the surface of the shoulders was not modified. Another difference between the SMAs and dense graded mixtures was that no RAS was used in the shoulder mixtures. As a result, they have relatively lower ABR. It is also noted that a Pine GB2 Superpave gyratory compactor was used to compact the reheated samples and make cylindrical specimens. All SMA testing samples were compacted to $6.0 \pm 0.5\%$ air void while the target air void for dense graded mixtures was $7.0 \pm 0.5\%$.

It is worth mentioning that the plan grade of binder used in the Tollway SMAs is PG76-22. This means that it is expected that the extracted binder, which includes both a modifier (polymer or rubber) and recycled binder (usually RAP and RAS) is required to pass the performance grading criteria at 76°C for the PG high temperature (PGHT) and -22°C for the PG low temperature (PGLT). As for the shoulder mixtures, the plan grade is PG 64-22. The less stringent requirement on the PGHT of the plan grade is attributed to the considerably lower traffic load that the shoulders experience throughout their service life. However, the plan PGLT requirement is the same as SMAs and shoulder mixtures

since both types were used on the surface of the roads and will experience the same low-temperature environmental conditions.

Aggregate gradations of the mixtures investigated are shown in Figure 6-2. It can be seen that the gradation of all SMAs are similar and possess a nominal maximum aggregate size of 12.5 mm. Likewise, the gradation of dense-graded mixtures are very close to one other, with 9.5 mm NMAAS in each case. Despite the similarities in the aggregate gradations, it should be noted that the aggregate type used by each asphalt contractor can and does vary in the Chicago area. Therefore, the overall characteristics of the aggregate skeleton in each mix investigated herein are unique.

The last column of Table 6-2 indicates the continuous PG of the extracted binder from the studied mixtures. The Superpave suite of tests including dynamic shear rheometer (DSR) and bending beam rheometer (BBR) tests were performed to determine the PG of the extracted binder. Binder recovery and testing was performed by STATE Testing, LLC, in East Dundee, IL. As the binder was already mixed with the aggregates in the asphalt plants, it is assumed that the recovered binder has gone through short term aging and rutting criterion of $G^*/\sin\delta$ equal to 2.2 was applied for DSR testing results on the recovered binder to obtain the continuous high temperature grade. Testing at multiple high, low and intermediate temperatures was needed to establish the continuous binder grade, by interpolation of results. Additionally, a max creep stiffness value of 300 MPa and a minimum m-value of 0.3 were used to establish the continuous extracted binder PG grade for low temperature. It should be noted that the extracted binder may not be necessarily representative of the binder system within the mix. This is due to different blending levels of virgin and recycled binder achieved in asphalt plants compared to the

ones in the extraction and recovery process. In addition, the practicality of the extraction and recovery of the rubber modified binders (e.g. 1835, 1845, and 1840) is still under question.

Table 6-2. Details of the mixture ingredients

Mix. No	Mix Type	Base	Binder	Plan	Grade	ABR by	RAP	ABR by	RAS	NMAS	Extracted	Binder
1844	SMA										88.2- 21.7	
	Friction Surface	SBS 70-28		76-22	10.8	16.0	12.5					
1835	SMA	46-34									75.3- 22.5	
	Friction Surface	+10%ECR		76-22	25.1	16.1	12.5					
1824	SMA										85.6- 29.8	
	Friction Surface	SBS 64-34		76-22	20.4	16.7	12.5					
1845	SMA	46-34									75-29.1	
	Friction Surface	+10.5%Lehig h		76-22	23.9	15.4	12.5					

1836	SMA	SBS 64-34	76-22	16.2	16.3	12.5	85.7-
	Surface						30.5
1840	SMA	58-28	76-22	15.9	9.8	12.5	72.2-29
	Surface	+12%GTR					
1818	Dense	64-22	64-22	20.4	0.0	9.5	72.9-
	Shoulder						23.8
1834	Dense	58-28	64-22	20.0	0.0	9.5	67.5-
	Shoulder						28.8

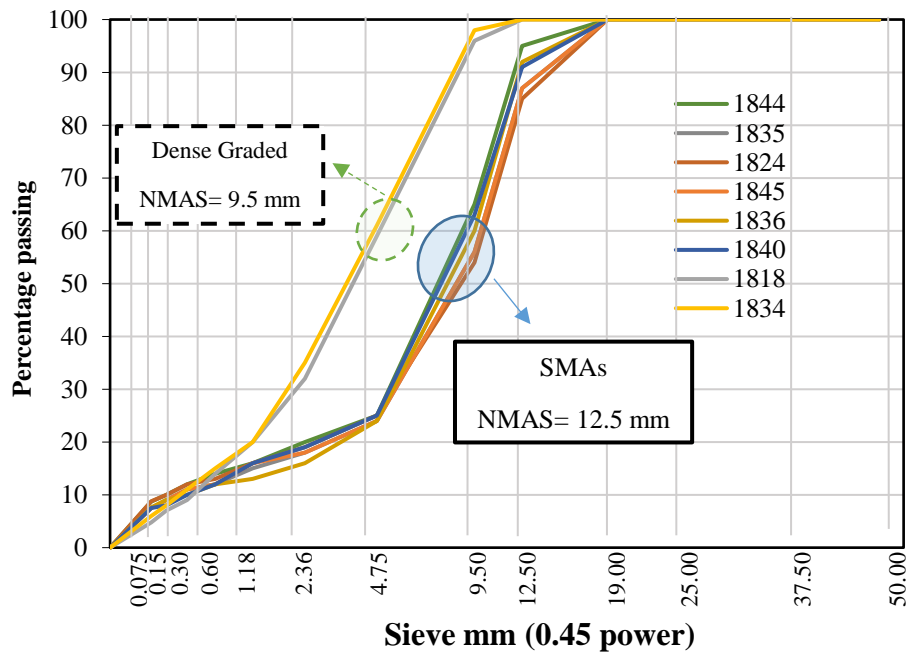


Figure 6-2. Aggregate gradation chart for the mixtures

6.4. Results and Discussions

6.4.1. Experimental Testing Results at Low Temperature

Looking at the pavement temperature with 98% reliability using LTPP binder software, it can be seen that the required PGLT of the binder in the state of Illinois is in the range of -22 to -27°C. The PGLT of -22 is mainly required in the southern part of Illinois while the -27 limit is identified for the very northern part of the state. Therefore, the PGLT of plan grade of the binder in the upper parts of Illinois should be lower than -22 to reach 98% reliability. As per ASTM D-7313, the DC(T) test is performed at 10 degrees warmer than the binder grade. The Illinois Tollway currently uses a -22°C plan low temperature grade, and thus testing at -12°C used in the DC(T). The relatively high DC(T) thresholds used at the Illinois Tollway reflect the high project criticality of Tollway road surfaces, and the fact that a slight adjustment has been made to facilitate the fact that northern Illinois is somewhat colder than the assumed -22°C PGLT used for base binder plan grades.

Figure 6-3 shows the DC(T) fracture (G_f) testing results at -12°C. The error bars provide the range of the values obtained for the three replicates tested in DC(T) fracture. In addition to the bars shown in the figure, the table below the figure provides the name of the mix, the average fracture energy and also the ABR of each mix. As shown in the figure, all the SMA friction surface type mixtures could pass the 750 J/m² criterion which is currently practiced by the Tollway. The difference between the highest and lowest recorded fracture energy is less than 100 J/m² which implies that the resistance of the mixtures to low temperature cracking is expected to be similar. On the other hand, the surface SMA mixture had significantly lower fracture energy than the friction surface mixtures. 1836 recorded the lowest fracture energy (596.5 J/m²) and similar to 1840

which had 483.7 J/m², the sampled production mix did not pass the 700 J/m² required for SMA surface mixtures in design. This may be possibly attributed to aging during sample storage (3 months on average) followed by reheating of the mix. Also noted was:

- The base binder system used in 1824 and 1836 mixture is the same (SBS 64-34). Although the 1824 mixture had a higher amount of ABR, it has an additional 270 J/m² of fracture energy. This comparison reveals the importance of aggregate quality and its prominent role in low temperature cracking resistance of the mix.
- Although the 1840 mix had the lowest amount of recycling, it could not pass the fracture energy criteria. Using a softer base binder on the low temperature side, adding a rejuvenator, and/or utilizing higher quality aggregate are strategies that could be used in the future to boost the fracture energy in this mix.
- A softer binder system used in 1834 mix is assumed to result in a 75 J/m² higher fracture energy as compared to mix 1818. Differences in aggregate quality might also contribute to the difference in DC(T) fracture energy of these two mixtures.

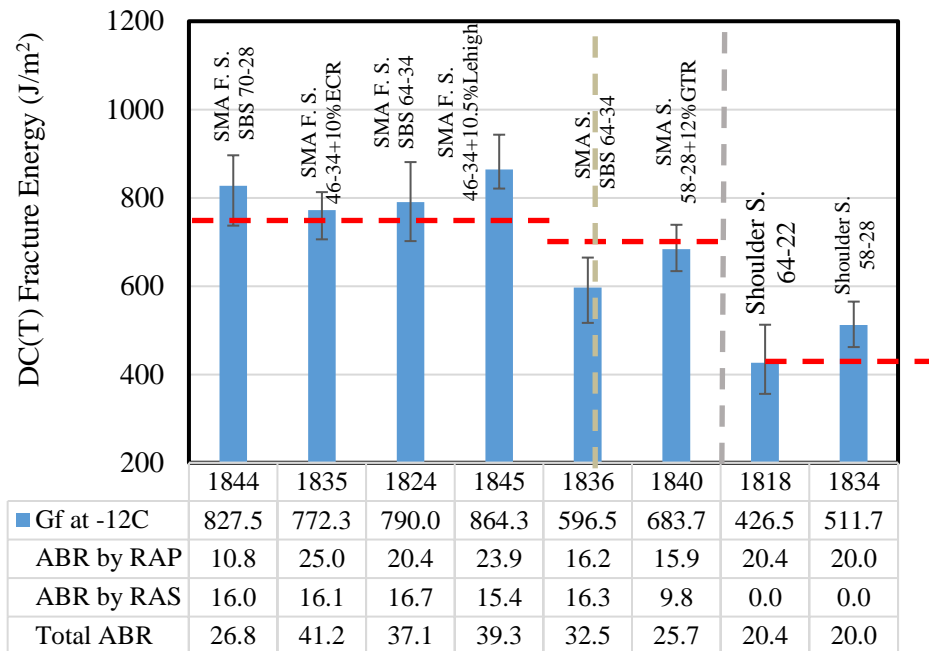


Figure 6-3. DC(T) fracture energy at -12°C

As testing temperature drops, asphalt binder becomes stiffer and as a result, the asphalt sample exhibits more brittle behavior. The reduction in flexibility of the mix leads to reduced fracture energy. Therefore, it is expected to obtain lower fracture energies at -18°C compared to -12°C. As shown in Figure 6-4, the DC(T) fracture energy of all the mixtures at -18 are lower than those at -12°C. Experiencing a drop of about 260 J/m², mix1824, which is an SBS modified mix, showed the highest temperature sensitivity. On the other hand, the 1835 mix which is modified with a dry process Engineered Crumb Rubber (ECR-type GTR) showed almost the same fracture energy at -18°C as compared to -12°C. Assuming that the same DC(T) criteria were applied by Tollway at -18°C, only the 1835 would pass.

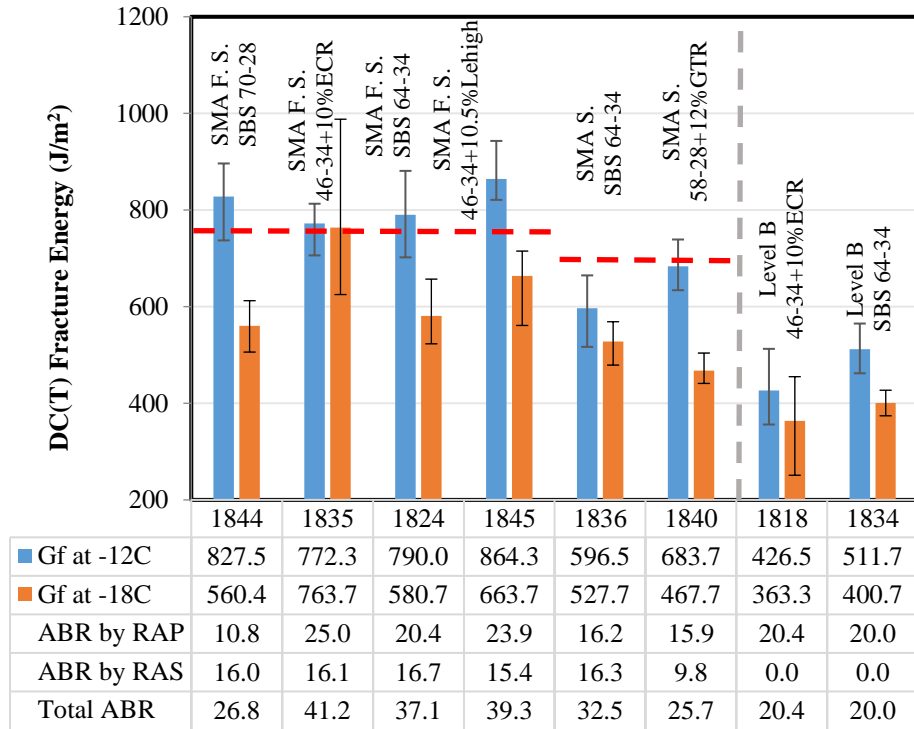


Figure 6-4. Comparing DC(T) fracture energy at -12°C and -18°C

6.4.2. Comparing the cracking performance of asphalt mixture with extracted and recovered binder

In this section, the performance of the recovered binders and their counterpart mixtures were compared to one another as shown in Figure 6-5. The PGLT of the mix was determined using the DC(T) fracture energy mainly performed at two different temperatures (-12 and -18°C). Linear interpolation (or slight extrapolation in a few cases) was then performed in an arithmetic plotting domain to find the temperature at which the fracture energy equals the criterion currently set by the Illinois Tollway. Then, the PG grade of the mix was calculated by subtracting 10°C from the temperature value determined from interpolation. The 10°C deduction is due to the DC(T) test being carried out at 10 degrees warmer than the binder PGLT (ASTM D-7313). A detailed discussion on each mixture and its extracted binder PGLT is provided as follows.

- 1844:** Comparing to the plan PGLT, the recovered binder PGLT is only 0.3°C warmer as its PGLT was determined to be -21.7°C. In order for the extracted binder to safely pass the plan PGLT criterion, a softer base binder could be used. Another option would be to use less recycled materials. Conversely, the mixture was found to pass the 750 J/m² DC(T) mixture requirement at -12°C. However, as the temperature testing decreased to -18, the DC(T) fracture energy dropped below the 750 J/m² criterion. Linear interpolation predicts a testing temperature of -13.7 at which the DC(T) fracture energy would be 750 J/m². This implies a pavement temperature of -23.7°C at which the asphalt mix would be crack resistant. The determined continuous mix PGLT temperature is relatively close to the PGLT of the binder in this case.

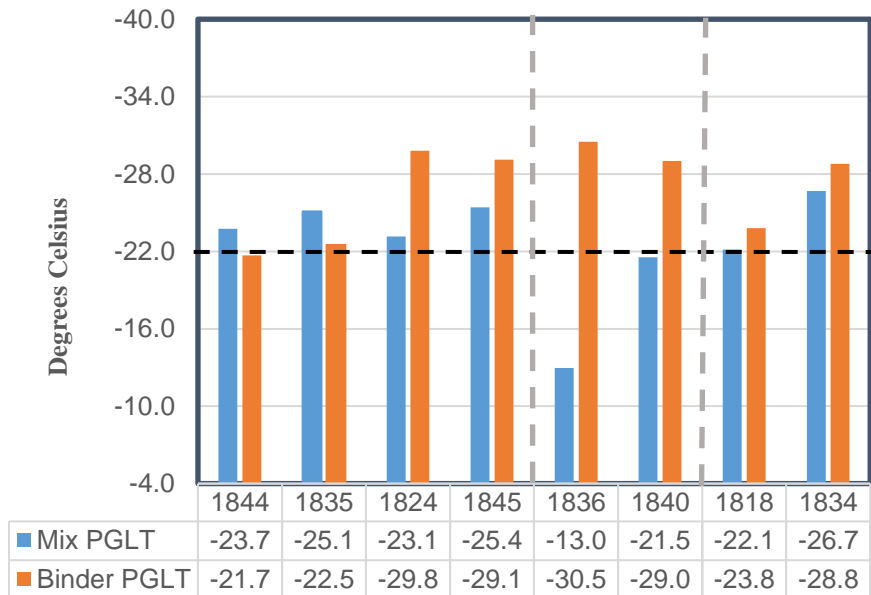


Figure 6-5. Comparing the mixture and extracted PGLT

- 1835:** This mix was modified by engineered crumb rubber which is added to the mix through a dry process. Before the addition of the rubber and recycled

materials, the base binder had a PGLT grade of -34. An ABR of 41.2% led to two grade bumps on the low temperature side such that the PGLT of the extracted binder is -22.5°C. It should be noted that due to difficulties associated with the extraction and recovery of the GTR-modified rubber, the tested recovered binder may not fully capture the benefits of the crumb rubber. Regarding the performance grade of the mix at low temperature, the DC(T) fracture energy difference at two tested temperatures (-12 and -18°C) is negligible. Therefore, the linear interpolation between the two temperatures may not result in a representative value. Therefore, the DC(T) test was performed at -24°C and then a linear fit was used to determine the temperature at which the fracture energy equals 750 J/m² (Figure 6-6). This temperature is calculated as -15.1°C, so the mix grade would be -25.1°C. Similar to 1844, the cracking performance of the mix is slightly better than the extracted binder.

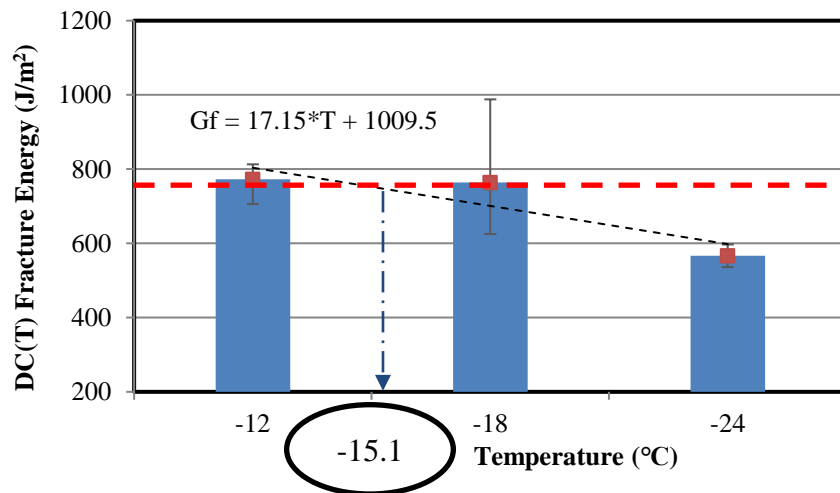


Figure 6-6. Determination of 1835 mix PGLT

- 1824: The SBS modified binder system, which had a PGLT of -34 experienced only one grade bump on the low side after addition of 37.1% ABR from RAP and

RAS. Despite the impressive grade determined for the recovered binder, the mixture showed a significant drop in DC(T) fracture energy at -18°C compared to the one at -12°C. This, again, implies the importance of the aggregate role at cracking performance of the mixture. As the crack resistance of the binder was assured through the PG tests, using a higher quality aggregate is recommended to obtain equally good performance for the mixture. Finally, it should be noted that both the PGLT of the mix and the binder both met the plan PGLT.

- 1845: This mix utilized a 46-34 binder system which was then modified by 10.5% Lehigh rubber through a wet process. After introducing the 39.3% ABR, the extracted binder experienced one grade bump on the PGLT side. As mentioned in the discussion for 1835, the effect of rubber might not be completely captured in the extracted binder as the rubber particles are not expected to fully dissolve in the binder. Therefore, the PG grade of the extracted binder may not thoroughly represent the rheological properties of the binder within the mix. Similar to the 1824 mix, the noticeable difference in fracture energies at -12 and -18°C led to a slightly less promising performance at low temperature as compared to that of the recovered binder.
- 1836: Comparing with mix 1824, this mix had the same binder system (SBS 64-34). Also, both of these mixtures had a very similar amount of ABR. As a result, the extracted binder in these two mixtures was close to one other. However, these two binder systems showed completely different performance after being mixed with aggregates. The 1836 mix did not pass the 700 J/m² requirement at -12°C for

Tollway surface mixtures. Therefore, this mix may be more cracking prone than the other studied SMA mixes. For this mix, using higher quality aggregates or tweaking the binder system would be recommended to improve the PGLT.

- 1840: The base binder for this mix was reported as PG58-28, which was then modified by adding 12% GTR. The combined effect of the 25.7% ABR and the rubber used in the mix rendered a continuous binder PGLT grade of -29°C. Similar to the other rubber modified mixtures (1835 and 1845), the extracted binder may not be fully representative of the binder system in the mix as the rubber may not be completely mixed with the binder. Although the extracted binder was found to meet the plan PGLT, the estimated mix PGLT did not meet the plan PGLT of -22°C.
- 1818: A PG 64-22 binder along with 20.4 ABR by RAP was used in this shoulder surface mix. The DC(T) fracture energy at -12°C was 426.5 J/m², just passing the 425 J/m² currently required for shoulder mixtures. This is consistent with typical practice, where the threshold for using a softer base binder is generally thought to be in the 15 to 20% ABR range (AASHTO PP 78-17). Similar to the SMAs, the plan PGLT of the shoulder mixtures is -22°C. Both the extracted binder and the mix met the plan PGLT. Compared to the previously discussed mixtures, the binder used in mix 1818 was not modified and did not contain RAS. Due to the lower heterogeneity in the mix, the resultant PGLT of the mix turned out to be very close to the binder continuous PGLT grade.

- 1834: Compared to mix 818, this mix used a softer base binder (PG58-28) and the ABR due to RAP was 20%, which is slightly lower than the 25% used in mix 1818. Therefore, it was expected for this mix to have a softer extracted binder. In addition, assuming the quality of the aggregates used in these two mixtures to be similar, 1834 should outperform the 1818 mix in cracking resistance due to the softer binder base binder and lower amount of RAP. As shown in Figure 6-5, the extracted binder from mix 1834 was one grade softer than the one obtained for mix 1818. Also, similar to mix 818, the difference between the PGLT of the mix and extracted binder is very low. This observation is attributed to the less complex combination of the binder system, modification, and recycled materials used in the shoulder mixtures.
- In this section, the performance grade of the mixtures and their extracted binders at low temperature was studied. Except for two mixtures (1844 and 1835), the extracted binder exhibited similar or slightly better performance than the asphalt mixtures. This indicates that the aggregates have an important impact on the crack resistance of the asphalt mixtures. Ignoring the role of aggregate and relying only on the binder performance grade may result in a crack prone asphalt pavement. Morphology, including partial blending of binder from recycled materials (especially RAS) and the positive effects of the presence of softened/swelled GTR particles in the mastic, are clearly only captured through mixture evaluation. A particularly large discrepancy was observed in the 1836 mix, which recorded a mix PGLT of -13°C while its extracted binder had a PGLT of -30.5. Also, the extracted binder from more complex and heterogeneous mixtures (e.g. rubber

modified) might not thoroughly represent the rheological properties of the binder system within the mixture due to the difficulties and uncertainties associated with the extraction process. Therefore, having an idea about the resistance of the mixture which is the product that will be ultimately used in the pavement will provide a more practical and accurate insight toward the crack resistance of modern, heterogeneous asphalt paving mixtures.

6.4.3. Experimental Testing Results at High Temperature

The Hamburg wheel tracking test was carried out in order to evaluate the rutting susceptibility of the mixtures. As mentioned in Table 6-1, the required number of wheel pass for Tollway SMAs is 20,000 and for shoulder mixtures is 15,000. Also, based on the current version of Tollway specification, the allowable rut depth at the required number of passes for SMA mixtures is 6 mm and for shoulder mixtures is 12.5 mm. The measured rut depth under the Hamburg test along with the requirements for each mixture type is shown in Figure 6-7. From the figure, clearly, Tollway SMAs have low rutting levels, as the maximum rut depth recorded was 3.3 mm in mix 1835. This means that the studied SMAs benefit from a robust aggregate structure and binder system, which is consistent with the observed resistance to permanent deformation of similar mixtures placed in the field over the past decade (Buttlar and Wang 2016; Buttlar and Rath 2017). Similarly, the 1818 shoulder mix had low Hamburg rutting as compared to the requirement. However, the 1834 mix, which used a softer binder system as compared to the 1818 mix, exhibit a higher rutting potential as it had the highest amount of rutting (9.8 mm) among the tested mixtures. On the other hand, this shoulder mix is not designed for

heavy traffic loads, and the higher Hamburg rut depth opens the door to obtain higher fracture energy with relatively economical mix design.

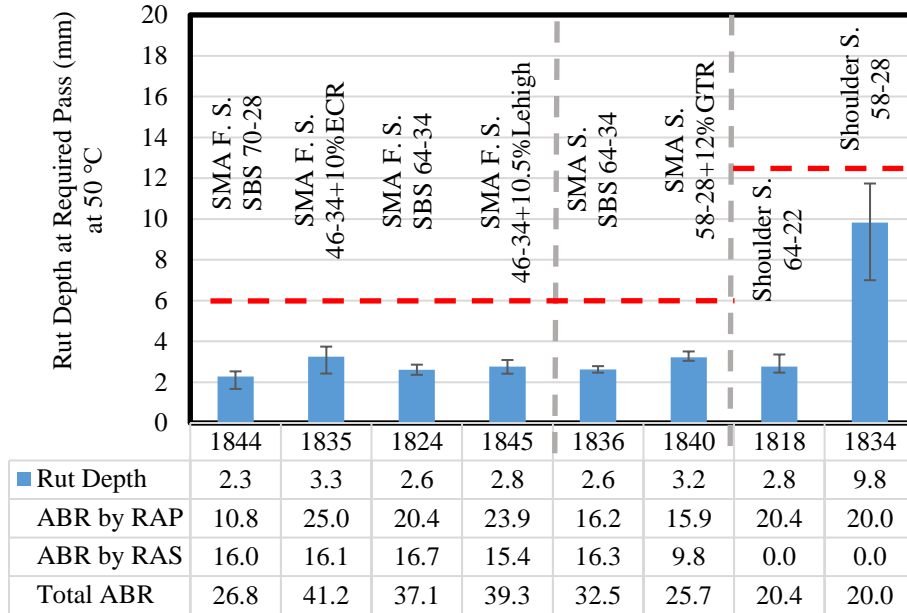


Figure 6-7. Hamburg testing results at 50°C

Figure 6-8 compares the measured rut depth at multiple temperatures. As seen in Figure 6-8, the SMA mixtures had low rutting at 50°C, and therefore, Hamburg testing was also conducted at 64°C in the second run. As the testing temperature increased, the rut depth of the SMAs increased and most mixes approached the allowable rut depth for SMAs. Although the rut depth of the 1845 mix reached the max value defined by Illinois Tollway, the other SMAs were then tested at a higher temperature in order to approach or exceed the maximum allowable rut depth. As for the 1818 mix, the second testing temperature was selected to be 58°C. Similar to SMA mixtures, the 1818 mix experienced a higher rut depth as the temperature increased. Conversely, as the rut depth of the 1834 mix was already relatively high at 50°C, lower test temperature of 40°C was selected as the second temperature. As shown in the figure, there is a significant drop of 7.4 mm in

rut depth as the testing temperature is decreased by 10°C. This shows a relatively high sensitivity to temperature in this mixture, likely due to the aggregate structure.

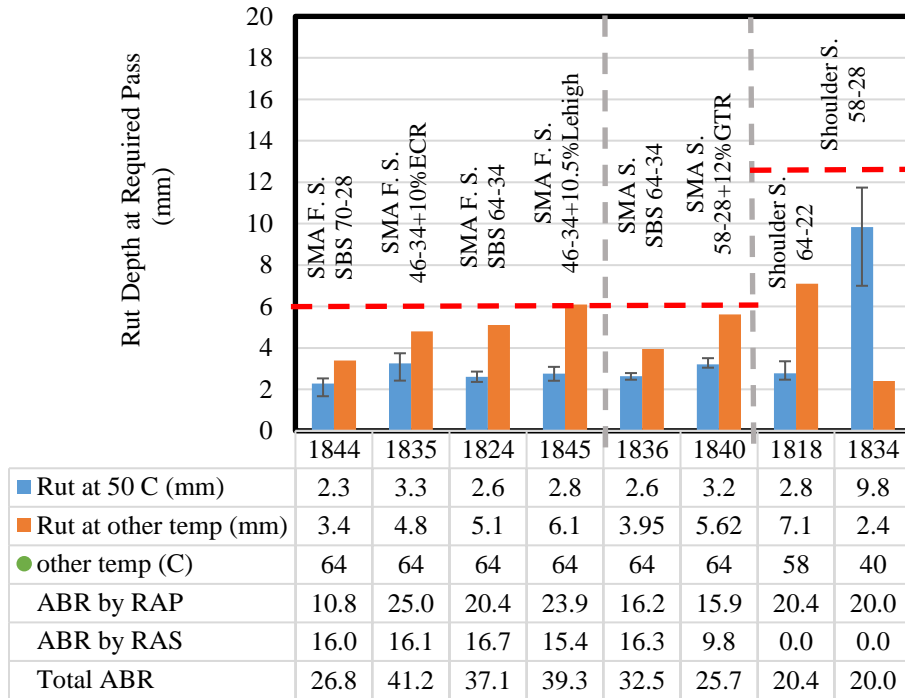


Figure 6-8. Comparing Hamburg testing results at multiple temperatures

6.4.4. Comparing the rutting performance of asphalt mixture with recovered binder

In this section, the high temperature performance grade of the mixtures and their extracted binder at high temperature (PGHT) is examined. The PGHT of the mix has been calculated through linear interpolation (extrapolation) of the Hamburg testing results at two different temperatures. In the newly developed procedure herein, the maximum temperature at which the mixture could meet the criteria was first determined, as shown in Figure 6-9. Then, 14 degrees Celsius was added to the calculated number, as an estimated shift factor between test temperature and the plan high temperature grade for Chicago, Illinois. The resultant temperature is then reported as the mix PGHT. This mix PGHT is then compared to the extracted binder PGHT as shown in Figure 6-9. As already

shown in Figure 6-8, the 1844 mix did not experience an appreciable rut depth under Hamburg test at 20,000 passes at 64°C, which is somewhat remarkable considering the high temperature and a high number of wheel passes. Therefore, the extrapolation between the two measured rut depths at 50 and 58°C led to a predicted threshold test temperature of 96.4°C, where the mix is expected to accumulate 6 mm of rut depth. Shifting by the proposed 14°C interval, the predicted mixture PGHT of 110.4°C was achieved, the highest among the tested mixtures.

Other findings from this analysis are summarized as follows:

- **1844:** Despite the relatively low amount of ABR (26.5%) in mix 1844, both the extracted binder and the mix PGHT were able to meet the plan PGHT of 76°C. That being said, the resistance of the mix to rutting is considerably higher than the extracted binder. Similar to the low temperature, the combination of the appropriate binder system and high quality aggregates appears to have resulted in a robust mix, which performs very well at extremely high and low temperatures.
- **1835:** Although the binder test results showed that the binder could not meet the plan PGHT of 76°C, the effect of the GTR used in the mixture might not have been captured in the recovered binder testing. The combination of a relatively soft binder (PG46-34), high amount of ABR (41.2%), ECR-type dry GTR modification, and SMA aggregates in the 1835 mix resulted in a very low amount of rut depth even at elevated temperatures.
- **1824:** This is the only one among the studied mixtures where its extracted binder PGHT was higher than that of the mix PGHT. Still, the mix PGHT easily met the

plan PGHT. These results suggest that using aggregates with even higher quality in a future mix design could unlock the full potential of this mixture system.

- **1845:** Unlike all other SMAs, the rutting resistance of this mix was borderline. Given the high amount of ABR (39.3%) used in this mix in addition to the 10.5% rubber, it was expected to achieve a high PGLT. However, there was a significant difference between the rut depth at 50 and 64°C which indicated the sensitivity of the mix to high temperature. To solve the temperature sensitivity issue, a higher UTI binder could be used instead of PG 46-34. Also, it is worth mentioning that the rutting performance of the extracted binder was not satisfactory. This could be attributed to the absence of the complete effect of rubber in the extracted binder.
- **1836:** Both the mix and recovered binder easily exceeded the plan PGHT, where 1836 ranked second in terms of the rutting resistance among the SMAs. The PGHT of the recovered binder was 85.7°C, very close to that of the 1824 mix, and which used the same binder system and a similar amount of recycled materials.
- **1840:** The 1840 mix also met the plan PGHT. Although the 25.7% of ABR and 12% GTR was expected to lead to three grade bumps and increase the PGHT of the neat binder from 58 to 76, the recovered binder PGHT was only predicted at 72.2°C. Therefore, it appeared that the effect of the ground tire rubber was not fully captured by continuous grading of the recovered binder.
- **1818:** Similar to the PGLT, the PGHT of the extracted binder and the mix was very similar. Both the recovered binder and the mix could easily pass the plan PGHT of 64. Although the rut depth of this mix at 58°C was considerably higher

than that achieved when testing at 50°C, the less stringent requirement of the shoulder mixtures (12.5 mm at 15000 passes) resulted in a high computed PGHT for this mix. The use of PG64-22 along with 20.4% ABR by RAP seemed to have helped both the mix and the recovered binder meet the plan PGHT grade.

- 1834:** Perhaps because the binder system of this shoulder mix was not modified (similar to 1818), the continuous grading of the mix and recovered binder was very close. Compared to mix 1818, 1834 used a softer base binder (PG58-28). This was clearly reflected in the PGHT of the mix and also the recovered binder. As a result, a difference of almost 6 degrees was observed between the PGHT of the 1818 and 1834 mixes for both the recovered binder and mixture (1834 mixture was softer, and possessed a lower PGHT).

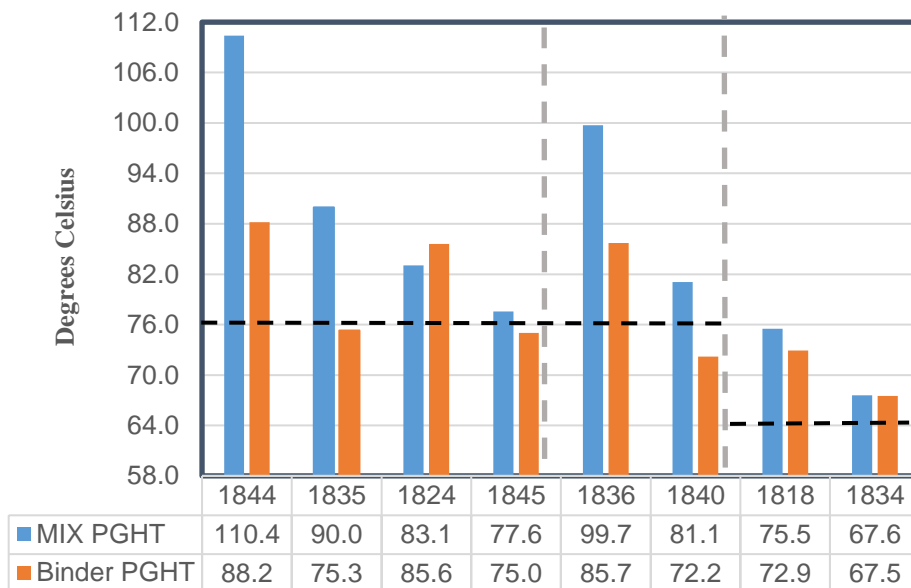


Figure 6-9. Comparing mix and binder performance grades

In this section, the rutting resistance of the mixtures and their extracted binders were studied. Comparing the PGHT of the extracted binder with that of the mix, it could be observed that the PGHT of the mixtures is often higher than that of the recovered binder for Illinois Tollway mixtures. This observation could be attributed to the dominant role of the SMA aggregates at high temperature, which are present in all but the 1818 and 1834 mixes. Also, none of the recovered binders from rubber modified mixtures, including mixes 1835, 1845, and 1840 could reach the plan PGLT. However, using the new mixture continuous grading system, all three mixes met rutting criteria. This again shows that relying merely on recovered binder results, especially for more complex mixtures such as mix 1835, might be misleading. To avoid this, mixture performance testing and continuous mix grading is recommended to better characterize these mixtures, and can be used in performance engineered design to more confidently assure long term performance of the pavement while allowing economical, sustainable mixtures to be developed.

6.4.5. Usable Temperature Interval of Mixtures and Binders

The usable temperature interval (UTI) is a measure of temperature susceptibility of the binders. The higher UTI implies the lower susceptibility of the binder and the wider range of temperature that the binder is able to properly function. The UTI of a binder is determined by adding the PGHT to the absolute value of the PGLT. In addition to the binder, the UTI of the mixture could be determined once the PGLT and the PGHT of the mixtures were calculated. Figure 6-10 shows the comparison between the mix and binder UTI. It can be observed that most of the studied mixtures had similar UTI as compared to their extracted binders. That being said, the UTI of the 1835 and 1844 mixtures were notably higher than their extracted binders as their markers resided high above the

equality line. This also indicates that the temperature susceptibility of these mixtures is lower than that which was predicted from the recovered binders. Other observations from this figure include:

- The location of the 1844 mix (light blue cross) far above the unity line suggests that the combination of the binder system, recycled materials, and the aggregates performed even better than that predicted by the recovered binder. In other words, the quality of the aggregates helped the performance of the mix in terms of low temperature cracking and rutting.
- Considering only the extracted binder testing results, it might be concluded that the 1835 mix (solid gray triangle) would not perform very well at either high or low temperatures. However, the extracted binder from this mix might not be representative, due to extraction and recovery issues associated with the ECR-type GTR which is added through a dry process. The UTI of the mixture, which is a more reliable indication of the mix performance, shows that this SMA mix is able to perform adequately at both high and low temperatures.
- The PGLT and PGHT of the 1824 recovered binder are slightly better than that of the mix. As a result, the 1824 marker (solid yellow diamond) is below the equality line. This suggests that a higher quality aggregate structure and/or higher UTI binder system (and/or another additive) could be considered in the future if it was desired to boost the UTI of this mix.
- The low temperature performance of the 1845 mix (blue asterisk) was the most outstanding among the SMAs while its rutting resistance was the lowest. This

means that this mix is ideal to be used in areas with even colder climatic conditions. Also, this leaves room for the addition of more recycled materials and makes the mixture even more sustainable and economical.

- The UTI of the 1836 recovered binder (rigid green circle) is the highest among the studied binders. However, the mixture did not perform as well and its marker is below the equality line. Specifically, the 1836 mix showed very brittle behavior and might suffer from significant cracking potential. As the recovered binder suggested suitable cracking resistance, the aggregate structure and quality might need modification in order to improve the mix PGLT and ultimately, the UTI of the mix.
- The difference in the PGLT of the 1840 (rigid blue square) was canceled out by the difference in the PGHT when comparing binder and mixture results in both tests (the low temperature binder PGLT was superior to the mix PGLT, and vice-versa for PGHT). Therefore, the blue solid square marker is very close to the equality line in terms of UTI. It is also worth mentioning that the amount of ABR used in this mix is relatively low (25.7%), so increased recycling would be a possibility only if other binders and mixture aspects were adjusted. As the UTI of this mix is relatively low, an improved binder system, GTR system and/or a more robust aggregate structure could be attempted in the future.
- The expected (plan) UTI of the 1818 (shoulder mix) is 86 ($64-22=86$). Having both a mixture and recovered binder UTI of more than 95 suggests this dense graded mix will lead to a high-performance shoulder surface. In this mix, the

binder and mixture UTI are very close to one other. This is likely attributed to the low complexity in the mix, as the binder is not modified and the ABR by RAS is zero. In the future, using a neat binder system of PG 58-28 could improve the UTI and make additional room for recycled materials.

- The UTI of the 1834 mix is also very close to that of the recovered binder.

Although the UTI of 1834 is lower than 1818, the advantage of this mix is its higher crack resistance (better PGLT) which is more preferable for shoulders as cracking is probably the main concern in this application.

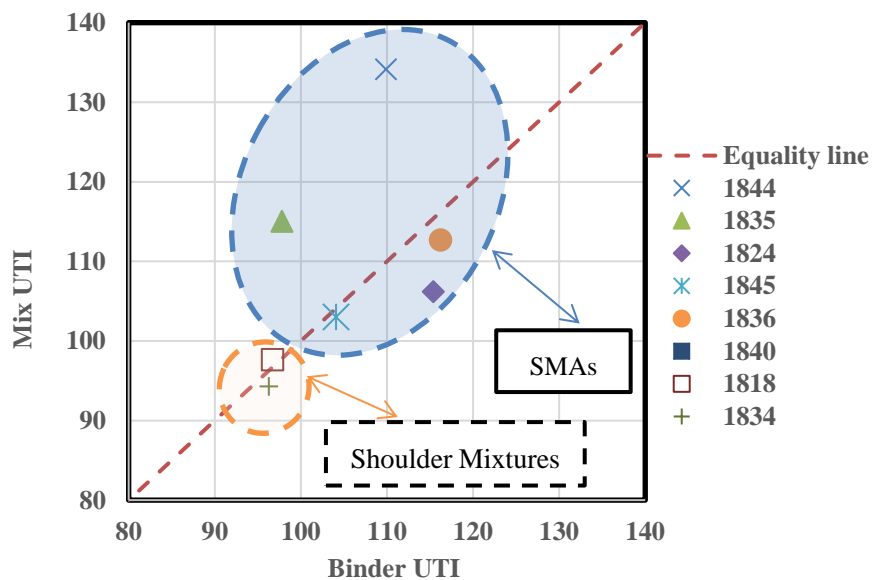


Figure 6-10. Mix vs. Binder UTI

Finally, it is noted that the aforementioned comparison between the binder and mixture continuous grade and UTI was made possible by the relative concordance of high and low temperature binder and mixture testing in Superpave, Hamburg and DC(T) tests.

Although the I-FIT and IDEAL have become popular asphalt mixture cracking tests, their current inability to be performed at low temperatures precludes their use in determining

mixture continuous grade or UTI. It is also acknowledged that much more work will be needed to fine-tune and to validate the proposed continuous mix grading method. These research needs include:

- Local validation of proposed DC(T) and Hamburg limits against field performance data. The authors are currently collaborating on a study aimed at this goal for the Illinois Tollway, scheduled for completion in March of 2020.
- Modeling-based validation of shifts between Hamburg and DC(T) test temperatures and environmental conditions for differing levels of reliability, and for differing positions in the pavement structure. This will assist in allowing tailored specifications to be developed in different regions worldwide.
- Development of a simplified DC(T) test. While the current DC(T) test has proven to be accurate and related to low-temperature field performance, it is somewhat more complex, and more costly as compared to other tests. Research is being conducted to evaluate the potential for a rapid, inexpensive low temperature test that can predict the DC(T) fracture energy, but which is more conducive for use in both design and routine material control/acceptance.
- Further development and deployment of Machine Learning based prediction models. As presented at AAPT 2019, machine learning based models have shown good ability to predict performance tests such as the DC(T), and more recently, the Hamburg wheel track test. By training these models with a wider data set, they will have excellent utility in helping agencies to rapidly develop continuous mix grading protocols and performance engineered (“balanced”) mix design

specifications for their particular climate regions, traffic levels, and pavement configurations.

6.5. Summary and Conclusions

In this study, DC(T) and Hamburg tests were employed in a new method to determine a continuous mixture performance grade, which is a useful tool in the larger field of performance-engineered mix design. To this end, the aforementioned performance tests were performed at multiple temperatures, and using Illinois Tollway performance test criteria, results were used to produce a first-glimpse at a new Continuous Mixture Performance Grading system. These results, along with comparison of continuous mixture PG with that of the extracted binder continuous PG grades, the following conclusions can be drawn:

- Generally, the PGLT of the extracted binder is slightly lower than that of the Illinois Tollway SMA mixtures PGLT, which requires very high-quality aggregates.
- The PGHT of the mixture is typically higher than the binder PGHT. This is also attributed to the high quality aggregates used in Tollway mixtures, and perhaps to the composite nature of modern, RAP, RAS and/or GTR mixtures. It should be mentioned that ambiguities still exist in blending levels between RAP/RAS and neat binders within extraction and recovery process.
- The continuous performance grade of the recovered binders from rubber modified mixtures might not be completely representative. Therefore, in order to assure that

the mixture can meet the plan grade, mixture performance grading as proposed herein may prove to be both a simpler and superior method for the design and control of GTR-modified mixtures.

- Less heterogeneous asphalt mixtures (such as 1818 and 1834 in this study) appear to be more likely to have similar PGLT and PGHT grades as compared to those obtained with their extracted binders.

Chapter 7

SUMMARY, CONCLUSIONS, AND FUTURE WORKS

In this dissertation, a systematic framework for performance specification evaluation and calibration was developed and deployed. This framework takes into account the link between lab and field performance results and the effect of aging in establishing specification thresholds. In addition, test repeatability and uncertainty associated with distress detection and measurement were incorporated, using a simple-yet-rational statistics-based reliability approach. The approaches followed in this study, the key findings, and major recommendations are now summarized.

Low Temperature Cracking Control – According the field investigations and site visits, transverse cracking was the main concern for the Illinois Tollway facilities and also Missouri roads. Therefore, an extensive effort has been put into the performance tests that are believed to mitigate the cracking of asphalt and avoid cracking prone mixes.

- The indirect tensile (IDT) strength test -12 °C exhibited the best repeatability (lowest COV); however, it did a poor job of distinguishing between mixtures.
- The DC(T) test was found to rank mixtures in close accordance with expected, relative field performance trends.
- Due to its high repeatability, excellent correlation with field results, and ability to change testing temperature based on environmental conditions of the project location, the DC(T) was recommended to be retained in the Tollway's asphalt mixture design specification.
- A systematic procedure was used to set DC(T) limits, which were then compared to existing DC(T) thresholds, followed by a consensus approval/adjustment step. This procedure involved setting baseline fracture energy thresholds for minimum

acceptable cracking resistance based on field results, then adding to this baseline in a conservative fashion.

Rutting Control - Similar to other agencies, the Illinois Tollway has had a positive experience in using the Hamburg test to conservatively control permanent deformation. The ability of the Hamburg to effectively control stripping in lieu of the TSR test was also of interest to the Tollway.

- Hamburg specification thresholds for the various mix types used by Tollway were evaluated as a function the depth of placement of those layers relative to the surface of the pavement. A summary of key research evaluations applied in support of validating or adjusting Hamburg thresholds include:
 - Based on laser-measured rut depths by ARAN-style pavement conditional assessment vehicles, Hamburg testing at 50 °C at 20,000 passes appeared to be appropriate for the control of rutting in Tollway SMA-type mixtures.
 - Computed temperature profiles and plots led to temperate-wheel pass equivalents were used to arrive at more highly tailored specification thresholds.

Stripping Control - Degradation of the bond between aggregate and binder in the presence of water leads to stripping distress (or moisture damage). In this research, tests were carried out on loose and compacted asphalt materials to evaluate resistance to moisture damage. The tensile strength ratio (TSR) test and stripping inflection point (SIP) parameter calculated using Hamburg test results were obtained for compacted samples while the boiling water test was performed on loose asphalt mixtures.

- The Iowa method triggers the SIP consideration only if the slope ratio is equal to or greater than two. Despite the fact that SIP can detect the stripping potential for mixtures with a considerable amount of rut depth at the end of 20,000 wheel passes, its slope ratio might be misleading for mixtures with very low accumulated rut depths.
- It is recommended that the Iowa stripping evaluation be waived for mixtures exhibiting less than-or-equal to 4.0 mm of rutting in the Hamburg test at 20,000 passes. In these cases, the mixture should be reported as non-stripping.

In collaboration with the project TRP to identify a number of good and poor performing sections placed during 2008 to 2015, which were visually surveyed in May of 2019.

These included both mainline and shoulder sections. This provided an excellent opportunity to link the laboratory performance testing results with actual field performance. The following observations were made after this investigation:

- Sixteen different sections including six mainline and six shoulder mixtures were tested in the lab using most of the candidate cracking and rutting tests evaluated in this study.
 - The COV of the DC(T) test was found to be the lowest among different mix categories, although considerably higher in some cases and more variable overall as compared to the 2018 testing results on plant-produced, lab-compacted specimens.
 - Based on the field observations, a DC(T) fracture energy of 400 J/m² was determined to be the threshold, long-term aged fracture energy recommended for shoulder surface mixtures.

- Performance indices and parameters such as IRI, CRS, and rut depth along with images from were used to compare the performance of different sections and to correlate them to lab and field observations.
- In addition to overall serviceability as characterized by CRS, a detailed analysis of the type, extent, and severity of surface distresses was conducted on the data set provided by ARA, and an average severity concept was introduced.
- As a part of performance prediction of the asphalt mixtures, a new method called the DC(T) creep test was introduced to characterize the viscoelastic behavior of asphalt mixtures at low temperatures.
 - The relationship between the CMOD responses of DC(T) creep tests and viscoelastic creep compliance can be used to precisely identify the viscoelastic properties of asphalt concrete at low temperatures.
- Using the DC(T) and Hamburg test results at multiple temperatures, a new method to determine a continuous mixture performance grade, which is a useful tool in the larger field of performance-engineered mix design.
 - The introduced grading system can address the difficulties associated with the performance grading of the extracted and recovered binder, especially in the case of more heterogenous and modern mixtures.

It is believed that meeting the newly proposed test thresholds will strike an even better balance in mixture performance and mixture economy for the Tollway. In addition, the specification continues to keep the door open for future innovations. These include the introduction of new, sustainable mixture design approaches and materials as they become available.

More work will be needed to further develop and apply the methods presented in this study. These research needs include:

- Local validation of proposed DC(T) and Hamburg limits against more field performance obtained from both mainlines and shoulder surface.
- Statistical analysis on the correlation between the laboratory test and field performance (such as bubble plot) to introduce more rigorous reliability levels into the specification.
- Modeling the temperature distribution and heat flux through different layers of the pavement structure and predicting the thermally induced stress, especially from the low-temperature cracking standpoint.
- Further development and deployment of Machine Learning based prediction models, which will assist agencies in developing continuous mix grading protocols and performance engineered (“balanced”) mix design specifications for their particular climate regions, traffic levels, and pavement configuration.
- Modeling-based validation of shifts between Hamburg and DC(T) test temperatures and environmental conditions for differing levels of reliability, and for differing positions in the pavement structure. This will assist in allowing tailored specification to be developed in different regions worldwide.

REFERENCES

- [1] S. Buchanan, Balanced Mix Design Task Force: Update of Activities, in: NAPA Asphalt Mix ETG Meeting, Salt Lake City, UT, 2017.
- [2] F. Zhou, S. Hu, G. Das, T. Scullion, High RAP mixes design methodology with balanced performance., United States. Federal Highway Administration, 2011.
- [3] S.B. Cooper, L.N. Mohammad, S. Kabir, W. King, Balanced asphalt mixture design through specification modification: Louisiana's experience, *Transp. Res. Rec.* 2447 (2014) 92–100. <https://doi.org/10.3141/2447-10>.
- [4] R. West, C. Rodezno, F. Leiva, F. Yin, Development of a framework for balanced mix design, *NCHRP Proj.* (2018) 7–20.
- [5] F. Zhou, T. Scullion, Overlay tester: A rapid performance related crack resistance test, Texas Transportation Institute, Texas A & M University System, 2005.
- [6] H. Ozer, I.L. Al-Qadi, J. Lambros, A. El-Khatib, P. Singhvi, B. Doll, Development of the fracture-based flexibility index for asphalt concrete cracking potential using modified semi-circle bending test parameters, *Constr. Build. Mater.* 115 (2016) 390–401. <https://doi.org/10.1016/j.conbuildmat.2016.03.144>.
- [7] F. Zhou, S. Im, L. Sun, T. Scullion, Development of an IDEAL cracking test for asphalt mix design and QC/QA, *Asph. Paving Technol. Assoc. Asph. Paving Technol. Tech. Sess.* 86 (2017) 549–577. <https://doi.org/10.1080/14680629.2017.1389082>.
- [8] K.P. Biligiri, K.E. Kaloush, M.S. Mamlouk, M.W. Witczak, Rational modeling of

- tertiary flow for asphalt mixtures, *Transp. Res. Rec.* 2001 (2007) 63–72.
- [9] T. Aschenbrener, Evaluation of Hamburg wheel-tracking device to predict moisture damage in hot-mix asphalt, *Transp. Res. Rec.* 1492 (1995) 193.
- [10] D. Newcomb, F. Zhou, Balanced Design of Asphalt Mixtures, MnDOT Res. (2018) 68.
- [11] N. Tran, G. Huber, F. Leiva, B. Pine, F. Yin, Mix Design Strategies for Improving Asphalt Mixture Performance, 2019.
- [12] ASTM D7313, Standard Test Method for Determining Fracture Energy of Asphalt-Aggregate Mixtures Using the Disk-Shaped Compact Tension Geometry, 2013. <https://doi.org/10.1520/D7313>.
- [13] R. Roque, W.G. Buttlar, The development of a measurement and analysis system to accurately determine asphalt concrete properties using the indirect tensile mode (with discussion), *J. Assoc. Asph. Paving Technol.* 61 (1992).
- [14] J.P. Hallin, Development of the 2002 guide for the design of new and rehabilitated pavement structures: Phase II, Rep. Natl. Coop. Highw. Res. Program, *Transp. Res. Board, Natl. Res. Counc.* (2004).
- [15] M.O. Marasteanu, X. Li, T.R. Clyne, V.R. Voller, D.H. Timm, D.E. Newcomb, Low Temperature Cracking of Asphalt Concrete Pavements, (2004) 210.
- [16] E. V. Dave, W.G. Buttlar, S.E. Leon, B. Behnia, G.H. Paulino, IlliTC – low-temperature cracking model for asphalt pavements, *Road Mater. Pavement Des.* 14 (2013) 57–78. <https://doi.org/10.1080/14680629.2013.812838>.

- [17] B. Jahangiri, M.M. Karimi, N. Tabatabaee, Relaxation of hardening in asphalt concrete under cyclic compression loading, *J. Mater. Civ. Eng.* 29 (2017).
[https://doi.org/10.1061/\(ASCE\)MT.1943-5533.0001814](https://doi.org/10.1061/(ASCE)MT.1943-5533.0001814).
- [18] M.E. Tuttle, H.F. Brinson, Prediction of the long-term creep compliance of general composite laminates, *Exp. Mech.* 26 (1986) 89–102.
<https://doi.org/10.1007/BF02319961>.
- [19] E. Zegeye Teshale, H.K. Stolarski, M.O. Marasteanu, Determination of Creep Compliance of Asphalt Concrete from Notched Semi-Circular Bend (SCB) Test, *Exp. Mech.* 53 (2013) 919–928. <https://doi.org/10.1007/s11340-012-9688-z>.
- [20] A. T322, Standard Method of Test Determining the Creep Compliance and Strength of Hot Mix Asphalt (HMA) Using the Indirect Tensile Test Device, *Am. Assoc. State Highw. Transp. Off.* 07 (2007).
- [21] W.G. Buttlar, R. Roque, Development and evaluation of the strategic highway research program measurement and analysis system for indirect tensile testing at low temperatures, *Transp. Res. Rec.* (1994).
- [22] A. Zofka, M. Marasteanu, M. Tuross, Investigation of asphalt mixture creep compliance at low temperatures, *Road Mater. Pavement Des.* 9 (2008) 269–285.
<https://doi.org/10.1080/14680629.2008.9690169>.
- [23] AASHTO T313-05, Standard Method of Test for Determining the Flexural Creep Stiffness of Asphalt Binder Using the Bending Beam Rheometer (BBR), *Stand. Specif. Transp. Mater. Methods Sampl. Test.* 12 (2005) 1–23.
<https://doi.org/10.1520/D6648-08R16.2>.

- [24] D.N. Richardson, S.M. Lusher, Determination of Creep Compliance and Tensile Strength of Hot-Mix Asphalt for Wearing Courses in Missouri, 2008.
- [25] A. Roberto, E. Romeo, A. Montepara, R. Roncella, Effect of fillers and their fractional voids on fundamental fracture properties of asphalt mixtures and mastics, *Road Mater. Pavement Des.* 21 (2020) 25–41.
<https://doi.org/10.1080/14680629.2018.1475297>.
- [26] R.S. McDaniel, A. Shah, G.A. Huber, A. Copeland, Effects of reclaimed asphalt pavement content and virgin binder grade on properties of plant produced mixtures, *Asph. Paving Technol. Assoc. Asph. Paving Technol. Tech. Sess.* 81 (2012) 369–397. <https://doi.org/10.1080/14680629.2012.657066>.
- [27] P.K. Das, Y. Tasdemir, B. Birgisson, Low temperature cracking performance of WMA with the use of the Superpave indirect tensile test, *Constr. Build. Mater.* 30 (2012) 643–649. <https://doi.org/10.1016/j.conbuildmat.2011.12.013>.
- [28] B. Behnia, E. Dave, S. Ahmed, W. Buttlar, H. Reis, Effects of Recycled Asphalt Pavement Amounts on Low-Temperature Cracking Performance of Asphalt Mixtures Using Acoustic Emissions, *Transp. Res. Rec. J. Transp. Res. Board.* 2208 (2011) 64–71. <https://doi.org/10.3141/2208-09>.
- [29] B. Hill, D. Oldham, B. Behnia, E.H. Fini, W.G. Buttlar, H. Reis, Evaluation of low temperature viscoelastic properties and fracture behavior of bio-asphalt mixtures, *Int. J. Pavement Eng.* 19 (2018) 362–369.
<https://doi.org/10.1080/10298436.2016.1175563>.
- [30] J. Wills, S. Caro, A. Braham, Influence of material heterogeneity in the fracture of

asphalt mixtures, *Int. J. Pavement Eng.* 8436 (2017) 1–14.

<https://doi.org/10.1080/10298436.2017.1334461>.

- [31] A. Zofka, I. Yut, M. Marasteanu, L. Khazanovich, Comparison of data interpretation procedures for indirect tensile creep test for linear viscoelastic materials, *Road Mater. Pavement Des.* 11 (2010) 411–441.
<https://doi.org/10.1080/14680629.2010.9690340>.
- [32] M. Marastean, R. Velasquez, A.C. Falchetto, A. Zofka, Temperature Creep Compliance of Asphalt Mixtures, *IDEA Progr. Final Rep. NCHRP.* 133 (2009).
- [33] Pedro Romero, USING THE BENDING BEAM RHEOMETER FOR LOW TEMPERATURE TESTING OF Prepared For : Utah Department of Transportation Submitted By : University of Utah Authored By :, (2016).
- [34] X. Gong, P. Romero, Z. Dong, Y. Li, Investigation on the low temperature property of asphalt fine aggregate matrix and asphalt mixture including the environmental factors, *Constr. Build. Mater.* 156 (2017) 56–62.
<https://doi.org/10.1016/j.conbuildmat.2017.08.142>.
- [35] F. Kaseer, A. Bajaj, A.E. Martin, E. Arámbula-Mercado, E. Hajj, Strategies for Producing Asphalt Mixtures with High RAP Content, *J. Mater. Civ. Eng.* 31 (2019) 1–16. [https://doi.org/10.1061/\(ASCE\)MT.1943-5533.0002910](https://doi.org/10.1061/(ASCE)MT.1943-5533.0002910).
- [36] A.S.M. Asib, P. Romero, F. Safazadeh, An equivalence between methods of aging for determining the low-temperature performance of hot-mix asphalt concrete mixtures containing reclaimed asphalt pavement, *Constr. Build. Mater.* 223 (2019) 198–209. <https://doi.org/10.1016/j.conbuildmat.2019.06.204>.

- [37] M. Wagoner, W. Buttlar, G. Paulino, P. Blankenship, Investigation of the Fracture Resistance of Hot-Mix Asphalt Concrete Using a Disk-Shaped Compact Tension Test, *Transp. Res. Rec.* 1929 (2005) 183–192. <https://doi.org/10.3141/1929-22>.
- [38] C.M. Stewart, J.G. Reyes, V.M. Garcia, Comparison of fracture test standards for a super pave dense-graded hot mix asphalt, *Eng. Fract. Mech.* 169 (2017) 262–275. <https://doi.org/10.1016/j.engfracmech.2016.10.016>.
- [39] M. Marasteanu, A. Zofka, M. Turos, X. Li, R. Velasquez, X. Li, W. Buttlar, G. Paulino, A. Braham, E. Dave, Investigation of low temperature cracking in asphalt pavements national pooled fund study 776, (2007).
- [40] W. Buttlar, J. Meister, B. Jahangiri, H. Majidifard, P. Rath, Performance Characteristics of Modern Recycled Asphalt Mixes in Missouri, Including Ground Tire Rubber, Recycled Roofing Shingles, and Rejuvenators, 2019. <https://orcid.org/0000-0002-1545-0165>.
- [41] W. Buttlar, B. Jahangiri, P. Rath, H. Majidifard, L. Urrea, J. Meister, H. Brwon, Development of a Performance-Related Asphalt Mix Design Specification for the Illinois Tollway, n.d.
- [42] W.G. Buttlar, B.C. Hill, H. Wang, W. Mogawer, Performance space diagram for the evaluation of high- and low-temperature asphalt mixture performance, *Road Mater. Pavement Des.* 0 (2016) 1–23. <https://doi.org/10.1080/14680629.2016.1267446>.
- [43] B. Jahangiri, H. Majidifard, J. Meister, W.G. Buttlar, Performance Evaluation of Asphalt Mixtures with Reclaimed Asphalt Pavement and Recycled Asphalt

Shingles in Missouri, *Transp. Res. Rec.* 2673 (2019) 392–403.

<https://doi.org/10.1177/0361198119825638>.

- [44] P. Rath, J.E. Love, W.G. Buttlar, H. Reis, Performance analysis of asphalt mixtures modified with ground tire rubber modifiers and recycled materials, *Sustain.* 11 (2019) 1792. <https://doi.org/10.3390/su11061792>.
- [45] A.F. Braham, W.G. Buttlar, T.R. Clyne, M.O. Marasteanu, M.I. Turos, The effect of long-term laboratory aging on asphalt concrete fracture energy, *J. Assoc. Asph. Paving Technol.* 78 (2009).
- [46] W. Flügge, *Viscoelasticity - 2nd revised edition*, 1975.
<https://doi.org/10.1007/978-3-662-02276-4>.
- [47] L. Khazanovich, The elastic-viscoelastic correspondence principle for non-homogeneous materials with time translation non-invariant properties, *Int. J. Solids Struct.* 45 (2008) 4739–4747. <https://doi.org/10.1016/j.ijsolstr.2008.04.011>.
- [48] G. Wijk, Some new theoretical aspects of indirect measurements of the tensile strength of rocks, *Int. J. Rock Mech. Min. Sci. Geomech. Abstr.* 15 (1978) 124.
[https://doi.org/10.1016/0148-9062\(78\)91493-6](https://doi.org/10.1016/0148-9062(78)91493-6).
- [49] E. V. Dave, G.H. Paulino, W.G. Buttlar, Viscoelastic Functionally Graded Finite-Element Method Using Correspondence Principle, *J. Mater. Civ. Eng.* 23 (2011) 39–48. [https://doi.org/10.1061/\(ASCE\)MT.1943-5533.0000006](https://doi.org/10.1061/(ASCE)MT.1943-5533.0000006).
- [50] M.M. Karimi, N. Tabatabaee, B. Jahangiri, M.K. Darabi, Constitutive modeling of hardening-relaxation response of asphalt concrete in cyclic compressive loading,

Constr. Build. Mater. 137 (2017).

<https://doi.org/10.1016/j.conbuildmat.2017.01.116>.

- [51] M.M. Karimi, N. Tabatabaee, H. Jahanbakhsh, B. Jahangiri, Development of a stress-mode sensitive viscoelastic constitutive relationship for asphalt concrete: experimental and numerical modeling, *Mech. Time-Dependent Mater.* 21 (2017) 383–417. <https://doi.org/10.1007/s11043-016-9335-7>.
- [52] M.K. Darabi, R.K. Abu Al-Rub, E.A. Masad, D.N. Little, Constitutive modeling of fatigue damage response of asphalt concrete materials with consideration of micro-damage healing, *Int. J. Solids Struct.* 50 (2013) 2901–2913.
<https://doi.org/10.1016/j.ijsolstr.2013.05.007>.
- [53] M.K. Darabi, R.K. Abu Al-Rub, E.A. Masad, D.N. Little, Cyclic Hardening-relaxation viscoplasticity model for asphalt concrete materials, *J. Eng. Mech.* 139 (2013) 832–847. [https://doi.org/10.1061/\(ASCE\)EM.1943-7889.0000541](https://doi.org/10.1061/(ASCE)EM.1943-7889.0000541).
- [54] H. Jahanbakhsh, M.M. Karimi, N. Tabatabaee, Experimental and numerical investigation of low-temperature performance of modified asphalt binders and mixtures, *Road Mater. Pavement Des.* 18 (2017) 1353–1374.
<https://doi.org/10.1080/14680629.2016.1220864>.
- [55] S. Aflaki, P. Hajikarimi, Implementing viscoelastic rheological methods to evaluate low temperature performance of modified asphalt binders, *Constr. Build. Mater.* 36 (2012) 110–118. <https://doi.org/10.1016/j.conbuildmat.2012.04.076>.
- [56] M. Jaczewski, J. Judycki, P. Jaskula, Asphalt concrete subjected to long-time loading at low temperatures – Deviations from the time-temperature superposition

principle, *Constr. Build. Mater.* 202 (2019) 426–439.

<https://doi.org/10.1016/j.conbuildmat.2019.01.049>.

- [57] N. Saboo, A. Mudgal, Modelling creep and recovery response of asphalt binders using generalized burgers model, *Pet. Sci. Technol.* 36 (2018) 1627–1634.
<https://doi.org/10.1080/10916466.2018.1496109>.
- [58] A. User, S. Reference, *Abaqus User Subroutines Reference Manual*, (n.d.).
- [59] R.A. Schapery, On the characterization of nonlinear viscoelastic materials, *Polym. Eng. Sci.* 9 (1969) 295–310.
- [60] R.M. Haj-Ali, A.H. Muliana, Numerical finite element formulation of the Schapery non-linear viscoelastic material model, *Int. J. Numer. Methods Eng.* 59 (2004) 25–45. <https://doi.org/10.1002/nme.861>.
- [61] NCHRP, *Guide for Mechanistic-Empirical Design of New and Rehabilitated Pavement Structures*. Final Report, NCHRP Project 1-37A., Washington, DC, 2004.
- [62] E. V. Dave, C. Hoplin, Flexible pavement thermal cracking performance sensitivity to fracture energy variation of asphalt mixtures, *Road Mater. Pavement Des.* 16 (2015) 423–441. <https://doi.org/10.1080/14680629.2015.1029697>.
- [63] M.R. Islam, R.A. Tarefder, Coefficients of Thermal Contraction and Expansion of Asphalt Concrete in the Laboratory, *J. Mater. Civ. Eng.* 27 (2015) 1239–1247.
[https://doi.org/10.1061/\(ASCE\)MT.1943-5533.0001277](https://doi.org/10.1061/(ASCE)MT.1943-5533.0001277).
- [64] J. D'Angelo, R. Kluttz, R. Dongr??, K. Stephens, L. Zanzotto, Revision of the

Superpave high temperature binder specification: The multiple stress creep recovery test, *Asph. Paving Technol. Assoc. Asph. Paving Technol. Tech. Sess.* 76 (2007) 123–162.

- [65] R.M. Anderson, G.N. King, D.I. Hanson, P.B. Blankenship, Evaluation of the relationship between asphalt binder properties and non-load related cracking, *J. Assoc. Asph. Paving Technol.* 80 (2011).
- [66] J. Shen, S. Amirkhanian, S.J. Lee, B. Putman, Recycling of laboratory-prepared reclaimed asphalt pavement mixtures containing crumb rubber-modified binders in hot-mix asphalt, *Transp. Res. Rec.* (2006) 71–78. <https://doi.org/10.3141/1962-09>.
- [67] M. Attia, M. Abdelrahman, Enhancing the performance of crumb rubber-modified binders through varying the interaction conditions, *Int. J. Pavement Eng.* 10 (2009) 423–434. <https://doi.org/10.1080/10298430802343177>.
- [68] A. Copeland, J. D'Angelo, R. Dongré, S. Belagutti, G. Sholar, Field evaluation of high reclaimed asphalt pavement-warm-mix asphalt project in Florida: Case study, *Transp. Res. Rec.* (2010) 93–101. <https://doi.org/10.3141/2179-11>.
- [69] F. Xiao, B. Putman, S. Amirkhanian, Laboratory investigation of dimensional changes of crumb rubber reacting with asphalt binder, *Road Mater. Pavement Des.* (2006). [http://www.clemson.edu/ces/arts/Dimensional Changes of Crumb Rubber Binder.pdf](http://www.clemson.edu/ces/arts/Dimensional%20Changes%20of%20Crumb%20Rubber%20Binder.pdf).
- [70] L.N. Mohammad, I.I. Negulescu, Z. Wu, C. Daranga, W.H. Daly, C. Abadie, Investigation of the use of recycled polymer modified asphalt binder in asphalt concrete pavements (with discussion and closure), *J. Assoc. Asph. Paving*

Technol. 72 (2003).

- [71] F. Morea, R. Marcozzi, G. Castaño, Rheological properties of asphalt binders with chemical tensoactive additives used in Warm Mix Asphalts (WMAs), *Constr. Build. Mater.* 29 (2012) 135–141.
<https://doi.org/10.1016/j.conbuildmat.2011.10.010>.
- [72] O. Sirin, H.J. Kim, M. Tia, B. Choubane, Comparison of rutting resistance of unmodified and SBS-modified Superpave mixtures by accelerated pavement testing, *Constr. Build. Mater.* 22 (2008) 286–294.
<https://doi.org/10.1016/j.conbuildmat.2006.08.018>.
- [73] G.A.J. Mturi, J. O’Connell, S.E. Zoorob, M. De Beer, A study of crumb rubber modified bitumen used in South Africa, *Road Mater. Pavement Des.* 15 (2014) 774–790. <https://doi.org/10.1080/14680629.2014.910130>.
- [74] T. Ma, Y. Zhao, X. Huang, Y. Zhang, Characteristics of desulfurized rubber asphalt and mixture, *KSCE J. Civ. Eng.* 20 (2016) 1347–1355.
<https://doi.org/10.1007/s12205-015-1195-1>.
- [75] A.I. Kanaan, H. Ozer, I.L. Al-Qadi, Testing of fine asphalt mixtures to quantify effectiveness of asphalt binder replacement using recycled shingles, *Transp. Res. Rec.* 2445 (2014) 103–112. <https://doi.org/10.3141/2445-12>.
- [76] H. Ozer, I.L. Al-Qadi, J. Lambros, A. El-Khatib, P. Singhvi, B. Doll, Development of the fracture-based flexibility index for asphalt concrete cracking potential using modified semi-circle bending test parameters, *Constr. Build. Mater.* 115 (2016) 390–401. <https://doi.org/10.1016/j.conbuildmat.2016.03.144>.

- [77] S. Im, F. Zhou, New and Simpler Cracking Test Method for Asphalt Mix Designs, *Transp. Res. Rec. J. Transp. Res. Board.* (2017) 1–10.
<https://doi.org/10.3141/2631-01>.
- [78] M.P. Wagoner, W.G. Buttlar, G.H. Paulino, Disk-shaped compact tension test for asphalt concrete fracture, *Exp. Mech.* 45 (2005) 270–277.
<https://doi.org/10.1177/0014485105053205>.
- [79] E. Kaloush, Kamil ; Witczak, M. W. ; Roque, Reynaldo ; Brown, Stephen ; D’Angelo, John ; Marasteanu, Mihai ; Masad, Tertiary Flow Characteristics of Asphalt Mixtures, *Asph. Paving Technol.* 71 (2002) 248–280.
- [80] T. Aschenbrener, Evaluation of Hamburg wheel-tracking device to predict moisture damage in hot-mix asphalt, *Transp. Res. Rec.* (1995) 193–201.
- [81] J.W. Arnold, B. Behnia, M.E. McGovern, B. Hill, W.G. Buttlar, H. Reis, Quantitative evaluation of low-temperature performance of sustainable asphalt pavements containing recycled asphalt shingles (RAS), *Constr. Build. Mater.* 58 (2014). <https://doi.org/10.1016/j.conbuildmat.2014.02.002>.
- [82] W.G. Buttlar, B.C. Hill, H. Wang, W. Mogawer, Performance space diagram for the evaluation of high- and low-temperature asphalt mixture performance, *Road Mater. Pavement Des.* 18 (2017) 336–358.
<https://doi.org/10.1080/14680629.2016.1267446>.
- [83] R.C. Williams, W.G. Buttlar, S. Ahmed, B. Hill, Laboratory evaluation of field produced hot mix asphalt containing post-consumer recycled asphalt shingles and fractionated recycled asphalt pavement, *Asph. Paving Technol.* 80 (2011) 377–

418.

- [84] E.T. Zegeye, K.H. Moon, M. Turos, T.R. Clyne, M.O. Marasteanu, Low Temperature Fracture Properties of Polyphosphoric Acid Modified Asphalt Mixtures, 24 (2012) 1089–1096. [https://doi.org/10.1061/\(ASCE\)MT.1943-5533.0000488](https://doi.org/10.1061/(ASCE)MT.1943-5533.0000488).
- [85] X. Li, A.F. Braham, M.O. Marasteanu, W.G. Buttlar, R.C. Williams, Effect of Factors Affecting Fracture Energy of Asphalt Concrete at Low Temperature, Road Mater. Pavement Des. 9 (2008) 397–416. <https://doi.org/10.1080/14680629.2008.9690176>.
- [86] B. Javilla, L. Mo, F. Hao, B. Shu, S. Wu, Multi-stress loading effect on rutting performance of asphalt mixtures based on wheel tracking testing, Constr. Build. Mater. 148 (2017) 1–9. <https://doi.org/10.1016/j.conbuildmat.2017.04.182>.
- [87] H. Haghshenas, Y. Kim, Research on High-RAP Asphalt Mixtures with Rejuvenators and WMA Additives Nebraska Transportation Research on High-RAP Asphalt Mixtures with Rejuvenators and WMA Additives Hamzeh Haghshenas Department of Civil Engineering, (2016).
- [88] L. Walubita, J. Zhang, G. Das, X. Hu, C. Mushota, A. Alvarez, T. Scullion, Hot-Mix Asphalt Permanent Deformation Evaluated by Hamburg Wheel Tracking, Dynamic Modulus, and Repeated Load Tests, Transp. Res. Rec. J. Transp. Res. Board. 2296 (2012) 46–56. <https://doi.org/10.3141/2296-05>.
- [89] B. Jahangiri, H. Majidifard, J. Meister, W.G. Buttlar, Performance Evaluation of Asphalt Mixtures with Reclaimed Asphalt Pavement and Recycled Asphalt

Shingles in Missouri, *Transp. Res. Rec.* (2019).

<https://doi.org/10.1177/0361198119825638>.

- [90] L.F. Walubita, A.N.M. Faruk, J. Zhang, X. Hu, S.I. Lee, The Hamburg rutting test - Effects of HMA sample sitting time and test temperature variation, *Constr. Build. Mater.* 108 (2016) 22–28. <https://doi.org/10.1016/j.conbuildmat.2016.01.031>.
- [91] D. Swiertz, C. Ling, P. Teymourpour, H.U. Bahia, Using the Hamburg Wheel Tracking Test to Characterize Asphalt Mixtures in Cool Weather Regions, *J. Transp. Res. Board.* (2017) 9–15. <https://doi.org/https://doi.org/10.3141/2633-03>.
- [92] R.C. Williams, D. Ph, D.S. Haugen, W.G. Buttlar, R. a Bentsen, J. Behnke, Characterization of Hot Mix Asphalt Containing Post-Consumer Recycled Asphalt Shingles and Fractionated Reclaimed Asphalt Pavement, (2011).
- [93] W.G. Buttlar, H. Wang, Laboratory investigation of Illinois Tollway Stone Matrix Asphalt mixtures with varied levels of asphalt binder replacement, (2016).
- [94] W.G. Buttlar, P. Rath, Illinois Tollway Project Illinois Tollway I-88 Ground Tire Rubber Test Sections, (2017).
- [95] Paul Kovacs, Cynthia Williams, Illinois Tollway continues to be a big asphalt player for contractors, (2019). <https://www.roadsbridges.com/illinois-tollway-continues-be-big-asphalt-player-contractors>.
- [96] F. Xiao, S.N. Amirkhanian, Road Materials and Pavement Design Resilient Modulus Behavior of Rubberized Asphalt Concrete Mixtures Containing Reclaimed Asphalt Resilient Modulus Behavior of Rubberized Asphalt Concrete

Mixtures Containing Reclaimed Asphalt Pavement, (2011) 37–41.

<https://doi.org/10.3166/RMPD.9.633-649>.

- [97] C.A. Cipione, R.R. Davison, B.L. Burr, C.J. Glover, J.A. Bullin, Evaluation of solvents for extraction of residual asphalt from aggregates, *Transp. Res. Rec.* (1991).
- [98] J.C. Petersen, Chemical composition of asphalt as related to asphalt durability, in: *Dev. Pet. Sci.*, Elsevier, 2000: pp. 363–399.
- [99] T. Ma, E. Mahmoud, H.U. Bahia, Estimation of Reclaimed Asphalt Pavement Binder Low-Temperature Properties Without Extraction Development of Testing Procedure, (2010) 58–65. <https://doi.org/10.3141/2179-07>.
- [100] A. Booshehrian, W.S. Mogawer, R. Bonaquist, How to construct an asphalt binder master curve and assess the degree of blending between RAP and virgin binders, *J. Mater. Civ. Eng.* 25 (2013) 1813–1821. [https://doi.org/10.1061/\(ASCE\)MT.1943-5533.0000726](https://doi.org/10.1061/(ASCE)MT.1943-5533.0000726).
- [101] S. Zhao, B. Huang, X. Shu, Investigation on binder homogeneity of RAP/RAS mixtures through staged extraction, *Constr. Build. Mater.* 82 (2015) 184–191. <https://doi.org/10.1016/j.conbuildmat.2015.02.013>.
- [102] J. Xu, P. Hao, D. Zhang, G. Yuan, Investigation of reclaimed asphalt pavement blending efficiency based on micro-mechanical properties of layered asphalt binders, *Constr. Build. Mater.* 163 (2018) 390–401. <https://doi.org/10.1016/j.conbuildmat.2017.12.030>.

- [103] B.L. Burr, R.R. Davison, H.B. Jemison, C.J. Glover, J.A. Bullin, Asphalt hardening in extraction solvents, *Transp. Res. Rec.* (1991).
- [104] J.S. Daniel, J.L. Pochily, D.M. Boisvert, Can more reclaimed asphalt pavement be added? Study of extracted binder properties from plant-produced mixtures with up to 25% reclaimed asphalt pavement, *Transp. Res. Rec.* (2010) 19–29.
<https://doi.org/10.3141/2180-03>.
- [105] A.I. Kanaan, H. Ozer, I.L. Al-Qadi, Testing of fine asphalt mixtures to quantify effectiveness of asphalt binder replacement using recycled shingles, *Transp. Res. Rec.* 2445 (2014) 103–112. <https://doi.org/10.3141/2445-12>.
- [106] M. Heitzman, Design and construction of asphalt paving materials with crumb rubber modifier, *Transp. Res. Rec.* 1339 (1992).
- [107] Y. He, M.Z. Alavi, D. Jones, J. Harvey, Proposing a solvent-free approach to evaluate the properties of blended binders in asphalt mixes containing high quantities of reclaimed asphalt pavement and recycled asphalt shingles, *Constr. Build. Mater.* 114 (2016) 172–180.
<https://doi.org/10.1016/j.conbuildmat.2016.03.074>.
- [108] D.W. Christensen Jr, T. Pellinen, R.F. Bonaquist, Hirsch model for estimating the modulus of asphalt concrete, *J. Assoc. Asph. Paving Technol.* 72 (2003).
- [109] J.S. Daniel, W.S. Mogawer, Determining the Effective PG Grade of Binder in RAP Mixes, (2010). <https://doi.org/10.1017/CBO9781107415324.004>.
- [110] E. Hajj, L. Salazar, P. Sebaaly, Methodologies for estimating effective

performance grade of asphalt binders in mixtures with high recycled asphalt pavement content, *Transp. Res. Rec.* (2012) 53–63. <https://doi.org/10.3141/2294-06>.

[111] P. Rath, H. Majidifard, B. Jahangiri, W. Buttlar, Recent Advances in Ground Tire Rubber Recycling in Midwest Pavements, in: *Association of Asphalt Paving Technologists*, 2019.

[112] AASHTO PP 7817, Standard Practice for Design Considerations When Using Reclaimed Asphalt Shingles (RAS) in Asphalt Mixtures, 3 (2017) 1–7.

[113] NAPA, National Asphalt Pavement Association: Fast Facts, (2009).

[114] F. Zhou, S. Hu, T. Scullion, Integrated Asphalt (Overlay) Mixture Design, Balancing Rutting and Cracking Requirements, 2006.

[115] Federal Highway Administration (FHWA), Asphalt Mixture Performance Tester (AMPT), (2013).

[116] AASHTO, Standard method of test for determining the creep compliance and strength of hot mix asphalt using the indirect tensile test device (T 322), 2010.

[117] T. Mandal, ENHANCEMENT OF THE ASPHALT THERMAL CRACKING ANALYSER (ATCA) TEST TO ALLOW MEASURING CRITICAL PROPERTIES AFFECTING CRACKING OF ASPHALT MIXTURES, (2016).

[118] D.W. Christensen, R.F. Bonaquist, Evaluation of Indirect Tensile Test (IDT) Procedures for Low-Temperature Performance of Hot Mix Asphalt, 2004. <https://doi.org/10.17226/13775>.

- [119] AASHTO, Standard method of test for thermal stress restrained specimen tensile strength (TP 10), 1993.
- [120] T. Aschenbrener, Investigation of Low Temperature Thermal Cracking In Hot Mix Asphalt, (1995).
- [121] ASTM, ASTM D7313-13: Standard Test Method for Determining Fracture Energy of Asphalt-Aggregate Mixtures Using the Disk-Shaped Compact Tension Geometry, ASTM Int. Stand. (2013) 2–8. <https://doi.org/10.1520/D7313>.
- [122] ASTM, ASTM E399-12e3, Standard Test Method for Linear-Elastic Plane-Strain Fracture Toughness K_{Ic} of Metallic Material, (2012).
- [123] I. Al-Qadi, H. Ozer, J. Lambros, D. Lippert, A. El Khatib, T. Khan, P. Singh, J.J. Rivera-Perez, Testing Protocols to Ensure Mix Performance w/ High RAP and RAS, Illinois Cent. Transp. (2015) 209.
- [124] AASHTO, Standard method of test for determining the fracture energy of asphalt mixtures using the semicircular bend geometry (SCB) (TP 105-13), 2013.
- [125] Z. Wu, L. Mohammad, L. Wang, M. Mull, Fracture Resistance Characterization of Superpave Mixtures Using the Semi-Circular Bending Test, J. ASTM Int. 2 (2005) 1–15. <https://doi.org/10.1520/JAI12264>.
- [126] TRB Superpave Committee, Superior Performing Asphalt Pavement SUPERPAVE Performance by Design, 2005.
- [127] AASHTO, Standard method of test for determining the rutting susceptibility of hot mix asphalt (HMA) using the asphalt pavement analyzer (APA) (TP 63), 2007.

- [128] J.F. Rushing, D.N. Little, N. Garg, Selecting a rutting performance test for the airport asphalt mixture design, *Road Mater. Pavement Des.* 15 (2014) 1–23.
<https://doi.org/10.1080/14680629.2014.926626>.
- [129] AASHTO T322-07, Determining Creep Compliance and Strength of Hot Mix Asphalt (HMA) Using the Indirect Tensile Test Device, 2011.
- [130] M.O. Marasteanu, W.G. Buttlar, H. Bahia, C. Williams, E. Al., Investigation of Low Temperature Cracking in Asphalt Pavements, National Pooled Fund Study Phase-II, 2012.

APPENDIX A: REVIEW ON THE PERFORMANCE TESTS

A review of the existing literature related to asphalt performance specifications was undertaken. The literature review included the following topics: asphalt performance testing, agency practices regarding Performance Based Specifications (PBS), and studies related to PBS development and test methods and protocols related to PBS. The results of the literature review are described in the following sections.

Asphalt roads make up for more than 90% of the USA's pavement infrastructure [113]. Such wide usage warrants a sturdy and robust design of the asphalt mix to make it last long and wear less. Before the Superpave mixture design protocol was in place, a lot of procedures followed for designing mixes to address particular distresses were empirical, for example Hubbard-Field or Marshall Test used to predict permanent deformation [114]. Superpave introduced volumetric mix design, which, albeit being a step forward, had considerable gaps in accurately predicting the field performance of the asphalt mixtures. This shortcoming motivated researchers to adopt laboratory mixture testing under simulated loading mimicking the field conditions. These 'performance tests' can provide key insights to the mixture field performance in terms of fatigue cracking, thermal cracking, rutting, moisture resistance, and other key distresses. Table 1 presents few such laboratory mix performance tests.

Table A-1. Assessment of Available Performance Tests for Use in Routine Mixture Design [115]

Property	Method	Standardization		Criteria		Complexity		Equipment		
		Method	Precision	Mix Design Pass/Fail	Performance Prediction Model	Method	Analysis	Availability	Reliability	Cost
Modulus	AMPT Dynamic Modulus	Yes	Yes	NA	Yes	Moderate	Moderate	Yes	High	Moderate
	Simple Shear	Yes	Yes		Yes	Moderate	Moderate	Yes	Moderate	High
	Indirect Tension Dynamic Modulus	No	No		Yes	Moderate	Moderate	No	Moderate	High
Permanent Deformation	AMPT Flow Number	Yes	Yes	Yes	Yes	Moderate	Low	Yes	High	Moderate
	Repeated Shear	Yes	Yes	Yes	Yes	Moderate	Moderate	Yes	Moderate	High
	High Temperature Indirect Tensile Strength	Draft	No	Yes	No	Low	Low	Yes	High	Low
	Asphalt Pavement Analyzer	Yes	No	Yes	No	Moderate	Low	Yes	High	Moderate
	Hamburg Wheel Tracking Device	Yes	No	Yes	No	Moderate	Low	Yes	High	Moderate
Load Associated Cracking	Flexural Fatigue	Yes	No	No	Yes	High	Moderate	Yes	High	Moderate
	AMPT Continuum Damage	No	No	No	Yes	High	High	Yes	High	Moderate
	Energy Ratio	No	No	Yes	Yes	High	High	Yes	High	High
	Fracture Energy	No	No	No	Yes	Low	Low	Yes	High	High
Thermal Cracking	IDT Creep and Strength	Yes	No	No	Yes	High	High	Yes	High	High
	Disc Shaped Compact Tension	Yes	Yes	Yes	Yes	High	Low	Yes	High	High
	Semi Circular Bend	Draft	No	Yes	No	Moderate	Low	Yes	High	High
Moisture Sensitivity	Tensile Strength Ratio	Yes	Yes	Yes	No	Moderate	Low	Yes	High	Low
	Hamburg Wheel Tracking Device	Yes	No	Yes	No	Moderate	Low	Yes	High	Moderate

The following sections summarize the current mixture performance tests grouped according to the parameter they measure or the distress they characterize.

A.1. Mixture Tests to Mitigate Thermal Cracking

Thermal cracking, or low-temperature cracking, is one of the primary distresses of asphalt pavements in cold climates. As the temperature drops, thermal stresses develop due to the differential contraction of the binder and aggregate in the asphalt mastic. When the thermal stresses exceed the tensile strength of the asphalt mixture, the pavement develops cracks. The popular tests for characterizing thermal stresses in asphalt mixtures are Disc-Shaped Compact Tension test (DC(T)), Indirect Tensile creep and strength test (IDT), Semi-Circular Bending test (SCB), and Thermal Stress Restrained Specimen Test (TSRST).

A.1.1. Overview of the IDT

The IDT test is performed to ascertain the tensile strength and the creep properties of the asphalt mixture specimen, which are critical factors of thermal cracking characteristics.

The test is done in accordance with the AASHTO T322 standard [116]. The specimen is loaded diametrically, inducing horizontal tensile stress in the mid-portion of the specimen. The creep test is done at 0 °C, -10 °C, and -20 °C, and the tensile strength test is done at -10 °C. The relaxation modulus data, obtained by converting the creep compliance data, is used to estimate the thermal stresses and calculate the critical cracking temperature [117,118].

A.1.2. Overview of TSRST Test

TSRST (AASHTO TP 10) [119] is a simple test wherein a rectangular asphalt mixture specimen is allowed to cool but is restrained on shorter edges, leading to development of thermal stresses within the specimen and ultimately cracking when the thermal stresses exceed the tensile strength of the specimen. It was developed at Oregon State University as a part of SHRP (Aschenbrener, 1995). After fabricating the specimens, they are glued to the plates and conditioned in a cooling chamber at 5 °C for an hour to impose thermal equilibrium in the specimen. LVDTs are used to measure the deformation of the sample while the temperature of the chamber is reduced. A closed-loop loading frame is used to restrain the shorted edges of the specimen at the original length, inducing thermal stresses. The end result of this test is a thermal stress-temperature plot.

A.1.3. Overview of DC(T) Test

The Disk-Shaped Compact Tension (DC(T)) (ASTM D7313-13) [121] test is used to measure the low-temperature cracking potential of the asphalt mixtures. Wagoner et al.

came up with a suitable configuration (shown in Figure 1) for this test using ASTM E-399 [122] as a starting point and then modified it for asphalt materials [42]. A big advantage of the DC(T) test lies in its ability to test cylindrical cores obtained from field or compacted in Superpave Gyrotory Compacter (SGC) and its large fracture surface area [78]. The DC(T) test temperature is generally 10°C higher than the PG low temperature grade of the binder used in the asphalt mixture. The specimen is pulled through the drilled holes, forcing the crack to propagate in perpendicular direction. The notch is made to pre-determine the crack path. The test is conducted at a constant Crack Mouth Opening Displacement (CMOD) rate of 1mm/min (0.017 mm/s). It is stopped when the post-peak loading reaches 0.1kN. A typical load-CMOD curve is shown in Figure 2. The area under the curve, normalized by the initial fracture area of the specimen, is reported as the fracture energy of the asphalt mixture specimen. The standard method of testing is outlined in ASTM D7313-13 standard [121].

A.1.4. Overview of SCB Test

The Semi-Circular Bending (SCB) test utilizes a simple three-point bending mechanism to determine the cracking resistance of the asphalt mixture specimen. The test uses a semi-circular specimen and load is applied at the center of specimen periphery, as shown in Figure 3. [123]. The test can be conducted in low temperatures as well as intermediate temperatures. The low temperature cracking resistance test standard is outlined in AASHTO TP105-13 [124] and utilizes the same method as the DC(T) test to calculate fracture energy. The intermediate temperature SCB test was developed by Wu et al. in 2005, using 25°C as the test temperature for the SCB test. The authors used the concept of critical J-integral, which was found to be sensitive to the changes in binder types and

nominal maximum aggregate size (NMAS), both affecting the fracture resistance of the mixtures [6,125].

A.1.5. Overview of IDEAL-CT Test

In a research study by Zhou et al. (2017), the indirect tensile asphalt cracking test (IDEAL-CT) which is similar to the indirect tensile (IDT) test was developed [7]. The IDEAL-CT is normally run at room temperature and a loading rate of 50 mm/min. Figure 6 shows the IDEAL-CT setup with typical results. The IDEAL-CT was compared to the Texas OT and Illinois SCB tests using over 25 laboratory and field plant mixes. All three tests ranked all of these mixes in the same order with respect to crack resistance. The IDEAL-CT showed a strong correlation with the field distresses of fatigue, reflective, and thermal cracking. According to the authors, the IDEAL-CT is straightforward to perform, requires minimal training, and is fast as the test completes within one minute. The IDEAL-CT was found to be rugged with respect to specimen thickness, loading rate, test temperature, and air voids.

A.2. Mixture Tests to Mitigate Rutting

Permanent deformation (rutting) in asphalt pavement is a result of consolidation and shear flow caused by traffic loading in hot weather. This results in a gradual accumulation of volumetric and shear strains in the HMA layers. The measured deformation of different layers of flexible pavement revealed that the upper 100 mm (4 in.) serves the main portion of the pavement rut depth such that the asphalt layer accumulates up to 60 percent of total permanent deformation. Lack of shear strength of the asphalt layer to resist the repeated heavy static and moving loads results in downward movement of the surface and provides the potential for upheaval and microcracks along

the rut edges. In addition to structural failure issues, safety concerns arise due to vehicle steering difficulties and the potential for increased hydroplaning. Although Superpave mixture design protocols have led to a general reduction in the manifestation of rutting on pavements [126], the ever-increasing traffic and advent of newer materials in asphalt mixture still call for the inclusion of a performance-based test specification. Rutting, or permanent deformation, is an accumulation of unrecoverable strains on the pavement structure due to repeated traffic loads. Wheel load tracking (WLT) tests are the most common performance tests used to control rutting potential in HMA mixes. The WLT methods simulate traffic by applying thousands of wheel load passes, simulating traffic loads on HMA specimen in an accelerated fashion at a selected temperature such as 50 °C.

A.2.1. Overview of WLA tests

Wheel load tracking (WLT) tests are the most common performance tests for measuring rutting potential of HMA mixes. The WLT methods simulate traffic by passing over standardized wheels simulating real-life traffic loads on HMA specimen at a given temperature. The two most common WLT test devices are Hamburg Wheel Tracking Test (HWTT) and the Asphalt Pavement Analyzer (APA) (formerly known as Georgia-loaded wheel tester). The HWTT is performed in accordance to AASHTO T324 standard. A loaded steel wheel, weighing approximately 71.7 kg tracks over the samples placed in a water bath at 50°C. The vertical deformation of the specimen is noted against the number of wheel passes. The test is stopped when either the specimen deforms by 20mm or the number of passes exceeds 20,000.

A.2.2. Overview of APA test

The APA uses a similar principle with an aluminum wheel and can also simulate the effect of tire pressure, unlike HWTT. It is performed in accordance with the AASHTO TP63 standard [127]. Both the methods can also be used to determine the moisture sensitivity of the HMA mixtures since the wheel loads are simulated under-water. There are several other test methods to measure permanent deformation such as the Static Creep triaxial test and repeated load triaxial test that use flow time and flow number respectively as parameters to ascertain rutting characteristics of a mixture. Rutting is also related to the dynamic modulus of the mixture [128].

APPENDIX B: OTHER PERFORMANCE TESTING RESULTS

B.1. I-FIT Testing Results

The flexibility index (FI) is an empirical index parameter that is computed as the total fracture energy divided by the absolute value of the slope of the post-peak softening curve. FI is proposed to provide a means to identify brittle mixtures that are prone to premature cracking, and was specifically developed to be sensitive to recycled material content (AASHTO TP124-16). The FI parameter is calculated as follows.

$$FI = \frac{G_f}{|m|} (0.01) \quad [B-1]$$

where G_f is computed in a similar manner as to the DC(T) test, and m represents the slope of the post-peak softening curve. There are numerous ways to estimate the slope of a curve resulting from a material test, which posed an inherent challenge from the perspective of test standardization in the development of tests such as the I-FIT. At present, to address this source of variability, the slope parameter is typically determined using a sophisticated software program available from the Illinois Center for Transportation (visit <https://ict.illinois.edu/2016/07/01/i-fit-software-now-available-on-ict-website/>). To fabricate samples, a notch is cut along the axis of symmetry of a semi-circular bend specimen to a depth of 15 ± 1 mm. Test specimens are then conditioned in the environmental chamber at $25 \text{ }^\circ\text{C}$ for 2 hrs. \pm 10 min. After a contact load of 0.1 kN is reached, the test is carried out at a rate of 50 mm/min load line displacement (LLD). The test is considered to be complete when the load drops below 0.1 kN, which is identical to the DC(T) test termination definition. A sampling rate of 40 samples per second was used to collect the data during the test. A software named “SCB TestQuip LLC. V2.0.0rc4”

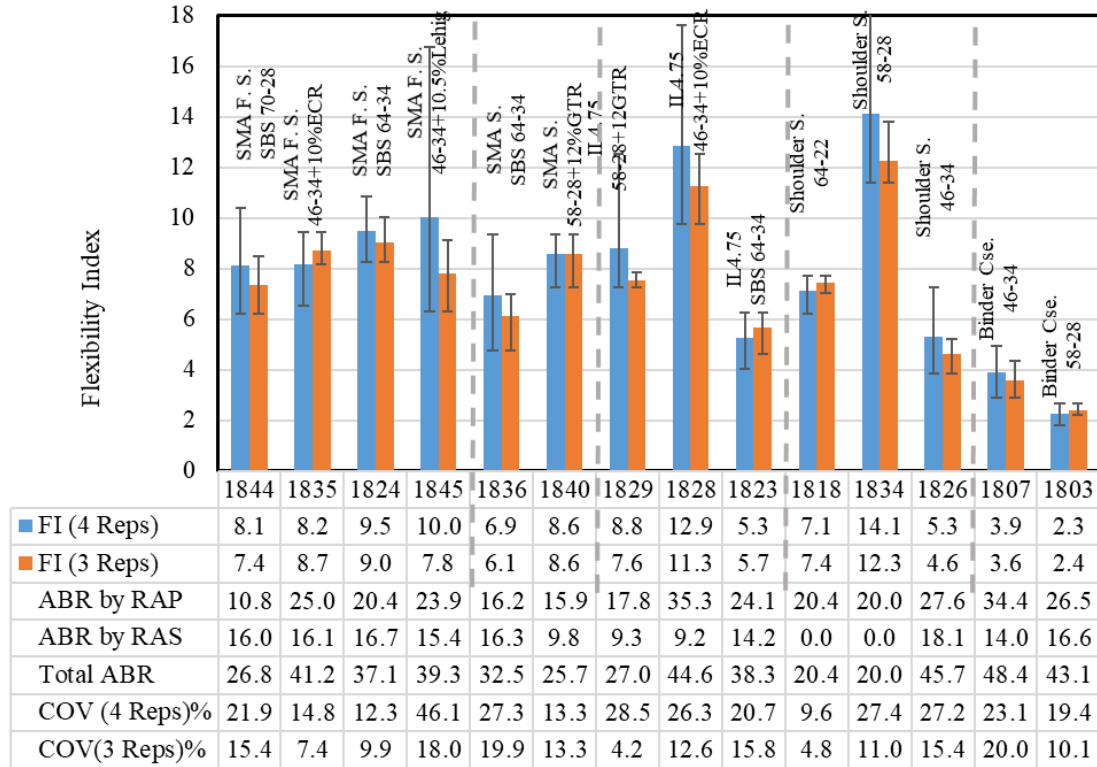
was then applied to analyze the collected load-displacement data and calculated the FI parameter.

Figure B.1 presents the results of I-FIT testing performed on the samples conditioned at 25 °C. The blue bars represent the average of four replicates. As inferred from the large error bars, which display the upper and lower FIs obtained for each mix, the repeatability of the I-FIT test itself may be viewed as borderline (too high). In order to lower the FI variability, researchers in Illinois proposed that the replicate with the furthest FI from the average FI be removed, followed by a recalculation of the average of three remaining replicates (denoted herein as ‘FI 3 Reps’). Although this approach is questionable from a statistical standpoint and may produce significant movement in the average (upwards or downwards), it clearly achieves the goal of reducing the reported variability in the averaged results. Figure B.1 also compares these two averages (four replicates vs. three replicates).

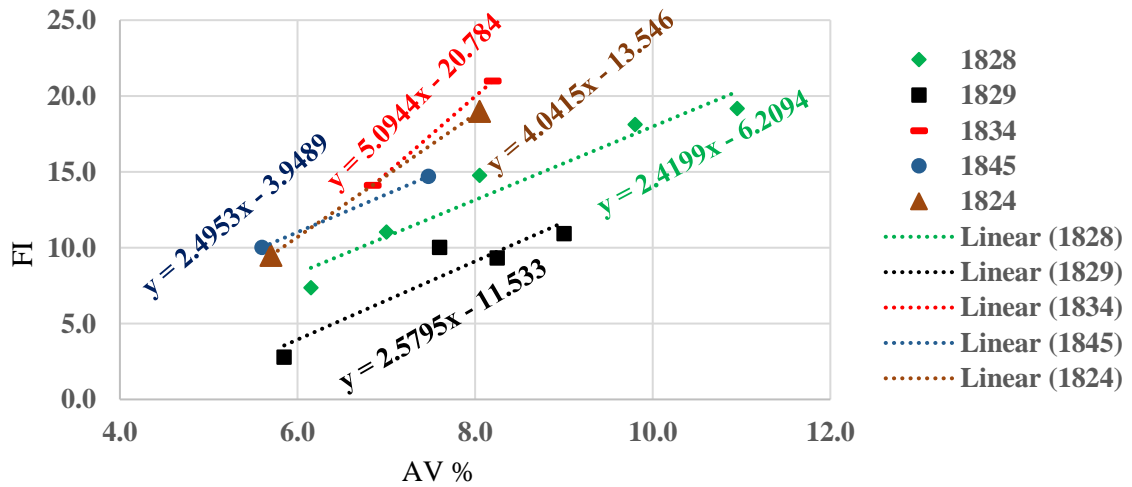
Examining the FI trends, the cracking performance of the different groups of Tollway mixtures were not in close correspondence with expected, relative cracking performance trends. For example, two mixtures in the IL-4.75 group (1829 and 1828) possessed FIs that were higher than those of SMA friction surface mixes. In addition, 1834, which is a shoulder surface mix, yielded the highest FI amongst the studied mixtures. As will be shown later, the FI parameter is heavily dependent on aging. As these plant-produced mixtures have been reheated for sample preparation, the FIs values, including relative trends, might have been significantly affected.

Figure B.2 shows the I-FIT testing results for specimens having varied levels of air voids. A straight line was fitted to data to quantify the sensitivity of the FI parameter to air voids. As the slopes suggests, air void content has a very significant effect on the FI. For example, the FI for the 1828 mix would increase by 2.4 for each percent increase in air void content. It is worth mentioning that the effect of air void on the I-FIT test was not the main goal of this study and the extra testing was done on the fabricated samples having air void levels outside of the acceptable range (6 ± 0.5 for SMAs and 7 ± 0.5 for dense graded mixes). Based on this relatively limited number of tested mixes, the maximum and minimum FI change per percent increase in air voids was found to be 5.1 and 2.4, respectively.

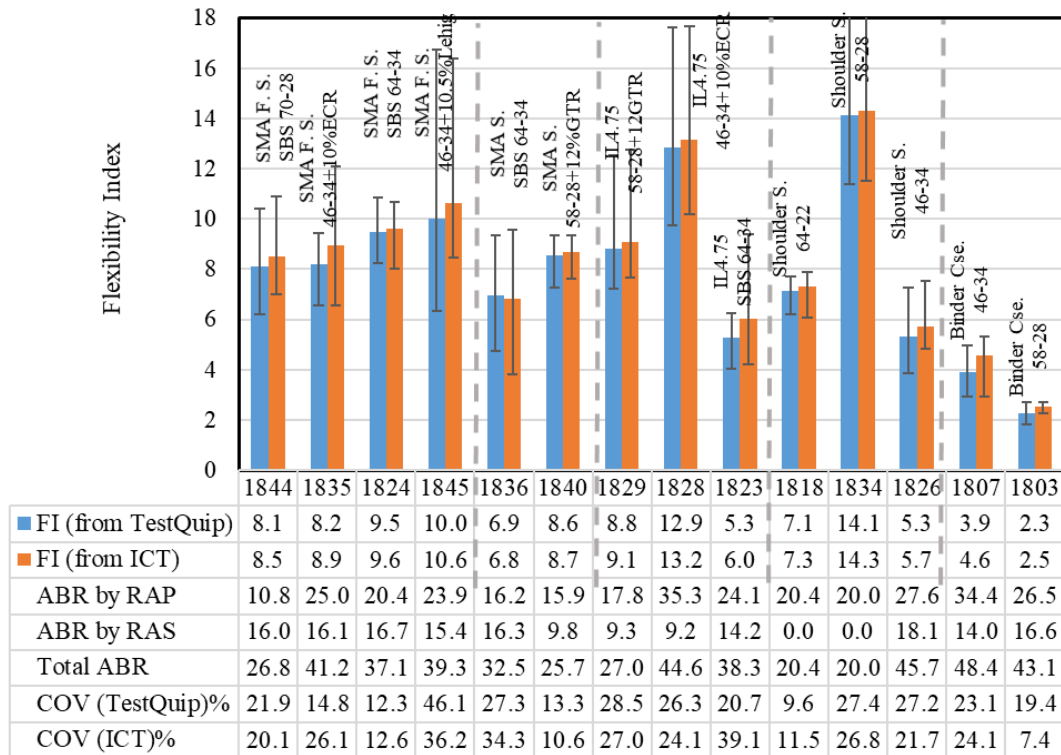
Figure B.3 compares the average FI values from four replicates calculated through the TestQuip software with the outputs from the software provided by Illinois Center for Transportation (ICT). As seen, the difference between the FIs is not considerable and could be mainly attributed to the differences in curve fitting techniques including the slope (derivative) computation method used.



B.1. I-FIT testing results (four replicates vs. three replicates)



B.2. Effect of air voids on FI



B.3. Comparing FIs calculated from Test Quip and ICT software

I-FIT testing was performed on the sliced top lift of the field cores. Four replicates were prepared and tested and the average of the FI parameter for twelve sections are presented in Figure B.4. Similar to the previous figure, the error bars show the range of the FIs calculated for the four replicates. Although the FIs for the SMAs are generally higher than those of dense graded mixtures (as expected), the I90-10E section, as a shoulder mix had the highest FI among the tested sections. I90-5.12 was another section that has an FI of 4.7 which is comparable to the FI of the SMAs. Among the six SMA mixtures, I88-60.5, which is a four-year-old SMA friction surface mix with an SBS 70-28 recoded the highest FI. As the I-FIT test is very sensitive to aging (based on the aging results in Chapter 3), it is expected that the FI of this section will drop significantly as it reaches the age of the other sections. The I90-6.6 mix, which performed well in DC(T) test and was

ranked as the third-best SMA, yielded the poorest performance in I-FIT test among the SMA, with an FI of 3.7.

Comparing I90-7.25 and I90-5.12, which have the same binder system but different combinations of recycled materials, illustrates how the FI is sensitive to RAS binder. As a result, the FI of I90-5.12 is significantly higher than that of I90-7.25, although I90-5.12 is one year older than I90-7.25.

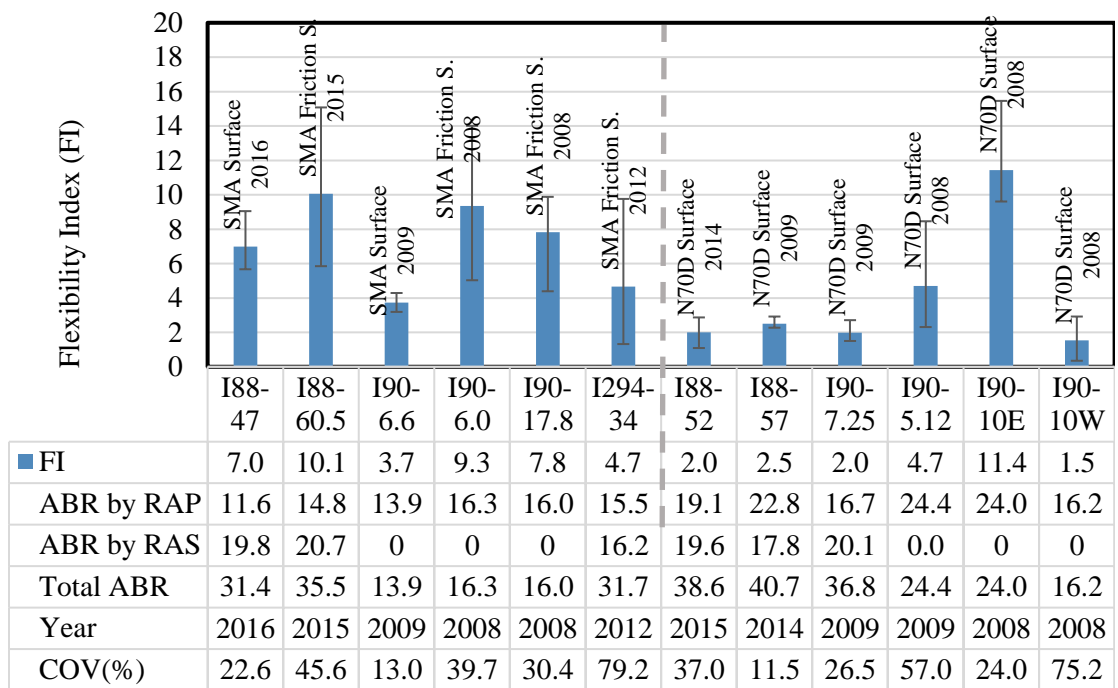


Figure B.4. I-FIT testing results for the top lift of the field cores

Figure B.5. compares the FIs for two different lifts of the field cores collected from three sections. As shown in the figure, all of these three sections are SMAs. Unlike the DC(T) fracture energy, there is a significant difference between the FI of different lifts. As mentioned before, I-FIT tests is very sensitive to aging and the bottom lift of field cores had less aging than the top lift. This was especially reflected in I90-6.6 where the same

mix was used in both lifts but the FI of the bottom lift was 170 % higher than the top lift. For the other two sections, I90-6.0 and I294-34, although the top lift is a SMA friction surface mix which benefits from very high quality aggregates, the FI of the bottom lift, which are SMA binders, are higher than the top lifts.

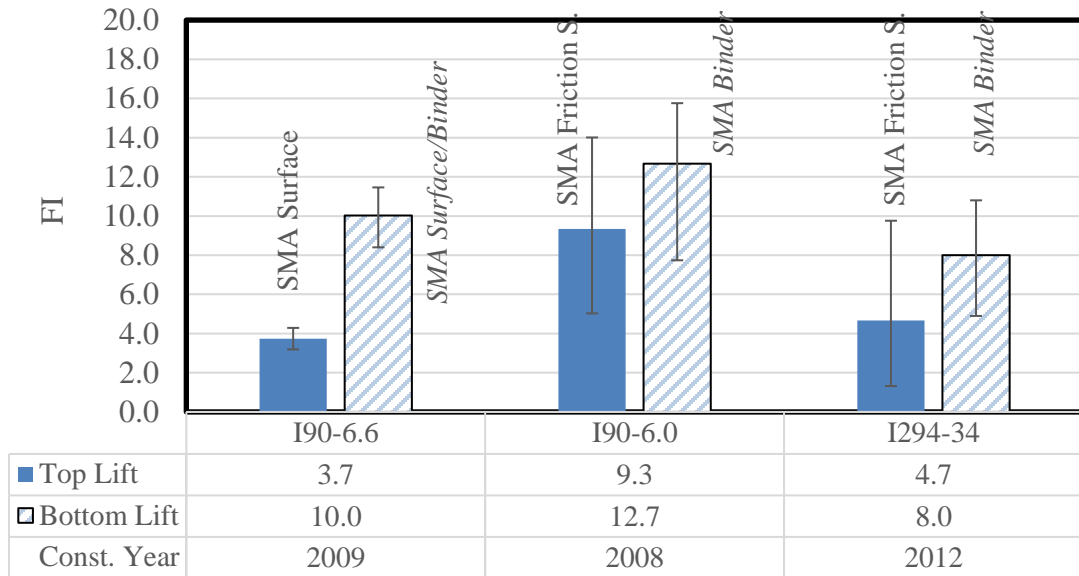


Figure B.5. Comparing the FIs for top and bottom lifts of the field cores

B.2. IDEAL-CT Testing Results

The IDEAL-CT test was developed to characterize the potential of cracking in asphalt mixes at room temperature. The test set-up is similar to the traditional indirect tensile strength test, but it is performed at 25°C under a constant loading rate of 50 mm/min until failure occurs (ASTM D 8225-19). The specimens are cylindrical with a diameter of 100 or 150 mm and a thickness of 38, 62, 75, or 95 mm, depending on the specification followed. The specimens do not require gluing, notching, drilling or additional cutting. The procedure of the test includes conditioning the specimens in a temperature-controlled chamber for a minimum of 2 hours at 25 °C. After conditioning, the specimens were

placed in a Test Quip™ load frame set up for the IDEAL test. A seating load of 0.1 kN was applied in order to make appropriate contact between the loading heads and the sample. The sample was then loaded under a displacement control mode of 50 mm/min while the loading level was collected by the device.

The cracking parameter for the IDEAL-CT is derived from the load vs. ram displacement curve. The larger the CT-index, the better the cracking resistance of the mixture according to the test developers. A minimum of CT-index for SMAs proposed is 145 while the recommended CT-index for Superpave dense graded mixes is 105 (Zhou, 2018). The CT index equation for a specimen of 62 mm thickness is as follows.

$$CT_{index} = \frac{G_f}{|m_{75}|} \times \left(\frac{l_{75}}{D}\right) \times \left(\frac{t}{62}\right) \quad [B-2]$$

where,

G_f = Fracture energy (AREA under the curve normalized by the area fractured)

AREA= Area under the load-displacement curve, until a terminal load of 0.1 kN is reached

m_{75} = Modulus parameter (absolute value of the slope at 75% of peak load)

l_{75} = Vertical displacement when the load is reduced to 75% of peak load

l_{75}/D = Strain tolerance parameter (when load is reduced to 75% of peak load)

D = Specimen diameter

t = Specimen thickness

In this study, the IDEAL-CT test was performed on cylindrical samples compacted to 95 mm and conditioned for two hours in an environmental chamber. Three replicates were

fabricated for each mix and tested to calculate the CT index. Similar to the previous testing figures, the error bars in Figure B.6 shows the range of the calculated CTs for each mix. As shown, most of the SMA mixtures could not meet the threshold of 145, which is recommended for Texas. The dense graded mixtures had a difficult time reaching the minimum recommended CT-index threshold of 105. Given the fact that most of the SMA mixtures produced relatively high DC(T) fracture energy values and FI values in excess of 8.0, the CT-index thresholds recommended by developers for the Texas climate might be too stringent for Tollway mixtures. It is also worth mentioning that reheating the samples might have reduced the crack resistance of the mixtures due to excessive aging.

- Similar to the other two cracking tests (DC(T) and I-FIT), 1836 (SMA surface) recorded the lowest score in the IDEAL-CT test among SMA mixtures.
- The 1845 and 1840 mixtures, which are both GTR modified, recorded the best CT scores among the SMAs.
- Similar to the other two cracking tests (DC(T) and I-FIT), 1823 mix had the lowest CT score in the IL-4.75 group.
- The 1807 mix, which benefits from a softer binder as compared to 1803, had significantly better cracking performance based on IDEAL-CT results.

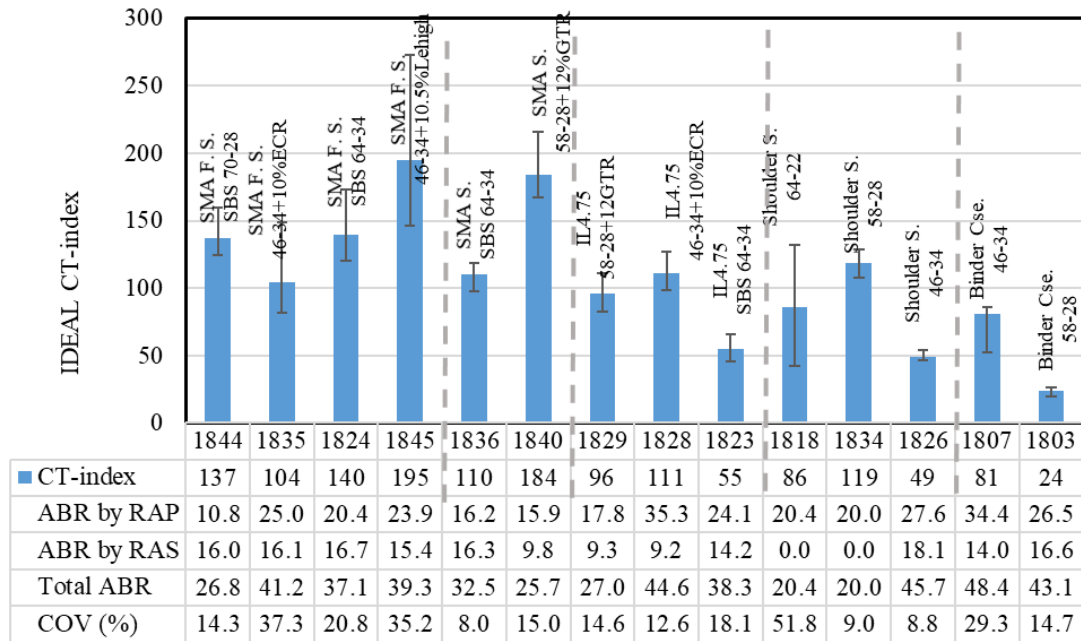


Figure B.6. Results from IDEAL-CT testing (95 mm sample thickness)

The IDEAL-CT test was the third cracking test which was carried out on the field cores. The averages of the CT index using three replicates for different sections are presented in Figure B.7. It should be noted that the recently published IDEAL-CT specification (ASTM D8228-19) calls for 62 mm as the thickness of the testing samples. However, the thickness of the lifts was not enough to meet that requirement and 50 mm slices were tested. Similar to I-FIT test results, the I88-60.5 and I90-10E have the highest CT score among the SMAs and dense graded mixtures, respectively. That being said, the SMA friction surface mixtures did not outperform the SMA surface mixtures. The IDEAL displayed a considerably lower COV as compared to I-FIT. Similar to DC(T) test results, the shoulder mixtures performed very similarly in this test, where the CT score ranged from 64 to 139.

As shown in Figure B.8, the CT scores of the bottom lifts for two sections (I60-6.6 and I90-6.0) are higher than their corresponding top lift. However, the I294-34 section recorded a higher CT index for its top lift.

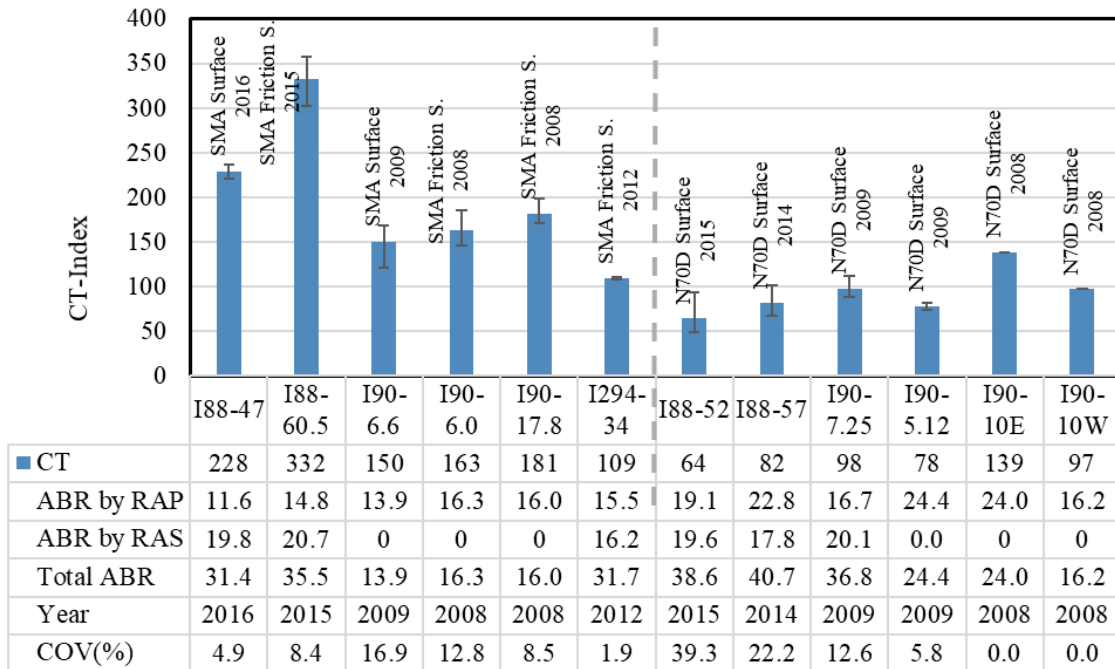


Figure B.7. IDEAL-CT testing results for the top lift of the field cores

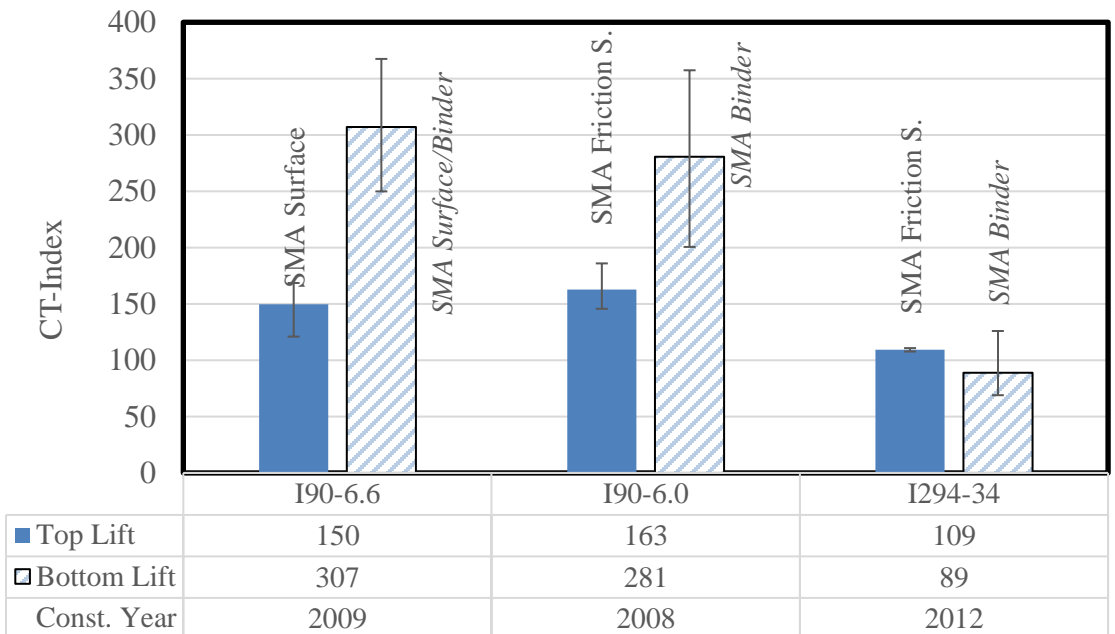


Figure B.8. Comparing the IDEAL-CTs for top and bottom lifts of the field cores

Table B.1 present more details regarding the variability associated with parameters obtained from the IFIT and IDEAL cracking tests. As shown, the average COV of the fracture energy (FE) calculated in IDEAL-CT test is 4.6 %, which is much lower than that of the I-FIT test. This is likely due to the larger sample size used, and thus, larger fracture process zone size relative to the inherent material RVE. Moreover, the post peak slope calculated through the IDEAL-CT test is generally less than half as compared to the I-FIT post peak slope. This is a factor explaining why the slope calculated by the IDEAL-CT method is less variable and therefore more reliable than that found in the IFIT. It was found that the COV of the final indices did not vary as much (20.9 vs. 22.7 %) in the case of the plant-produced mixtures.

Table B.1. COVs of different parameters obtained from IDEAL CT and I-FIT tests

Mix. ID	IDEAL-CT test				I-FIT test		
	FE	Slope	L ₇₅	CT	FE	Slope	FI
1844	9.4	11.6	5.2	14.3	16.4	13.7	21.9
1835	4.5	16.8	13.2	37.3	23.1	22.0	14.8
1824	6.1	16.2	8.3	20.8	9.2	5.1	12.3
1845	6.8	13.5	13.4	35.2	18.9	23.0	46.1
1836	2.8	7.9	4.0	8.0	14.2	39.9	27.3
1840	6.4	5.2	6.2	15.0	10.0	24.1	13.3
1829	2.5	6.3	8.7	14.6	8.3	19.1	28.5
828	0.9	5.4	6.6	12.6	7.2	19.0	26.3
1823	1.9	9.2	7.3	18.1	41.1	50.9	20.7
1818	5.0	20.1	10.1	51.8	7.9	14.9	9.6
1834	4.1	10.7	2.6	9.0	5.1	24.1	27.4
1826	4.4	4.9	4.3	8.8	4.6	23.8	27.2
1807	4.5	16.2	6.9	32.5	8.8	22.6	23.1
1803	5.4	13.9	6.9	14.7	9.5	19.8	19.4
AVG	4.6	11.3	7.4	20.9	13.2	23.0	22.7

B.3. IDT Creep and Strength Testing Results

Following AASHTO T322-07, 2011, the Superpave Indirect Tensile Test (IDT) can be used to perform creep compliance and strength testing of asphalt mixtures. Field-cored or gyratory-compacted samples with heights ranging from 38 to 50 mm and diameters in the range of 150 ± 9 mm are generally used. Three testing temperatures with 10 °C intervals are recommended for use, which are often taken as 0, -10, and -20 °C. Alternatively, temperatures can be selected to encompass the low-performance grade (PG) of the asphalt binder and can use a different temperature spacing, such as 0, -12, and -24 °C [130]. A creep test duration of 1000 seconds is generally required to ensure overlap between creep curves when constructing the master curve. Since the creep compliance should normally be characterized in the linear viscoelastic range, loading levels should be kept sufficiently low in order to retain this linearity. Therefore, a maximum deformation on the horizontal clip gage of 0.019 mm for 150 mm diameter samples is suggested to stay within the linear range. In addition, to circumvent the noise problems and drift inherent in sensors (displacement extensometers), a minimum deformation of 0.00125 mm at a 30-second loading time is recommended.

The IDT creep and strength tests were carried out using a Cooper universal testing machine (UTM) at MAPIL with the capacity of 100 kN. IDT creep and strength tests were performed following AASHTO T-322. To carry out the IDT creep test, three samples were conditioned at three different temperatures including 0, -12 and -24 °C. Each sample was kept at the testing temperature for 2 hours. The conditioned sample was then put into the IDT fixture. In order to compensate the temperature loss due to opening the chamber door and installing the extensometers, the sample was kept for another half

an hour to reach the testing temperature. During this time, the response of extensometers was monitored to ensure temperature stabilization and the absence of sensor drift. Monitoring the response of the extensometer also helps in detecting potential problems with the attachment of the extensometers, which could affect the data. Next, a seating load of 0.1 kN was applied to the sample. The seating load fixes the sample position in the IDT fixture, ensures rapid creep loading without impact, and eliminates some of the slight nonlinearity exhibited at low load levels. In the test, the load level is rapidly increased as a steep slope-load function until the target creep load is reached, which may differ at each temperature. The closed-loop controls are tuned such that the creep load is attained in less than one second. The creep load was then maintained for 1000 seconds while displacements were recorded. Table B.2 shows the testing parameters used in IDT creep test. Equation 4 presents the general equation used to convert load and deflection values to creep compliance (AASHTO T-322-17).

Table B.2. Loading Properties in IDT Creep Test

Testing	Chamber	Seating	Ramp	Creep	Creep
0	-1.5	0.1	1	4	1000
-12	-14	0.1	1	8	1000
-24	-26	0.1	1	20	1000

$$D(t) = \frac{\Delta X_{tm,t} * D_{avg} * b_{avg}}{P_{avg} * GL} * C_{cmpl} \quad [B-3]$$

where,

D(t)= Creep compliance as a function of time (1/GPa)

$\Delta X_{tm,t}$ = Trimmed mean of normalized horizontal deformation (mm)

D_{avg} = Averaged diameter (mm)

b_{avg} = Averaged thickness (mm)

P_{avg} = Averaged applied load (kN)

GL = Guage length (mm)

C_{cmpl} = Creep compliance correction factor

After plotting the creep compliance curves at different temperatures versus time in a log-log space, the curves are shifted horizontally relative to the curve at the referenced temperature to construct a unique continuous curve, called the master curve. A power law function is then fitted to the master curve as shown in Eq. 5.

$$D(t) = D_0 + D_1 t^m \quad [\text{B-4}]$$

where D_0 and D_1 and m are model constant values and t denotes time.

The strength test is performed by applying an increasing load at a constant displacement rate until failure occurs in the specimen. Extensometers were removed prior to strength testing to avoid damage, as tensile strength was estimated using a simple 2D, plane-stress based solution.

$$S_t = \frac{2P_{max}}{\pi * b * D} \quad [\text{B-5}]$$

where

S_t = Tensile strength (MPa)

P_{max} = Maximum recorded load (kN)

b= Sample thickness (mm)

D= Sample diameter (mm)

Figure B.9 shows the IDT strength testing results performed on SMA slices with 50 mm thickness after being conditioned at -12 °C for 2 hours. As can be seen in this figure, the strength of the SMA mixtures are very similar to each other and there is no significant difference between the strengths. It is also worth mentioning that unlike the other cracking performance tests, the SMA surface mixes are exhibiting a slightly higher strength as compared to the SMA friction surface mixtures under the IDT strength test. The Tollway 2018 mixtures are also compared to selected dense-graded Missouri highway mixtures in this figure. It is interesting to note that the strength of the Missouri highway mixtures is higher than the Tollway mixtures. Additionally, the DC(T) fracture energy in the same Missouri highway mixtures was around 400 J/m², and measured creep compliance was relatively low, which indicates stiff and brittle behavior at low temperatures. This follows the general trend of high stiffness being related to high strength but low fracture resistance. This also follows the current thinking regarding the shortcomings in using simple tensile strength measurements as a parameter to rank low temperature cracking resistance (Buttlar et al., 2019).

Prior to IDT strength testing, the IDT creep test was conducted on the samples and the IDT creep compliance master curves were generated as shown in Figure B.10. The creep compliance master curve, which is the output of the IDT creep test can be used to model the viscoelastic behavior of the mixtures and to predict the amount of low temperature cracking expected in the pavement.

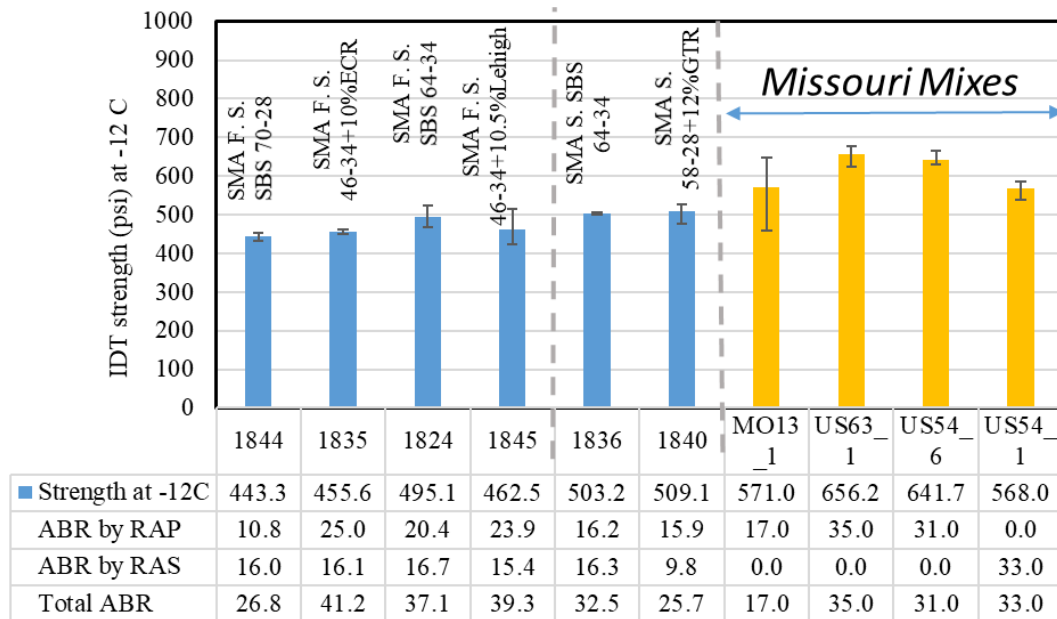


Figure B.9. IDT strength testing results at -12 °C

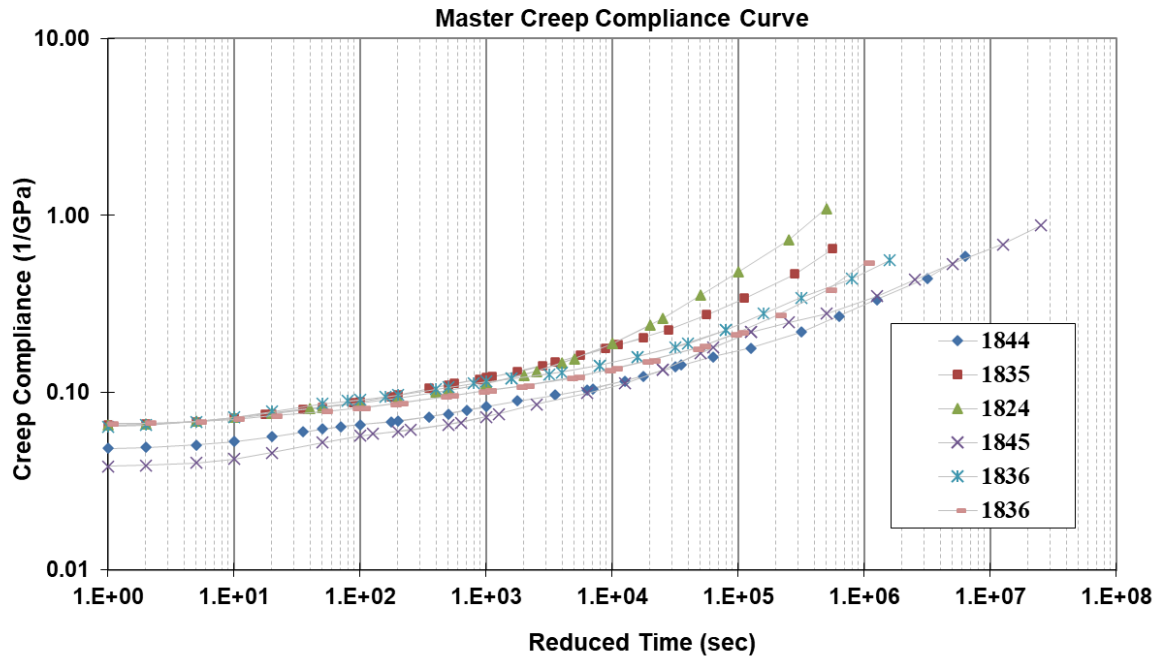


Figure B.10. IDT creep compliance master curves (Reference temperature: -24°C)

VITA

Mr. Behnam Jahangiri Koohbanani is a PhD candidate in the Department of Civil and Environmental Engineering at the University of Missouri-Columbia (MU, Advisor: Bill Buttlar). He also holds an MSc degree in Pavement Engineering from Sharif University of Technology (Advisor: Nader Tabatabaee), and a BSc degree in Civil Engineering from Isfahan University of Technology. As a Graduate Research Assistant at Missouri Asphalt Pavement and Innovation Lab (MAPIL), he has been working on cutting-edge research areas related to smart infrastructure systems and innovative construction materials to address real-world concerns in the asphalt industry. His PhD dissertation is focused on the development of performance specifications for the Illinois Tollway. He is also involved in the characterization of a wide variety of modern and heterogeneous asphalt mixtures containing recycled materials RAP, RAS, rubber, and waste plastic for the Missouri Department of Transportation and for industry. Finally, he conducts research in advanced machine learning/artificial intelligence methods for material characterization, and deployment of sensors for civil infrastructure condition assessment.